

UC Davis

UC Davis Electronic Theses and Dissertations

Title

U-Pb Geochronology of Mid-Crustal Rocks Exhumed Along the Denali Fault in the Eastern Alaska Range

Permalink

<https://escholarship.org/uc/item/83p3h5dk>

Author

Grant, Belyn Nicole

Publication Date

2022

Peer reviewed|Thesis/dissertation

U-Pb Geochronology of Mid-Crustal Rocks Exhumed Along the Denali Fault in the Eastern
Alaska Range

By

BELYN NICOLE GRANT
THESIS

Submitted in partial satisfaction of the requirements for the degree of

MASTER OF SCIENCE

in

Earth and Planetary Sciences

in the

OFFICE OF GRADUATE STUDIES

of the

UNIVERSITY OF CALIFORNIA

DAVIS

Approved:

Sarah Roeske, Chair

Michael Oskin

Kenneth Ridgway

Committee in Charge

2022

Abstract

For much of its length, the Denali fault juxtaposes the Wrangellia Composite terrane against the ancestral North American margin. However, the location of the main geologic boundary between the Wrangellia Composite terrane and the North American margin is obscured in the Alaska Range Suture Zone. In the Eastern Alaska Range, where persistent and rapid exhumation has been occurring since ~23 Ma, the origin and protolith of the rocks north of the Denali fault is unknown. We present new U-Pb detrital zircon geochronology from seven samples collected in the eastern Alaska Range located within this region of focused exhumation. The prevalence of suspected metamorphic grains, grains affected by lead loss, and newly crystallized grains due to regional plutonism provided challenges when filtering our data. Grains from each data set with U/Th ratios > 10 , Uranium content $> 5,000$ ppm, or U-Pb ages $> 3\%$ error were removed. Additionally, neo-crystallized grains were identified and removed based on the known distribution of U-Pb zircon ages of plutons in the immediate field area. The maximum depositional age of our samples ranges from Late Devonian to Middle Triassic. These findings contradict previous mapping and suggest that many assemblages in the eastern Alaska Range will be mapped differently with future detailed mapping. It is possible rocks to the north of the Denali fault in the eastern Alaska Range have ties with the ancestral North American margin, which would be expected based on geographic location and would imply these rocks have remained in place. Alternatively, it is also possible that one of our samples has sediment sourced from the southern portion of the Alexander terrane, and two of our samples have sediment sourced from the Endicott Arm of the southeastern Yukon Tanana terrane. If these correlations are correct, this requires >1000 kilometers of transport, which requires slip on a separate structure from the Denali fault.

Acknowledgements

I am incredibly thankful for all the different forms of support I've experienced over the last few years.

First, thank you to Sarah Roeske for making this research possible and for guiding me on this journey, in the field and in the lab. I've learned so much! I am grateful for funding from the Alaska Geological Society, Geological Society of America, and the UC Davis Earth and Planetary Sciences Department. Additional funding for this project came from an NSF Tectonics grant awarded to Sarah Roeske. I am indebted to Eric Cowgill, Magali Billen, Mike Oskin, and Ken Ridgway for not only serving on my committees but also providing incredibly helpful mentorship. Many thanks to the staff at Arizona Laserchron Center and to Greg Baxter for preparing my thin sections beautifully and answering countless questions.

Thank you to Fiona for being my research buddy, lab buddy, office buddy, and field buddy. These last two years would not have been same without you, that is for certain. I am so appreciative to Trevor Waldien, Dylan Vasey, and Elaine Young for the conversations I thought would be five minutes and ended up being hours long - thank you for diving into the complexities.

Finally, I'm grateful to my dog, McPhee, for getting me outside on a regular basis and to my parents for watching him when I couldn't. Forever thanks to Brian for spending his time listening to me talk about rocks rather than climbing them.

Table of Contents

ABSTRACT	ii
ACKNOWLEDGEMENTS	iii
TABLE OF CONTENTS	iv
LIST OF FIGURES	v
LIST OF TABLES	vi
I. INTRODUCTION	1
II. GEOLOGIC BACKGROUND	4
III. FIELD DESCRIPTIONS.....	13
IV. METHODS.....	25
V. RESULTS.....	27
VI. DISCUSSION.....	49
VII. CONCLUSION	68
REFERENCES	69
APPENDICES	73
A. Filtered U-Pb detrital zircon data from samples collected in the eastern Alaska Range...	73
B. Geologic sketch map of field locales in the eastern Alaska Range	73
C. U-Pb detrital zircon data from samples collected in the eastern Alaska Range	75

List of Figures

Figure 1: Terrane map of the northern Cordillera	3
Figure 2: Hillshade of southern Alaska showing major terrane boundaries.....	4
Figure 3: Geologic compilation map of eastern Alaska Range from the USGS with sample locales	13
Figure 4a – 4d: Field photographs of the rock assemblages in proximity to the Nenana Glacier.	17
Figure 5a – 5k: Field photographs of the rock assemblages adjacent to the Susitna Glacier....	20
Figure 6a – 6f: Field photographs of the rock assemblages in proximity to the Black Rapids Glacier	22
Figure 7a – 7j: Samples selected for detrital zircon analysis in each field area	24
Figure 8: Eastern AK Range U-Pb zircon ages	29
Figures 9a – 9e: Histogram, kernel density estimate plot, maximum depositional age, Age vs. U plot, and Age vs. U/Th plot for sample 15LT17	30
Figure 10a – 10f: Histogram, kernel density estimate plot, maximum depositional age, Age vs. U plot, and Age vs. U/Th plot for sample 21BG32.....	33
Figure 11a – 11e: Histogram, kernel density estimate plot, maximum depositional age, Age vs. U plot, and Age vs. U/Th plot for sample 10CH01b.....	36
Figure 12a – 12e: Histogram, kernel density estimate plot, maximum depositional age, Age vs. U plot, and Age vs. U/Th plot for sample 19CSR46.....	39
Figure 13a – 13f: Histogram, kernel density estimate plot, maximum depositional age, Age vs. U plot, and Age vs. U/Th plot for sample 15LT03	42
Figure 14a – 14e: Histogram, kernel density estimate plot, maximum depositional age, Age vs. U plot, and Age vs. U/Th plot for sample 21BG24.....	45
Figure 15a – 15d: Histogram, kernel density estimate plot, maximum depositional age, Age vs. U plot, and Age vs. U/Th plot for sample 21BG08.....	48
Figure 16: Geologic map of the eastern Alaska Range	51
Figure 17: Example of a cross-plot of the KDE for two samples	53

Figure 18: Kernel density estimate plots (red curves) and histograms (blue bars) for detrital zircon U-Pb data for all six of our samples	55
Figure 19: Kernel density estimate plots of all samples with highlighted age ranges of dominant detrital zircon age populations from parautochthonous North America and the northern section of the Yukon-Tanana terrane	59
Figure 20: Kernel density estimate plots of all samples with highlighted age ranges of dominant detrital zircon age populations from the Endicott Arm of southeast Yukon-Tanana....	60
Figure 21: Kernel density estimate plots of all samples with highlighted age ranges of dominant detrital zircon age populations from the Alexander Terrane	62
Figure 22: Kernel density estimate plots of all samples with highlighted age ranges of dominant detrital zircon age populations from the Windy-McKinley Terrane	63
Figure 23: Kernel density estimate plots of all samples with highlighted age ranges of dominant detrital zircon age populations from the Wrangellia Terrane	64
Figure 24: Kernel density estimate plots of all samples with highlighted age ranges of dominant detrital zircon age populations from unit TRcs	65
Figure 25: Simplified terrane map of the northern Cordillera.....	68
Figure 26: Simplified geologic map of the eastern Alaska Range showing sample locations relative to the Hines Creek fault and Nenana Glacier fault.....	68
Appendix	
Figure B1: Overview map for figures B2 and B3	59
Figure B2: Geologic sketch of the eastern Alaska Range in proximity of the Nenana Glacier	60
Figure B3: Geologic sketch of the eastern Alaska Range in proximity of the Susitna Glacier.....	60

List of Tables

Table 1: Summary of sample name, locale (Figure 16), and maximum depositional age	28
Table 2: Comparisons between all seven of our samples using the cross-correlation coefficient	56
Table 3: Summary of Potential Detrital Zircon Sources	57

I. Introduction

The western North American Cordillera was built primarily from continental fragments, island arcs, and ocean basin terranes that accreted to the margin of North America (Laurentia) throughout the Phanerozoic (Figure 1; Colpron et al., 2007; Dickinson, 2004). Located in the northernmost part of the Cordillera, the crust of southern Alaska grew from collision of the Wrangellia island arc against the North American margin (Colpron et al., 2007). The late Jurassic to late Cretaceous oblique collision of Wrangellia closed the intervening marine basins (Figure 2; Ridgway et al., 2002).

The Denali fault lies approximately along this Mesozoic collisional boundary, truncating the Alaska Range suture zone and juxtaposing the Wrangellia composite terrane against the North American margin. The Denali fault is a major intra-continental dextral strike slip fault that has accommodated 480 km of displacement since 52 Ma (Waldien et al., 2021b). The large-scale northward translation of crust accommodated along the Denali fault drastically rearranged the North American margin in the Cretaceous (Lanphere, 1978).

The onset of Yakutat microplate collision at ca. 30-25 Ma resulted in transpressional deformation along the Denali fault system and triggered exhumation in the eastern Alaska Range (Haeussler, 2008; Benowitz et al., 2011). On the north side of the Denali fault in the eastern Alaska Range, low-temperature thermochronology data define a zone of sustained exhumation. This exhumation has been occurring in an extremely focused region approximately 20 km long and 5 km wide since 25 Ma (Benowitz et al., 2014). $^{40}\text{Ar}/^{39}\text{Ar}$ cooling ages of biotite and muscovite suggest a minimum of 11 km of exhumation since 24 Ma (Benowitz et al., 2014). Strikingly, rocks south of the Denali fault at the same longitude have only experienced about 5 km of exhumation since the Oligocene (Benowitz et al., 2011). This exhumation has resulted in

exposure of greenschist to amphibolite facies rocks in the eastern Alaska Range. The deformation accommodating this exhumation north of the Denali fault is accommodated by shortening perpendicular to the Denali fault, indicating the rocks have been exhumed vertically with very little lateral translation for at least 24 million years (Tait, 2017; Benowitz et al., 2014). There is no consensus about the location of the original boundary between the North American margin in the Mesozoic and the Wrangellia composite terrane within the highly deformed Alaska Range suture zone. The motivation behind my study is to provide better constraints on the location of the original suture and determine where this suture zone is in relation to the region of localized exhumation. To this end, the goal of this study is to determine the depositional history and provenance of the rocks located within the region of localized exhumation. Determining if the depositional history of these rocks is related to the Wrangellia composite terrane or the ancestral North American margin has very different implications about the location of the original suture zone between Wrangellia composite terrane and North America. If these rocks are related to the Wrangellia composite terrane, this indicates the original suture zone between Wrangellia and North America is in between the Denali fault and the Hines Creek fault; whereas if these rocks are related to the ancestral North American margin, this indicates the original suture zone is located south of the Denali fault.

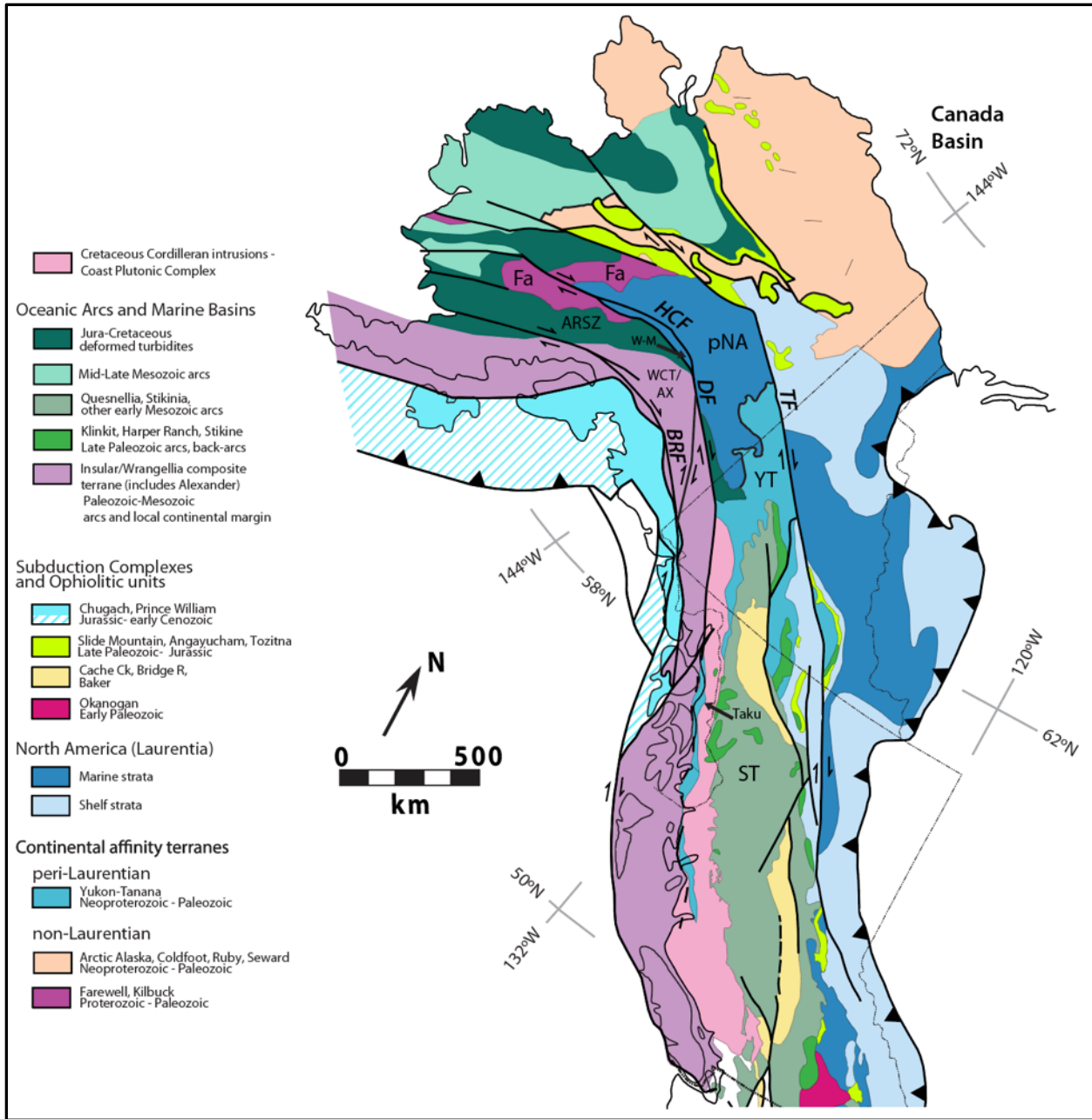


Figure 1: Terrane map of the northern half of the North American Cordillera. Modified from Busby et al., 2023. Inset depicts terranes grouped by tectonic setting. Note the dark blue and light blue terranes depict marine and shelf strata of the ancestral North American margin. ARSZ: Alaska Range Suture Zone; BRF – Border Ranges Fault; Ck – creek; DF – Denali fault; Fa – Farewell; HCF – Hines Creek fault; pNA – paraautochthonous North America; R – river; ST – Stikinia; Taku – Taku terrane (included within Yukon-Tanana terrane); TF – Tintina fault; YT – Yukon-Tanana; W-M – Windy-McKinley (included within paraautochthonous North America); WCT/AX – Wrangellia composite Terrane (includes Alexander).

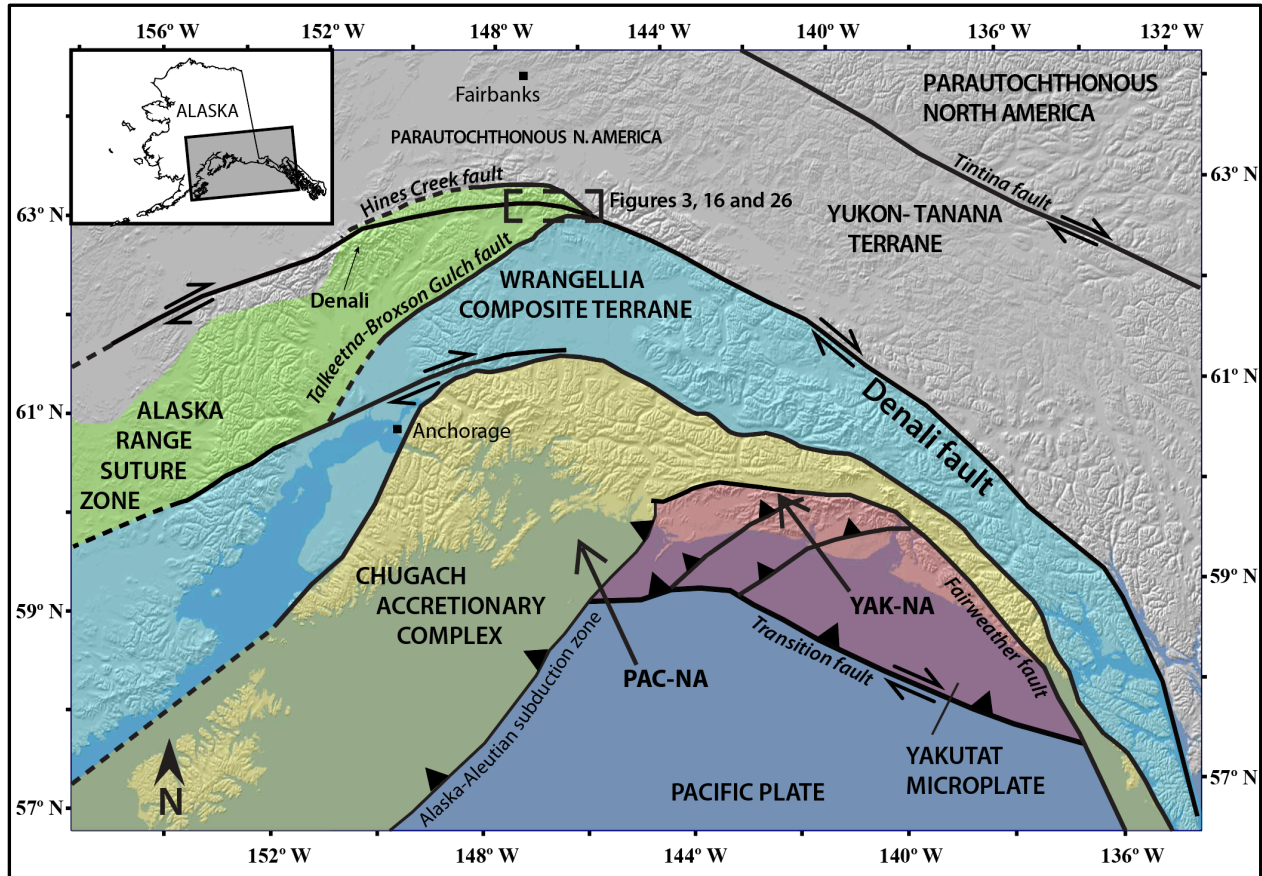


Figure 2: Hillshaded topography of southern Alaska showing major terrane boundaries. Modified from Waldien et al., 2018). The Alaska Range Suture Zone is bound by the Hines Creek fault to the north and the Talkeetna-Broxson Gulch fault to the south. Significant crustal deformation in southern Alaska is caused by flat-slab subduction of the Yakutat microplate. Rate of Yakutat plate motion relative to North America (YAK-NA) is from Elliot et al., 2010. Rate of Pacific plate motion relative to North America (PAC-NA) is from Plattner et al., 2007. The outline of our study area is indicated by the dashed black rectangle. The location of Figures 3, 16 and 26 is indicated by the dashed black rectangle.

II. Geologic Background

Previous mapping in the eastern Alaska Range

The crust of central Alaska is comprised of multiple terranes that were translated along the margin by extensive Cenozoic strike-slip faulting along the Denali fault (Colpron et al., 2007). As a result of this process and despite considerable mapping efforts, there are multiple fault-bounded slivers in the eastern Alaska Range of unknown origin. Consequently, little is

known about the basic rock assemblages, depositional history, and terrane affiliation of the rocks in this region. My field area is located on the boundary between two 1:250,000 quadrangles: the Healy quadrangle to the west (Csejtey et al., 1992), and the Mt. Hayes quadrangle to the east (Nokleberg et al., 1992). Large disparities exist between exiting geologic maps of the two quadrangles, as the Healy quadrangle was mapped according to lithologic units whereas the Mt. Hayes quadrangle was mapped according to terrane affiliation.

Original mapping of the Mt. Hayes quadrangle in the eastern Alaska Range focused on a suite of narrow terranes lying along the northern side of the Denali fault including the Windy, Pingston, McKinley, and Aurora Peak terranes (Nokleberg and Richter, 2007). The Windy, Pingston, and McKinley terranes are Paleozoic and Mesozoic continental margin strata that are related to North America (Nokleberg and Richter, 2007). Where my field site lies within the Mt. Hayes quadrangle, it is mapped as the Aurora Peak terrane, a distinct unit lying between the Hines Creek fault and Denali fault. The Aurora Peak terrane is a predominantly metasedimentary unit with a wide range of rock types: calcareous schist, quartz mica schist, marble, and metavolcanic rock (Brewer, 1982; Nokleberg and Richter, 2007). Age constraints of the metasedimentary rocks are Silurian to Triassic based on conodont fragments (Nokleberg and Richter, 2007).

Potential correlative terranes along strike

Considering the slip history of the Denali fault and the fact that my study area lies within one kilometer of the fault at all field locales, correlative terranes may be located a considerable distance away due to strike-slip displacement. For example, extensive sinistral Mesozoic strike slip faulting along the margin translated parts of the Yukon-Tanana terrane over ~1000 km south (Gehrels et al., 2009). For this reason, I will consider not only terranes located in the immediate

vicinity of my field area in south-central Alaska, but also terranes that extend into southwest Yukon, southeast Alaska and northwestern British Columbia (Pecha et al., 2016).

The terranes in the northern Cordillera can be grouped into two broad categories: those local or semi-related to the ancestral North American (Laurentian) margin and those terranes exotic to the margin (Colpron et al., 2007). When referring to the ancestral North American passive margin, many use the term parautochthonous North America (pNA). In addition to the Laurentia – affinity rock units, I will consider exotic terranes, including the Wrangellia terrane, the Alexander terrane, and the Farewell terrane (Figure 1). For brevity, I will omit the word ‘terranne’ from the following descriptions.

Yukon-Tanana and parautochthonous North America

Yukon-Tanana is considered separate from parautochthonous North America because it is a rifted fragment of the continental margin of Laurentia. However, the literature not infrequently groups Yukon-Tanana with the ancestral North American margin (Figure 1). Yukon-Tanana is an extensive peri-cratonic arc fragment that rifted from the North American margin in the Mississippian. Yukon-Tanana rejoined the parautochthonous North American margin as an intervening ocean basin (Slide Mountain and related assemblages) progressively closed in Permian to early Triassic time (Nelson and Gehrels, 2007).

The northern section of Yukon-Tanana shares more characteristics with parautochthonous North America than the southern portion of Yukon-Tanana. Specific similarities between parautochthonous North America and Yukon-Tanana include the Snowcap assemblage, the oldest basement unit in Yukon-Tanana (Nelson and Gehrels 2007). The Snowcap assemblage is a package of primarily siliciclastic rocks of continental margin affinity intruded by Devonian-Mississippian plutons (Colpron et al., 2006; Nelson and Gehrels, 2007).

The southern section of Yukon-Tanana found in southeast Alaska is comprised of the Endicott Arm assemblage, the Port Houghton assemblage, and the Tracy Arm assemblage. The pre-Devonian (mainly Neoproterozoic to early Paleozoic) Tracy Arm assemblage is interpreted to have been deposited on a shallow passive margin and is intruded by Silurian and Devonian plutons that yield ages of 440 – 360 Ma (Pecha et al., 2016). The Silurian-Devonian Endicott Arm assemblage is composed of a magmatic arc composed of metavolcanic rocks intruded by intermediate plutonic rocks. The Endicott Arm yields distinct populations of Precambrian U-Pb zircon ages with peaks at 2694 Ma, 1732 Ma, 1620 Ma, 1485 Ma and 1444 Ma (Pecha et al., 2016). The Mississippian-Pennsylvanian Port Houghton assemblage is characterized by quartz-rich turbidites interbedded with metavolcanics and subordinate marble overlying a basal metaconglomerate (Pecha et al., 2016). Each assemblage yields distinct U-Pb ages. The basal conglomerate yields U-Pb detrital zircon ages from 390 – 325 Ma with one group of Precambrian grains from 2030 – 1730 Ma (Pecha et al., 2016). The U-Pb detrital zircon ages from the overlying sedimentary and metavolcanic assemblage yields a bimodal Paleozoic age distribution from 455 – 345 Ma and a Precambrian group from 670 – 530 Ma (Pecha et al., 2016).

The detrital zircon age distributions show an affinity between Yukon-Tanana assemblages and paraautochthonous North America assemblages with similar peaks at 2800 – 2600 Ma and 2100 – 1800 Ma (Dusel-Bacon et al., 2017; Nelson and Gehrels, 2007). Similarly, most pNA and Yukon-Tanana age distributions share scattered peaks from 1500 – 1000 Ma (Nelson and Gehrels, 2007). Most samples from paraautochthonous North America lack ages in the 1600 – 1500 Ma age range, the “North American magmatic gap” (Dusel-Bacon et al., 2017). Both pNA and Yukon-Tanana are dominated by Devonian-Early Mississippian igneous events

with plutons in the 350 – 370 Ma age range (Dusel-Bacon et al., 2017; Pecha et al., 2016). Unique to Yukon-Tanana are Pennsylvanian to Permian magmatic events (Dusel-Bacon et al., 2017). Yukon-Tanana is intruded by Triassic to Jurassic plutons that also intrude Stikinia (Dusel-Bacon et al., 2017).

Stikinia

Stikinia is a Paleozoic to Mesozoic arc terrane composed of volcanic and volcaniclastic assemblages that has a complex accretionary history within the northern Cordillera (George et al., 2021). Stikinia is located in southeast Alaska and British Columbia, east of Wrangellia and Alexander, and directly adjacent to Yukon Tanana (Figure 1). Common detrital zircon age populations within Stikinia include 250 – 160 Ma, with minor populations at 340 – 290 Ma and small Precambrian sub-populations (George et al., 2021). Stikinia is intruded by Late Triassic to Early Jurassic plutons that it shares with Yukon-Tanana (Colpron et al., 2007).

Windy-McKinley

The Windy-McKinley is located in the Yukon to the north of the Denali fault and is frequently included within parautochthonous North America (Figure 1). The Windy-McKinley is composed of three subdivisions. One assemblage is composed of fine-grained, calcareous metaclastic rocks that are intruded by a Middle Triassic gabbro (Murphy, 2006). A second assemblage is composed of quartz-rich, calcareous metasediments, granite, and schist. The third is an ophiolitic assemblage of gabbro, chert, greenstone, and serpentinized dunite and harzburgite (Murphy, 2006). U-Pb isotopic analysis of zircon from a gabbro intrusion yielded a crystallization age of Late Triassic (229 Ma) (Murphy, 2006). Detrital zircon U-Pb analyses yield an age distribution with peaks at 600 – 400 Ma, 1300 – 900 Ma, 2000 – 1500 Ma, and 2800 – 2500 Ma (Murphy, 2006).

Taku terrane

The Taku occurs in southeast Alaska between the inboard Yukon-Tanana and Stikinia terranes and the outboard Wrangellia and Alexander terranes (Figure 1). The Carboniferous through Triassic Taku terrane is composed of carbonate, volcanic, and marine sedimentary rocks (Geisler et al., 2016). Detrital zircon ages reported from metasediments within the Taku terrane have abundant grains from 362 – 376 Ma and subpeaks at 435, 290, and 261 (Geisler et al., 2016). The oldest unit of the Taku terrane is the Carboniferous through Permian Windham Group which consists of volcaniclastics with 387 – 369 Ma detrital zircons (Geisler et al., 2016).

Unit TRcs of the central Alaska Range

The unit TRcs (a Triassic calcareous sedimentary unit) is found on many regional maps of central Alaska (Figure 3). TRcs is upper Triassic to Jurassic marine calcareous sedimentary unit that was deposited on the northwestern margin of Laurentia (Till et al., 2007). The age of unit TRcs is constrained by conodonts found in several locations in the central Alaska Range (Till et al., 2007). Detrital zircon populations found within unit TRcs include dominant populations between 458 – 240 Ma and 676 – 463 Ma, and subordinate population peaks at 2725 Ma, 2060 Ma, 1885 Ma, 1764 Ma, 1672 Ma, 1491 Ma, and 1050 Ma (Keough et al., 2021). The detrital zircon population between 700 – 500 Ma is relatively uncommon in rocks of Yukon-Tanana and parautochthonous North America and suggests recycling of sediment from Caledonian and Baltic sources (Keough et al., 2021). Devonian to Mississippian detrital zircon grains are likely sourced from the plutonic suite of the same age intruding Yukon-Tanana (Keough et al., 2021). Based on common conodont occurrences, some workers speculate that TRcs of the central Alaska Range may be related to upper Triassic marine strata associated with the Slide Mountain complex (Till et al., 2007). Others have made the case that TRcs is related to

the Farewell terrane due to detrital zircon age population populations at 1600 – 1000 Ma and 488 – 416 Ma (Keough et al., 2021).

Wrangellia composite terrane

The Wrangellia composite terrane is comprised of the Wrangellia, Alexander, and Peninsular terranes (Figure 1). Wrangellia and Alexander have a shared history by middle Pennsylvanian time and were juxtaposed with the Peninsular terrane between Permian and Cretaceous time (Trop et al., 2002). This section will focus on the Wrangellia terrane.

The Wrangellia terrane is a dominantly mafic, Paleozoic to Mesozoic oceanic plateau-arc system consisting of Carboniferous arc-derived volcanic and volcaniclastic strata and Permian carbonate strata overlain by the Triassic Nikolai flood basalt (Nokleberg et al., 1985). In south-central Alaska, Wrangellia is predominately characterized by Late Paleozoic Skolai arc which forms the core of the Wrangellia terrane in south-central Alaska and is comprised of Carboniferous strata intruded by gabbro-diorite plutons and other silicic intrusions (Beard and Barker, 1989). The igneous intrusive units that are associated with the Carboniferous volcaniclastic strata yield U-Pb zircon ages of 315 – 301 Ma (Waldien et al., 2021a). Unconformably overlying the Carboniferous strata, the flood basalts yield ages of 230 – 225 Ma (Greene et al., 2010). One study focusing on the Wrangellia terrane in the region of south-central Alaska found age distributions that overwhelmingly yielded a single peak at ~310 Ma (Romero et al., 2020). Silicic intrusions within the Skolai arc have U-Pb zircon ages of 290 – 320 Ma (Beard and Barker, 1989).

Alexander Terrane

Alexander is a crustal fragment that likely evolved along a convergent plate margin from the Neoproterozoic through the Early Devonian, stretching from southeast Alaska to

northwestern British Columbia and consisting of a northern and southern portion with distinct histories (Figure 1; Gehrels and Saleeby, 1987). The northern portion of the terrane formed in proximity to a continental landmass and is comprised of primarily Paleozoic shelf facies strata while the southern portion of the terrane experienced arc-type magmatism (White et al., 2016). Arc-type volcanism and plutonism was widespread throughout the terrane from Early Ordovician to Silurian, producing abundant detrital zircon ages from 480 – 420 Ma (Gehrels et al., 1996).

The timing of magmatism varied across the terrane. Magmatism in the northern portion of the terrane started at 520 Ma and continued through 390 Ma, with most reported grains from 480 – 420 (White et al., 2016). In the southern part of the terrane magmatism started at 470 and ended at 400, with a peak of U-Pb zircon ages centered at ~441 Ma (White et al., 2016). In summary, Early Paleozoic (500 – 400 Ma) detrital zircon grains are common throughout the terrane. In the northern Cordillera, 500 – 400 Ma grains are relatively rare and point to the Alexander terrane as a potential source.

Southern Alexander is more likely to yield older grains, however the entire terrane shares Precambrian detrital zircon populations from 2050 – 1630 Ma, 1500 – 1310 Ma, and 1260 – 990 Ma (White et al., 2016). Alexander is not composed of any rocks older than 595 Ma, indicating the likely source of these grains was a nearby continental source at some point in the terrane's history (Gehrels et al., 1996). The southern part of the terrane also yields detrital zircon populations younger than 400 Ma. Upper Paleozoic and Triassic strata of the southern part of the terrane yield grain populations ~360 Ma and ~290 Ma (White et al., 2016).

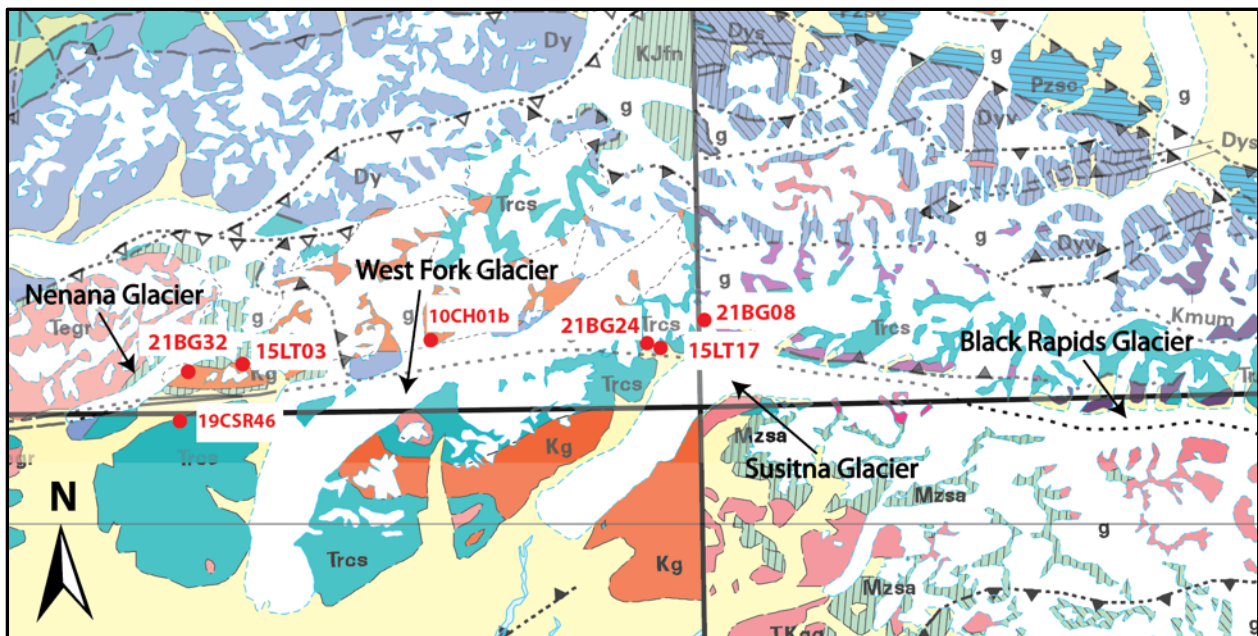
Farewell Terrane

The Farewell is located in western Alaska, inboard of the Wrangellia and Alexander terranes (Figure 1). The oldest exposed basement rocks of Farewell are within Paleoproterozoic

to Neoproterozoic metamorphic core complexes (Malkowski and Hampton, 2014). The youngest part of the Farewell terrane is the Mystic sub-terrane, a Devonian to Cretaceous unit composed of carbonate, siliciclastic, and volcanic rocks (Dumoulin et al., 2018). One study reports abundant detrital zircon U-Pb ages from the Mystic subterrane to be in the range of 419 – 359 Ma and 2000 – 1800 Ma (Dumoulin et al., 2018).

Ages of regional plutons

Regional plutonism is common in our immediate field area in the eastern Alaska Range. Known U-Pb zircon crystallization ages of plutons in the region include a pluton less than one kilometer away from the Nenana Glacier that is 67 Ma and three plutons within 2 kilometers of the Susitna Glacier that are 38.6, 63.2, and 97 Ma. All plutons are located north of the Denali fault (Benowitz et al., 2022). Due to the close proximity of these plutons to our sample locations, detrital zircons with these ages are potentially neo-crystalline grains or metamorphic grains.



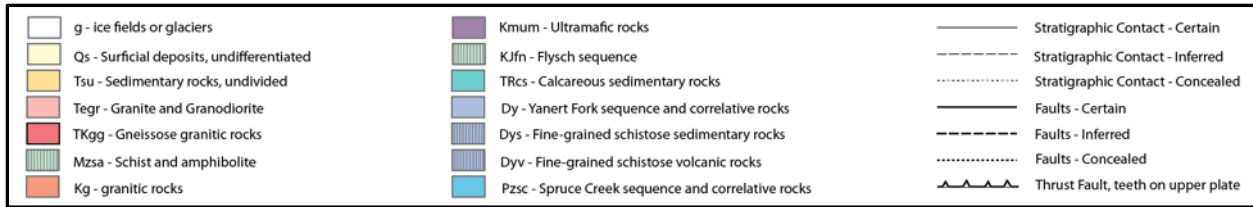


Figure 3: Geologic compilation map of eastern Alaska Range from the USGS (Wilson et al., 1998). Sample locales are depicted in red. Glaciers are labelled for reference.

III. Field Descriptions

Here I describe the rocks within my field area that I sampled to determine potential correlative terranes. The field area is divided into three locales. These locales are described in proximity to regional glaciers. Outcrops are typically exposed in small stream drainages perpendicular to the trace of the Denali fault. Mapping was limited due to ice cover and glacial deposit cover and was conducted based on a series of transects.

Rock assemblages between the Nenana Glacier and West Fork Glacier

The rock assemblages in between the Nenana Glacier and West Fork Glacier are primarily greenschist grade (Figure 3). In this locale the assemblage is relatively homogenous with abundant fine-grained biotite-muscovite schist and moderately foliated orthogneiss (Figure 4). The foliation strikes northwest and is steeply dipping to the northeast. Biotite-muscovite schists have compositional layering on the scale of millimeters (Figure 4A). Composition of biotite-muscovite schist does not vary in this region. The schist unit is fine-grained and has alternating dark biotite and muscovite-rich horizons and light quartz-rich horizons (Figures 4B and 4C). Orthogneiss is pervasively weathered throughout the outcrop (Figure 4D). For multiple samples from this region, thin section analysis revealed fabrics intensely altered by hydrothermal processes to the extent that identification of the primary protolith is difficult.

Rock assemblages between the West Fork Glacier and Susitna Glacier

The rock assemblages in the field locale in between the West Fork Glacier and the Susitna Glacier are upper amphibolite to granulite facies (Figure 3). In this locale the assemblage is characterized by foliated orthogneiss, foliated biotite-quartz schist and carbonate. The strike of the foliation in this locale is dominantly west/northwest, steeply dipping to the northeast and is highly consistent. The section is dominantly composed of biotite-quartz schist intermingled with orthogneiss on centimeter to meter scale (Figure 5A, 5B). Less common units include mafic, ultramafic, and calc-schist units.

The biotite-quartz schist unit, with varying amounts of hornblende and plagioclase, consistently displays a strong, planar fabric. Schist outcrops exhibited compositional layering on the scale of millimeters to tens of centimeters and is commonly banded blue, gray, white, and weathers rust red (Figure 5C). Locally the layers are tightly folded on millimeter to centimeter scale. Composition varies between quartz-rich horizons and finer-grained, biotite-rich horizons.

The gneiss unit is light to medium gray, with felsic layers rich in plagioclase and varying amounts of quartz, and mafic layers rich in biotite and plagioclase (Figure 5D). The gneiss exhibits strong flattening foliation and locally exhibits isoclinal folding. Color varies from white in color where it is felsic/leucocratic, and dark gray in color where it is intermediate to mafic in composition. Outcrops of gneiss are comprised of medium-grained groundmass consisting of biotite, plagioclase, and quartz, with rounded and elongate plagioclase feldspar porphyroclasts 1-10 millimeters long (Figure 5E).

Carbonate outcrops are massive and 5 to 15 meters thick. Locally, massive white carbonate grades into white with light gray bands. White and gray banded carbonate shows consistent foliation. Locally, carbonate is isoclinally folded on the scale of tens of centimeters

and is in contact with fine-grained biotite-quartz schist (Figure 5F). The massive carbonate sections are relatively pure with little quartz-feldspar component. Less abundant rock types include mafic and ultramafic bodies on the scale of 5 mm to 3 meters incorporated with carbonate and metasedimentary units (Figures 5G, 5H, 5I, 5J). Ultramafic bodies consist of pyroxene with lesser amounts olivine, the latter replaced by serpentine, and contains boudins rich in serpentine. Marble in proximity to ultramafic bodies is white and gray in color and tightly folded (Figure 5K).

Rock assemblages north of the Denali fault, adjacent to the Black Rapids Glacier

Approximately 38 km east along strike from the Susitna Glacier locales, in proximity to the Black Rapids Glacier, the rock assemblage is a highly variable greenschist-facies assemblage (Figure 3, Figure 6). The unit consists of abundant chert, outcrops of relatively pure marble with little quartzofeldspathic sediment incorporated, serpentinite, and greenschist. Greenschist outcrops are steeply dipping and composed of abundant chlorite and amphibole rich layers (Figure 6A, 6B). Chert outcrops are purple with centimeters to tens of centimeters thick bedding horizons (Figure 6C, 6D). Serpentinite outcrops are 10-15 meters thick, bright turquoise and dark green in color, and exhibit smooth faces (Figures 6E, 6F). Field work in this locale was limited to 6 hours where we covered an area of approximately 0.5 square kilometer.

Rocks targeted for detrital zircon sampling

Samples selected for detrital zircon analysis in each field area are shown in Figure 7. These samples are not necessarily representative of the entire rock assemblage at each field locale because sampling for detrital zircon necessarily meant targeting relatively quartz-rich metasedimentary rocks.

Samples collected during previous field seasons

I also analyzed samples collected from our research group during previous field seasons. Sample 19CSR46 is the only sample located south of the Denali fault (Figure 3). This sample is a slaty graphitic phyllite dominated by fine-grained chlorite-muscovite-quartz layers and minor quartz-rich layers. Sample 15LT03 is a quartz-plagioclase-biotite schist that is locally intruded by felsic orthogneiss and was collected in between the Nenana Glacier and West Fork Glacier (Figure 3). Sample 15LT17 is a very fine-grained quartz-plagioclase-biotite schist that was collected in proximity to the Susitna Glacier (Figure 3). Sample 10CH01b is a biotite-plagioclase-quartz schist that was collected in proximity to the West Fork Glacier (Figure 3).

Summary of the most abundant rock assemblages in each locale

The typical rock assemblages sampled between the Nenana Glacier and West Fork Glacier (the western locale in our field area) are homogenous fine-grained biotite-muscovite schist and moderately foliated orthogneiss. The units in this region are greenschist facies.

The most commonly sampled rock assemblages between the West Fork Glacier and the Susitna Glacier (the eastern locale in our field area) are foliated biotite-quartz schist and foliated orthogneiss, with less abundant carbonate and mafic units. The units in this region are primarily upper amphibolite to granulite facies.

The rock assemblages observed at the Black Rapids Glacier locale are low-grade and extremely variable with abundant chert, marble, serpentinite, and greenschist. Due to a lack of quartz-rich rocks in this locale, we did not sample any of these rock assemblages for detrital zircon dating.

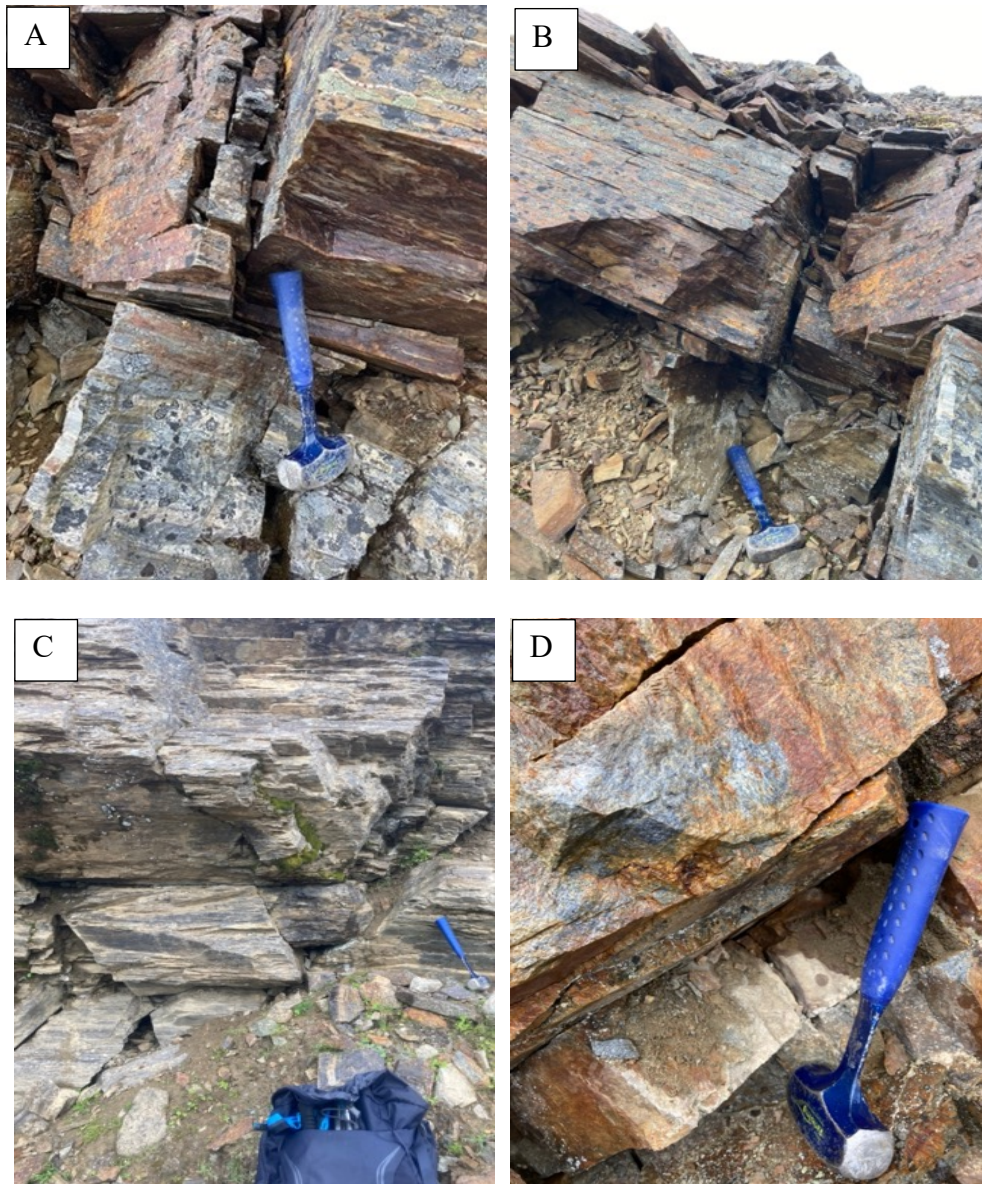


Figure 4: Field photographs of the rock assemblages in proximity to the Nenana Glacier. A) Compositional layering of biotite-quartz schist on the millimeter scale resulting in horizons of blue, white, gray, purple. B) Extremely fine-grained biotite-quartz schist. C) Fine-grained muscovite-biotite schist. D) Extremely altered orthogneiss weathering to a rusty red color.

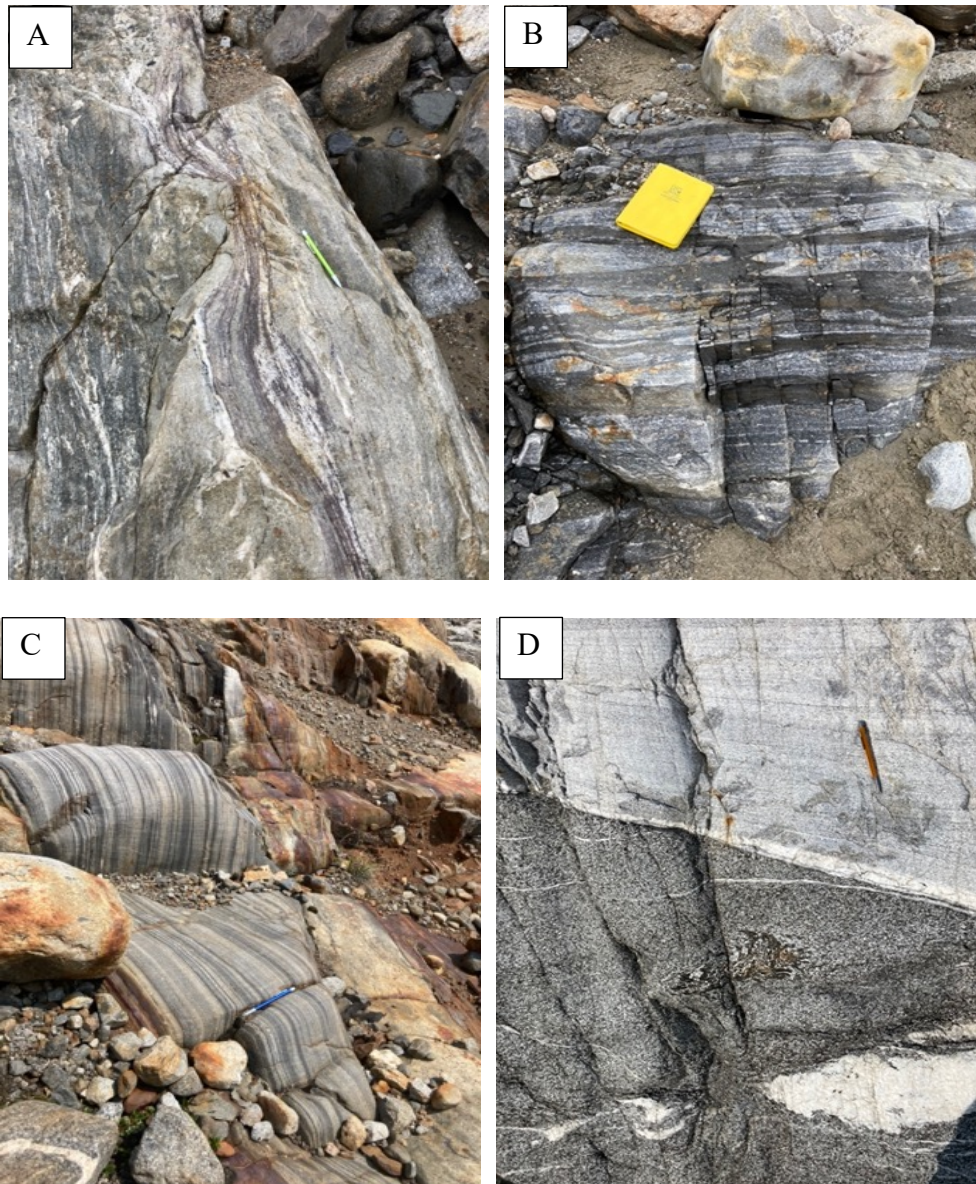


Figure 5

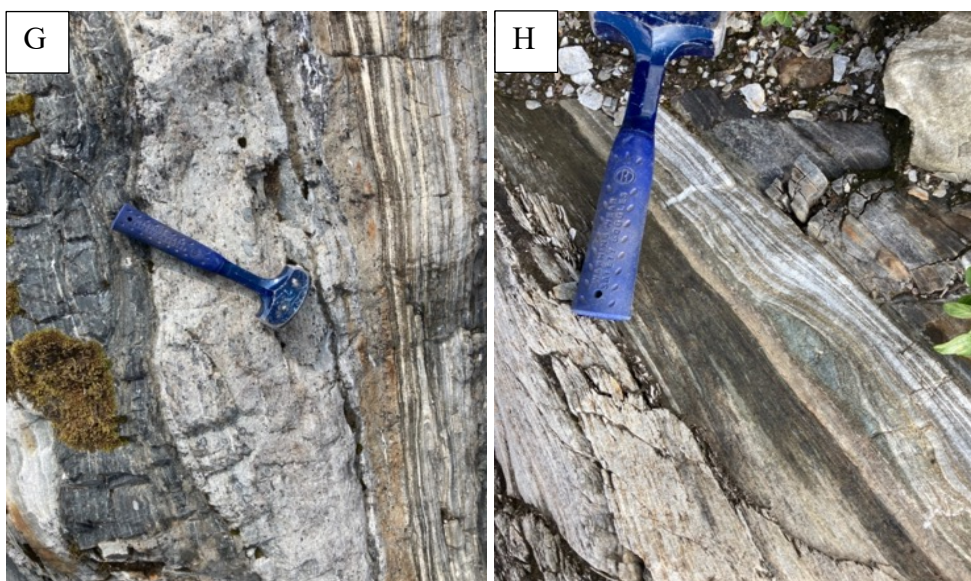


Figure 5

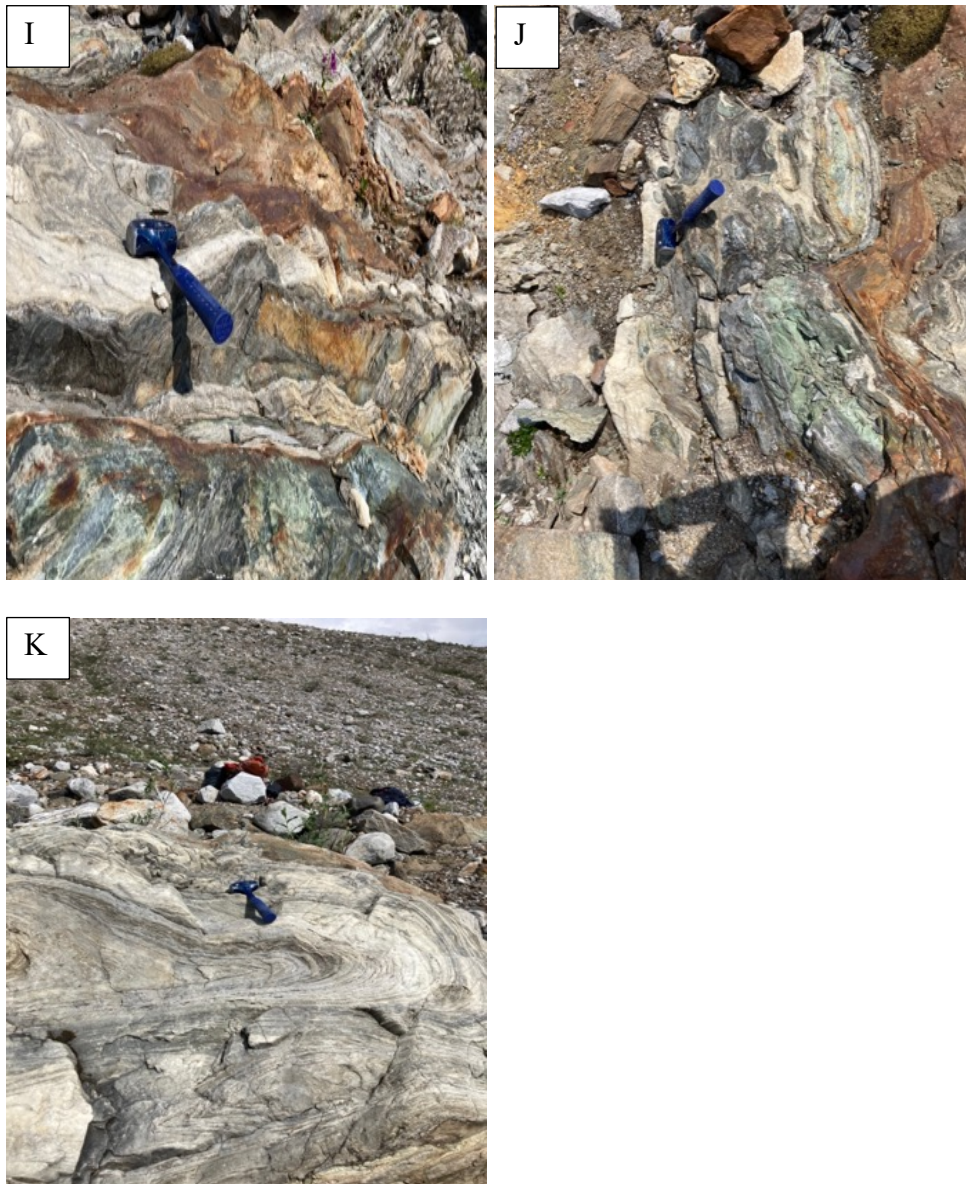


Figure 5: Field photographs of the rock assemblages adjacent to the Susitna Glacier. A) Strongly foliated intermediate orthogneiss and purple biotite-rich schist intermingling on a scale of centimeters. B) Orthogneiss intermingled with amphibole-rich schist on the scale of centimeters. C) typical outcrop of biotite-quartz schist. D) Typical orthogneiss with variable felsic and intermediate composition. E) Intermediate orthogneiss is locally mylonitic with rounded, flattened 3-5 centimeter feldspars, indicating grain-size reduction. F) Locally, carbonate unit is in contact with fine-grained biotite-quartz schist. G) Intermingling between ultramafic, carbonate, and metasedimentary units. H) Serpentine-rich boudins within ultramafic unit. I) The contact between the ultramafic body and carbonate is an irregular, wavy boundary with plastic deformation of both units. J) Margins of ultramafic body show evidence of hydrothermal alteration. K) Marble in proximity to ultramafic body is white and gray in color and is isoclinally folded on the scale of centimeters to meters.

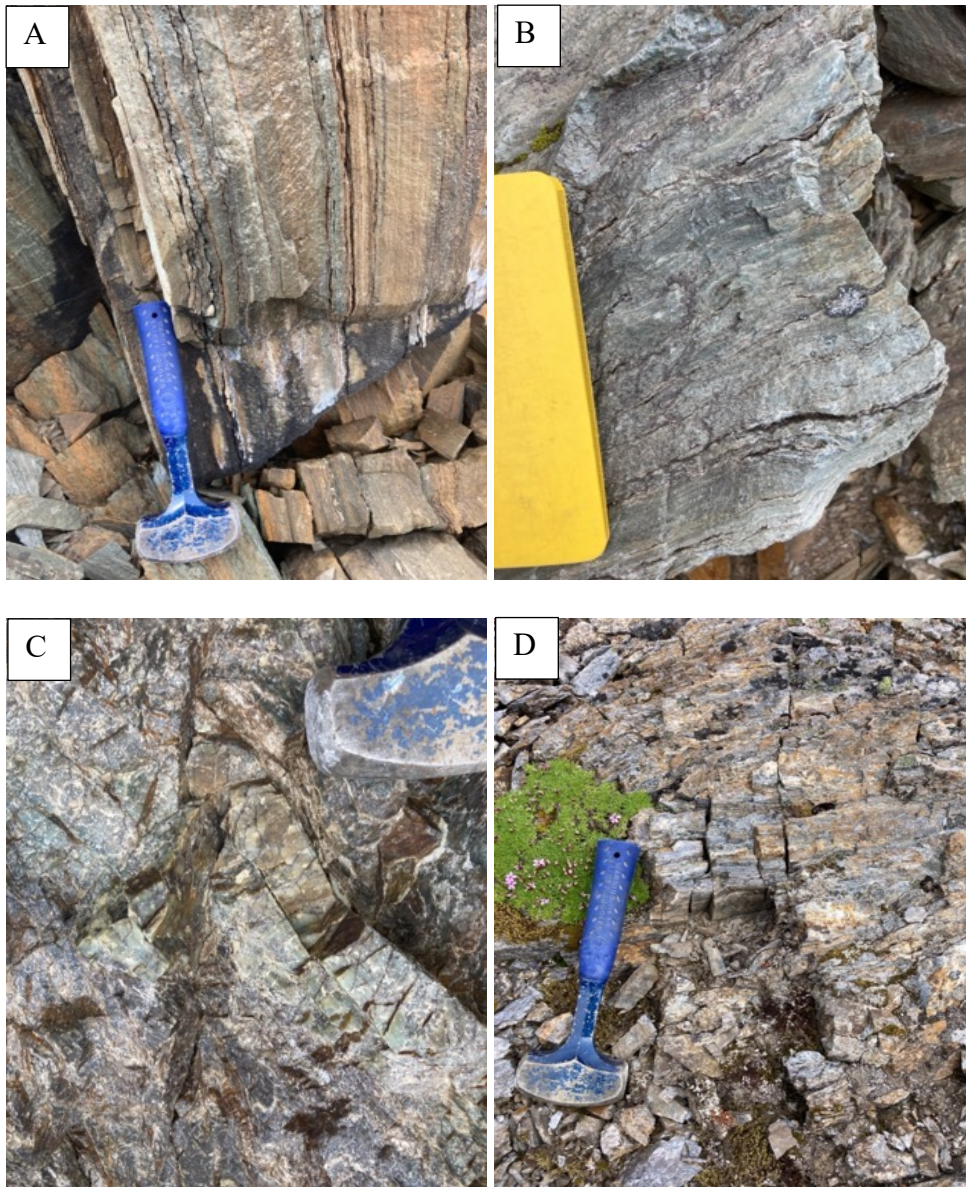


Figure 6

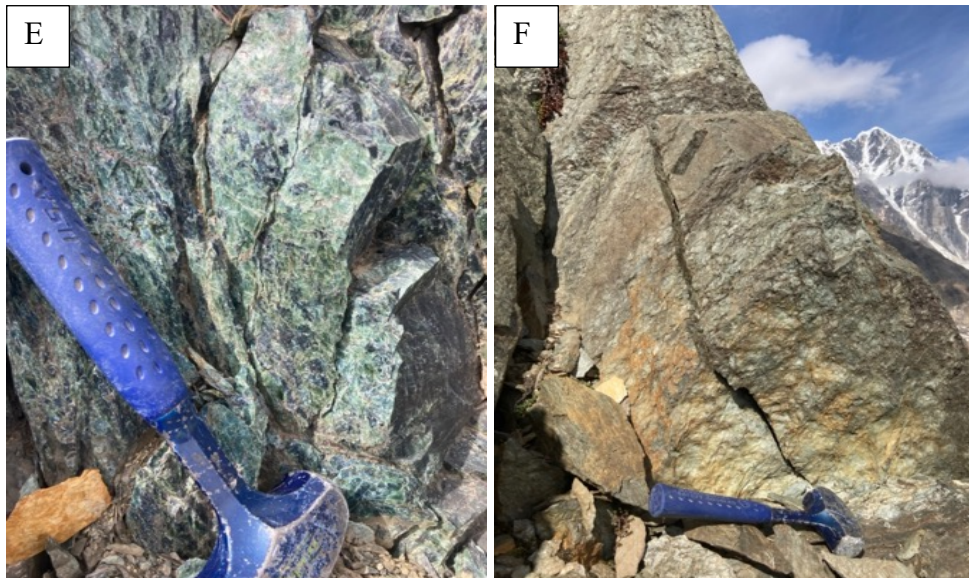


Figure 6: Field photographs of the rock assemblages in proximity to the Black Rapids Glacier. A, B) Outcrop of steeply dipping, chlorite and amphibole rich- greenschist with horizons of carbonate, 5 meters thick. C) Chert outcrop with original bedding horizons approximately 3 to 7 centimeters thick. D) Chert outcrops are purple and green with color variations throughout field region. Outcrops are typically 10 meters thick. E) Serpentinite outcrop, 10-15 meters thick. Serpentinite is bright turquoise and dark green and exhibits smooth faces. F) Mafic and ultramafic outcrop 10 meters thick that weathers to orange color.

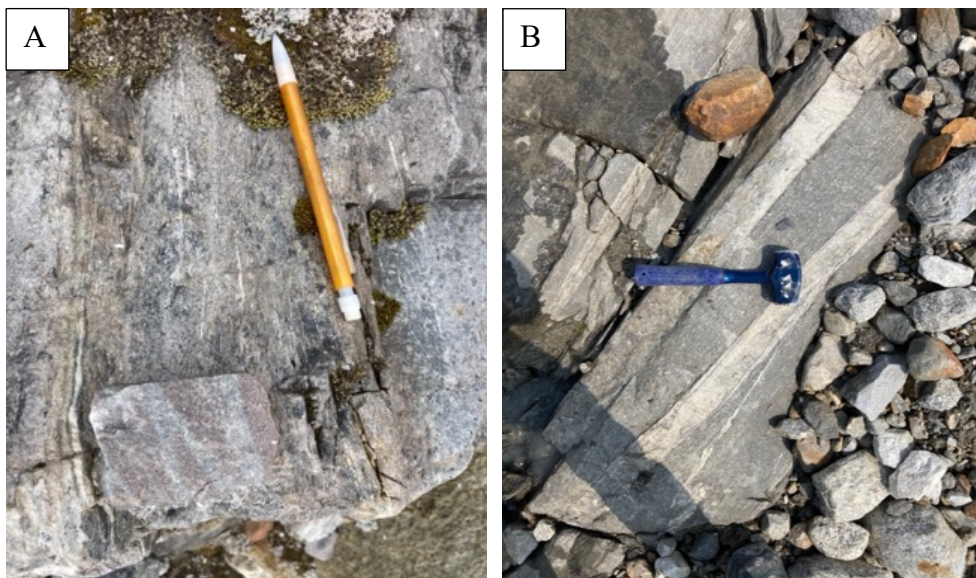


Figure 7



Figure 7

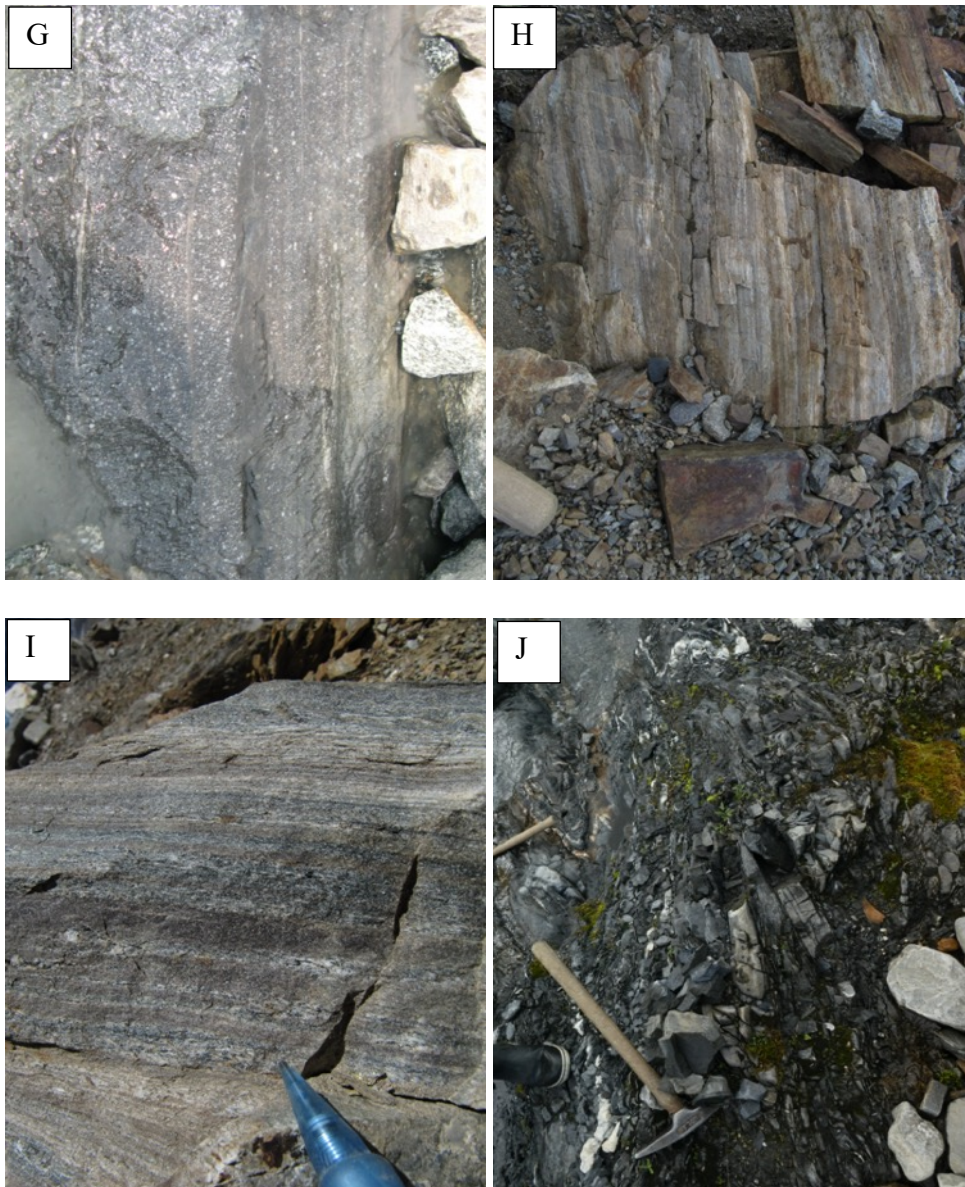


Figure 7: Samples selected for detrital zircon analysis in each field area. A) Sample 21BG24. Plagioclase-biotite-quartz schist. Schistose fabric defined by coarse quartz-rich horizons and finer-grained biotite-rich horizons. Horizons vary in thickness from millimeters to tens of centimeters. Millimeter scale bands of white and gray, weathers to rusty red color. B, C) Sample 21BG08. Clinopyroxene-amphibole-biotite schist. Schist is dark-gray, fine-grained, with schistose foliation defined by amphibole. Mineral assemblage is comprised primarily of clinopyroxene, amphibole, and plagioclase, with accessory minerals biotite, quartz, and epidote. D, E) Sample 21BG32. Biotite-muscovite-quartz schist. Fabric defined by biotite with bands of muscovite, and lesser amounts plagioclase. Locally horizons include lenses of partial melt. F) Detailed photograph of sample 10CH01b; G) Outcrop photograph of sample 10CH01b; H) Sample 15LT03; I) Detailed photograph of sample 15LT17; J) Outcrop photograph of sample 19CSR46

IV. Methods

Geologic mapping

I conducted mapping at 1:10,000 scale during the summer of 2021 (Appendix B). Access to the field area was provided by helicopter. All mapping is based on foot traverses conducted from a central base camp. Base maps used for field mapping were created from IFSAR Alaska digital terrain models. Sample locations were recorded using handheld GPS devices.

Detrital Zircon U-Pb Geochronology

Sample Preparation

At UC Davis, I prepared the detrital zircon samples for analysis by using standard crushing techniques. I used a mortar and pestle for the initial rock crushing stage, then used a disk mill to crush the sample into a grain size approximately 3 mm in width. I sieved the material using a top sieve to remove the fraction larger than 250 microns. With the remaining material smaller than 250 microns, I removed the magnetic particles with a hand magnet and washed the sample in a large beaker to remove dust. I then used a standard miner's gold pan to remove the less dense fraction. I used a Frantz isodynamic mineral separator to remove minerals that are magnetic at 1 amp. Finally, I used water-based Lithium Polytungstate heavy liquid with a density of 2.85 g/cm³ to further separate zircon from the rest of the mineral separate. The remaining mineral separate was further concentrated by pouring the sample onto a glass slide and picking out non-zircon material using an optical microscope.

All samples were crushed, panned, and sieved at UC Davis using the methods outlined below. Samples 21BG08 and 15LT17 were prepared for analysis at UC Davis by pouring zircon and other heavy mineral grains onto double-stick tape containing zircon reference standards. A 1" round epoxy mount is cured, polished, and imaged using the Cameca SX-100 electron

microprobe at UC Davis. Back-scatter electron images were taken to create maps of the mounts to identify zircon grains.

Samples 21BG32, 21BG24, and 21BG14 were sent to Arizona LaserChron Center for mineral separation using conventional mineral separation processes as outlined in Gehrels et al., 2008. 21BG14 was not used in our analyses because there were not enough detrital zircon grains in the sample. Samples were prepared for analyses by pouring onto a 1" epoxy mount, and polished to 1 micron finish. Back-scatter electron images were taken using a Hitachi 3400N SEM.

U-Pb Geochronologic Analysis

U-Pb analyses were conducted in the LA-ICP-MS laboratory at the University of Arizona LaserChron Center. U-Pb analyses were conducted using laser ablation-inductively coupled plasma mass spectrometry (LA-ICP-MS) using the Thermo Element2 High Resolution ICPMS. Analyses from samples 21BG08 and 15LT17 were conducted using a 15- μm spot diameter size. Analyses from samples 21BG32, 21BG24, 10CH01b, 15LT03, and 19CSR46 were conducted using a 20- μm spot diameter size. Samples 15LT03 and 19CSR46 were analyzed using the Thermo Element2 High Resolution ICPMS in February of 2020.

Initial data reduction and filtering using a 10% discordance filter was completed using AgeCalcML, the standard protocol of the Arizona Laserchron Center (Sundell et al., 2021). The samples analyzed for this study experienced greenschist to upper amphibolite grade metamorphism and consequently the zircon may have undergone metamorphic recrystallization and lead loss (Appendix A). To account for this possibility, I filtered the data to remove U-Pb ages according to the following criteria: Uranium content higher than 5,000 ppm, U-Pb ages that were above a 3% error, and U/Th ratios greater than 10 (Appendix C).

After filtering for suspect metamorphic and newly crystallized igneous grains from the youngest age population, I used Isoplot R (Vermeesch, 2018) to calculate the maximum depositional age (MDA) for each sample using the weighted mean of the youngest cluster of three or more grains that overlap with 2σ uncertainty and have an MSWD of 1 or less. The reported ages are based on $^{206}\text{Pb}/^{238}\text{U}$ ages for grains <1.0 Ga and the $^{206}\text{Pb}/^{207}\text{Pb}$ ages for grains >1.0 Ga (Gehrels et al., 2006).

An important phenomenon to note is that every sample analyzed has zircons with ages younger than the MDA, but these ages did not fail any of the filter criteria. Two possible explanations for these ages are: 1) these ages are geologically meaningful, and our method of calculating the MDA makes them outliers; or 2) there is undetected Pb loss in these grains. In the results section below, I will refer to these ages as “outlier ages”.

It is possible some of these ages are metamorphic grains that experienced lead loss due to partial recrystallization during high-temperature metamorphism. For example, 15LT17 has three outlier grains younger than the MDA. However, these grains also have U/Th ratios of $\sim 7 - 9$, which is not enough to fail our filter criteria (U/Th ratio > 10) but is nonetheless significantly higher than the U/Th ratio of most ages. Other samples that contain these outlier grains do not have high U/Th ratios. One explanation for these grains is lead lost due to crystal plastic deformation at low temperatures creating fast-diffusion pathways or hydrothermal dissolution-reprecipitation (Schoene, 2014).

V. Results

Detrital zircon U-Pb age distributions from seven samples collected in the eastern Alaska Range are reported below (Table 1). Samples are arranged from the youngest maximum depositional age at the top to the oldest maximum depositional age at the bottom. The prevalence

of suspected metamorphic grains, grains affected by lead loss, and newly crystallized grains due to regional plutonism presented challenges when filtering our data. Grains from each data set were removed based on the filter criteria outlined in the methods section (Table 1). Additionally, neo-crystallized grains were identified based on the known distribution of U-Pb zircon ages of plutons in the immediate field area, where regional plutonism produced distinct populations at ~40 Ma, ~55-70 Ma, and ~95 Ma (Figure 8; Benowitz et al., 2022). Our U-Pb detrital zircon age distributions are presented as Kernel Density Estimates (KDE) using AgeCalcML data reduction software from the Arizona Laserchron Center.

Sample	MDA	Period	Locale		Detrital Zircon U-Pb population age peaks	N = total grains analyzed	N = total number of ages removed	N = filtered ages	Percent Paleozoic grains
			Lat.	Long.					
15LT17	246.08 +/- 3.79	Middle Triassic	63.528°	-147.055°	246, 420	108	9	99	99%
21BG32	259.8 +/- 2.23	Permian	63.513°	-147.643°	260, 297, 323, 376, 517, 1859	266	196	70	63%
10CH01b	275.15 +/- 1.79	Permian	63.534°	-147.342°	275, 387, 480, 990, 1400, 1620, 1728	142	7	135	48%
19CSR46	321.9 +/- 2.43	Early Pennsylvanian	63.492°	-147.652°	390, 576, 1052, 1450, 1667, 2714	286	9	277	20%
15LT03	326.84 +/- 2.43	Late Mississippian	63.518°	-147.568°	327, 405, 1854	71	46	25	50%
21BG24	362.95 +/- 3.42	Late Devonian	63.529°	-147.056°	363, 449, 1116, 1321, 1439, 1632, 1779	66	5	61	38%
21BG08			63.543°	-146.999°		114	112	2	50%

Table 1: Summary of sample name, locale, and maximum depositional age. Samples are arranged from youngest MDA at the top to the oldest MDA at the bottom. The total number of ages removed includes suspect metamorphic grains, neo-crystallization grains, grains with Uranium content > 5,000 ppm, or U-Pb ages > 3% error.

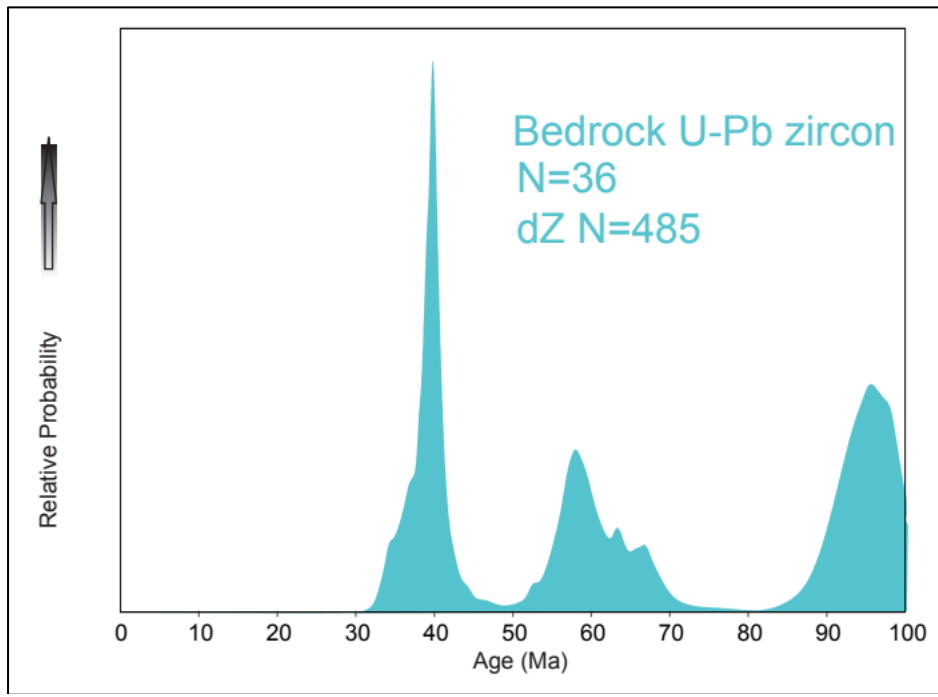


Figure 8: Eastern AK Range U-Pb zircon ages with distinct populations at 38.6 Ma, 63.2 Ma, and 97 Ma (Benowitz et al., 2022).

Sample 15LT17

Sample 15LT17 has a dominant age peak at 420 Ma (Figures 9a and 9b). Sample 15LT17 has a maximum depositional age of 246 Ma (early Triassic) (Figure 9c). No grains were removed due to high Uranium content (Figure 9d). One suspect metamorphic age was removed due to a high U/Th ratio (Figure 9e). Eight grains were removed because the ages had a percent error higher than 3%. Three outlier grains were removed. After removing these grains, the total number of grains analyzed for this sample is 99.

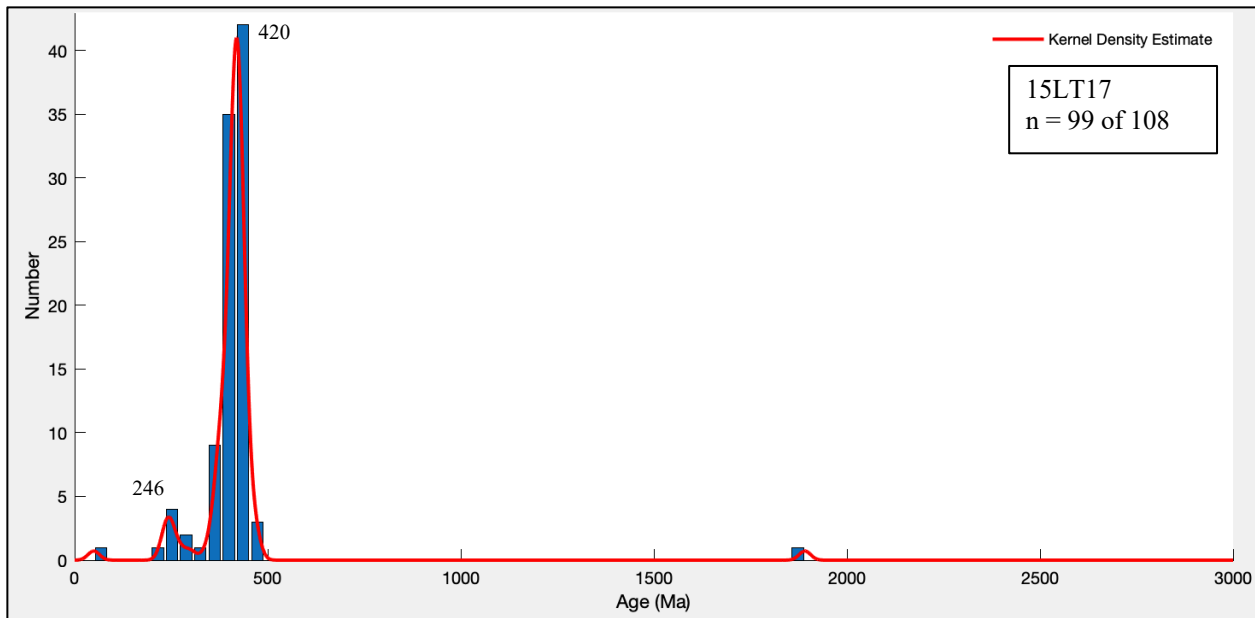


Figure 9a: Histogram and kernel density estimate (KDE) for sample 15LT17. Each histogram bin is approximately 35 million years. N is the number of analyses reported on the plot out of the total number of grains analyzed.

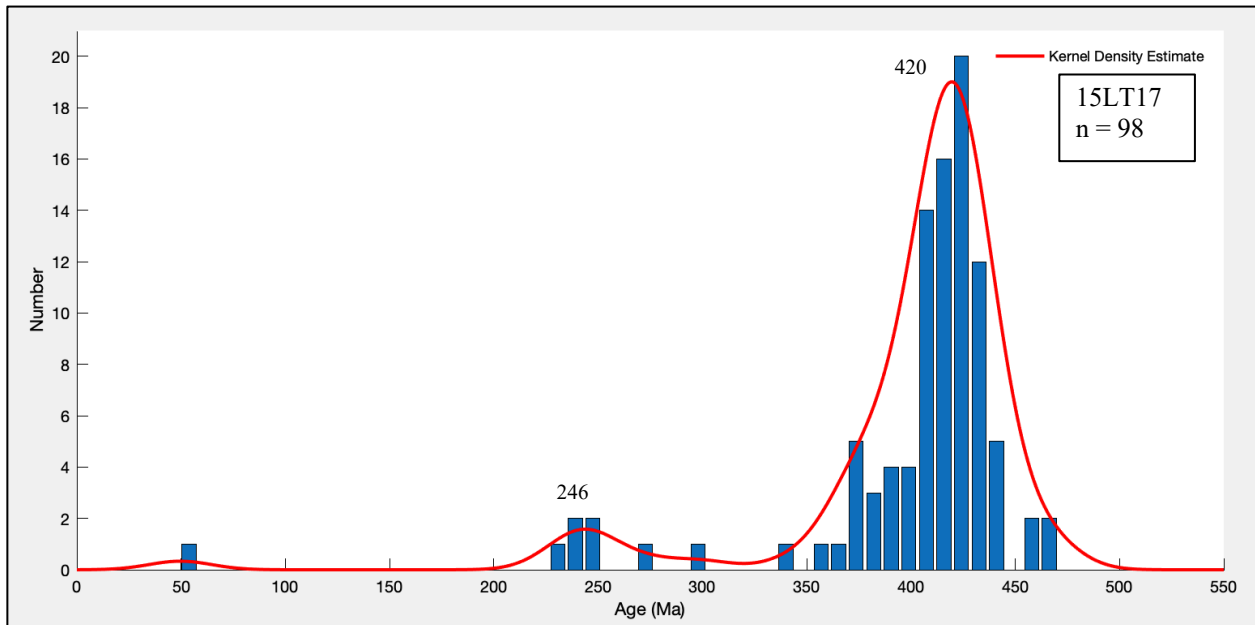


Figure 9b: Histogram and kernel density estimate (KDE) of the Paleozoic age distribution for sample 15LT17. Each histogram bin is approximately 10 million years. N is the number of analyses reported on the plot.

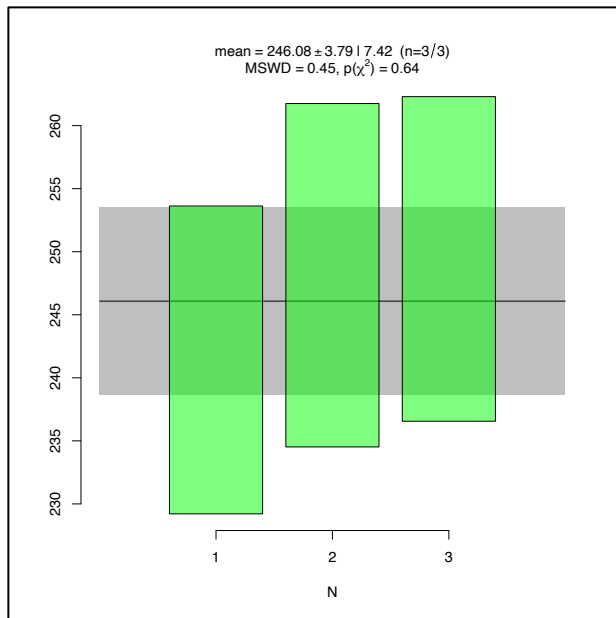


Figure 9c: Maximum depositional age of sample 15LT17 using the weighted mean of the youngest cluster of three or more grains that overlap with 2σ uncertainty.

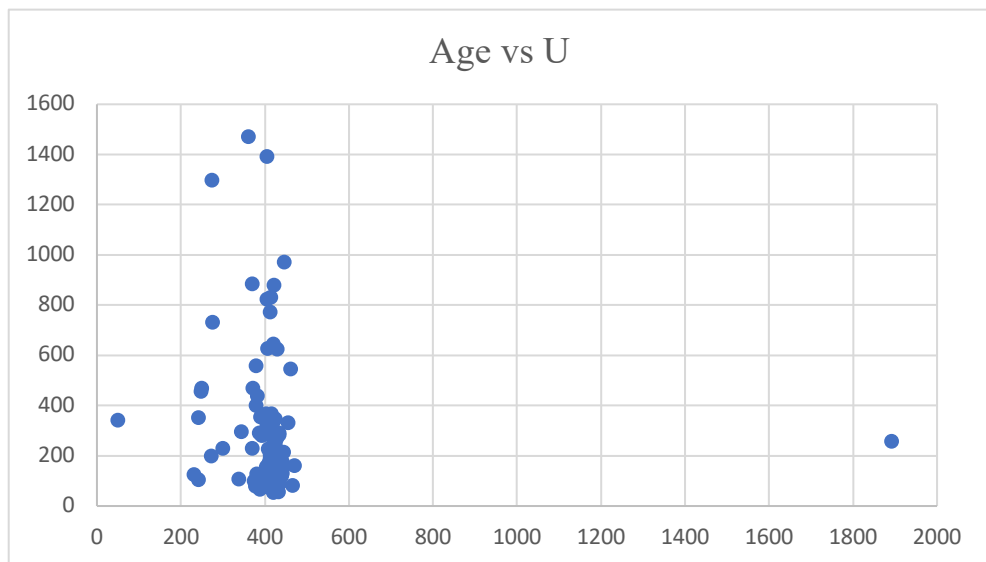


Figure 9d: Age vs. Uranium plot for sample 15LT17. No grains were removed due to high Uranium content.

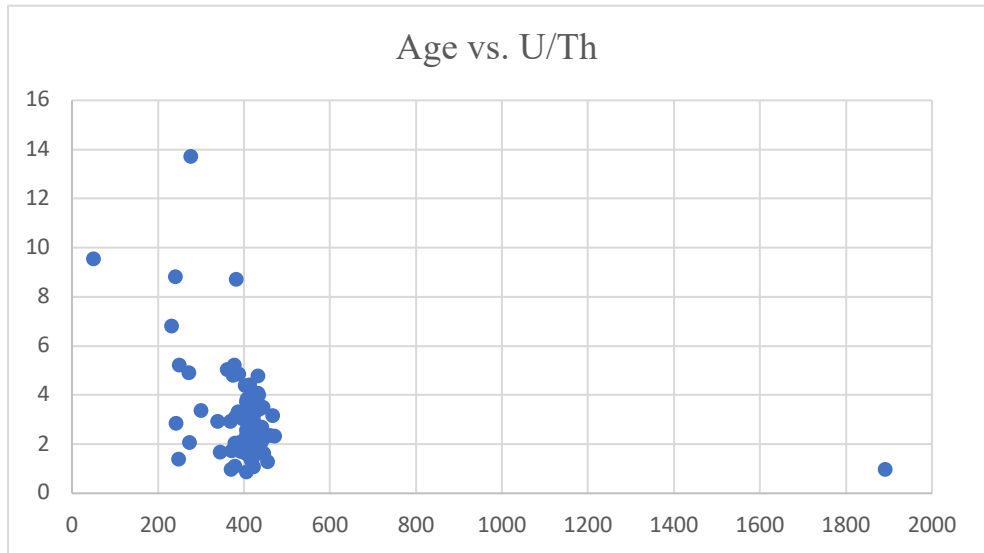


Figure 9e: Age vs. Uranium/Thorium plot for sample 15LT17. One grain was removed from our analysis due to a U/Th ratio greater than 10.

Sample 21BG32

Sample 21BG32 has a dominant peak at 323 Ma and a sub-peak at 1859 Ma (Figures 10a and 10b). 190 grains were removed from the analysis due to being newly crystallized grains whose ages are consistent with known ages of regional plutons (Figure 10c). Sample 21BG32 has a maximum depositional age of 260 Ma (late Permian) (Figure 10d). No grains were removed due to high uranium content and three suspect metamorphic ages were removed due to high U/Th ratios (Figures 10e and 10f). Three grains were removed because the ages had a percent error higher than 3%. Three outlier grains were removed. After removing these grains, the total number of grains analyzed for this sample is 70.

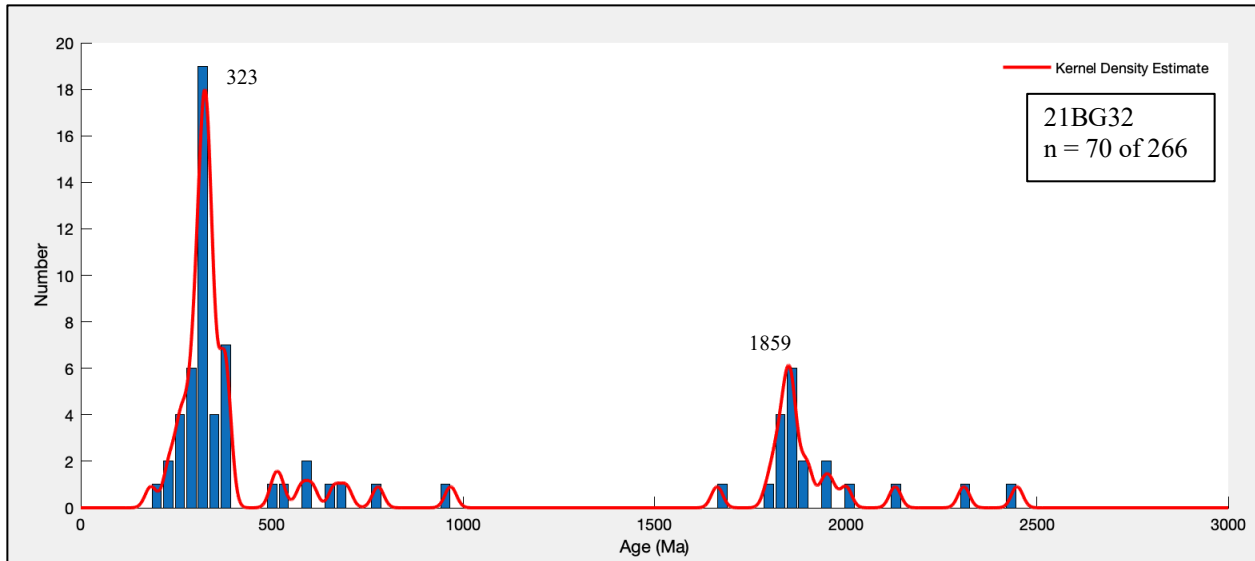


Figure 10a: KDE and cumulative density plot of sample 21BG32. Histogram and kernel density estimate (KDE) for sample 10CH01b. Each histogram bin is approximately 35 million years. N is the number of analyses reported on the plot out of the total number of grains analyzed.

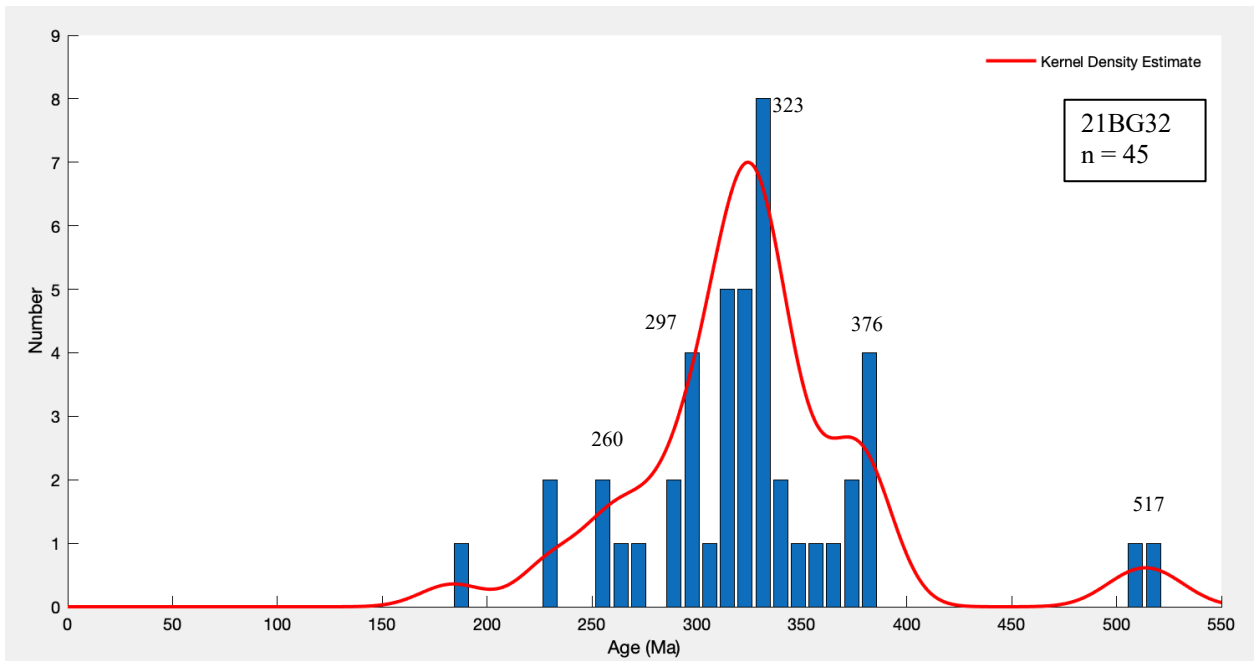


Figure 10b: Histogram and kernel density estimate (KDE) of the Paleozoic age distribution for sample 21BG32. Each histogram bin is approximately 10 million years. N is the number of analyses reported on the plot.

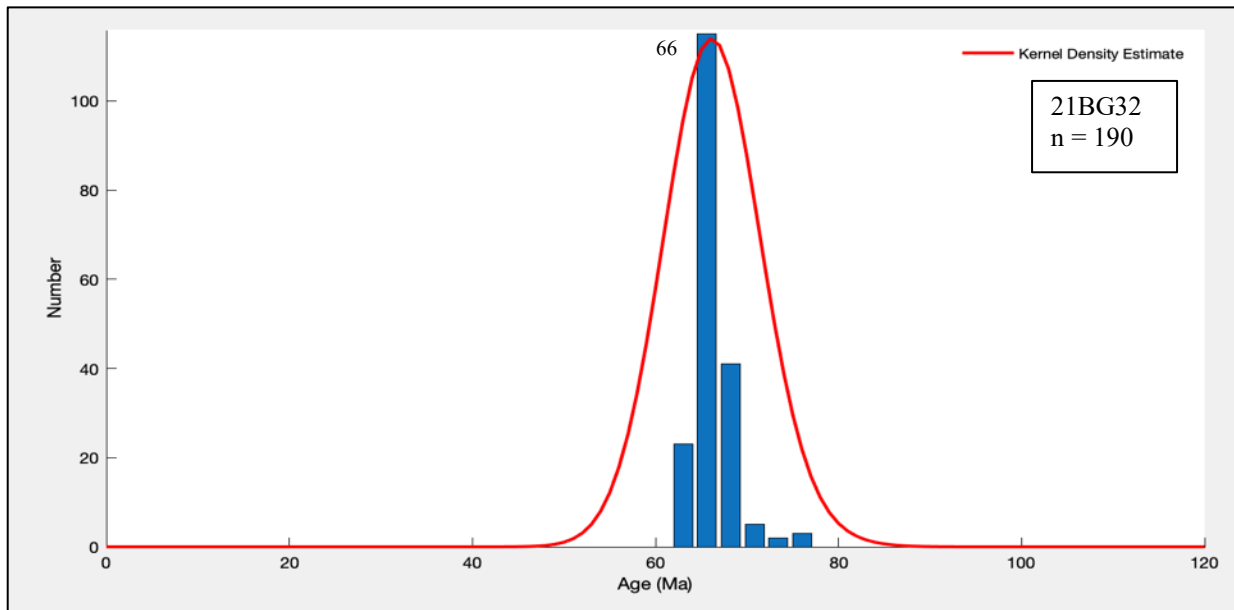


Figure 10c: Histogram and kernel density estimate (KDE) of all metamorphic and neo-crystallized grains younger than 130 Ma in sample 21BG32. These ages reflect the age range of regional plutons and the immediate proximity of orthogneiss dated at 66 Ma (Benowitz et al., 2022). Each histogram bin is approximately 10 million years. N is the number of analyses reported on the plot.

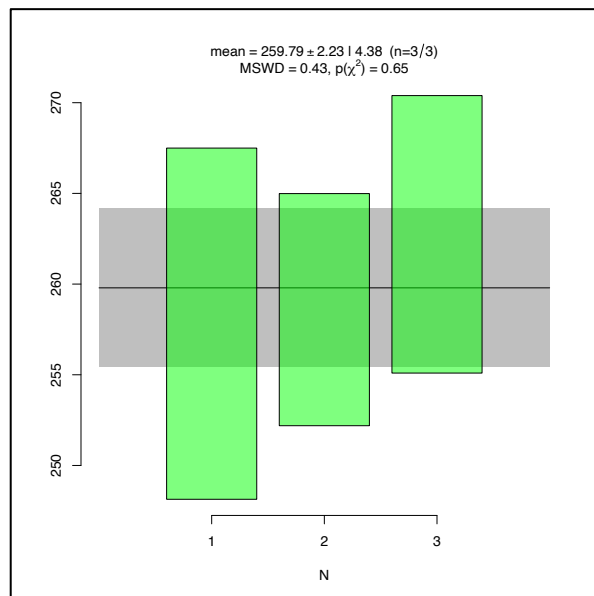


Figure 10d: Maximum depositional age of sample 21BG32 using the weighted mean of the youngest cluster of three or more grains that overlap with 2σ uncertainty.

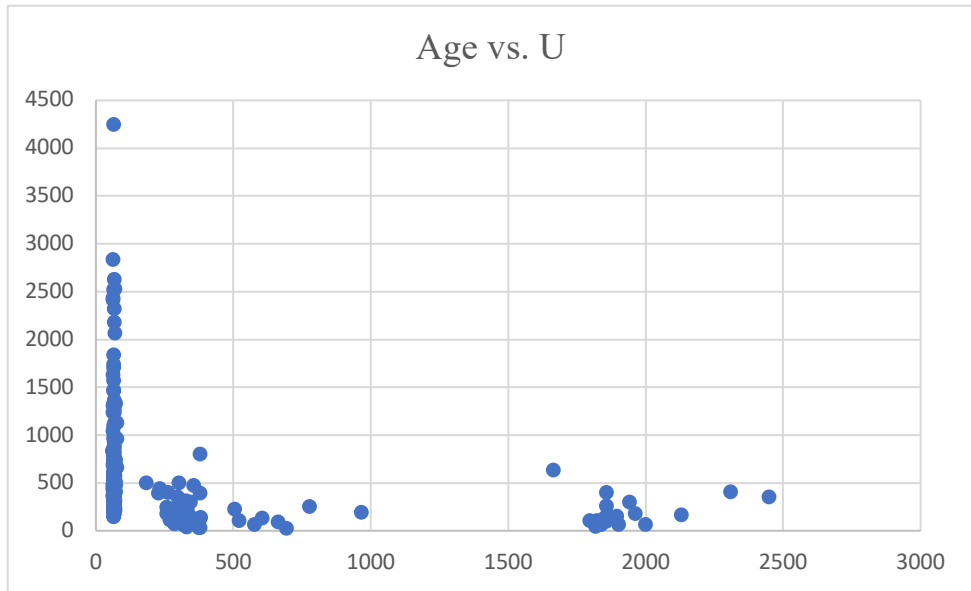


Figure 10e: Age vs. Uranium plot for sample 21BG32. No grains were removed due to high uranium content.

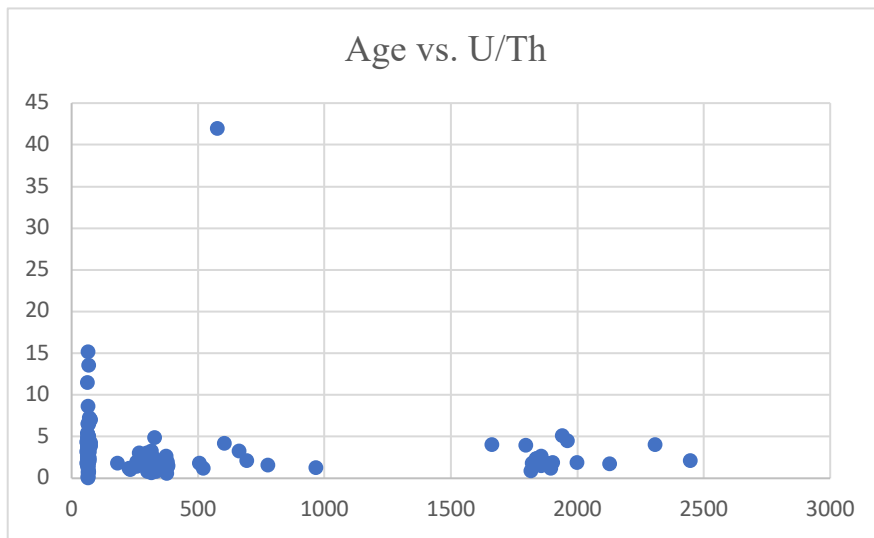


Figure 10f: Age vs. Uranium/Thorium plot for sample 21BG32. Three grains were removed from our analysis due to a U/Th ratio greater than 10.

Sample 10CH01b

Sample 10CH01b yields a dominant age peak at 387 Ma, 1620 Ma, and 1728 Ma, and sub-peaks at 1400 Ma, 990 Ma, and 289 Ma (Figures 11a and 11b). Sample 10CH01b has a maximum depositional age of 275 Ma (middle Permian) (Figure 11c). This sample also has small, scattered peaks from 2900 – 1800 Ma. No grains were removed due to high Uranium

content (Figure 11d). One suspect metamorphic age was removed due to a high U/Th ratio (Figure 11e) and 3 grains were removed due to neo-crystallization. Three grains were removed because the ages had a percent error higher than 3%. After removing these grains, the total number of grains analyzed for this sample is 135.

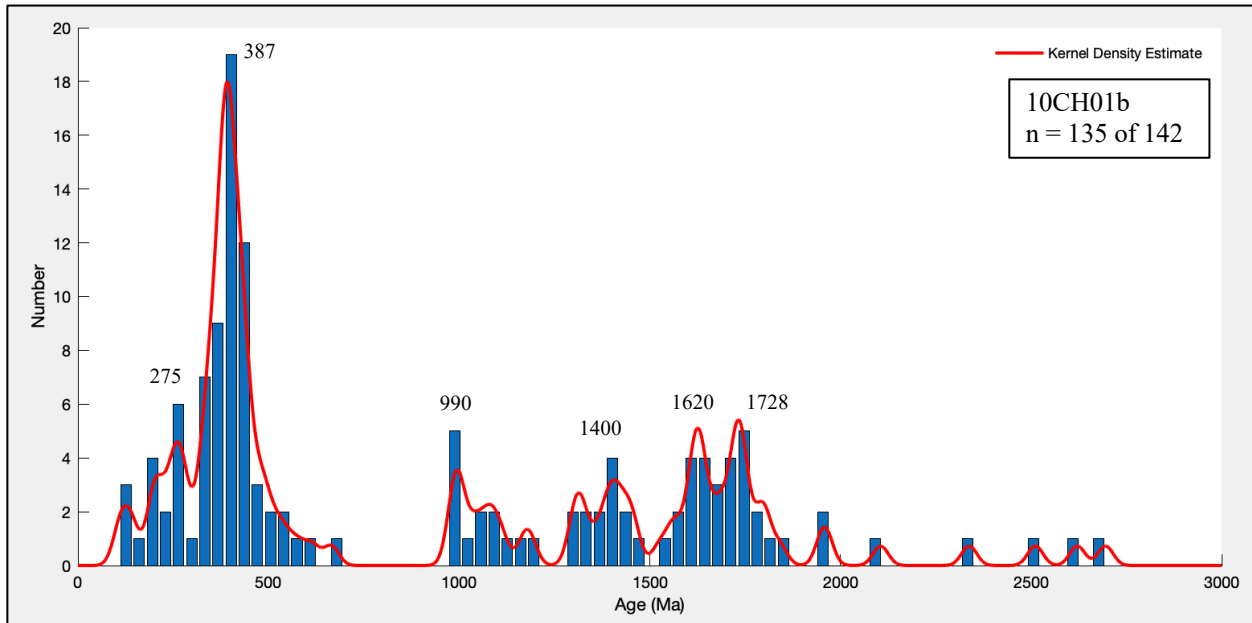


Figure 11a: KDE and cumulative density plot of sample 10CH01b. Histogram and kernel density estimate (KDE) for sample 10CH01b. Each histogram bin is approximately 35 million years. N is the number of analyses reported on the plot out of the total number of grains analyzed.

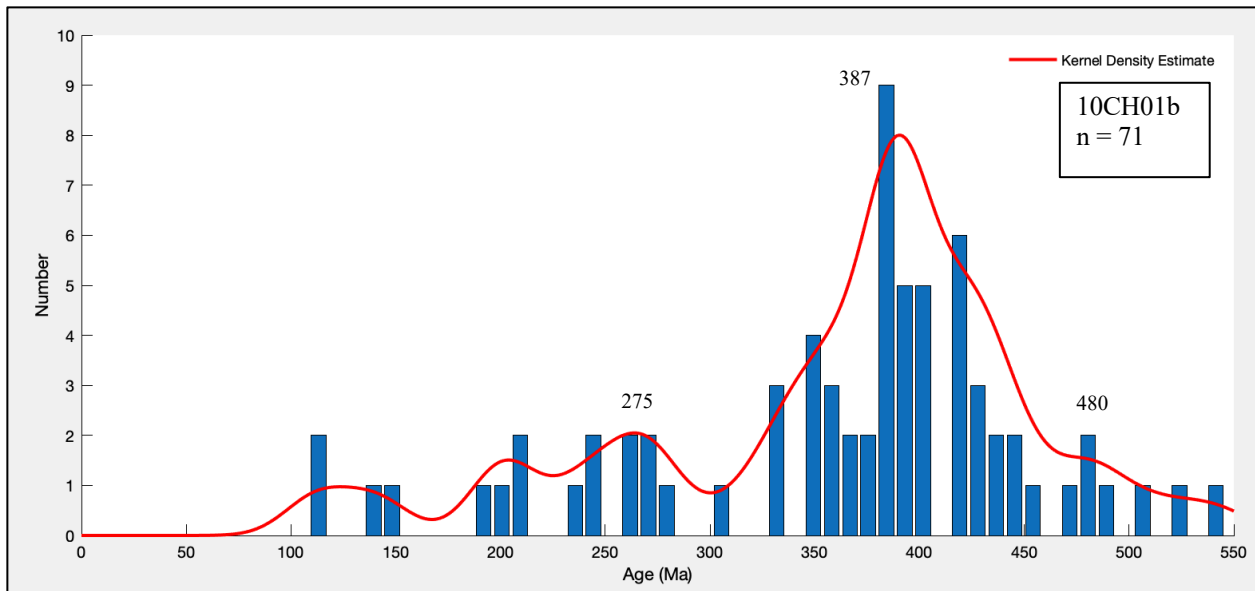


Figure 11b: Histogram and kernel density estimate (KDE) of the Paleozoic age distribution for sample 10CH01b. Each histogram bin is approximately 10 million years. N is the number of analyses reported on the plot.

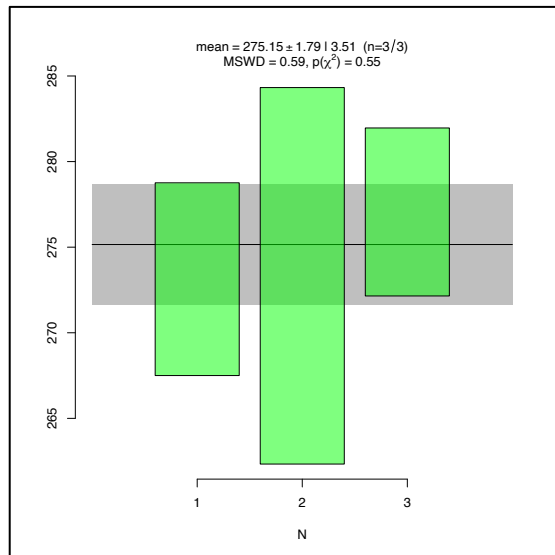


Figure 11c: Maximum depositional age of sample 10CH01b using the weighted mean of the youngest cluster of three or more grains that overlap with 2σ uncertainty.

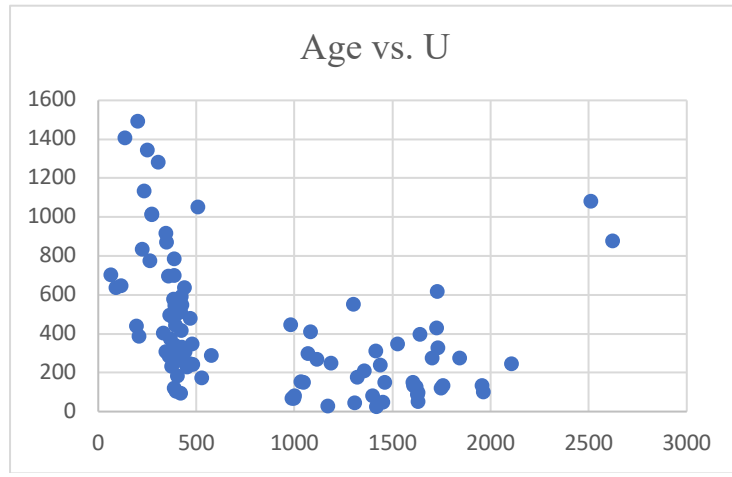


Figure 11d: Age vs. Uranium plot for sample 10CH01b. No grains were removed due to high uranium content.

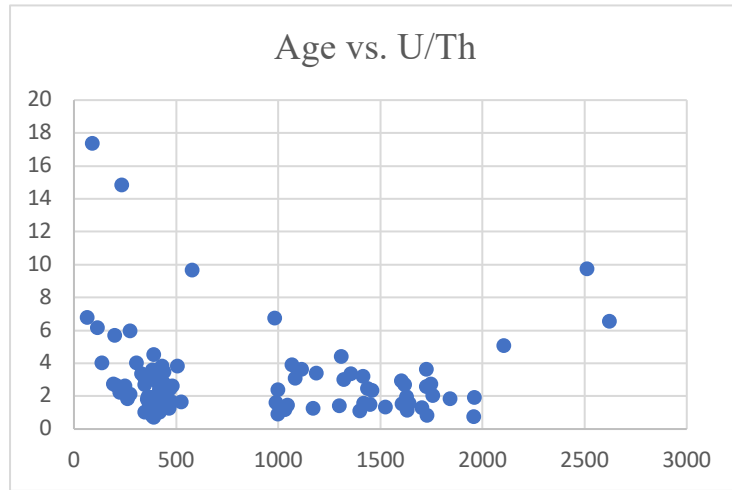


Figure 11e: Age vs. Uranium/Thorium plot for sample 10CH01b. One grain was removed from our analysis due to a U/Th ratio greater than 10.

Sample 19CSR46

Sample 19CSR46 has dominant peaks at 390 Ma, 576 Ma and 1052 Ma, and sub-peaks at 2714 Ma, 2021 Ma, 1886 Ma, 1760 Ma, 1667 Ma, and 1450 Ma (Figures 12a and 12b). Sample 19CSR46 has a maximum depositional age 321 Ma (late Mississippian) (Figure 12c). No grains were removed due to high Uranium content (Figure 12d). Nine suspect metamorphic ages were removed due to high U/Th ratios (Figure 12e). No grains were removed due to high Uranium content. After removing these grains, the total number of grains analyzed for this sample is 277.

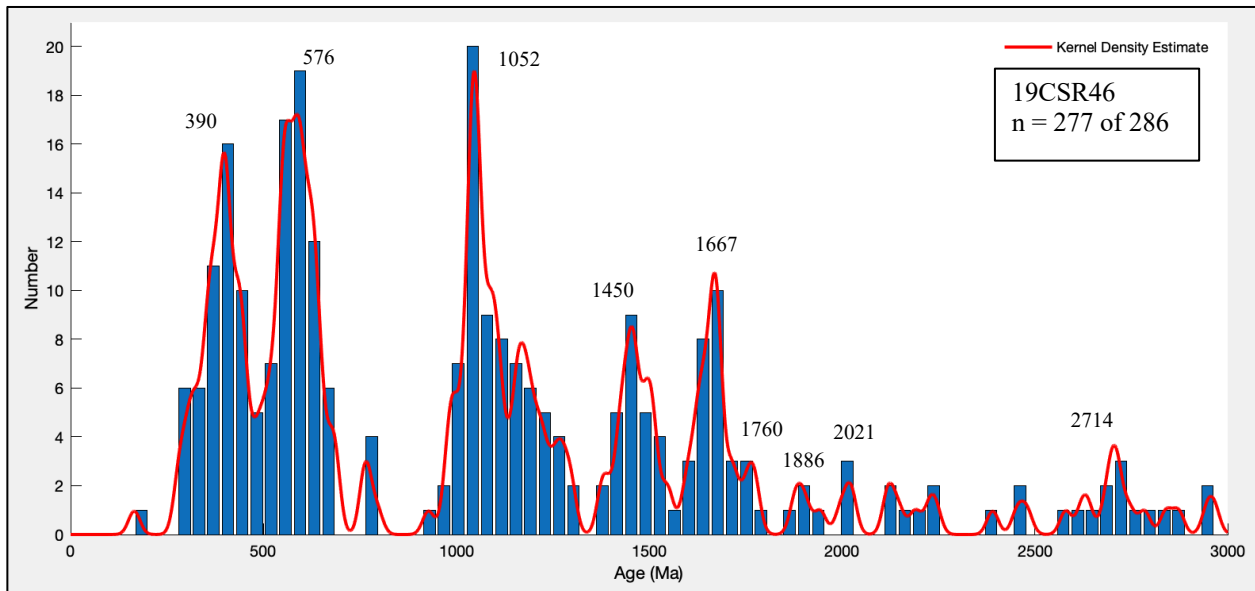


Figure 12a: Histogram and kernel density estimate (KDE) for sample 19CSR46. Each histogram bin is approximately 35 million years. N is the number of analyses reported on the plot out of the total number of grains analyzed.

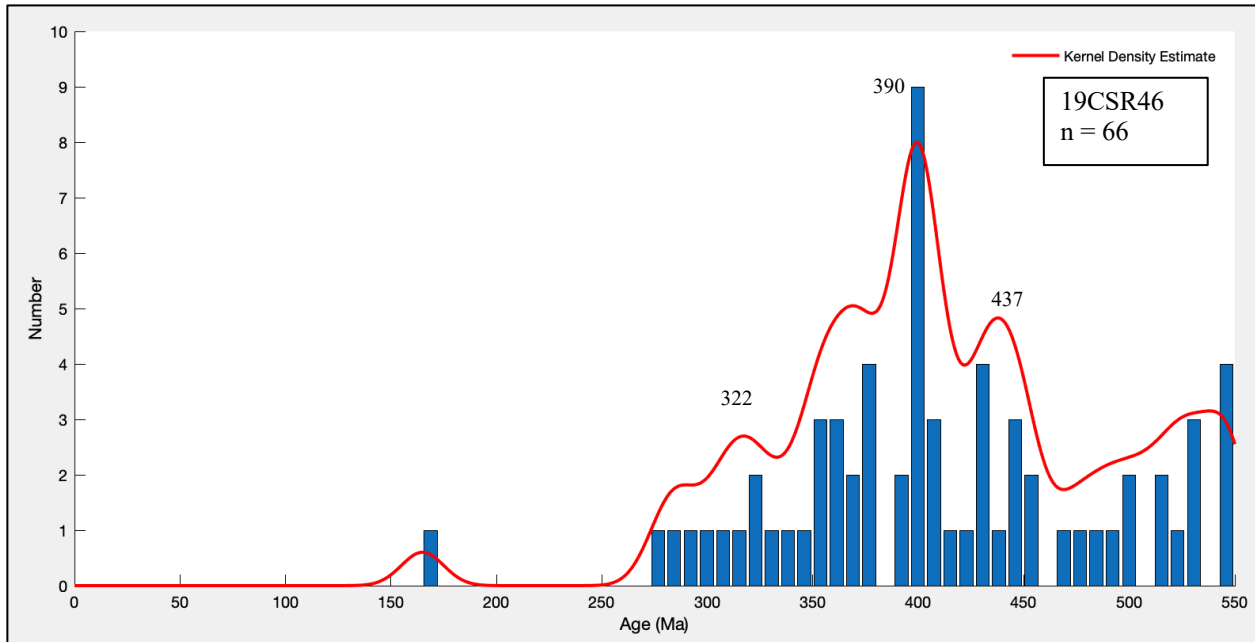


Figure 12b: Histogram and kernel density estimate (KDE) of the Paleozoic age distribution for sample 19CSR46. Each histogram bin is approximately 10 million years. N is the number of analyses reported on the plot.

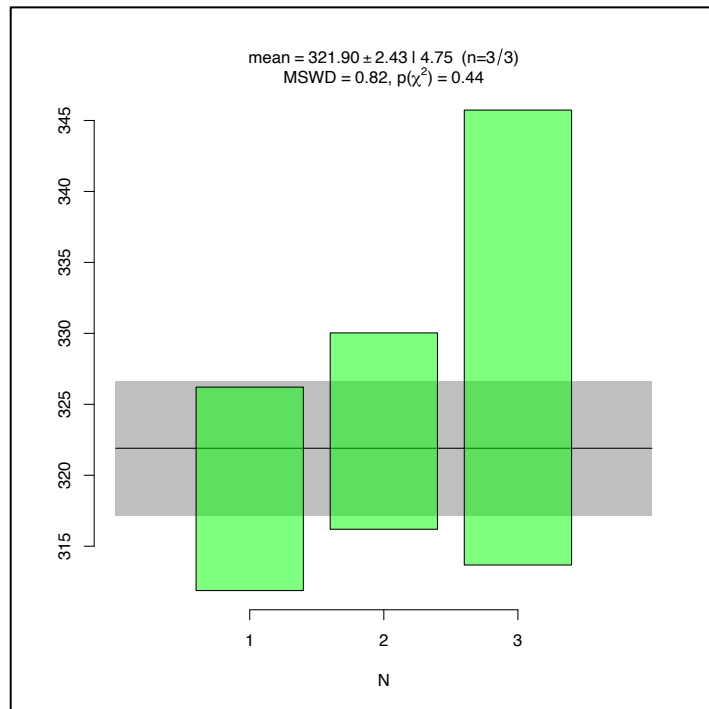


Figure 12c: Maximum depositional age of sample 19CSR46 using the weighted mean of the youngest cluster of three or more grains that overlap with 2σ uncertainty.

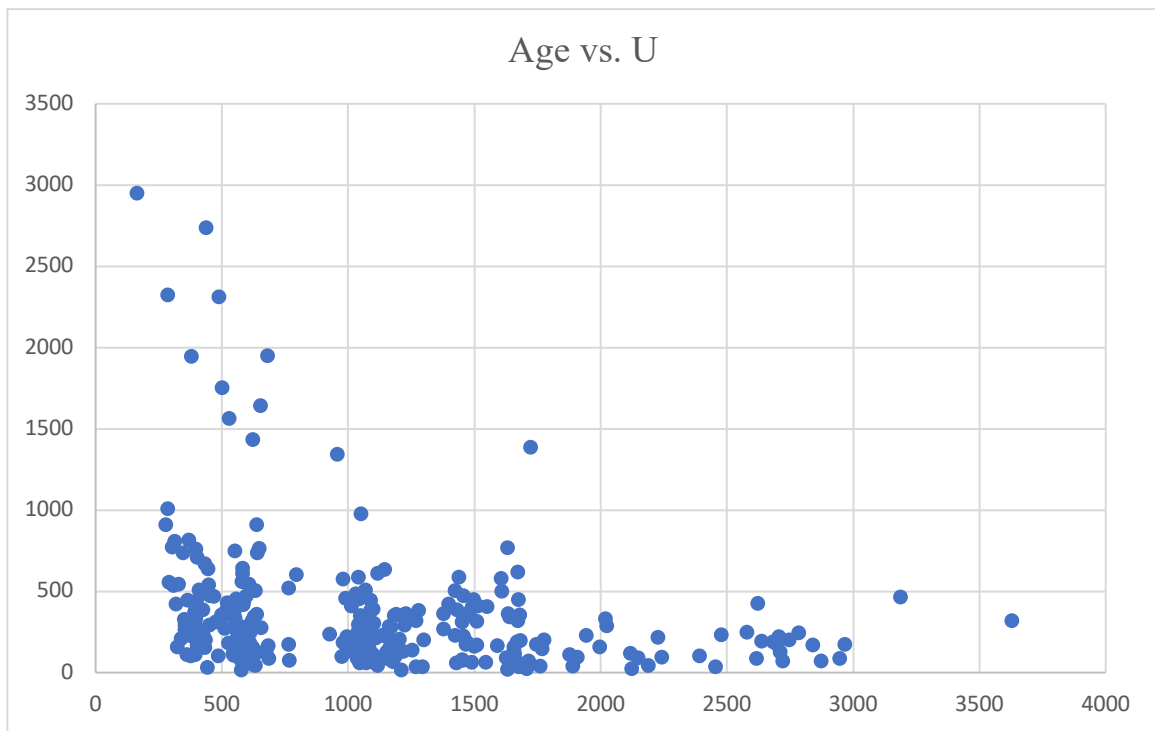


Figure 12d: Age vs. Uranium plot for sample 19CSR46. No grains were removed due to high Uranium content.

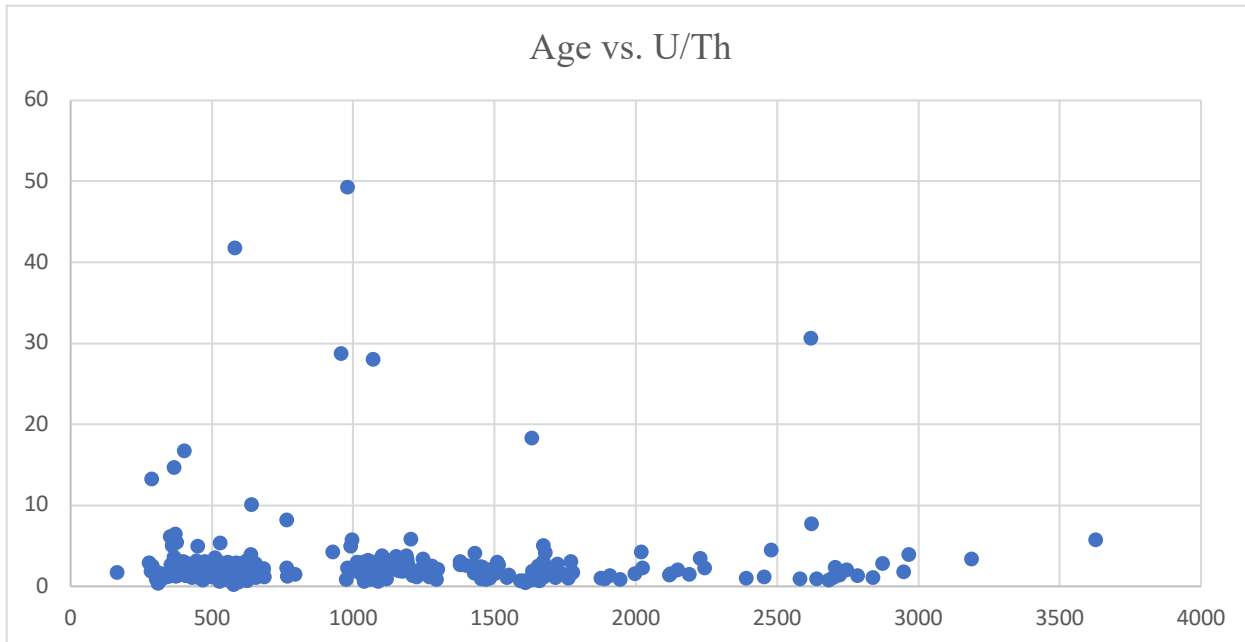


Figure 12e: Age vs. Uranium/Thorium plot for sample 19CSR46. Nine grains were removed from our analysis due to a U/Th ratio greater than 10.

Sample 15LT03

Sample 15LT03 has a dominant peak at 1854 Ma and a sub-peak at 405 Ma (Figures 13a and 13b). Thirty-eight neo-crystallization ages were removed from the analysis based on the known U-Pb age populations in the region (Figure 13c). Sample 15LT03 has a maximum depositional age of 327 Ma (late Mississippian) (Figure 13d). No grains were removed due to high Uranium content (Figure 13e). Six suspect metamorphic ages were removed due to high U/Th ratios (Figure 13f). Two grains were removed because the ages had a percent error higher than 3%. After removing these grains, the total number of grains analyzed for this sample is 25.

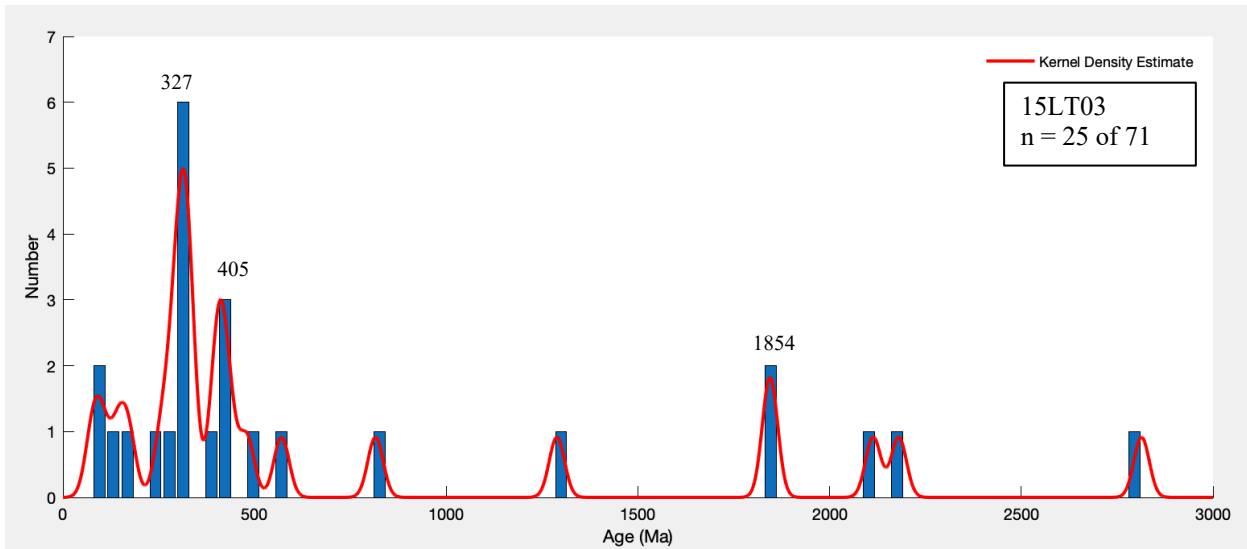


Figure 13a: Histogram and kernel density estimate (KDE) for sample 15LT03. Each histogram bin is approximately 35 million years. N is the number of analyses reported on the plot out of the total number of grains analyzed.

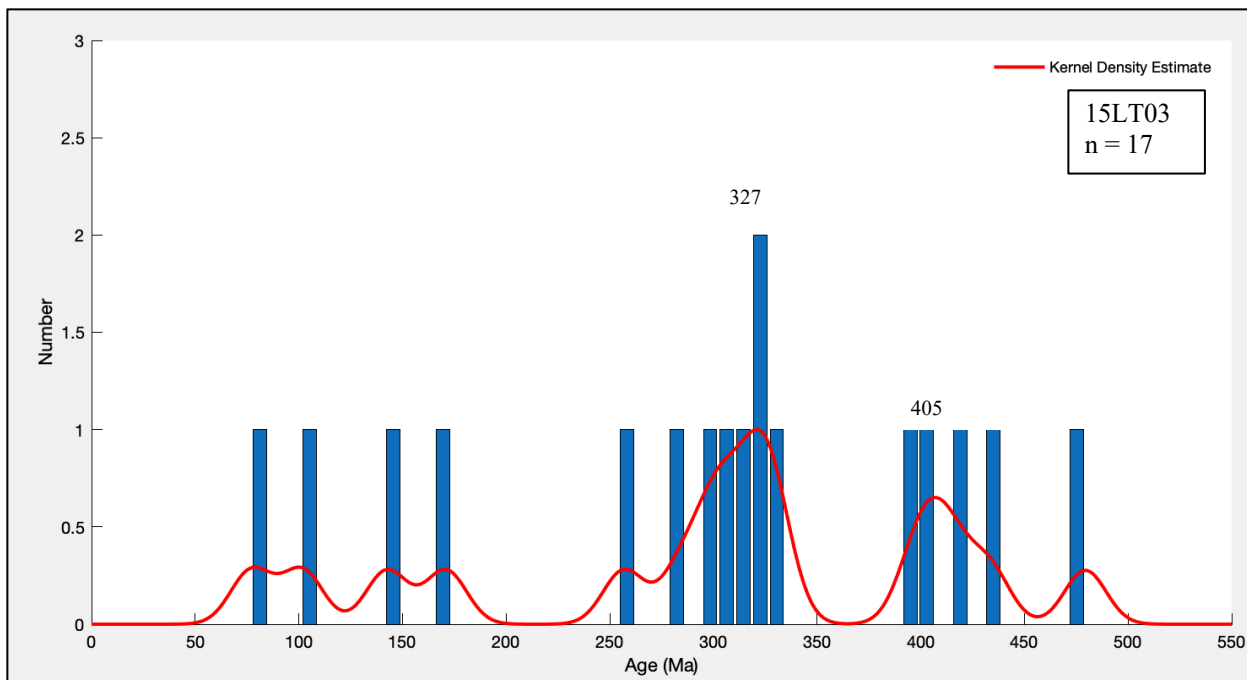


Figure 13b: Histogram and kernel density estimate (KDE) of the Paleozoic age distribution for sample 15LT03. Each histogram bin is approximately 10 million years. N is the number of analyses reported on the plot.

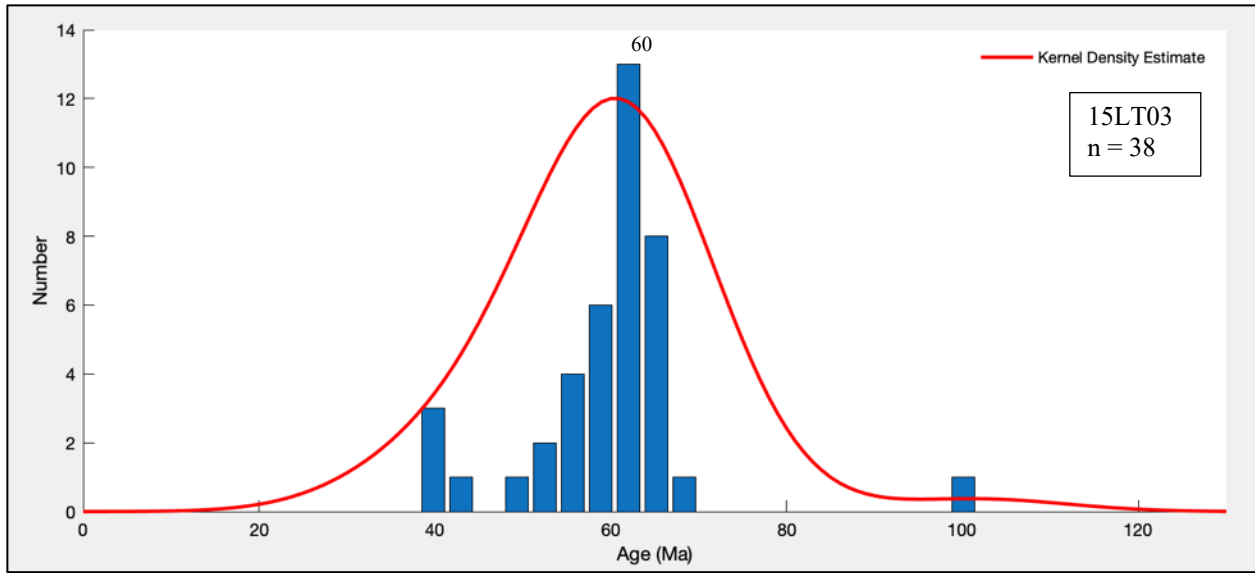


Figure 13c: Histogram and kernel density estimate (KDE) of all metamorphic and neo-crystallized grains younger than 130 Ma in sample 15LT03. These ages reflect the age range of regional plutons (Benowitz et al., 2022). Each histogram bin is approximately 10 million years. N is the number of analyses reported on the plot.

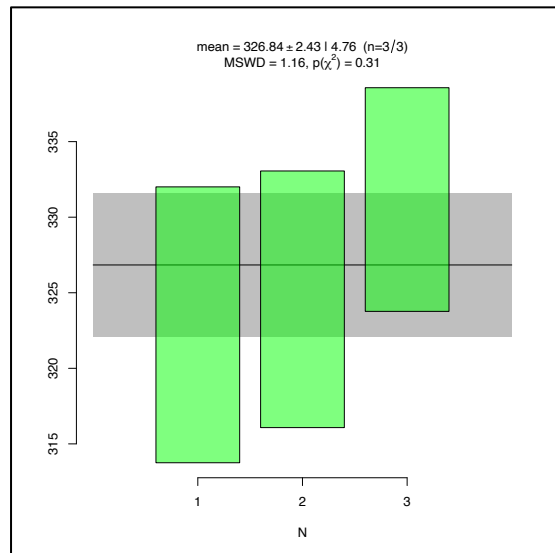


Figure 13d: Maximum depositional age of sample 15LT03 using the weighted mean of the youngest cluster of three or more grains that overlap with 2σ uncertainty.

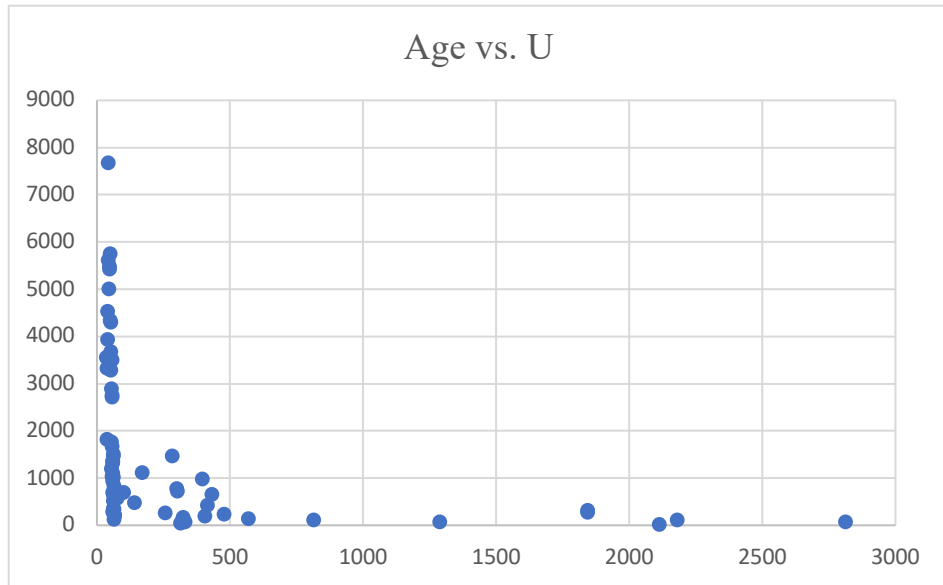


Figure 13e: Age vs. Uranium plot for sample 15LT03. No grains were removed due to high Uranium content.

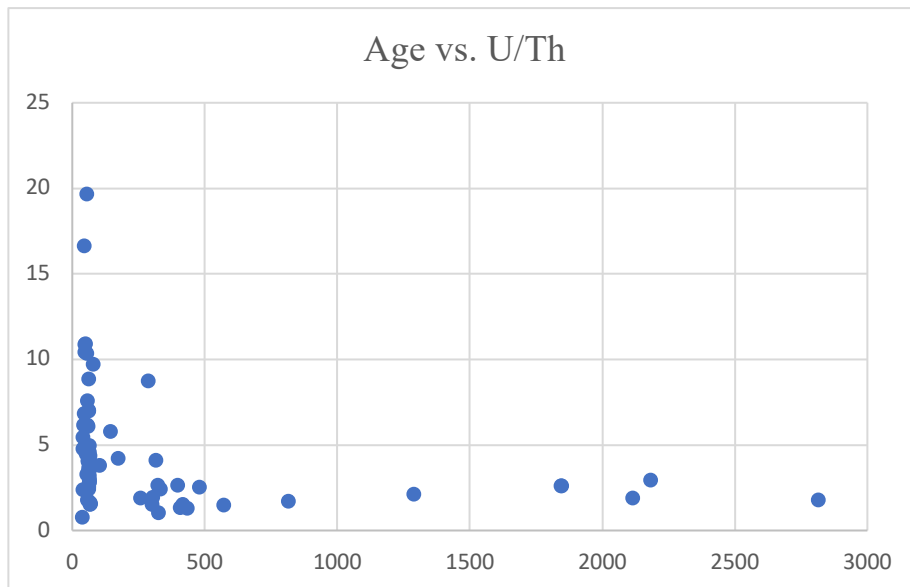


Figure 13f: Age vs. Uranium/Thorium plot for sample 15LT03. Six grains were removed from our analysis due to a U/Th ratio greater than 10.

Sample 21BG24

Sample 21BG24 has a dominant peak at 449 Ma and sub-peaks at 1116 Ma, 1321 Ma, 1439 Ma, 1632, and 1779 Ma (Figures 14a and 14b). Sample 21BG24 has a maximum depositional age of 363 Ma (late Devonian) (Figure 14c). One grain was removed due to high Ur content and three suspect metamorphic ages were removed due to high U/Th ratios (Figures 14d

and 14e). One grain was removed because the age had a percent error higher than 3%. After removing these grains, the total number of grains analyzed for this sample is 61.

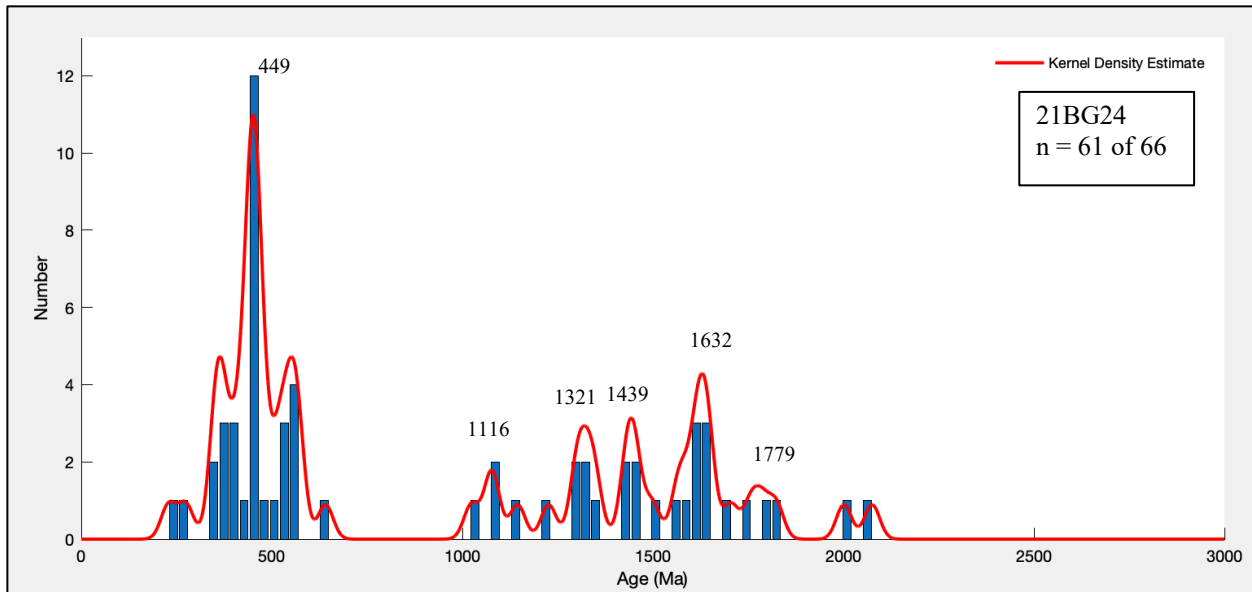


Figure 14a: Histogram and kernel density estimate (KDE) for sample 21BG24. Each histogram bin is approximately 35 million years. N is the number of analyses reported on the plot out of the total number of grains analyzed.

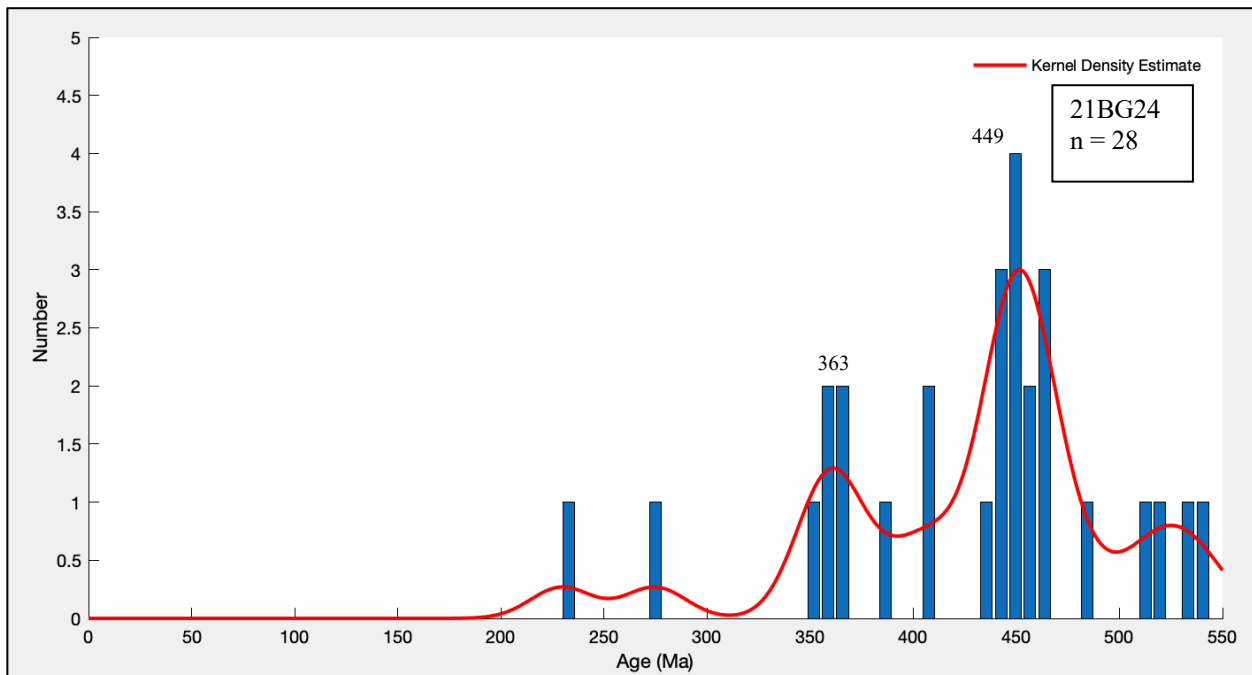


Figure 14b: Histogram and kernel density estimate (KDE) of the Paleozoic age distribution for sample 21BG24. Each histogram bin is approximately 10 million years. N is the number of analyses reported on the plot.

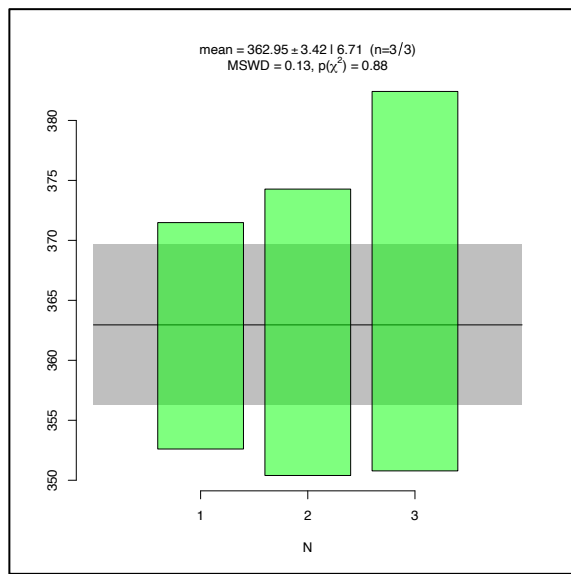


Figure 14c: Maximum depositional age of sample 21BG24 using the weighted mean of the youngest cluster of three or more grains that overlap with 2σ uncertainty.

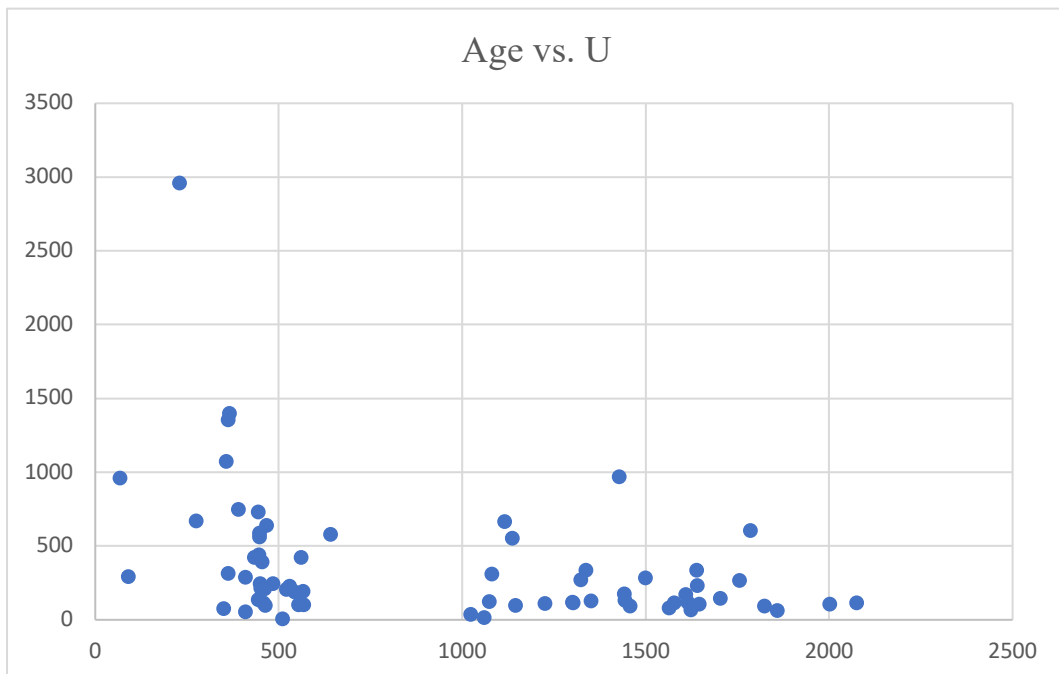


Figure 14d: Age vs. Uranium plot for sample 21BG24. One grain was removed due to high uranium content.

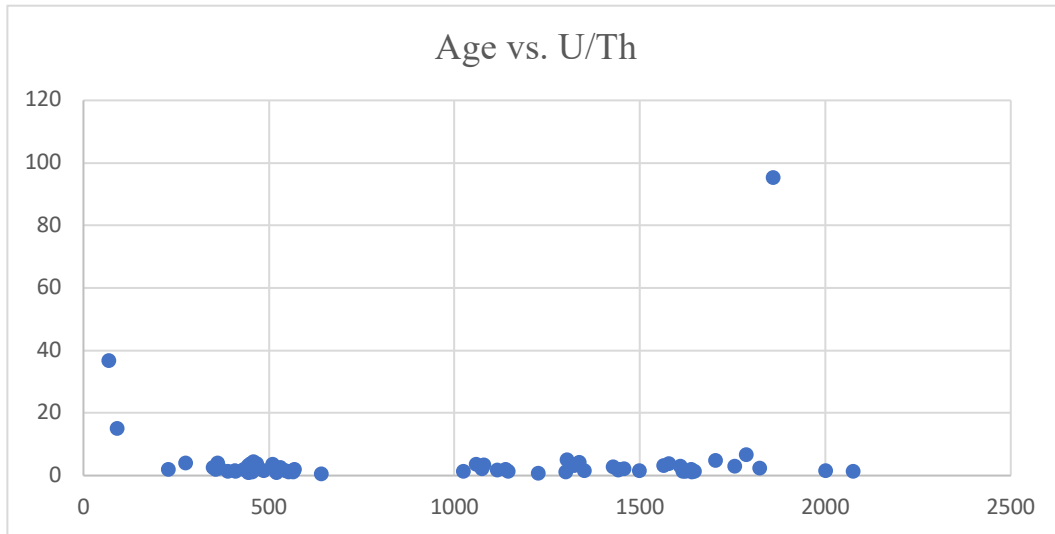


Figure 14e: Age vs. Uranium/Thorium plot for sample 21BG24. Three grains were removed from our analysis due to a U/Th ratio greater than 10.

Sample 21BG08

Determining the dominant peaks for sample 21BG08 is difficult due to the removal of a majority of analyzed grains due to suspect metamorphism and neo-crystallization, as discussed below. Ninety-four grains were removed from the analysis due to being newly crystallized grains whose ages are consistent with known ages of regional plutons (Figure 15a). No grains were removed due to high Uranium content (Figure 15b). Additionally, fifteen suspect metamorphic ages were removed due to high U/Th ratios (Figure 15c). Three grains were removed because the age had a percent error higher than 3%. A maximum depositional age could not be calculated for sample 21BG08 because there were not enough U-Pb ages that overlapped with 2-sigma uncertainty. After removing these ages, the total number of grains analyzed for this sample is 2.

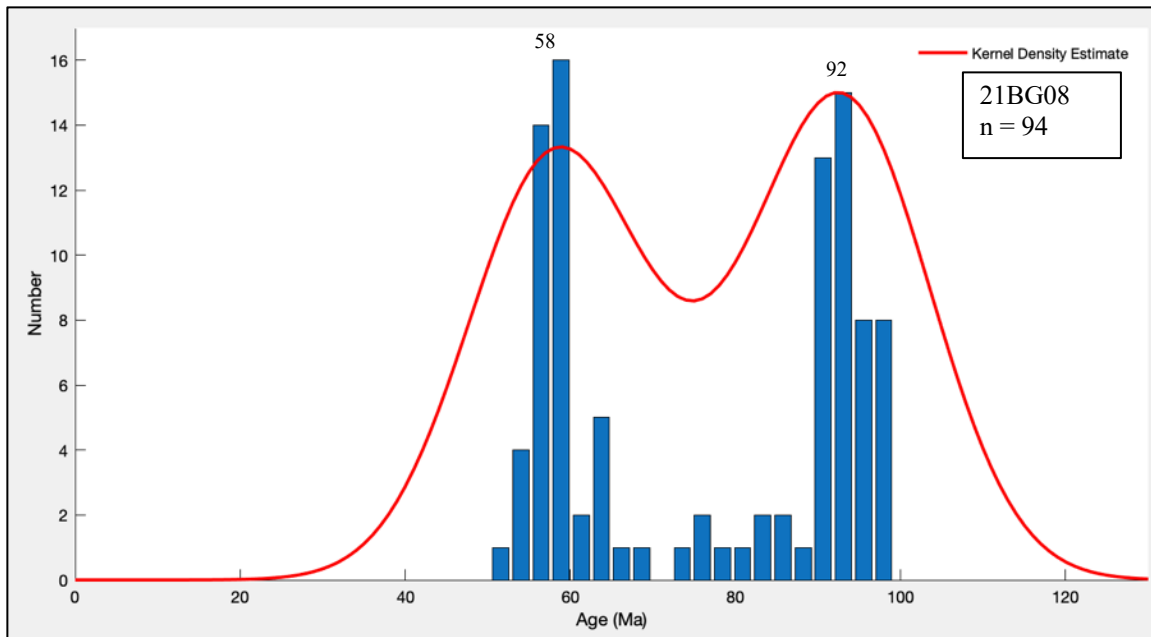


Figure 15a: Histogram and kernel density estimate (KDE) of all metamorphic and neo-crystallized grains younger than 130 Ma in sample 21BG08. These ages reflect the age range of regional plutons (Benowitz et al., 2022). Each histogram bin is approximately 10 million years. N is the number of analyses reported on the plot.

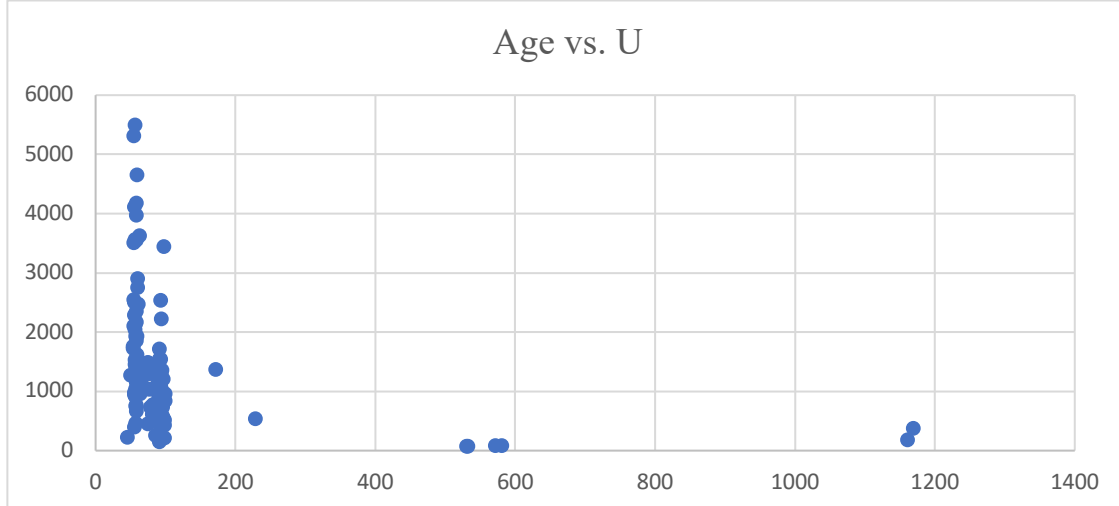


Figure 15b: Age vs. Uranium plot for sample 21BG08. No grains were removed due to high uranium content.

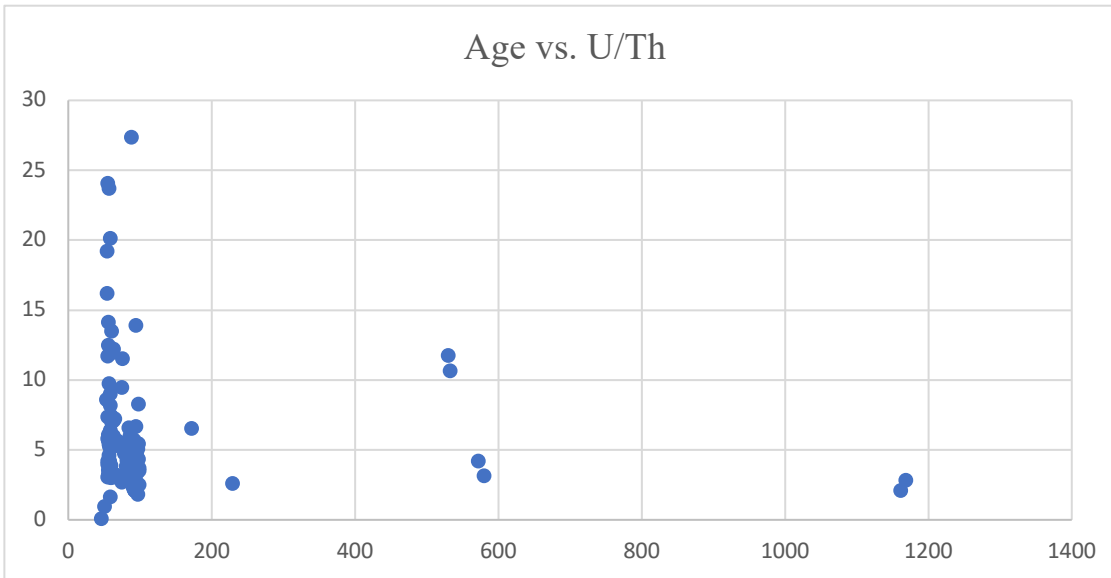


Figure 15c: Age vs. Uranium/Thorium plot for sample 21BG08. Fifteen grains were removed from our analysis due to a U/Th ratio greater than 10.

VI. Discussion

As discussed earlier, previous mapping of this region has produced locally inconsistent geologic maps. Many units are not continuous along strike from one quadrangle to the next. To address these issues, one of the goals of this project is to contribute to a more complete geologic map by providing an estimate of the depositional age of the units and providing more detailed rock unit descriptions. Additionally, my goal is to determine if our samples belong to the same unit and to determine if my samples are linked to any of the major terranes along strike in south-central Alaska.

Many disparities exist between our work and previous mapping. Previous mapping shows three different units in our field area (KJfm, Dy, TRcs), that are incorrect based on the inferred maximum depositional ages of our samples. For example, sample 10Ch01b has a maximum depositional age of 275 Ma, considerably younger than unit Dy as it is mapped (Figure 11c; Figure 16). Sample 21BG32, mapped as unit KJf, has a maximum depositional age of 260 Ma (Figure 10d, Figure 16). Sample 19CSR46 is mapped on the Healy quadrangle as unit TRcs;

however, our U-Pb analysis produced an early Pennsylvanian maximum depositional age of 321 Ma (Figure 12c, Figure 16). Additionally, sample 21BG24 was originally mapped on the Healy quadrangle as unit TRcs, a Triassic calcareous sedimentary rock (Figure 16). However, our U-Pb analysis revealed a Devonian maximum depositional age of 363 Ma for sample 21BG24 (Figure 14c).

It should be noted that there are fossil constraints on each of these units (Dy, KJf, and TRcs). The age constraint on unit KJf comes from a radiolarian fossil with a Jurassic or Cretaceous age located 47 km west along strike from sample 21BG32 (Murchey et al., 1983). Unit TRcs yields Late Triassic conodont fossils 26 km north of sample 19CSR46 (Sherwood and Craddock, 1979). Unit Dy contains Late Devonian conodont fossils 46 km west along strike from sample 10CH101b (Csejtey et al., 1992). To this end, I do not suggest these fossil constraints are inaccurate. Instead, I propose that many assemblages in the eastern Alaska Range will change with future detailed mapping.

The maximum depositional ages of my samples are notably very different despite the fact they are relatively close to each other geographically. This variability makes it difficult to do direct comparisons of the age distribution peaks. A difference in maximum depositional age of even a few million years (and some our samples are different by tens of millions of years) could result in sediment sources coming from very different areas. This wide range in maximum depositional ages of our samples is not entirely unsurprising given that most of these samples were collected within several hundred meters (all within one kilometer) of the Denali fault zone and the samples are uniformly strongly deformed and recrystallized at high temperatures (Tait, 2017; Benowitz et al., 2022).

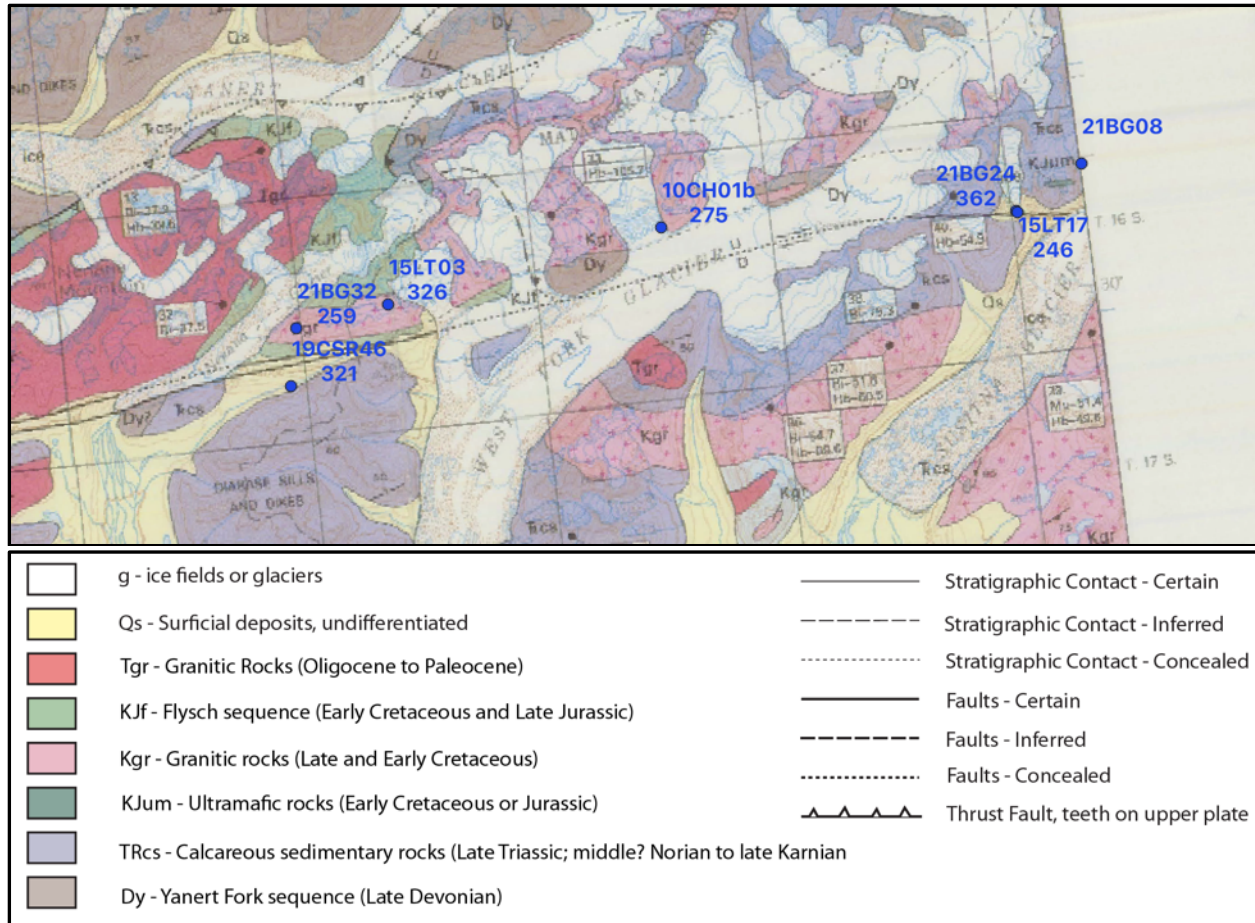


Figure 16: Geologic map of the eastern Alaska Range. Map overlay is the Healy quad (Csejtey et al., 1992). Blue circles are sample locales. The first line reports the sample number; the second line reports the MDA for that sample. Note that none of the inferred maximum depositional ages of our samples (with the possible exception of sample 15LT17) fit with the existing Healy quad map unit ages. It is important to note that samples 15LT03 and 21BG32 occur as screens of metasedimentary rock within the late Cretaceous pluton and are mapped as part of unit KJg as well as KJf, a Cretaceous-Jurassic marine meta-sedimentary unit. Similarly, sample 10CH01b is mapped as KJg as well as Dy, a Devonian marine metasedimentary and metavolcanic unit. Samples 21BG24 and 15LT17 were collected less than .5 km apart and only appear as a single blue circle on this map. As discussed in the results section, a maximum depositional age is not reported for sample 21BG08.

First order comparison: determining if samples belong to the same unit

I compared my samples to determine if they belong to the same unit. Determining correlation between rock units is commonly done by using the inferred maximum depositional age, comparing field evidence of rock types, and visually comparing the age distributions using kernel density estimates (KDEs) (Saylor and Sundell, 2016). Kernel density estimates were

generated using DZstats (Saylor and Sundell, 2016; Vermeesch, 2012). KDEs were generated using the optimized bandwidth that varies based on data density (Saylor and Sundell, 2016).

Various statistical methods can also be used to determine correlation between rock units. These quantitative methods include statistical tests such as the cross-correlation coefficient of the kernel density estimates (KDEs).

The cross-correlation coefficient of two KDEs can be a useful measurement in determining the similarity between two detrital zircon U-Pb age data sets. The cross-correlation coefficient is a statistical measurement of the cross-plot of two KDE plots. The cross-correlation coefficient is the coefficient of determination of a cross-plot of probability density plots or kernel density estimates of two samples for the same age interval (Saylor and Sundell, 2016). The cross-plot is sensitive to the presence or absence of peaks and to the relative magnitude of the peaks. For example, when comparing two samples with identical age distributions, the R^2 value of the cross-plot will be 1; when comparing two samples with no shared age peaks, the R^2 value of the cross-plot will be 0. For my analyses, I used the KDE for determining the cross-correlation coefficient. The R^2 value of the cross plot for samples that share some peaks will be between 0 and 1, with higher values indicating higher similarity. The cross correlation coefficient is more sensitive to the differences between samples (Saylor and Sundell, 2016). For sample sizes of $n > 375$, a KDE cross-correlation coefficient $> \sim .5$ indicates samples with the same source area and a coefficient of $< \sim .2$ indicates samples with different source areas (Saylor and Sundell, 2016). All of our datasets are smaller than 375 grains; however this method appears to be the most reliable for datasets of variable sample sizes (Saylor and Sundell, 2016). I used the software program DZstats to compute the cross-correlation coefficient (Saylor and Sundell 2016).

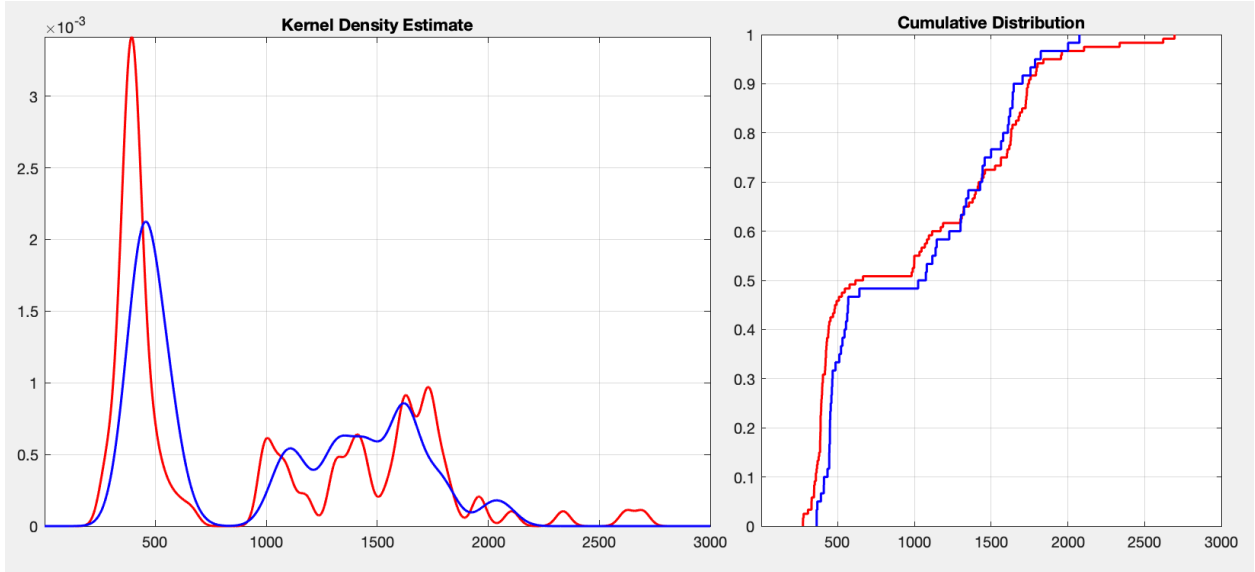


Figure 17: Example of a cross-plot of the KDE for two samples, 10CH01b (red line) and 21BG24 (blue line).

We propose our samples do not all belong to the same unit along strike. However, based on field observations, comparison of the detrital zircon age distributions, maximum depositional ages, and quantitative measures of similarity such as the cross-correlation coefficient, we do see some correlations between our samples.

Our results support correlation of samples 10CH01b and 21BG24, located in the eastern area of our field region (Figure 16). The lithology of these samples is relatively similar - both are biotite, plagioclase and quartz-rich schists with a likely volcanic protolith. These two samples do not have a similar maximum depositional age; however, they do have a cross-correlation coefficient of .614 (Figure 17; Table 2). Finally, samples 10CH01b and 21BG24 have similar U-Pb age distributions with similar main Paleozoic peaks and a similar spread of Precambrian sub-peaks (Figure 18).

Samples 15LT03 and 21BG32, located in the western area of our field region, also appear to be correlated (Figure 16). The western locales are relatively homogenous greenschist grade metasediments with distinct biotite-rich and quartz-rich horizons. Field observations of both

samples (schistose fabrics defined by coarse quartz-rich horizons and finer-grained biotite-rich horizons), supports correlation of these two samples (Figure 7E and 7H). The U-Pb age distributions of samples 15LT03 and 21BG32 supports a correlation with very similar Paleozoic peaks at 327 Ma and 323 Ma, respectively, and similar Precambrian sub-peaks at 1854 Ma and 1859 Ma, respectively (Figure 18). The cross-correlation coefficient between 15LT03 and 21BG32 is .402, however this number could be due to the low sample size for 15LT03 (Table 2).

The age distribution of the youngest sample, 15LT17, is unique from every other sample with a distinct mono-peak at 420 Ma (Figure 18). 99% of the grains in 15LT17 are Paleozoic, which also makes it unique from the rest of the samples. For this reason, we consider 15LT17 as representing a distinct unit from the other samples.

We considered whether these rock assemblages represent the same stratigraphic section and the rocks in the east have simply experienced more exhumation, exposing a deeper part of the section. However, the maximum depositional ages do not reflect this trend as the sample with the youngest MDA and the sample with the oldest MDA are located immediately adjacent to one another in the eastern end of the field area (Figure 16).

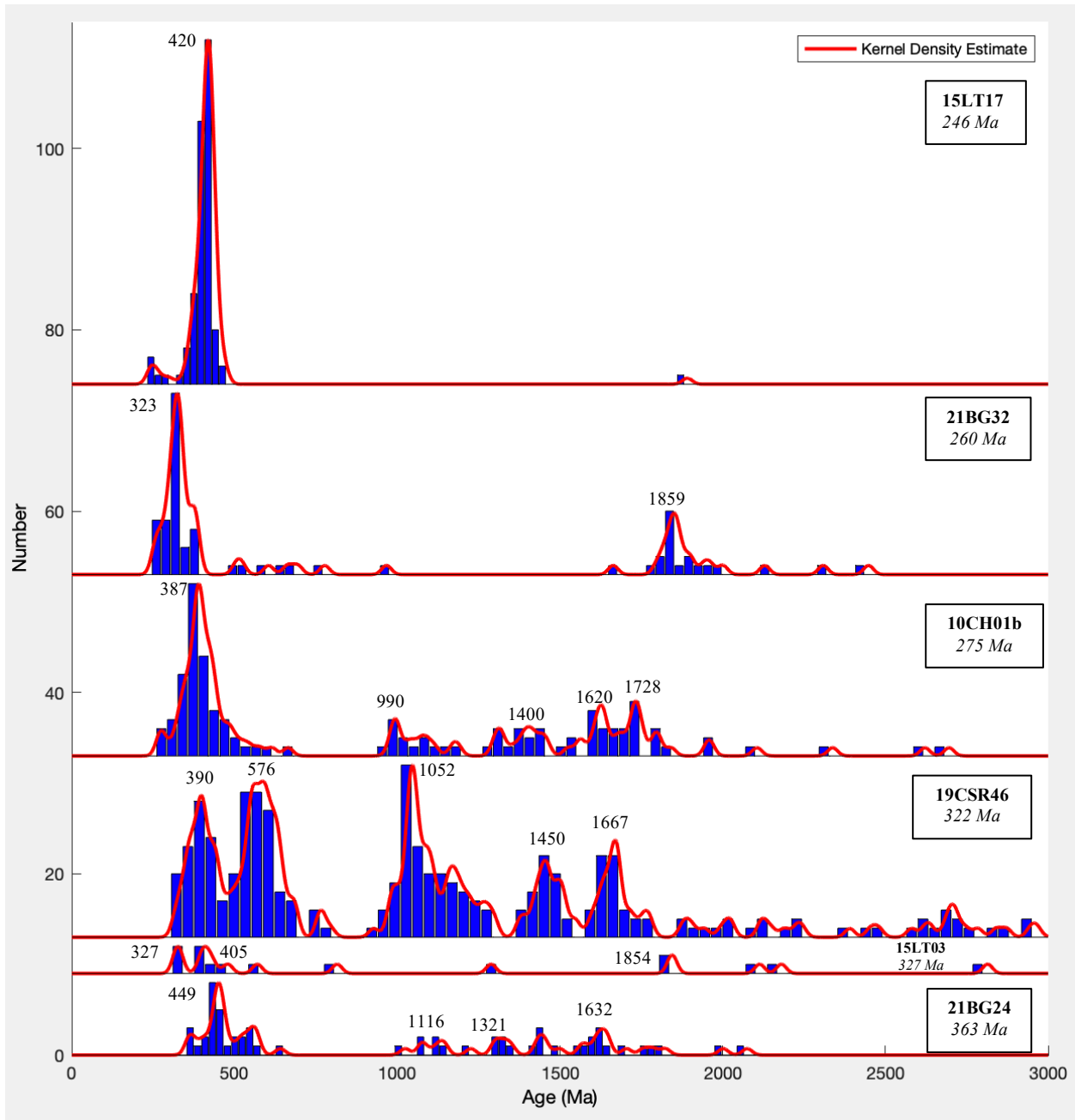


Figure 18: Kernel density estimate plots (red curves) and histograms (blue bars) for detrital zircon U-Pb data for all six of our samples. The bold text is the sample name and the italicized text is the MDA. Samples are arranged from youngest MDA at the top to the oldest MDA at the bottom. Each histogram bin is approximately 35 million years.

Cross-correlation Coefficient							
	15LT17	21BG32	10CH01b	19CSR46	15LT03	21BG24	21BG08
15LT17	1	0.009	0.446	0.106	0.192	0.25	0.06
21BG32		1	0.228	0.048	0.402	0.082	0.113
10CH01b			1	0.343	0.545	0.614	0.295
19CSR46				1	0.155	0.59	0.316
15LT03					1	0.345	0.524
21BG24						1	0.301
21BG08							1

Table 2: Comparisons between all seven of our samples using the cross-correlation coefficient. These comparisons consider the entire age distribution. Yellow cells have cross-correlation coefficients >.5.

Second-order comparison: Determining if our samples are related to units along strike

In this section I compare our samples to units along strike. All samples except 19CSR46 are located north of the Denali fault (Figure 16). If these rocks have remained in place, a northern Yukon-Tanana or parautochthonous North America sediment source is the most likely. However, if these rocks have been translated along the Denali fault (or a proto-Denali fault), then protoliths located farther away along strike are very plausible. Therefore, we will analyze both local sediment sources and sediment sources located at a distance along strike. Comparisons rely on the primary detrital zircon age populations from potential sediment sources along strike (Table 3).

Terrane	Sub-Terrane	Unit	Rock Type	Age of Unit	Primary Age Populations	Reference
Alexander	Saint Elias Mountains	Donjek Assemblage	shallow marine sedimentary and volcanic assemblage	Upper Cambrian- Middle Ordovician strata	565 - 760 Ma (dominant, 40 - 75%); 625, 640, 675, 710, 725, 880. 10%; 1000 - 1250, 1400 - 1480, 1600 - 1680.	Beranek et al., 2013a
	Saint Elias Mountains	Icefield Assemblage	terrestrial/shallow marine strata	Upper Silurian to lower Devonian	390 - 395 Ma, 405 - 490 Ma (total range 390 - 3372 Ma)	Beranek et al., 2013b
	Saint Elias Mountains (Craig Subterrane of Alexander basement)	Donjek Glacier Plutonic Suite	diorite to granodiorite intrusive complex	Early Permian	284 - 291 Ma	Beranek et al., 2014
	SE Alaska	Descon Arc	marine volcanic arc assemblage (volcanic and volcanic-rich sedimentary rocks)	Ordovician to Lower Silurian	461 to 591 Ma	White et al., 2016
	SE Alaska	Karheen Formation	conglomerates, clastic wedge strata	Devonian	418 to 472 Ma	White et al., 2016
	Banks Island Assemblage		quartz-rich metasediments	Ordovician to Permian	307, 367, 409, 434, 442, 478	Tochillin et al., 2014
Farewell	Mystic Subterrane		overlap assemblage	Devonian to Jurassic	Mississippian strata: primary peak 400 - 325, secondary peaks 480 - 415 and 2000 - 1800. Permian strata: 320 - 275 Ma, 460 - 415 Ma	Malkowski et al., 2014
	Mystic Subterrane	Sheep Creek, Mystic, Mount Dall conglomerate			256, 298, 347 - 335, 349, 369, 445 - 424, 425, 459 - 405, 1840	Dumolin et al., 2018
	Nixon Fork Subterrane	Metasedimentary and meta-igneous rocks and orthogneiss	carbonate platform	Late Neoproterozoic to Devonian	850 Ma (orthogneiss), 979 Ma, 921 Ma	Bradley et al., 2003; McClelland et al., 1999
	Dillinger Subterrane		deep water basin assemblage	Cambrian to Devonian		Dumolin et al., 2018
Wrangellia	Sicker Arc			Late Devonian to Early Permian	340, 310, 295 Ma	Beranek 2014
	Skolai Arc			Late Paleozoic	320 - 290 Ma	Beard and Barker, 1989
	Barnard Glacier pluton	(shared with Alexander)		Pennsylvanian	307 - 301 Ma	Beranek et al., 2014
Yukon-Tanana, Stikinia, parautochthonous North America, Quenellia	Taylor Mountain Batholith			Late Triassic to Early Jurassic	216 - 181	Dusel Bacon et al., 1996
	Augen Gneiss				380 - 360 Ma	Alienikoff et al., 1986
	Endicott Arm	metasedimentary		summary dominant peaks: 460 - 320 Ma	dominantly 450 - 350 Ma (with peaks at 421 and 337 Ma); 2770 - 2620 (peak age of 2694 Ma), 1890 - 1580 (peak ages of 1732 and 1620), 1520 - 1415 (peak ages of 1485 and 1444), and 1200 - 930 (peak ages of 1168, 1077, and 1026).	Pecha et al., 2016
		metavolcanic			425 - 355, peaks 421, 402, 378 Ma	Pecha et al., 2016
		metaplutonic			peaks: 428, 400, 381, 365	Pecha et al., 2016
	Stikinia		arc terrane		250 - 160 Ma (on Triassic-Jurassic sedimentary and igneous rocks)	George et al., 2021
	shared by pNA and Yukon-Tanana		Devonian to Early Mississippian igneous events		370 - 350 Ma	Colpron et al., 2007
	shared by Stikinia and Yukon-Tanana		Late Triassic to Early Jurassic plutons		220 - 206	Colpron et al., 2007
Taku	Taku				peak ages: 362, 370, 376 Ma	Geisler et al., 2016
Windy-McKinley					age ranges: 600 - 400 Ma, 1300 - 900 Ma, 2000 - 1500 Ma, and 2800 - 2500 Ma	Murphy, 2006
TRcs		submarine fan strata (marine calcareous sediments)	upper Triassic to Jurassic		458 - 240 Ma and 676 - 463 Ma, and subordinate population peaks at 2725 Ma, 2060 Ma, 1885 Ma, 1764 Ma, 1672 Ma, 1491 Ma, and 1050 Ma (Keough et al., 2021).	Keough et al., 2021

Table 3: Summary of Potential Detrital Zircon Sources

I first compare my samples to local sediment sources – parautochthonous North America and the northern part of the Yukon-Tanana terrane (Figure 1). All of my samples lack conspicuous peaks from 2800 – 2600 Ma, a defining age range in parautochthonous North America and northern Yukon-Tanana terrane (Table 3). Sample 21BG32 is the only sample that has a significant peak within one of the age ranges 2100 – 1800 Ma (Figure 19). However, 21BG32 has no grains within 1500 – 1000 Ma and it also has a striking peak at 323 Ma (Figure 19).

However, it is notable that my samples all share a broadly Devonian (Late Silurian through Mississippian) spread of peaks. A possible source of this sediment is the Devonian to Mississippian arc igneous events (Colpron et al., 2007). As discussed above, my samples do not have similar age distributions in the Precambrian. It is therefore possible that a diverse assemblage of country rocks with separate origins were emplaced in the Early Paleozoic and were intruded by the arc igneous events in the Devonian – Mississippian. It is possible that parautochthonous North America and Yukon-Tanana are sources of sediment for my samples.

We next compare our samples to the southern part of Yukon-Tanana that extends into southeast Alaska (Figure 1). The Southeast Yukon-Tanana terrane is composed of the Endicott Arm, Tracy Arm, and Port Houghton assemblages. Sample 10CH01b bears the most striking resemblance to the Endicott Arm (Figure 20). Sample 10CH01b has a strong peak at 450 – 350 Ma, as could be derived from extensive Ordovician through Carboniferous magmatism throughout southeast Yukon-Tanana (Figure 20, Table 3). The spread of ages between 1800 – 1000 Ma in sample 21BG24 is well captured by the range of ages within the Endicott Arm (Figure 20).

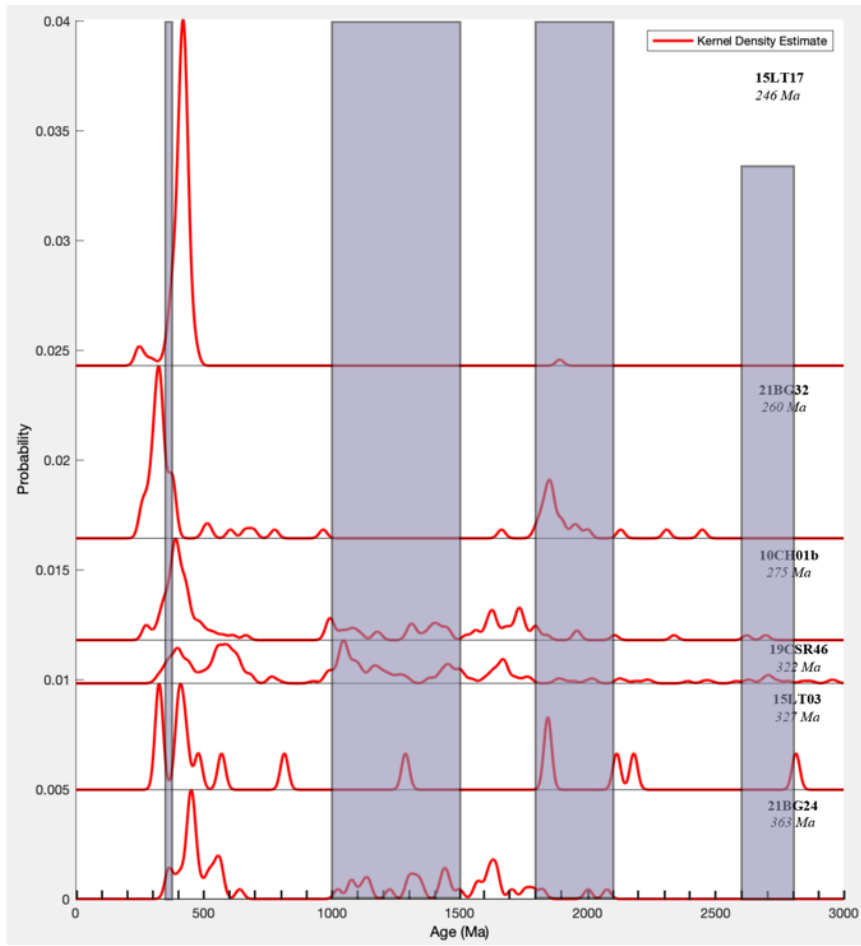


Figure 19: Kernel density estimate plots (red curves) for detrital zircon U-Pb data for six of our samples. Light purple bars highlight the age ranges of dominant detrital zircon age populations from paraautochthonous North America and the northern section of the Yukon-Tanana terrane (Colpron et al., 2007; Pecha et al., 2016).

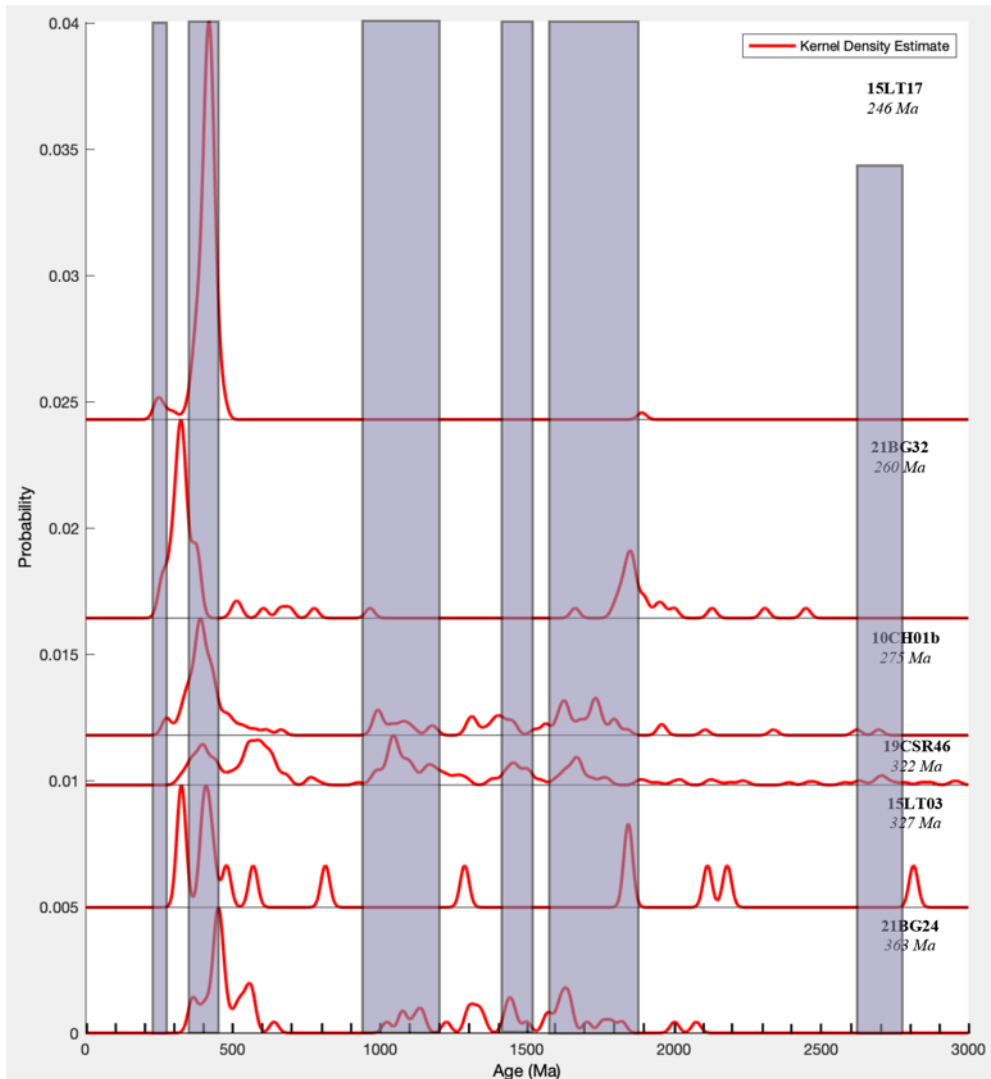


Figure 20: Kernel density estimate plots (red curves) for detrital zircon U-Pb data for six of our samples. Light purple bars highlight the age ranges of dominant detrital zircon age populations from the Endicott Arm of the southeast Yukon-Tanana terrane (Aleinikoff et al., 1996; Dusel-Bacon et al., 1995; George et al., 2020; Pecha et al., 2016).

My youngest sample, 15LT17, is the only sample that could be correlated with any of the outboard terranes within the Wrangellia composite terrane (Figure 1). Sample 15LT17 has a strong peak at 420 Ma with a sub-peak at 246 Ma and one grain age of 1891 Ma. A likely sediment source for 15LT17 is the Banks Island assemblage of the southern Alexander terrane in southeast Alaska (Figure 21). The dominant detrital zircon age populations of the southern Alexander terrane in southeast Alaska ranges from 429 to 417 Ma (Figure 21, Table 3).

It is also possible that sample 15LT17 is associated with the Windy-McKinley terrane (Figure 22). However, given the striking lack of Precambrian grains within the sample and the abundant Precambrian grains within the Windy-McKinley terrane, this is highly unlikely (Table 3).

The Wrangellia Terrane does not appear to be a likely sediment source for 15LT17 (Figure 23). The age ranges for the Skolai arc (320 – 290 Ma) and the Barnard Glacier Plutonic Suite (315 – 301 Ma) do not exhibit the strong peak at 420 Ma in sample 15LT17 (Figure 23, Table 3). While samples 15LT03 and 21BG32 have peak ages (327 Ma and 323 Ma, respectively) near this age range, both of these samples also have grains at ~1850 Ma (Figure 23). The Wrangellia Terrane does not contain Paleoproterozoic detrital zircon grains.

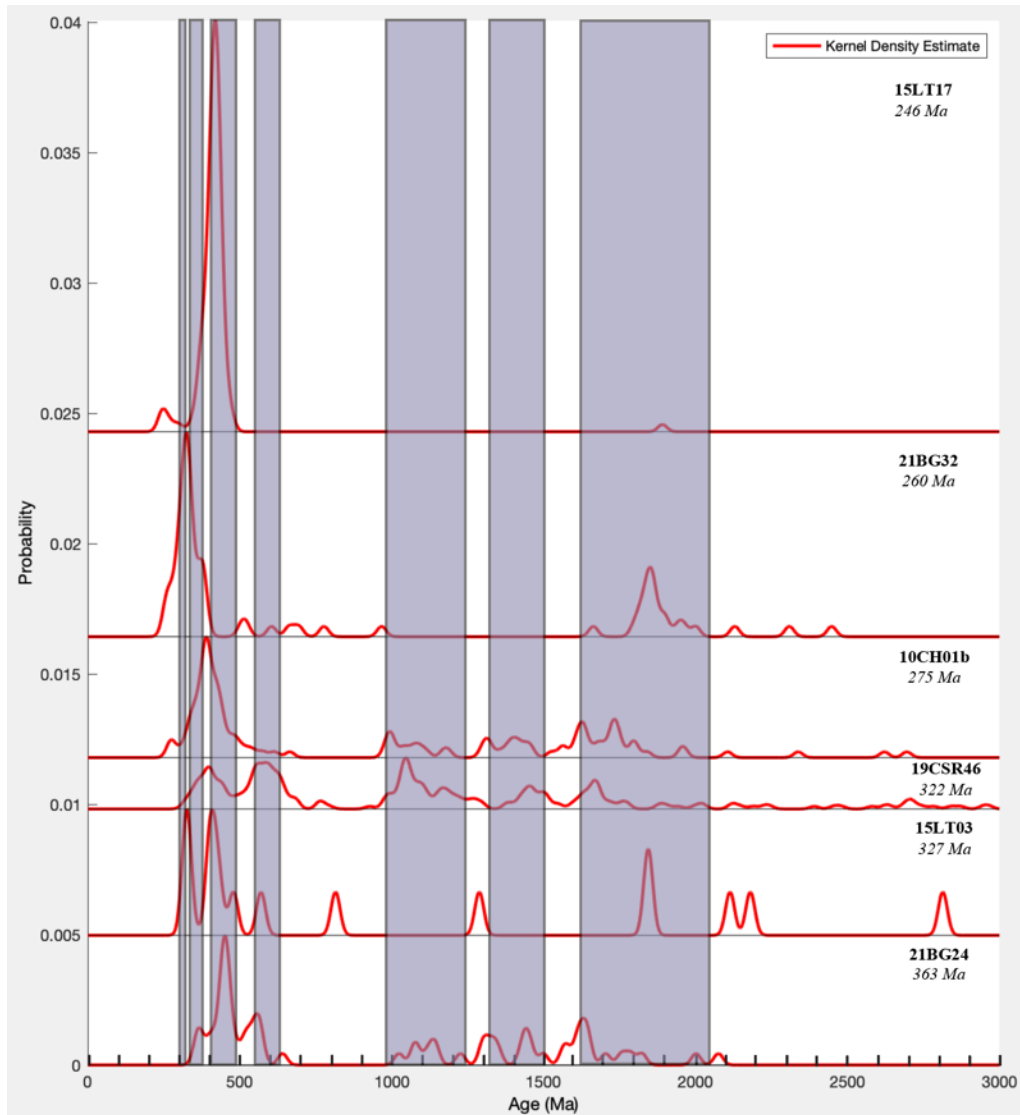


Figure 21: Kernel density estimate plots (red curves) for detrital zircon U-Pb data for six of our samples. Light purple bars highlight the age ranges of dominant detrital zircon age populations from the Alexander Terrane (Beranek et al., 2013a; Beranek et al., 2013b; Beranek et al., 2014; Tochilin et al., 2014; White et al., 2016).

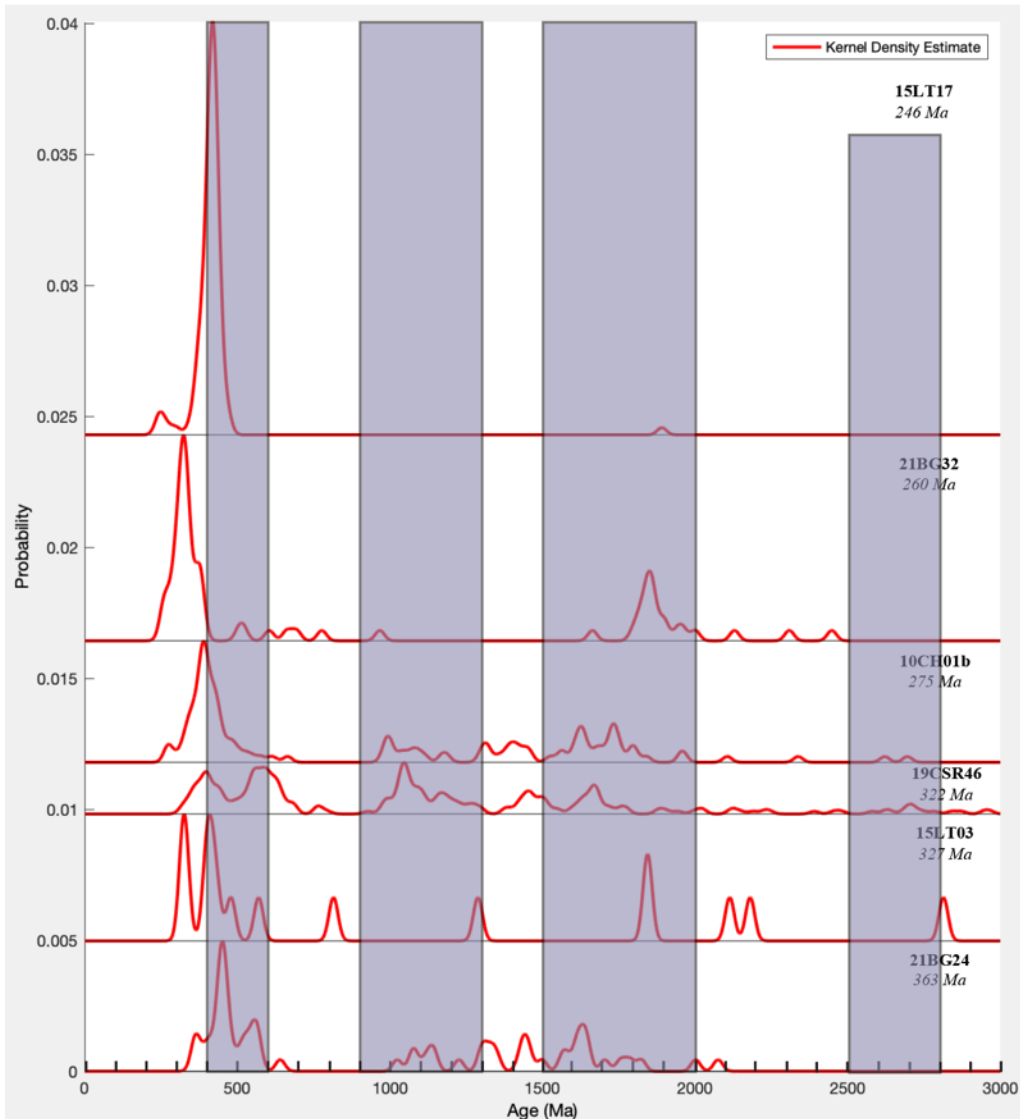


Figure 22: Kernel density estimate plots (red curves) for detrital zircon U-Pb data for six of our samples. Light purple bars highlight the age ranges of dominant detrital zircon age populations from the Windy-McKinley Terrane (Murphy, 2006).

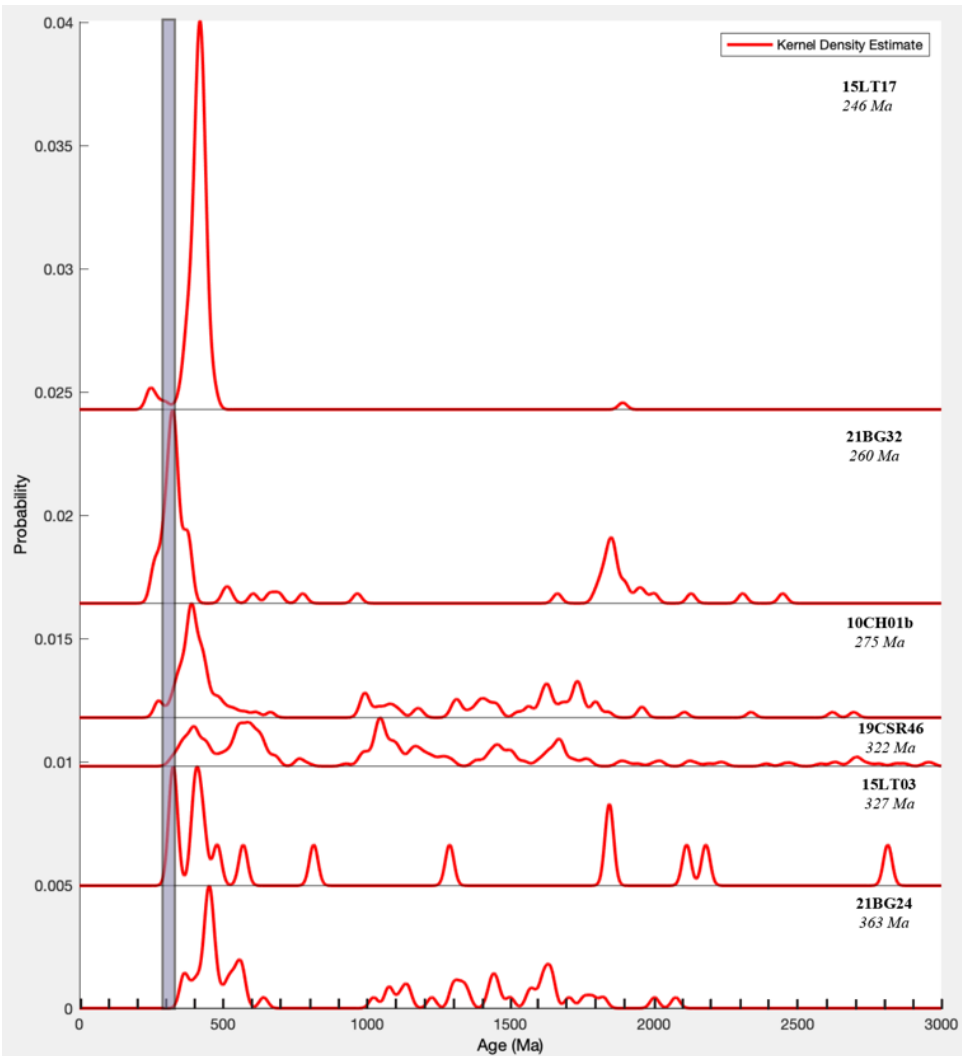


Figure 23: Kernel density estimate plots (red curves) for detrital zircon U-Pb data for six of our samples. Light purple bars highlight the age ranges of dominant detrital zircon age populations from the Wrangellia Terrane (Beranek et al., 2014; Beard and Barker, 1989).

Sample 19CSR46, the only one of our samples located south of the Denali fault, does not have a good match with any terrane along strike. The presence of a strong peak at 576 Ma strongly suggests 19CSR46 is not related to Yukon-Tanana or parautochthonous North America, as detrital zircon grains from 700 – 500 Ma are a relatively uncommon population in rocks related to Yukon-Tanana and parautochthonous North America. One possible correlation is with unit TRcs as described by Keough et al., 2021 (Table 3). The three dominant peaks within 19CSR46 at 390 Ma, 576 Ma, and 1052 Ma are well captured by the age range within TRcs

(Figure 24). Similarly, the spread of Precambrian sub-peaks are also within the age range of detrital zircon ages that define unit TRcs (Figure 24).

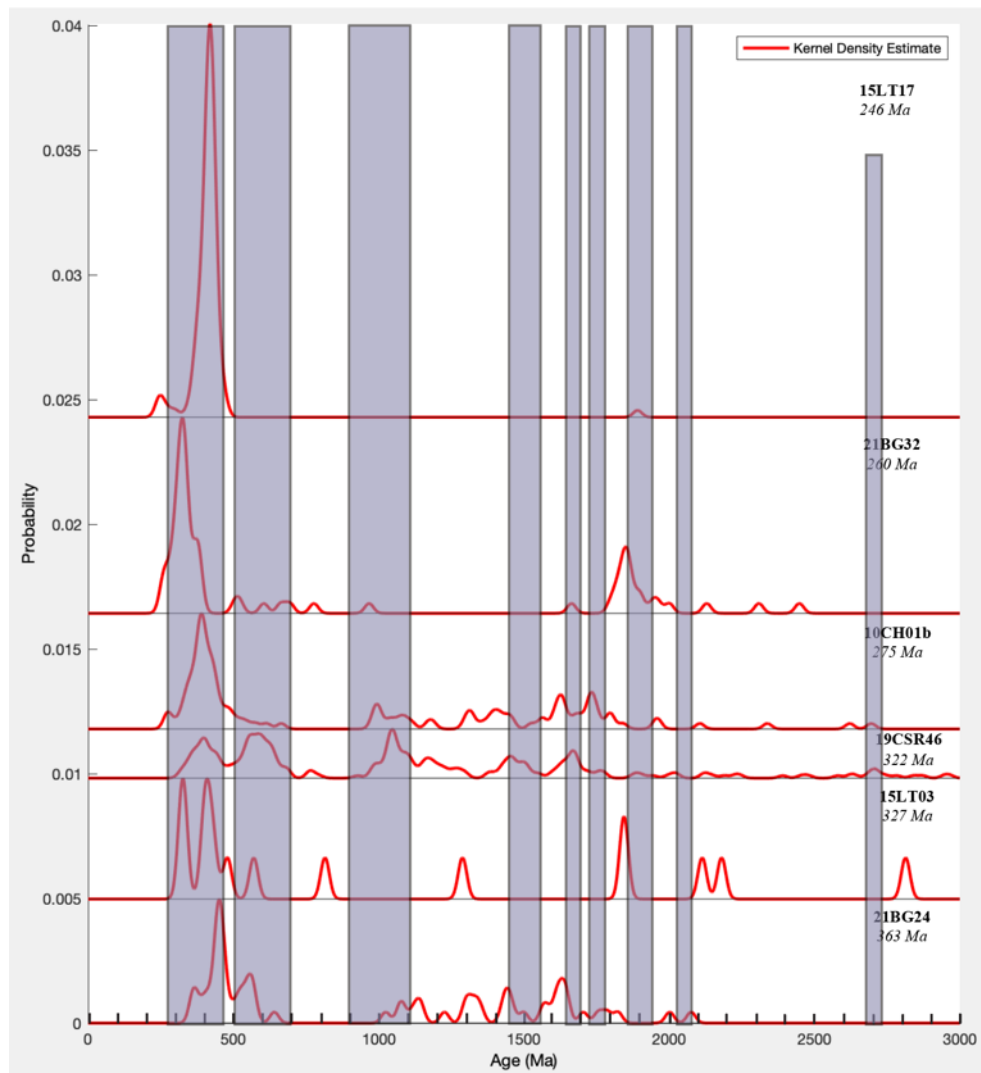


Figure 24: Kernel density estimate plots (red curves) for detrital zircon U-Pb data for six of our samples. Light purple bars highlight the age ranges of dominant detrital zircon age populations from unit TRcs found in Keough et al., 2021.

Implications

If these samples indeed have a common Devonian-Mississippian sediment source characteristic of parautochthonous North America, this would indicate our samples have remained in place and have ties with the ancestral North American margin.

However, if the correlations with the southern Alexander terrane and southeastern Yukon-Tanana terrane are correct, this implies our field area is located within the Wrangellia composite terrane and does not have ties to the ancestral North American margin. Given the possible correlation with the Endicott Arm of the southeast Yukon-Tanana terrane, this requires translation of these rocks over a great distance (>1000 kilometers) (Figure 25). The current Denali fault appears to have been highly localized along one strand throughout the Cenozoic (Regan et al., 2021). This would imply large-scale slip on a previously active strand of the Denali fault (a proto-Denali fault), on a major strike-slip fault further inboard, or on an unidentified structure.

As noted above, all our samples except one are located north of the Denali fault, and they were all collected within one kilometer of the Denali fault (Figure 16). Sample 15LT17, which is potentially related to the southern Alexander terrane, is the sample that is located the closest to the active strand of the fault. It is possible this sample was translated north entrained in the anastomosing strands of the Denali fault zone.

Given the correlation with the Endicott Arm of the southeast Yukon-Tanana terrane, this requires translation of these rocks over a great distance (>1000 kilometers). The current Denali fault appears to have been highly localized along one strand throughout the Cenozoic (Regan et al., 2021). This would imply large-scale slip on a previously active strand of the Denali fault (a proto-Denali fault), on a major strike-slip fault further inboard, or on an unidentified structure.

One option is the vertical, lithospheric-scale Hines Creek fault to the north of the Denali fault (Figure 26). The Hines Creek fault shows evidence for Cenozoic dip-slip motion; however, it has also been speculated that the Hines Creek fault accommodated significant Cretaceous strike-slip displacement (Benowitz et al., 2022, Hickman et al., 1978). A pluton intruding the

Hines Creek fault strand has a 95 Ma K-Ar cooling age, indicating that movement along the Hines Creek fault must pre-date 95 Ma (Wahrhaftig et al., 1975).

Alternatively, Warren Nokleberg noted a potential fault underneath the Nenana Glacier called the Nenana Glacier fault which he maps as a strand of the Denali fault system (Figure 26; Nokleberg and Richter, 2007). Additional evidence for the Nenana Glacier fault is difficult to acquire as it is mapped as lying underneath the Nenana Glacier or crossing extreme topography.

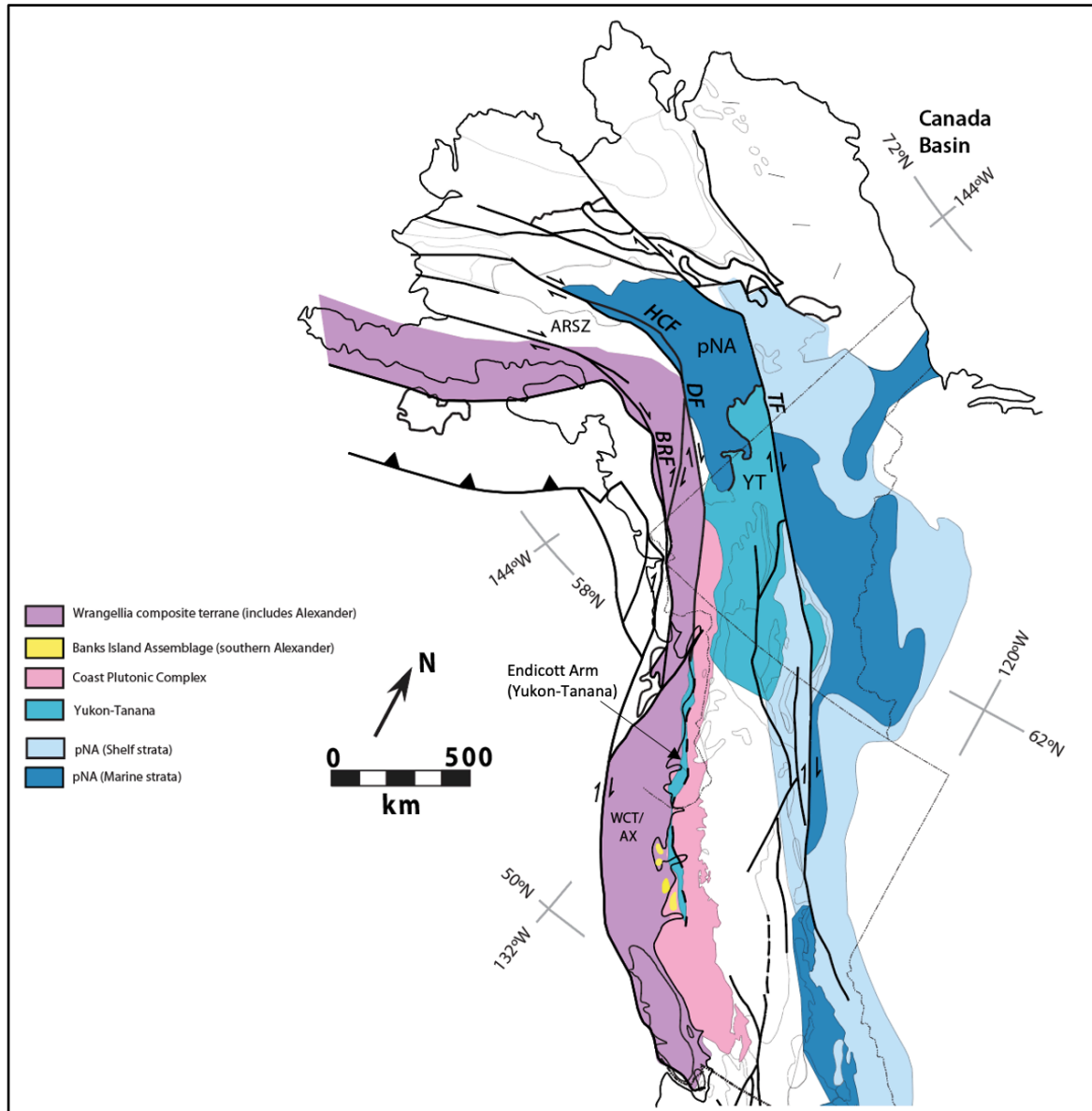


Figure 25: Simplified terrane map of the northern Cordillera. Modified from Busby et al., 2023. Key depicts terranes grouped by tectonic setting. Note the Banks Island Assemblage of the southern Alexander terrane and the Endicott Arm of the southeast Yukon-Tanana terrane are both outboard of the Denali fault. ARSZ – Alaska Range Suture Zone; BRF – Border Ranges Fault; DF – Denali fault; HCF – Hines Creek fault; pNA – parautochthonous North America; TF – Tintina fault; YT – Yukon-Tanana; WCT/AX – Wrangellia composite Terrane (includes Alexander).

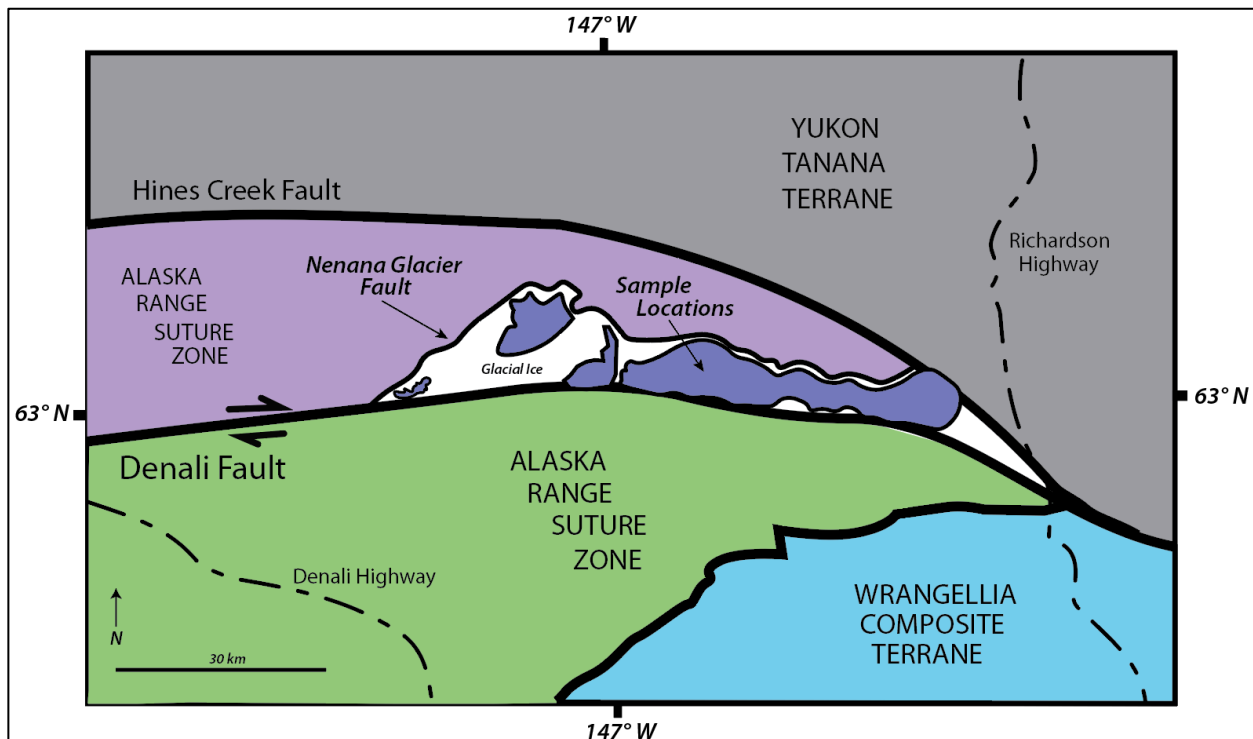


Figure 26: Simplified geologic map of the eastern Alaska Range showing sample locations relative to the Hines Creek fault and the Nenana Glacier fault. The proposed location of the Nenana Glacier fault is from Nokleberg and Richter, 2007.

VII. Conclusion

Rocks to the north of the Denali fault in the eastern Alaska Range are not interpreted to have sediment sourced from parautochthonous North America, as would be expected based on geographic location. Two of my samples appear to have sediment from the southern portion of the Alexander terrane, and two of my samples have a signature suggesting a source from the Endicott Arm of southeastern Yukon Tanana as the protolith. The fact that these rocks are located within 30 kilometers of one another along strike and yet have different terranes as source

areas could be a result of the fact that all samples were collected within one kilometer of the Denali fault, and may be separated by unmapped strands of this fault. If these correlations with southeastern Yukon Tanana and southern Alexander are correct, this requires >1000 kilometers of transport, which requires slip on a separate structure from the active trace of Denali fault. These results also imply my field area in the eastern Alaska Range is south of the original suture between the Wrangellia composite terrane and the North American margin.

VIII. References

- Aleinikoff, J. N., Dusel-Bacon, C., & Foster, H. L. (1986). Geochronology of augen gneiss and related rocks, Yukon-Tanana terrane, east-central Alaska. *Geological Society of America Bulletin*, 97(5), 626-637.
- Beard, J. S., & Barker, F. (1989). Petrology and tectonic significance of gabbros, tonalites, shoshonites, and anorthosites in a late Paleozoic arc-root complex in the Wrangellia terrane, southern Alaska. *The Journal of Geology*, 97(6), 667-683.
- Benowitz, J. A., Layer, P.W., Armstrong, P., Perry, S.E., Haeussler, P.J., Fitzgerald, P.G., VanLaningham, S. (2011). Spatial variations in focused exhumation along a continental-scale strike-slip fault: The Denali fault of the eastern Alaska Range. *Geosphere*, v. 7, no., 2, p. 1-13.
- Benowitz, J. A., Layer, P.W., Vanlaningham, S. (2014). Persistent long-term (c. 24 Ma) exhumation in the Eastern Alaska Range constrained by stacked thermochronology. *Geological Society of London Special Publications*, v. 378, p. 225 – 243.
- Benowitz, J. A., Roeske, S. M., Regan, S. P., Waldien, T. S., Elliott, J. L., & O'Sullivan, P. B. (2022). Large-scale, crustal-block vertical extrusion between the Hines Creek and Denali faults coeval with slip localization on the Denali fault since ca. 45 Ma, Hayes Range, Alaska, USA. *Geosphere*, 18(3), 1030-1054.
- Beranek, L. P., van Staal, C. R., McClelland, W. C., Israel, S., & Mihalynuk, M. G. (2013a). Baltic crustal provenance for Cambrian–Ordovician sandstones of the Alexander terrane, North American Cordillera: evidence from detrital zircon U–Pb geochronology and Hf isotope geochemistry. *Journal of the Geological Society*, 170(1), 7-18.
- Beranek, L. P., van Staal, C. R., McClelland, W. C., Israel, S., & Mihalynuk, M. G. (2013b). Detrital zircon Hf isotopic compositions indicate a northern Caledonian connection for the Alexander terrane. *Lithosphere*, 5(2), 163-168.
- Beranek, L. P., van Staal, C. R., McClelland, W. C., Joyce, N., & Israel, S. (2014). Late Paleozoic assembly of the Alexander-Wrangellia-Peninsular composite terrane, Canadian and Alaskan Cordillera. *Geological Society of America Bulletin*, 126(11-12), 1531-1550.
- Bradley, D. C., Dumoulin, J., Layer, P., Sunderlin, D., Roeske, S., McClelland, B., ... & Kusky, T. (2003). Late Paleozoic orogeny in Alaska's Farewell terrane. *Tectonophysics*, 372(1-2), 23-40.
- Brewer, W. M. (1982). Stratigraphy, structure, and metamorphism of the Mount Deborah area, central Alaska Range, Alaska [Ph.D. thesis]: Madison, University of Wisconsin, 318 p.

- Busby, C.J., Pavlis, T.L., Roeske, S.M., and Tikoff, B. (2023). The North American Cordillera during the Mesozoic to Paleogene: Selected questions and controversies, in Whitmeyer, S.J., Williams, M.L., Kellett, D.A., and Tikoff, B., eds., Laurentia: Turning Points in the Evolution of a Continent: Geological Society of America Memoir 220, p. 635–658, [https://doi.org/10.1130/2022.1220\(31\)](https://doi.org/10.1130/2022.1220(31)).
- Colpron, M., Nelson, J.L. and Murphy, D.C. (2007). Northern Cordilleran terranes and their interactions through time. *GSA Today*, v. 17 no. 4/5, p.4.
- Csejtey, B., Mullen, M. W., Cox, D. P., & Stricker, G. D. (1992). Geology and geochronology of the Healy Quadrangle, south-central Alaska, U.S. Geological Survey Miscellaneous Investigations, Series Map 1961, 63 p., 2 sheets, scale 1:250,000.
- Dickinson, W. R. (2004). Evolution of the North American cordillera. *Annual Review of Earth and Planetary Science.*, 32, 13-45.
- Dumoulin, J. A., Jones, J. V., Box, S. E., Bradley, D. C., Ayuso, R. A., & O'Sullivan, P. (2018). The Mystic subterrane (partly) demystified: New data from the Farewell terrane and adjacent rocks, interior Alaska. *Geosphere*, 14(4), 1501-1543.
- Dusel-Bacon, C., Aleinikoff, J. N., Moore, T. E., & Dumoulin, J. A. (1996). U-Pb zircon and titanite ages for augen gneiss from the Divide Mountain area, eastern Yukon-Tanana upland, Alaska, and evidence for the composite nature of the Fiftymile Batholith. *US Geological Survey Bulletin*, 2152, 131-141.
- Dusel-Bacon, C., Holm-Denoma, C. S., Jones, J. V., Aleinikoff, J. N., & Mortensen, J. K. (2017). Detrital zircon geochronology of quartzose metasedimentary rocks from paraautochthonous North America, east-central Alaska. *Lithosphere*, 9(6), 927-952.
- Elliott, J. L., Larsen, C. F., Freymueller, J. T., & Motyka, R. J. (2010). Tectonic block motion and glacial isostatic adjustment in southeast Alaska and adjacent Canada constrained by GPS measurements. *Journal of Geophysical Research: Solid Earth*, 115(B9).
- Gehrels, G. E., Butler, R. F., & Bazard, D. R. (1996). Detrital zircon geochronology of the Alexander terrane, southeastern Alaska. *Geological Society of America Bulletin*, 108(6), 722-734.
- Gehrels, G., Rusmore, M., Woodsworth, G., Crawford, M., Andronicos, C., Hollister, L., ... & Girardi, J. (2009). U-Th-Pb geochronology of the Coast Mountains batholith in north-coastal British Columbia: Constraints on age and tectonic evolution. *Geological Society of America Bulletin*, 121(9-10), 1341-1361.
- Gehrels, G. E., & Saleeby, J. B. (1987). Geologic framework, tectonic evolution, and displacement history of the Alexander terrane. *Tectonics*, 6(2), 151-173.
- Gehrels, G., Valencia, V., & Pullen, A. (2006). Detrital zircon geochronology by laser-ablation multicollector ICPMS at the Arizona LaserChron Center. *The Paleontological Society Papers*, 12, 67-76.
- Gehrels, G. E., Valencia, V. A., & Ruiz, J. (2008). Enhanced precision, accuracy, efficiency, and spatial resolution of U-Pb ages by laser ablation–multicollector–inductively coupled plasma–mass spectrometry. *Geochemistry, Geophysics, Geosystems*, 9(3). 1-13.
- George, S. W. M., Nelson, J. L., Alberts, D., Greig, C. J., & Gehrels, G. E. (2021). Triassic–Jurassic accretionary history and tectonic origin of Stikinia from U-Pb geochronology and Lu-Hf isotope analysis, British Columbia. *Tectonics*, 40(4), e2020TC006505.
- Giesler, D., Gehrels, G., Pecha, M., White, C., Yokelson, I., & McClelland, W. C. (2016). U-Pb and Hf isotopic analyses of detrital zircons from the Taku terrane, southeast Alaska. *Canadian Journal of Earth Sciences*, 53(10), 979-992.

- Greene, A. R., Scoates, J. S., Weis, D., Katvala, E. C., Israel, S., & Nixon, G. T. (2010). The architecture of oceanic plateaus revealed by the volcanic stratigraphy of the accreted Wrangellia oceanic plateau. *Geosphere*, 6(1), 47-73.
- Haeussler, P. J., Freymueller, J. T., Wesson, R. L., & Ekström, G. (2008). An overview of the neotectonics of interior Alaska: Far-field deformation from the Yakutat microplate collision. *Active Tectonics and Seismic Potential of Alaska: American Geophysical Union Geophysical Monograph*, 179, 83-108.
- Hickman, R. G., Craddock, C., & Sherwood, K. W. (1978). The Denali fault system and the tectonic development of southern Alaska. *Tectonophysics*, 47(3-4), 247-273.
- Keough, B. M., & Ridgway, K. D. (2021). Tectonic Growth of the Late Paleozoic-Middle Mesozoic Northwestern Margin of Laurentia and Implications for the Farewell Terrane: Stratigraphic, Structural, and Provenance Records from the Central Alaska Range. *Tectonics*, 40(7), e2021TC006764.
- Lanphere, M. A. (1978). Displacement history of the Denali fault system, Alaska and Canada. *Canadian Journal of Earth Sciences*, 15(5), 817-822.
- Malkowski, M. A., & Hampton, B. A. (2014). Sedimentology, U-Pb detrital geochronology, and Hf isotopic analyses from Mississippian–Permian stratigraphy of the Mystic subterrane, Farewell terrane, Alaska. *Lithosphere*, 6(5), 383-398.
- McClelland, W. C., Kusky, T., Bradley, D. C., Dumoulin, J., & Harris, A. G. (1999). The nature of Nixon Fork “basement,” west-central Alaska. In *Geological Society of America, Abstracts with Programs* (Vol. 31, No. 6, pp. A-78).
- Murchey, B., Jones, D. L., & Holdsworth, B. K. (1983). Distribution, age, and depositional environments of radiolarian chert in western North America. In *Developments in Sedimentology* (Vol. 36, pp. 109-125). Elsevier.
- Murphy, D. C. (2006). The three ‘Windy McKinley’ terranes of Stevenson ridge (115Jk), western Yukon. *Yukon Exploration and Geology*, 223-236.
- Nelson, J., & Gehrels, G. (2007). Detrital zircon geochronology and provenance of the southeastern Yukon–Tanana terrane. *Canadian Journal of Earth Sciences*, 44(3), 297-316.
- Nokleberg, W. J., Aleinikoff, J. N., Lange, I. M., Silva, S. R., Miyaoka, R. T., Schwab, C. E., & Zehner, R. E. (1992). Preliminary geologic map of the Mount Hayes quadrangle, eastern Alaska Range, Alaska. U.S. Geological Survey Open File Report 92-594, 39p., 1 sheet, scale 1:250,000.
- Nokleberg, W. J., Jones, D. L., & Silberling, N. J. (1985). Origin and tectonic evolution of the Maclarens and Wrangellia terranes, eastern Alaska Range, Alaska. *Geological Society of America Bulletin*, 96(10), 1251-1270.
- Nokleberg, W. J., Richter, D. H. (2007). Origin of narrow terranes and adjacent major terranes occurring along the Denali fault in the Eastern and Central Alaska Range, Alaska. *The Geological Society of America Special Paper* 431, p. 129 – 154.
- Pecha, M. E., Gehrels, G. E., McClelland, W. C., Giesler, D., White, C., & Yokelson, I. (2016). Detrital zircon U-Pb geochronology and Hf isotope geochemistry of the Yukon-Tanana terrane, Coast Mountains, southeast Alaska. *Geosphere*, 12(5), 1556-1574.
- Plattner, C., Malservisi, R., Dixon, T. H., LaFemina, P., Sella, G. F., Fletcher, J., & Suarez-Vidal, F. (2007). New constraints on relative motion between the Pacific Plate and Baja California microplate (Mexico) from GPS measurements. *Geophysical Journal International*, 170(3), 1373-1380.

- Regan, S. P., Benowitz, J. A., Waldien, T. S., Holland, M. E., Roeske, S. M., O'Sullivan, P., & Layer, P. (2021). Long distance plutonic relationships demonstrate 33 million years of strain partitioning along the Denali fault. *Terra Nova*, 33(6), 630-640.
- Ridgway, K. D., Trop J. M., Nokleberg, W. J., Davidson, C. M., Eastman K. R. (2002). Mesozoic and Cenozoic tectonics of the eastern and central Alaska Range: Progressive basin development and deformation in a suture zone. *GSA Bulletin*, v. 114, no. 12, p. 1480 – 1504.
- Romero, M. C., Ridgway, K. D., Gehrels, G. E. (2020). Geology, U-Pb geochronology, and Hf isotope geochemistry across the Mesozoic Alaska Range suture zone (south-central Alaska): Implications for Cordilleran Collisional Processes and Tectonic Growth of North America. *Tectonics*, 39, e2019TC005946.
- Saylor, J. E., & Sundell, K. E. (2016). Quantifying comparison of large detrital geochronology data sets. *Geosphere*, 12(1), 203-220.
- Schoene, B. (2014). 4.10-U–Th–Pb Geochronology. *Treatise on geochemistry*, 4, 341-378.
- Sherwood, K. W., & Craddock, C. (1979). *General geology of the central Alaska Range between the Nenana River and Mount Deborah*. State of Alaska, Department of Natural Resources, Division of Geological and Geophysical Surveys.
- Sundell, K. E., Gehrels, G. E., & Pecha, M. E. (2021). Rapid U-Pb geochronology by laser ablation multi-collector ICP-MS. *Geostandards and Geoanalytical Research*, 45(1), 37-57.
- Tait, L. D. (2017). Strain and Vorticity Analysis of Mid-Crustal Rocks Exhumed Along the Denali Fault in the Eastern Alaska Range. [M.S. thesis]: Davis, California, University of California, 76 p.
- Till, A. B., Harris, A. G., Wardlaw, B. R., & Mullen, M. (2007). Upper Triassic continental margin strata of the central Alaska Range: Implications for paleogeographic reconstruction, *Special Papers - Geological Society of America*, 431, 191-205.
- Tochilin, C. J., Gehrels, G. E., Nelson, J., & Mahoney, J. B. (2014). U-Pb and Hf isotope analysis of detrital zircons from the Banks Island assemblage (coastal British Columbia) and southern Alexander terrane (southeast Alaska). *Lithosphere*, 6(3), 200-215.
- Trop, J. M., Ridgway, K. D., Manuszak, J. D., & Layer, P. (2002). Mesozoic sedimentary-basin development on the allochthonous Wrangellia composite terrane, Wrangell Mountains basin, Alaska: A long-term record of terrane migration and arc construction. *Geological Society of America Bulletin*, 114(6), 693-717.
- Vermeesch, P. (2018). IsoplotR: A free and open toolbox for geochronology. *Geoscience Frontiers*, 9(5), 1479-1493.
- Wahrhaftig, C., Turner, D. L., Weber, F. R., & Smith, T. E. (1975). Nature and timing of movement on Hines Creek strand of Denali fault system, Alaska. *Geology*, 3(8), 463-466.
- Waldien, T. S., Roeske, S. M., Benowitz, J. A., Allen, W. K., Ridgway, K. D., & O'Sullivan, P. B. (2018). Late Miocene to Quaternary evolution of the McCallum Creek thrust system, Alaska: Insights for range-boundary thrusts in transpressional orogens. *Geosphere*, 14(6), 2379-2406.
- Waldien, T. S., Roeske, S. M., & Benowitz, J. A. (2021b). Tectonic underplating and dismemberment of the Maclarens-Kluane schist records Late Cretaceous terrane accretion polarity and ~ 480 km of Post-52 Ma dextral displacement on the Denali Fault. *Tectonics*, 40(10), e2020TC006677.

- Waldien, T. S., Roeske, S. M., Benowitz, J. A., Twelker, E., & Miller, M. S. (2021a). Oligocene-Neogene lithospheric-scale reactivation of Mesozoic terrane accretionary structures in the Alaska Range suture zone, southern Alaska, USA. *Geological Society of America Bulletin*, 133(3-4), 691-716.
- White, C., Gehrels, G. E., Pecha, M., Giesler, D., Yokelson, I., McClelland, W. C., & Butler, R. F. (2016). U-Pb and Hf isotope analysis of detrital zircons from Paleozoic strata of the southern Alexander terrane (southeast Alaska). *Lithosphere*, 8(1), 83-96.
- Wilson, F.H., Dover, J.H., Bradley, D.C., Weber, F.R., Bundtzen, T.K., and Haeussler, P.J. (1998). Geologic map of Central (interior) Alaska: U.S. Geological Survey Open-File Report 98-133-A, 62 p., 3 sheets.

IX. Appendix

Appendix A: Filtered U-Pb detrital zircon data from samples collected in the eastern Alaska Range

Sample	MDA	N = total grains analyzed	N = total number of ages removed	N = filtered ages	N = ages removed due to Pb loss (U content > 5,000 ppm)	N = ages removed due to high percent error	N = suspect metamorphic grains (high U/Th)	N = suspect neocrystalline grains
15LT17	246.08 +/- 3.79	108	9	99	0	8	1	0
21BG32	259.8 +/- 2.23	266	196	70	0	3	3	190
10CH01b	275.15 +/- 1.79	142	7	135	0	3	1	3
19CSR46	321.9 +/- 2.43	286	9	277	0	0	9	0
15LT03	326.84 +/- 2.43	71	46	25	0	2	6	38
21BG24	362.95 +/- 3.42	66	5	61	1	1	3	0
21BG08		114	112	2	0	3	15	94

Appendix B: Geologic sketch of the eastern Alaska Range including structural data, rock units, and sample locations

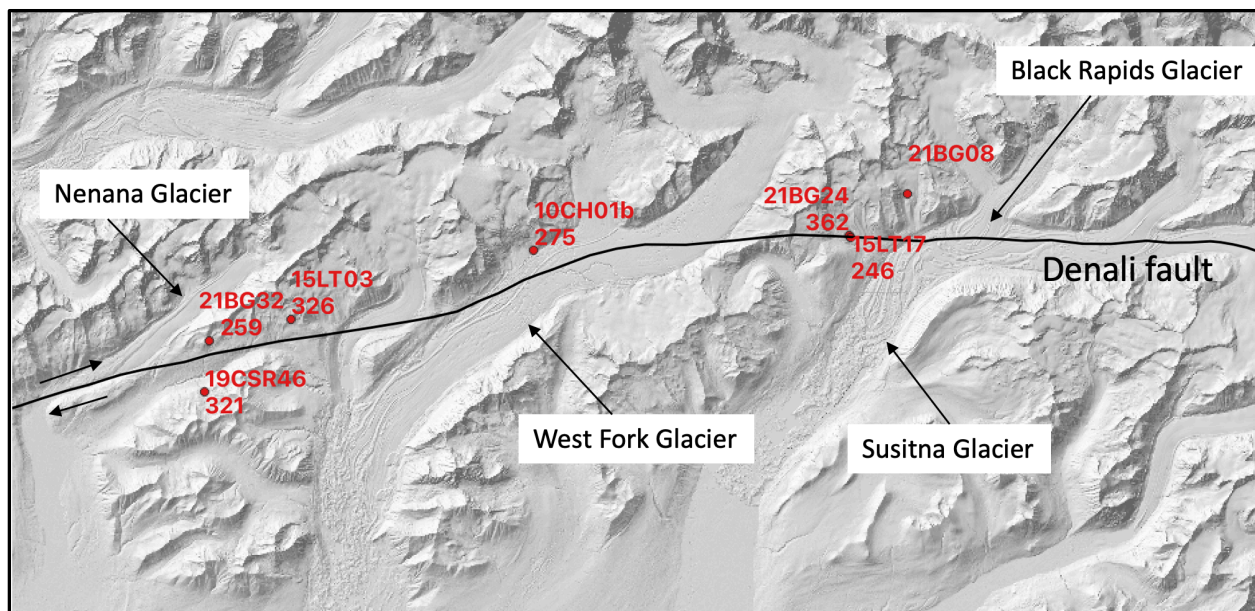


Figure B1: Overview map for figures B2 and B3. Red circles are sample locales. The first line reports the sample number; the second line reports the MDA for that sample

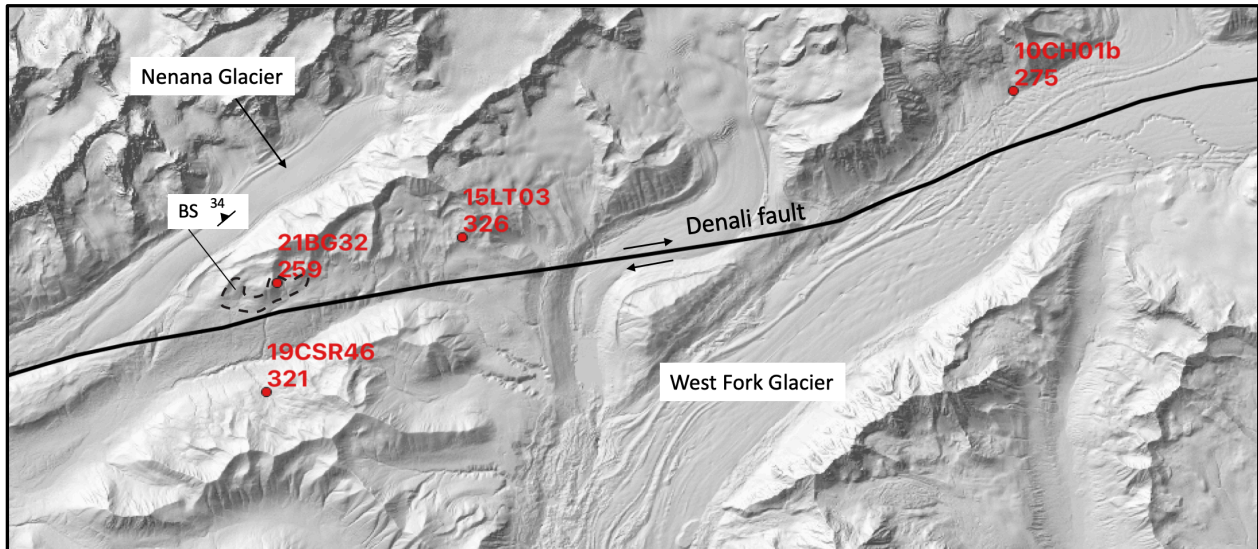


Figure B2: Geologic sketch of the eastern Alaska Range in the proximity of the Nenana Glacier. Red circles are sample locales. The first line reports the sample number; the second line reports the MDA for that sample. Typical strike and dip of foliation is reported for each locale. BS – biotite-quartz schist; GSS – garnet-sillimanite schist; CARB – carbonate/calcschist; OR – orthogneiss; UM – ultramafic

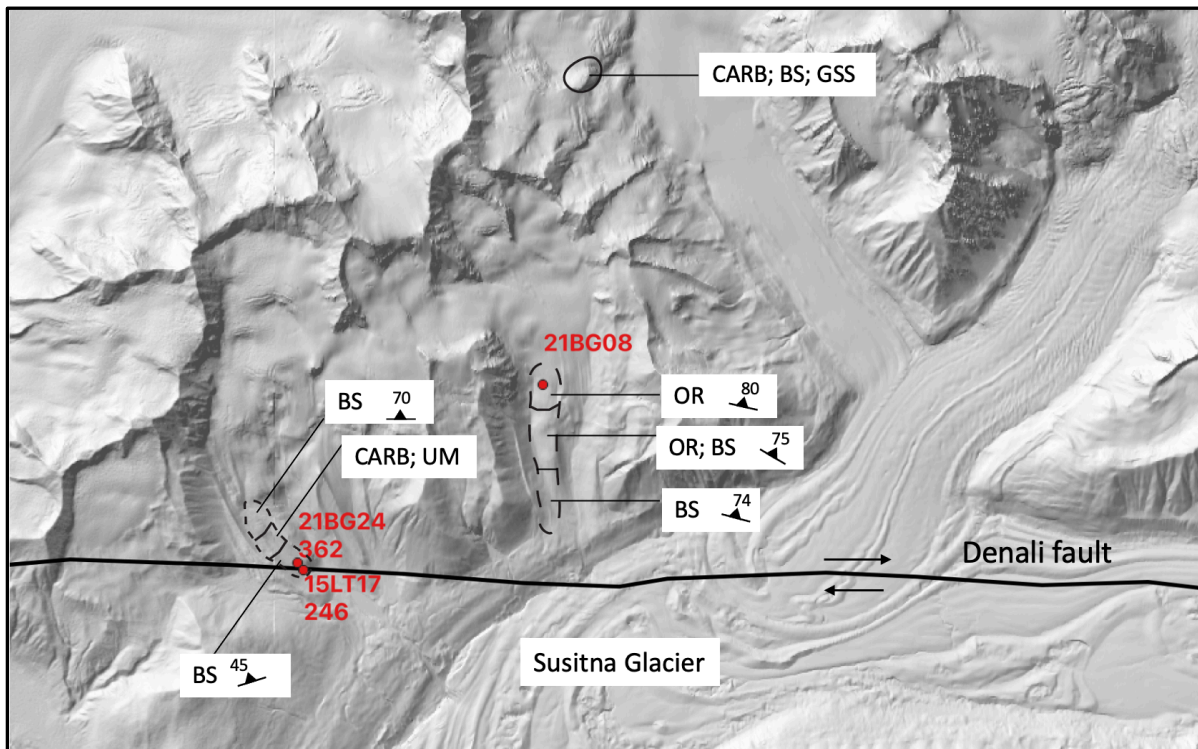


Figure B3: Geologic sketch of the eastern Alaska Range in the proximity of the Susitna Glacier. Red circles are sample locales. The first line reports the sample number; the second line reports

the MDA for that sample. Typical strike and dip of foliation is reported for each locale. BS – biotite-quartz schist; GSS – garnet-sillimanite schist; CARB – carbonate/calc-schist; OR – orthogneiss; UM – ultramafic

Appendix C: U-Pb detrital zircon data from samples collected in the eastern Alaska Range

Key

- % Error > 3
- U/Th > 10
- U > 5,000 ppm
- suspect neo-crystalline
- ages used for MDA

Sample 15LT17

Analysis	U (ppm)	Isotope ratios						Apparent ages (Ma)									Conc (%)	% Error		
		206Pb 204Pb	U/Th	206Pb* 207Pb*	± (%)	207Pb* 235U	± (%)	206Pb* 238U	± (%)	error corr.	206Pb* 238U	± (Ma)	207Pb* 235U	± (Ma)	206Pb* 207Pb*	± (Ma)	Best age (Ma)	± (Ma)		
Spot 101	340	6752	9.5	19.3445	2.9	0.0526	3.4	0.0077	1.7	0.50	49.6246	0.8	52.1	1.7	166.2	68.7	49.6	0.8	29.9	1.7
Spot 46	124	11513	6.8	16.4440	1.6	0.2984	2.8	0.0365	2.3	0.81	231.0227	5.2	265.2	6.6	578.8	35.9	231.0	5.2	39.9	2.3
Spot 66	104	9504	8.8	18.0734	1.4	0.2810	2.7	0.0380	2.4	0.87	240.6178	5.6	251.4	6.1	353.4	30.7	240.6	5.6	68.1	2.3
Spot 109	352	265832	2.8	18.0056	1.1	0.2914	2.9	0.0382	2.6	0.92	241.4202	6.2	259.7	6.6	427.9	25.4	241.4	6.2	56.4	2.6
Spot 43	457	28870	1.4	17.9824	1.7	0.2968	3.3	0.0392	2.9	0.86	248.1360	6.9	263.9	7.7	405.9	37.7	248.1	6.9	61.1	2.8
Spot 61	469	56801	5.2	18.0019	0.8	0.2994	2.8	0.0395	2.7	0.95	249.4272	6.6	265.9	6.6	413.7	19.0	249.4	6.6	60.3	2.6
Spot 103	199	2430	4.9	9.9236	6.6	0.5626	6.8	0.0430	1.6	0.23	271.5684	4.2	453.2	24.7	1524.6	124.2	271.6	4.2	17.8	1.5
Spot 12	1297	115681	2.1	17.1155	0.9	0.3451	3.6	0.0433	3.5	0.97	273.0637	9.4	301.0	9.5	523.7	19.7	273.1	9.4	52.1	3.4
Spot 72	731	27213	13.7	9.6660	1.0	0.6167	5.1	0.0436	5.0	0.98	275.2895	13.5	487.8	19.8	1670.1	18.0	275.3	13.5	16.5	4.9
Spot 71	228	1802338	3.4	17.0186	1.5	0.3839	1.9	0.0476	1.2	0.62	299.7245	3.4	329.9	5.2	548.6	31.9	299.7	3.4	54.6	1.1
Spot 59	106	215836	2.9	17.2122	1.5	0.4283	4.5	0.0538	4.3	0.94	338.0203	14.0	362.0	13.8	518.6	33.3	338.0	14.0	65.2	4.2
Spot 115	294	10951	1.7	16.4698	2.9	0.4477	3.4	0.0548	1.4	0.42	343.6819	4.8	375.6	10.7	577.7	67.7	343.7	4.8	59.5	1.4
Spot 36	1471	123393	5.0	17.9778	0.7	0.4373	1.1	0.0575	0.9	0.80	360.5325	3.1	368.3	3.4	417.7	14.9	360.5	3.1	86.3	0.9
Spot 121	229	88184	2.9	18.1350	0.9	0.4454	1.4	0.0589	1.0	0.75	368.6615	3.6	374.1	4.2	407.6	20.1	368.7	3.6	90.4	1.0
Spot 19	883	49020	1.0	17.5993	0.8	0.4576	1.8	0.0590	1.7	0.91	369.8234	6.0	382.6	5.9	460.3	16.8	369.8	6.0	80.3	1.6
Spot 70	468	150142	1.7	17.5661	1.9	0.4622	2.4	0.0592	1.6	0.64	370.8026	5.6	385.8	7.8	476.7	41.5	370.8	5.6	77.8	1.5
Spot 68	98	12039	4.8	17.7859	1.4	0.4510	1.8	0.0597	1.1	0.59	373.6512	3.8	378.0	5.6	404.4	32.1	373.7	3.8	92.4	1.0
Spot 21	77	4080	5.2	18.3658	1.6	0.4198	1.9	0.0602	1.0	0.51	376.6854	3.5	355.9	5.6	222.4	37.4	376.7	3.5	169.4	0.9
Spot 113	399	116210	2.0	17.7384	0.8	0.4674	1.3	0.0604	1.0	0.77	377.8665	3.6	389.4	4.1	458.5	18.1	377.9	3.6	82.4	1.0
Spot 62	557	123800	1.1	17.7403	0.8	0.4669	1.4	0.0605	1.1	0.81	378.5525	4.2	389.1	4.5	452.0	18.3	378.6	4.2	83.7	1.1
Spot 97	127	25857	3.1	17.7046	1.1	0.4658	1.5	0.0607	1.0	0.67	379.7436	3.8	388.3	5.0	439.5	25.4	379.7	3.8	86.4	1.0
Spot 92	437	53518	8.7	17.9702	0.7	0.4642	2.2	0.0611	2.1	0.94	382.1722	7.8	387.1	7.2	416.9	16.3	382.2	7.8	91.7	2.0
Spot 6	290	169440	3.3	17.9478	1.0	0.4705	1.6	0.0618	1.2	0.79	386.4862	4.7	391.5	5.1	421.3	21.5	386.5	4.7	91.7	1.2
Spot 55	66	4064	4.9	17.9904	1.7	0.4417	2.3	0.0620	1.6	0.69	387.6958	6.1	371.5	7.3	271.5	39.2	387.7	6.1	142.8	1.6
Spot 38	353	29091	2.1	18.0286	0.7	0.4690	1.1	0.0623	0.9	0.77	389.4749	3.3	390.5	3.7	396.4	16.2	389.5	3.3	98.2	0.9
Spot 102	279	135115	1.7	17.7845	0.9	0.4831	1.6	0.0626	1.3	0.84	391.3934	5.1	400.2	5.3	451.5	19.0	391.4	5.1	86.7	1.3
Spot 41	111	86236	3.0	17.8129	1.2	0.4871	2.0	0.0634	1.6	0.81	396.4830	6.3	402.9	6.7	440.1	26.6	396.5	6.3	90.1	1.6
Spot 31	350	42041	2.1	17.4772	0.6	0.4980	3.3	0.0639	3.2	0.98	399.3577	12.4	410.3	11.1	472.6	14.0	399.4	12.4	84.5	3.1
Spot 60	147	32939	4.4	18.1265	1.0	0.4835	1.4	0.0644	1.0	0.70	402.2253	3.9	400.4	4.7	390.1	22.7	402.2	3.9	103.1	1.0
Spot 56	156	29069	2.1	17.8899	1.1	0.4892	1.3	0.0644	0.7	0.54	402.3796	2.7	404.3	4.3	415.5	24.4	402.4	2.7	96.8	0.7
Spot 86	366	39309	3.0	18.1047	0.7	0.4863	1.4	0.0645	1.2	0.85	403.0906	4.7	402.4	4.7	398.4	16.3	403.1	4.7	101.2	1.2
Spot 17	1390	421715	1.6	17.9372	0.5	0.4934	1.1	0.0646	1.0	0.88	403.7443	3.9	407.2	3.8	427.0	12.2	403.7	3.9	94.6	1.0
Spot 39	321	185112	2.3	17.5736	0.8	0.5040	2.8	0.0647	2.7	0.96	404.1902	10.5	414.4	9.5	471.7	17.5	404.2	10.5	85.7	2.6
Spot 120	823	129168	2.1	17.8731	0.7	0.4978	1.2	0.0648	1.0	0.83	404.4514	3.9	410.2	4.0	442.7	14.8	404.5	3.9	91.4	1.0
Spot 108	76	36467	2.6	17.5599	1.5	0.5044	1.7	0.0648	0.9	0.52	404.8662	3.5	414.7	5.8	469.6	32.5	404.9	3.5	86.2	0.9
Spot 52	140	14801	3.7	18.0238	1.1	0.4850	1.4	0.0649	0.7	0.54	405.2407	2.9	401.5	4.5	380.1	25.5	405.2	2.9	106.6	0.7
Spot 90	107	53493	3.3	17.8457	1.3	0.4968	1.8	0.0649	1.2	0.68	405.2782	4.8	409.5	6.0	433.6	29.2	405.3	4.8	93.5	1.2
Spot 110	626	67086	0.9	17.8642	0.9	0.4985	1.6	0.0650	1.3	0.84	405.6848	5.2	410.7	5.3	439.0	19.2	405.7	5.2	92.4	1.3
Spot 35	158	29733	3.9	16.2917	2.6	0.5426	2.9	0.0651	1.2	0.41	406.3026	4.7	440.1	10.3	621.1	56.5	406.3	4.7	65.4	1.2
Spot 122	227	14116	2.4	18.0321	0.9	0.4878	1.3	0.0651	0.9	0.67	406.6293	3.5	403.4	4.4	384.9	21.7	406.6	3.5	105.6	0.9
Spot 124	149	66047	3.4	17.8119	1.2	0.5022	1.5	0.0652	0.9	0.60	407.4093	3.6	413.2	5.2	445.6	27.0	407.4	3.6	91.4	0.9
Spot 75	170	36477	3.8	17.9029	1.3	0.4988	3.4	0.0656	3.1	0.92	409.3567	12.4	410.9	11.4	419.4	29.4	409.4	12.4	97.6	3.0
Spot 111	84	8130	2.2	18.0660	1.1	0.4834	1.7	0.0656	0.8	0.47	409.4044	3.2	400.4	5.7	348.7	34.2	409.4	3.2	117.4	0.8
Spot 95	283	16634	2.2	17.9445	0.9	0.4947	1.3	0.0657	1.0	0.72	410.1513	3.8	408.1	4.5	396.5	20.8	410.2	3.8	103.5	0.9
Spot 50	148	28104	3.4	17.9551	1.2	0.4980	1.4	0.0658	0.8	0.56	410.7665	3.2	410.4	4.8	408.0	26.5	410.8	3.2	100.7	0.8
Spot 45	203	22546	1.8	17.4245	1.0	0.5135	1.5	0.0659	1.1	0.71	411.3751	4.2	420.8	5.1	473.0	23.2	411.4	4.2	87.0	1.0
Spot 7	771	71614	2.4	17.4737	0.7	0.5147	1.6	0.0659	1.4	0.90	411.6698	5.7	421.6	5.5	476.4	15.5	411.7	5.7	86.4	1.4
Spot 74	188	48412	1.9	16.5403	2.0	0.5454	2.3	0.0660	1.1	0.50	412.3020	4.6	442.0	8.1	599.4	42.3	412.3	4.6	68.8	1.1
Spot 11	831	135136	4.4	17.7172	0.9	0.5098	3.6	0.0662	3.5	0.97	412.9858	14.0	418.3	12.4	447.9	19.0	413.0	14.0	92.2	3.4
Spot 51	206	23215	2.2	17.7648	1.4	0.5058	4.1	0.0662	3.8	0.94	413.4253	15.3	415.6	13.9	427.8	31.9	413.4	15.3	96.6	3.7
Spot 79	366	20968</																		

Spot 80	127	30741	2.5	17.9145	1.1	0.5063	1.2	0.0667	0.7	0.53	416.2313	2.7	416.0	4.3	414.4	23.7	416.2	2.7	100.4	0.6
Spot 76	93	15738	3.6	18.0547	1.2	0.4983	1.4	0.0667	0.8	0.55	416.4643	3.2	410.6	4.9	377.4	27.0	416.5	3.2	110.3	0.8
Spot 32	205	264649	3.1	17.9180	0.8	0.5102	1.1	0.0668	0.9	0.75	416.8025	3.5	418.6	3.9	428.6	16.8	416.8	3.5	97.3	0.8
Spot 87	65	42061	4.1	17.8839	1.1	0.5103	1.6	0.0669	1.0	0.67	417.1758	4.2	418.7	5.3	427.0	25.6	417.2	4.2	97.7	1.0
Spot 18	227	20872	2.0	18.0551	0.8	0.5010	1.1	0.0669	0.8	0.71	417.1936	3.2	412.3	3.8	385.3	17.7	417.2	3.2	108.3	0.8
Spot 123	172	61550	2.5	18.1153	1.0	0.5060	1.3	0.0669	0.9	0.70	417.3290	3.8	415.8	4.6	407.2	21.4	417.3	3.8	102.5	0.9
Spot 64	329	133359	1.3	17.9627	1.0	0.5102	1.9	0.0669	1.6	0.84	417.5926	6.5	418.6	6.5	424.1	23.0	417.6	6.5	98.5	1.6
Spot 126	142	63776	3.7	18.1329	1.0	0.5075	1.2	0.0671	0.8	0.64	418.4913	3.2	416.7	4.2	407.0	21.3	418.5	3.2	102.8	0.8
Spot 81	53	8388	2.5	17.7436	1.2	0.5038	1.5	0.0672	0.9	0.59	419.4073	3.6	414.3	5.1	385.7	27.1	419.4	3.6	108.7	0.9
Spot 106	151	76099	2.3	17.5637	0.8	0.5251	1.2	0.0672	0.9	0.72	419.5210	3.5	428.5	4.2	477.3	18.5	419.5	3.5	87.9	0.8
Spot 26	643	330073	2.2	17.7193	0.6	0.5201	1.1	0.0672	0.9	0.82	419.5340	3.8	425.2	4.0	456.3	14.3	419.5	3.8	91.9	0.9
Spot 3	120	8915	3.6	17.4823	1.2	0.5124	2.0	0.0673	0.8	0.37	420.1475	3.1	420.1	7.0	419.7	42.4	420.1	3.1	100.1	0.7
Spot 10	83	10317	1.5	18.3124	1.3	0.4902	2.0	0.0674	0.7	0.37	420.2086	3.0	405.1	6.6	319.7	41.7	420.2	3.0	131.4	0.7
Spot 94	237	68881	3.0	18.0768	0.8	0.5107	1.1	0.0675	0.8	0.71	421.0328	3.2	418.9	3.7	407.1	17.1	421.0	3.2	103.4	0.7
Spot 30	204	24406	2.0	17.9961	0.9	0.5084	1.3	0.0675	1.0	0.75	421.0761	4.0	417.4	4.5	396.9	19.5	421.1	4.0	106.1	1.0
Spot 98	252	26090	1.1	17.7359	1.0	0.5175	1.3	0.0675	0.8	0.63	421.1727	3.4	423.5	4.6	436.1	22.8	421.2	3.4	96.6	0.8
Spot 73	880	59106	2.1	17.6332	0.8	0.5237	3.7	0.0676	3.6	0.98	421.4481	14.7	427.6	12.9	461.1	17.1	421.4	14.7	91.4	3.5
Spot 44	196	65855	2.6	17.9156	0.7	0.5155	1.3	0.0676	1.1	0.85	421.5056	4.3	422.2	4.3	425.8	14.7	421.5	4.3	99.0	1.0
Spot 1	65	6509	2.7	17.3175	1.2	0.5146	1.6	0.0677	0.9	0.59	422.1950	3.9	421.6	5.6	418.1	29.1	422.2	3.9	101.0	0.9
Spot 2	110	33419	2.6	18.0738	1.3	0.5090	1.6	0.0677	1.0	0.60	422.4302	3.9	417.8	5.5	392.3	28.8	422.4	3.9	107.7	0.9
Spot 54	247	37475	2.2	17.8735	0.8	0.5169	1.1	0.0678	0.8	0.70	422.9029	3.3	423.1	4.0	424.0	18.2	422.9	3.3	99.7	0.8
Spot 125	107	166111	2.8	17.7815	1.1	0.5176	1.6	0.0679	0.8	0.53	423.5103	3.4	423.6	5.4	423.8	29.5	423.5	3.4	99.9	0.8
Spot 93	346	72156	1.6	17.8873	0.8	0.5198	1.4	0.0680	1.1	0.83	423.8832	4.7	425.0	4.8	430.9	17.3	423.9	4.7	98.4	1.1
Spot 117	142	31648	2.7	17.7152	1.0	0.5242	1.3	0.0680	0.8	0.60	424.0725	3.1	428.0	4.4	449.0	22.7	424.1	3.1	94.5	0.7
Spot 91	245	49519	2.7	17.8614	0.9	0.5197	1.2	0.0680	0.8	0.68	424.1095	3.4	425.0	4.3	429.7	20.3	424.1	3.4	98.7	0.8
Spot 8	96	6434	3.3	17.1976	1.3	0.5214	1.6	0.0682	0.9	0.58	425.1121	3.9	426.1	5.6	431.4	29.4	425.1	3.9	98.5	0.9
Spot 83	82	13681	3.6	18.1273	1.4	0.5064	1.6	0.0682	0.8	0.49	425.4030	3.2	416.0	5.5	364.1	31.6	425.4	3.2	116.8	0.8
Spot 48	194	50985	2.5	17.7396	1.0	0.5259	1.3	0.0683	0.9	0.67	426.0377	3.7	429.1	4.7	445.5	22.3	426.0	3.7	95.6	0.9
Spot 67	135	23812	2.2	16.9016	1.2	0.5496	1.6	0.0683	1.1	0.68	426.2048	4.5	444.8	5.8	542.0	26.0	426.2	4.5	78.6	1.1
Spot 58	266	23716	2.1	17.7612	0.8	0.5223	1.3	0.0684	1.0	0.77	426.6374	4.1	426.7	4.6	427.1	18.7	426.6	4.1	99.9	1.0
Spot 116	155	12602	2.7	17.9988	0.8	0.5129	1.4	0.0685	0.8	0.62	426.9397	3.5	420.4	4.7	384.7	23.8	426.9	3.5	111.0	0.8
Spot 53	62	14221	3.7	17.7690	1.2	0.5202	1.6	0.0686	1.1	0.66	427.7667	4.4	425.3	5.5	411.6	26.7	427.8	4.4	103.9	1.0
Spot 69	102	55713	3.5	18.1415	1.2	0.5181	1.4	0.0687	0.7	0.53	428.4756	3.0	423.9	4.7	398.8	26.0	428.5	3.0	107.4	0.7
Spot 130	623	77628	1.7	17.5565	0.8	0.5382	1.4	0.0688	1.2	0.82	428.9785	4.8	437.2	5.0	480.9	17.6	429.0	4.8	89.2	1.1
Spot 84	137	51815	1.7	17.5038	0.9	0.5389	1.8	0.0691	1.6	0.87	430.5573	6.7	437.7	6.6	475.6	20.3	430.6	6.7	90.5	1.6
Spot 40	178	9422	2.5	18.0212	1.0	0.5129	1.4	0.0693	1.0	0.70	431.9778	4.2	420.4	5.0	357.3	23.3	432.0	4.2	120.9	1.0
Spot 13	56	7177	4.1	14.3229	3.8	0.6430	4.1	0.0693	1.5	0.36	432.0064	6.2	504.2	16.3	846.5	79.3	432.0	6.2	51.0	1.4
Spot 47	291	26429	2.0	17.7982	0.7	0.50303	1.1	0.0694	0.9	0.78	432.5746	3.7	432.0	4.0	429.1	15.8	432.6	3.7	100.8	0.9
Spot 9	187	75539	4.8	18.0027	1.1	0.5261	1.5	0.0694	1.0	0.69	432.7753	4.2	429.2	5.1	410.2	23.7	432.8	4.2	105.5	1.0
Spot 34	283	19998	1.6	18.2008	0.6	0.5160	1.0	0.0695	0.8	0.80	433.1320	3.4	422.5	3.5	364.8	13.7	433.1	3.4	118.7	0.8
Spot 4	180	49759	4.0	18.0250	0.8	0.5256	1.2	0.0695	0.8	0.71	433.4383	3.5	428.9	4.1	404.3	18.7	433.4	3.5	107.2	0.8
Spot 129	198	37157	2.0	17.9284	1.1	0.5321	1.7	0.0697	1.3	0.76	434.3113	5.4	433.2	5.9	427.2	24.1	434.3	5.4	101.7	1.2
Spot 37	119	1474232	2.5	17.6650	1.3	0.5404	1.5	0.0697	0.7	0.46	434.4198	2.9	438.7	5.3	461.1	29.4	434.4	2.9	94.2	0.7
Spot 107	89	38870	3.4	17.4541	1.3	0.5467	1.6	0.0698	1.0	0.59	434.9651	4.1	442.9	5.9	484.1	29.4	435.0	4.1	89.9	0.9
Spot 57	119	37048	2.1	18.1108	1.3	0.5293	1.8	0.0704	1.2	0.68	438.7729	5.1	431.4	6.2	392.0	28.8	438.8	5.1	111.9	1.2
Spot 127	130	9917	2.7	18.0301	1.0	0.5265	1.4	0.0708	1.0	0.70	440.8928	4.1	429.5	4.8	368.7	22.3	440.9	4.1	119.6	0.9
Spot 33	175	19706	2.4	17.8137	0.9	0.5369	1.2	0.0708	0.8	0.65	440.9950	3.4	436.3	4.4	411.9	21.0	441.0	3.4	107.1	0.8
Spot 100	214	33341	2.2	17.9724	0.7	0.5409	1.0	0.0713	0.8	0.76	443.9049	3.3	439.0	3.6	413.5	14.6	443.9	3.3	107.3	0.7
Spot 112	158	30037	3.5	17.5417	1.0	0.5548	1.5	0.0713	1.1	0.74	443.9954	4.9	448.1	5.6	469.2	23.0	444.0	4.9	94.6	1.1
Spot 128	970	204218	1.6	18.5540	2.0	0.5298	5.6	0.0714	5.3	0.94	444.8818	22.7	431.7	19.8	361.8	44.3	444.9	22.7	123.0	5.1
Spot 96	331	53104	1.3	17.2730	0.9	0.5778	1.2	0.0730	0.9	0.71	454.4611	3.8	463.0	4.6	505.8	19.2	454.5	3.8	89.8	0.8
Spot 49	544	140954	2.3	17.4564	0.6	0.5806	1.4	0.0740	1.3	0.91	460.3113	5.6	464.9	5.2	487.4	12.4	460.3	5.6	94.4	1.2
Spot 25	81	8868	3.2	17.0654	1.4	0.5856	1.7	0.0750	1.0	0.56	465.9545	4.4	468.1	6.5	478.5	31.8	466.0	4.4	97.4	0.9
Spot 88	159	28029	2.3	17.4933	1.0	0.5891	1.3	0.0757	0.9	0.64	470.5484	3.9	470.3	5.0	469.1	22.5	470.5	3.9	100.3	0.8
Spot 27	256	149009	1.0	8.5808	0.5	5.1127	2.8	0.3204	2.8	0.99	1791.8260	43.1	1838.2	23.7	1891.1					

Key
% Error > 3
U/Th > 10
U > 5,000 ppm
suspect neo-crystalline
ages used for MDA

Sample 21BG32

Analysis	U (ppm)	Isotope ratios										Apparent ages (Ma)									
		206Pb 204Pb	U/Th	206Pb* 207Pb*	± (%)	207Pb* 235U	± (%)	206Pb* 238U	± (%)	error corr.	206Pb* 238U	± (Ma)	207Pb* 235U	± (Ma)	206Pb* 207Pb*	± (Ma)	Best age (Ma)	± (Ma)	Conc (%)	% Error	
Spot 269	839	48364	1.8	20.4267	1.0	0.0621	3.7	0.0093	3.6	0.96	59.9529	2.1	61.2	2.2	110.4	24.0	60.0	2.1	54.3	3.5	
Spot 315	437	33305	4.4	20.2903	1.9	0.0641	2.1	0.0096	0.8	0.39	61.7372	0.5	63.1	1.3	115.9	45.9	61.7	0.5	53.2	0.8	
Spot 132	444	7104	3.2	20.6551	1.4	0.0614	2.1	0.0097	1.3	0.61	62.2118	0.8	60.5	1.2	NA	NA	62.2	0.8	1.3		
Spot 138	480	49223	4.8	19.6448	1.3	0.0674	2.5	0.0098	2.2	0.86	62.5648	1.4	66.2	1.6	199.2	29.6	62.6	1.4	31.4	2.2	
Spot 126	2414	85642	3.1	21.0463	0.6	0.0631	0.8	0.0098	0.6	0.72	62.6016	0.4	62.2	0.5	45.4	14.0	62.6	0.4	137.8	0.6	
Spot 234	2837	86624	5.4	20.0598	0.7	0.0663	1.1	0.0098	0.8	0.76	62.7542	0.5	65.2	0.7	154.9	17.2	62.8	0.5	40.5	0.8	
Spot 176	1040	29759	2.7	20.9900	0.9	0.0630	1.2	0.0098	0.8	0.64	62.8138	0.5	62.1	0.7	33.6	22.9	62.8	0.5	187.0	0.8	
Spot 116	359	6198	4.2	21.2185	1.2	0.0601	1.5	0.0098	0.9	0.57	62.9653	0.5	59.2	0.9	NA	NA	63.0	0.5	0.8		
Spot 182	375	63391	3.9	21.1537	1.3	0.0631	1.7	0.0098	1.0	0.62	62.9814	0.6	62.1	1.0	28.6	NA	63.0	0.6	220.5	1.0	
Spot 152	2436	56362	1.6	20.9031	1.0	0.0639	1.9	0.0098	1.7	0.86	63.1153	1.1	62.9	1.2	55.3	23.5	63.1	1.1	114.1	1.7	
Spot 233	689	653615	11.5	20.5173	0.8	0.0654	1.1	0.0099	0.7	0.65	63.2039	0.5	64.3	0.7	106.9	20.0	63.2	0.5	59.1	0.7	
Spot 228	1631	430408	1.8	20.8662	0.6	0.0644	0.9	0.0099	0.7	0.80	63.2236	0.5	63.3	0.6	67.8	13.2	63.2	0.5	93.3	0.7	
Spot 254	1235	46560	4.2	20.3843	1.5	0.0656	2.3	0.0099	1.7	0.73	63.2755	1.0	64.5	1.4	111.4	36.4	63.3	1.0	56.8	1.6	
Spot 117	1309	20938	4.5	20.9542	0.7	0.0637	1.5	0.0099	1.4	0.88	63.5985	0.9	62.7	0.9	28.3	17.8	63.6	0.9	224.6	1.3	
Spot 294	475	8570	3.6	20.2781	1.3	0.0645	1.5	0.0099	0.7	0.49	63.6412	0.5	63.5	0.9	56.8	30.6	63.6	0.5	111.9	0.7	
Spot 178	418	9086	2.2	20.9937	1.1	0.0625	1.4	0.0099	0.8	0.58	63.7953	0.5	61.5	0.9	NA	NA	63.8	0.5	0.8		
Spot 208	270	3548	2.7	20.6048	1.6	0.0602	1.9	0.0099	1.0	0.51	63.7997	0.6	59.3	1.1	NA	NA	63.8	0.6	1.0		
Spot 131	400	10933	3.1	20.6497	1.3	0.0640	1.7	0.0100	0.9	0.54	63.8424	0.6	63.0	1.0	31.8	NA	63.8	0.6	200.9	0.9	
Spot 252	505	31771	4.6	20.9751	0.9	0.0642	2.6	0.0100	2.5	0.93	63.9285	1.6	63.2	1.6	35.9	23.2	63.9	1.6	178.0	2.4	
Spot 63	570	13273	1.9	20.0608	1.0	0.0663	1.7	0.0100	1.0	0.57	64.0092	0.6	65.2	1.1	109.0	33.3	64.0	0.6	58.7	1.0	
Spot 91	791	99040	2.5	21.0008	0.9	0.0647	1.2	0.0100	0.8	0.62	64.0146	0.5	63.7	0.7	51.0	22.7	64.0	0.5	125.4	0.7	
Spot 207	622	4847	2.6	20.7352	1.1	0.0616	1.5	0.0100	1.0	0.66	64.0599	0.6	60.7	0.9	NA	NA	64.1	0.6	1.0		
Spot 105	351	49008	2.6	19.6789	1.3	0.0692	1.6	0.0100	0.9	0.58	64.1395	0.6	67.9	1.0	202.8	30.2	64.1	0.6	31.6	0.9	
Spot 238	1096	53722	2.8	21.1313	0.7	0.0642	1.2	0.0100	0.9	0.76	64.1469	0.6	63.2	0.7	28.5	18.0	64.1	0.6	224.8	0.9	
Spot 299	226	62085	3.3	20.2223	1.4	0.0672	1.9	0.0100	1.2	0.65	64.1565	0.8	66.1	1.2	135.5	33.5	64.2	0.8	47.4	1.2	
Spot 304	600	12296	1.8	20.3881	1.6	0.0655	1.9	0.0100	1.0	0.51	64.3941	0.6	64.4	1.2	66.2	39.4	64.4	0.6	97.3	1.0	
Spot 115	326	103606	4.4	20.6541	1.2	0.0665	1.5	0.0101	0.9	0.57	64.5765	0.6	65.3	1.0	93.7	29.3	64.6	0.6	68.9	0.9	
Spot 184	370	19259	3.0	20.8381	1.2	0.0650	1.5	0.0101	0.9	0.60	64.6093	0.6	63.9	1.0	37.4	29.7	64.6	0.6	172.9	0.9	
Spot 281	447	11503	3.4	21.4885	1.4	0.0624	2.0	0.0101	0.7	0.36	64.6424	0.5	61.5	1.2	NA	NA	64.6	0.5	0.7		
Spot 235	382	8417	2.0	19.8045	1.3	0.0671	1.5	0.0101	0.9	0.55	64.7009	0.5	65.9	1.0	110.0	30.3	64.7	0.5	58.8	0.8	
Spot 179	1463	9358	2.0	20.8667	0.6	0.0639	0.9	0.0101	0.7	0.72	64.7417	0.4	62.9	0.6	NA	NA	64.7	0.4	0.7		
Spot 52	358	11380	4.1	20.5080	1.4	0.0653	1.6	0.0101	0.7	0.44	64.8055	0.5	64.3	1.0	44.2	34.8	64.8	0.5	146.7	0.7	
Spot 58	296	5554	4.4	20.9776	1.9	0.0620	2.7	0.0101	1.0	0.36	64.8800	0.6	61.1	1.6	NA	NA	64.9	0.6	0.9		
Spot 247	862	71039	3.1	20.6289	0.8	0.0667	1.1	0.0101	0.7	0.63	64.8957	0.4	65.6	0.7	89.6	19.3	64.9	0.4	72.4	0.7	
Spot 308	375	8933	3.1	21.2212	1.6	0.0628	2.0	0.0101	1.0	0.52	64.9013	0.7	61.8	1.2	NA	NA	64.9	0.7	1.0		
Spot 83	1574	49076	3.8	20.7964	0.7	0.0661	0.9	0.0101	0.6	0.67	64.9280	0.4	65.0	0.6	67.8	15.5	64.9	0.4	95.8	0.6	
Spot 298	1706	69978	0.8	20.8112	0.4	0.0662	0.7	0.0101	0.5	0.81	64.9573	0.3	65.1	0.4	68.6	9.3	65.0	0.3	94.7	0.5	
Spot 135	526	6602	3.6	20.7543	1.0	0.0635	2.7	0.0101	0.7	0.27	64.9870	0.5	62.5	1.7	NA	NA	65.0	0.5	0.7		
Spot 285	288	15037	2.6	21.0355	1.3	0.0646	1.7	0.0101	1.0	0.56	65.0042	0.6	63.5	1.1	8.7	NA	65.0	0.6	750.8	1.0	
Spot 120	4251	193698	5.2	20.8037	0.5	0.0665	0.7	0.0101	0.6	0.76	65.0437	0.4	65.4	0.5	77.0	11.2	65.0	0.4	84.5	0.5	
Spot 127	735	19438	1.6	21.3442	1.0	0.0639	1.3	0.0101	0.8	0.61	65.0917	0.5	62.9	0.8	NA	NA	65.1	0.5	0.8		
Spot 183	1840	1426653	1.3	20.8905	0.6	0.0663	1.0	0.0101	0.8	0.80	65.1010	0.5	65.2	0.6	69.7	14.5	65.1	0.5	93.3	0.8	
Spot 143	604	12765	3.8	21.2083	0.9	0.0637	1.5	0.0102	0.6	0.42	65.1120	0.4	62.7	0.9	NA	NA	65.1	0.4	0.6		
Spot 85	729	11911	3.4	20.8724	1.0	0.0648	1.8	0.0102	0.8	0.47	65.1536	0.5	63.7	1.1	11.2	NA	65.2	0.5	579.5	0.8	
Spot 49	1738	26571	3.9	20.8736	0.7	0.0655	0.8	0.0102	0.5	0.55	65.1589	0.3	64.4	0.5	36.7	17.0	65.2	0.3	177.3	0.5	
Spot 114	209	5462	3.4	20.7827	1.5	0.0632	2.0	0.0102	0.9	0.44	65.2221	0.6	62.2	1.2	NA	NA	65.2	0.6	0.9		
Spot 266	287	6069	4.2	20.7423	1.2	0.0636	1.5	0.0102	0.8	0.53	65.2282	0.5	62.6	0.9	NA	NA	65.2	0.5	0.8		
Spot 283	235	2178	3.0	20.7195	1.1	0.0577	1.3	0.0102	0.6	0.46	65.2432	0.4	56.9	0.7	NA	NA	65.2	0.4	0.6		
Spot 142	786	11797	2.2	20.9028	0.9	0.0647	1.1	0.0102	0.7	0.61	65.2842	0.4	63.7	0.7	4.1	NA	65.3	0.4	1596.6	0.7	
Spot 112	407	7520	2.2	20.9067	1.2	0.0639	2.1	0.0102	0.9	0.43	65.2871	0.6	62.9	1.3	NA	NA	65.3	0.6	0.9		
Spot 267	971	101269	1.5	21.1093	0.7	0.0657	1.1	0.0102	0.8	0.78	65.2910	0.6	64.6	0.7	38.8	16.1	65.3	0.6	168.1	0.8	
Spot 148	328	15262	2.0	20.9930	1.3	0.0648	1.6	0.0102	0.9	0.56	65.3238	0.6	63.8	1.0	6.5	NA					

Spot 111	836	46349	3.0	21.1279	0.9	0.0655	1.2	0.0102	0.8	0.64	65.3731	0.5	64.4	0.8	30.1	22.3	65.4	0.5	217.2	0.8
Spot 311	143	4917	2.5	20.9155	2.2	0.0623	2.5	0.0102	1.0	0.39	65.3799	0.6	61.4	1.5	NA	NA	65.4	0.6	1.0	
Spot 305	303	117999	0.1	20.5976	0.5	0.0674	1.0	0.0102	0.9	0.86	65.4238	0.6	66.2	0.7	94.5	12.6	65.4	0.6	69.2	0.9
Spot 140	284	17730	2.1	20.8561	1.2	0.0656	1.5	0.0102	0.7	0.44	65.4307	0.4	64.5	0.9	31.1	31.5	65.4	0.4	210.5	0.6
Spot 118	323	4485	3.1	20.5895	1.3	0.0631	1.8	0.0102	1.2	0.67	65.4503	0.8	62.1	1.1	NA	NA	65.5	0.8	1.2	
Spot 275	327	8659	4.5	21.3847	1.1	0.0630	1.4	0.0102	0.7	0.49	65.4584	0.5	62.0	0.9	NA	NA	65.5	0.5	0.7	
Spot 274	677	66935	4.8	20.8742	0.9	0.0667	1.3	0.0102	0.8	0.66	65.4822	0.5	65.5	0.8	67.1	22.5	65.5	0.5	97.7	0.8
Spot 109	296	7105	4.7	20.6817	1.5	0.0646	1.9	0.0102	1.1	0.58	65.4900	0.7	63.6	1.2	NA	NA	65.5	0.7	1.1	
Spot 139	299	34895	2.4	20.5713	1.7	0.0672	1.9	0.0102	0.9	0.48	65.5128	0.6	66.0	1.2	84.9	39.5	65.5	0.6	77.2	0.9
Spot 261	296	24891	3.1	21.2600	1.2	0.0647	1.4	0.0102	0.8	0.55	65.5265	0.5	63.6	0.9	NA	NA	65.5	0.5	0.8	
Spot 162	742	43483	3.2	20.8316	0.9	0.0665	1.2	0.0102	0.8	0.66	65.5321	0.5	65.4	0.7	59.3	20.8	65.5	0.5	110.6	0.8
Spot 95	385	3729	3.3	20.6620	1.4	0.0621	2.2	0.0102	0.8	0.35	65.5466	0.5	61.1	1.3	NA	NA	65.5	0.5	0.8	
Spot 204	295	7339	3.3	17.3163	3.4	0.0777	3.7	0.0102	0.8	0.22	65.5482	0.5	76.0	2.7	417.7	79.8	65.5	0.5	15.7	0.8
Spot 163	305	11769	6.6	20.8949	1.2	0.0650	1.5	0.0102	0.8	0.56	65.5585	0.6	64.0	0.9	5.3	NA	65.6	0.6	1248.4	0.8
Spot 209	406	104548	2.2	20.2440	1.4	0.0686	1.6	0.0102	0.8	0.48	65.5823	0.5	67.4	1.0	132.9	32.4	65.6	0.5	49.3	0.7
Spot 288	285	5707	2.7	19.0960	1.4	0.0696	2.6	0.0102	1.0	0.39	65.6088	0.7	68.3	1.7	165.1	55.6	65.6	0.7	39.7	1.0
Spot 89	743	33727	3.5	21.1022	1.1	0.0657	1.2	0.0102	0.6	0.49	65.6097	0.4	64.6	0.8	26.5	25.8	65.6	0.4	247.4	0.6
Spot 295	2523	35660	2.8	21.0027	0.7	0.0659	0.9	0.0102	0.6	0.68	65.6126	0.4	64.8	0.6	36.3	16.0	65.6	0.4	180.5	0.6
Spot 199	1326	27927	2.8	20.9350	0.8	0.0660	1.1	0.0102	0.7	0.66	65.6254	0.5	64.9	0.7	37.2	19.4	65.6	0.5	176.6	0.7
Spot 57	322	587092	3.6	21.0064	1.5	0.0663	1.8	0.0102	0.9	0.53	65.6436	0.6	65.2	1.1	49.2	35.9	65.6	0.6	133.4	0.9
Spot 137	358	30431	4.9	20.9359	1.4	0.0661	1.7	0.0102	0.9	0.54	65.6513	0.6	64.9	1.1	39.1	34.3	65.7	0.6	168.0	0.9
Spot 18	686	47863	3.1	20.6624	0.9	0.0672	1.3	0.0102	0.9	0.74	65.6535	0.6	66.0	0.8	78.8	20.6	65.7	0.6	83.3	0.9
Spot 313	273	10160	2.4	21.1315	1.4	0.0641	1.6	0.0102	0.8	0.49	65.6895	0.5	63.1	1.0	NA	NA	65.7	0.5	0.8	
Spot 55	566	36374	2.4	21.0314	1.0	0.0658	1.3	0.0102	0.7	0.59	65.6947	0.5	64.7	0.8	27.3	24.7	65.7	0.5	240.8	0.7
Spot 77	590	11239	3.1	20.6587	1.1	0.0660	1.5	0.0102	0.9	0.64	65.7272	0.6	64.9	0.9	34.3	26.6	65.7	0.6	191.7	0.9
Spot 203	195	7316	3.7	20.1569	1.8	0.0666	2.1	0.0103	0.9	0.44	65.7489	0.6	65.5	1.3	54.7	44.6	65.7	0.6	120.2	0.9
Spot 42	377	52818	3.2	20.7984	1.0	0.0668	1.4	0.0103	1.0	0.67	65.7611	0.6	65.7	0.9	63.2	25.0	65.8	0.6	104.0	0.9
Spot 26	311	7322	3.5	21.2134	1.3	0.0632	2.8	0.0103	1.1	0.37	65.8136	0.7	62.2	1.7	NA	NA	65.8	0.7	1.0	
Spot 128	495	11320	3.4	21.0029	1.0	0.0649	1.3	0.0103	0.8	0.63	65.8188	0.5	63.9	0.8	NA	NA	65.8	0.5	0.8	
Spot 165	251	18868	3.5	21.4190	1.3	0.0643	1.5	0.0103	0.8	0.51	65.8496	0.5	63.3	0.9	NA	NA	65.8	0.5	0.8	
Spot 38	1470	46222	3.9	20.6868	0.8	0.0673	1.1	0.0103	0.8	0.69	65.8705	0.5	66.1	0.7	74.8	19.6	65.9	0.5	88.1	0.8
Spot 223	215	7112	3.6	21.0514	1.5	0.0636	1.8	0.0103	0.8	0.45	65.9318	0.5	62.6	1.1	NA	NA	65.9	0.5	0.8	
Spot 191	484	9036	3.9	20.9330	1.0	0.0647	1.6	0.0103	1.0	0.65	65.9319	0.7	63.7	1.0	NA	NA	65.9	0.7	1.0	
Spot 272	276	41390	3.3	20.9711	1.5	0.0666	1.8	0.0103	1.0	0.58	65.9323	0.7	65.4	1.1	46.9	35.0	65.9	0.7	140.5	1.0
Spot 76	417	23986	2.7	20.4975	0.8	0.0677	1.2	0.0103	0.8	0.64	65.9466	0.5	66.6	0.8	88.4	22.4	65.9	0.5	74.6	0.8
Spot 129	344	9411	2.6	21.2198	1.3	0.0640	1.6	0.0103	0.9	0.55	65.9500	0.6	63.0	1.0	NA	NA	65.9	0.6	0.9	
Spot 210	209	4492	3.5	21.0735	1.8	0.0619	2.0	0.0103	0.7	0.35	65.9538	0.5	61.0	1.2	NA	NA	66.0	0.5	0.7	
Spot 256	539	12677	2.8	21.0357	0.8	0.0651	1.1	0.0103	0.7	0.62	65.9668	0.4	64.0	0.7	NA	NA	66.0	0.4	0.7	
Spot 144	156	8266	3.3	20.7111	1.9	0.0653	2.2	0.0103	0.8	0.37	66.0026	0.5	64.2	1.4	NA	NA	66.0	0.5	0.8	
Spot 99	386	15572	2.3	21.0380	1.5	0.0657	1.7	0.0103	0.8	0.46	66.0365	0.5	64.6	1.1	10.7	NA	66.0	0.5	616.7	0.8
Spot 67	592	10769	3.9	20.7914	1.3	0.0656	1.5	0.0103	0.7	0.44	66.0366	0.5	64.5	1.0	9.0	NA	66.0	0.5	731.9	0.7
Spot 205	303	12647	3.5	21.1063	1.3	0.0649	1.6	0.0103	0.8	0.53	66.0513	0.5	63.9	1.0	NA	NA	66.1	0.5	0.8	
Spot 195	220	4473	2.9	20.4388	1.9	0.0641	2.3	0.0103	1.2	0.50	66.0647	0.8	63.1	1.4	NA	NA	66.1	0.8	1.2	
Spot 134	330	7312	3.7	21.2505	1.1	0.0633	1.5	0.0103	0.9	0.62	66.0969	0.6	62.4	0.9	NA	NA	66.1	0.6	0.9	
Spot 94	337	4000	2.0	20.9559	1.5	0.0620	1.8	0.0103	0.9	0.54	66.1086	0.6	61.1	1.0	NA	NA	66.1	0.6	0.9	
Spot 227	296	12329	3.0	20.6237	1.7	0.0664	2.2	0.0103	1.3	0.60	66.1247	0.9	65.3	1.4	34.7	NA	66.1	0.9	190.7	1.3
Spot 170	452	69712	3.5	21.0190	1.3	0.0668	1.6	0.0103	0.9	0.55	66.1522	0.6	65.7	1.0	47.8	31.2	66.2	0.6	138.3	0.8
Spot 206	551	382762	4.5	21.1663	1.3	0.0665	1.6	0.0103	1.0	0.62	66.2304	0.7	65.4	1.0	34.8	30.8	66.2	0.7	190.1	1.0
Spot 241	497	8379	3.0	20.9065	1.1	0.0650	1.8	0.0103	0.7	0.40	66.2374	0.5	63.9	1.1	NA	NA	66.2	0.5	0.7	
Spot 24	724	10508	3.2	20.9538	1.0	0.0653	1.4	0.0103	0.7	0.55	66.2399	0.5	64.2	0.8	NA	NA	66.2	0.5	0.7	
Spot 273	2182	36358	3.7	20.9493	0.6	0.0669	0.8	0.0103	0.6	0.71	66.2442	0.4	65.8	0.5	49.1	14.0	66.2	0.4	134.9	0.6
Spot 218	579	7195	3.6	21.0376	1.3	0.0640	1.6	0.0103	0.9	0.58	66.2502	0.6	63.0	1.0	NA	NA	66.3	0.6	0.9	
Spot 33	336	10402	2.8	20.5110	1.1	0.0667	1.3	0.0103	0.7	0.52	66.2505	0.4	65.6	0.8	41.3	26.2	66.3	0.4	160.3	0.7
Spot 270	257	12999	3.2	20.7313	1.7	0.0666	2.0	0.0103	1.0	0.50	66.3123	0.7	65.5	1.2	35.3	NA	66.3	0.7	187.6	1.0
Spot 141	428	7840	3.4	20.8948	1.0	0.0649	1.6	0.0103	1.2	0.73	66.3245	0.8	63.8	1.0	NA	NA	66.3	0.8	1.1	
Spot 56	198	11557	3.2	20.9050	1.6	0.0656	1.8	0.0103	0.7	0.39	66.3290	0.5	64.5	1.1	NA	NA	66.3	0.5	0.7	
Spot 231	437	21704	2.2	20.6470	0.9	0.0673	1.3	0.0103	0.8	0.64	66.3597	0.5	66.1	0.8	57.9	23.5	66.4	0.5	114.5	0.8
Spot 297	2320	105788	1.3	20.8976	0.6															

Spot 262	291	54301	4.1	20.7334	1.4	0.0678	1.7	0.0104	0.9	0.56	66.5182	0.6	66.6	1.1	70.6	33.1	66.5	0.6	94.2	0.9
Spot 181	219	4319	2.9	18.4936	2.5	0.0718	4.4	0.0104	1.5	0.34	66.5329	1.0	70.4	3.0	203.7	96.8	66.5	1.0	32.7	1.5
Spot 236	664	9197	5.1	20.4248	1.0	0.0670	1.2	0.0104	0.7	0.58	66.5644	0.5	65.9	0.8	41.4	24.3	66.6	0.5	160.7	0.7
Spot 158	199	21459	3.2	21.0950	1.3	0.0663	1.7	0.0104	1.1	0.66	66.6311	0.8	65.1	1.1	10.9	NA	66.6	0.8	610.2	1.1
Spot 96	518	9704	4.2	20.8814	1.3	0.0659	1.7	0.0104	1.0	0.61	66.6358	0.7	64.8	1.1	NA	NA	66.6	0.7	1.0	
Spot 229	452	8993	2.4	21.0847	1.3	0.0648	1.5	0.0104	0.7	0.48	66.6440	0.5	63.8	0.9	NA	NA	66.6	0.5	0.7	
Spot 197	422	10045	3.5	20.8217	1.2	0.0660	1.5	0.0104	0.9	0.56	66.6444	0.6	64.9	1.0	1.9	NA	66.6	0.6	3516.4	0.8
Spot 88	305	6478	3.9	21.2438	1.2	0.0636	1.9	0.0104	0.8	0.42	66.6461	0.5	62.6	1.1	NA	NA	66.6	0.5	0.8	
Spot 249	317	27163	2.5	21.0852	1.6	0.0665	2.1	0.0104	1.4	0.66	66.6489	0.9	65.4	1.4	19.2	NA	66.6	0.9	346.5	1.4
Spot 34	461	6956	3.9	21.0400	1.1	0.0644	2.1	0.0104	0.8	0.39	66.6659	0.5	63.4	1.3	NA	NA	66.7	0.5	0.8	
Spot 174	938	1201320	3.2	20.9184	0.6	0.0678	1.1	0.0104	0.9	0.82	66.6715	0.6	66.7	0.7	66.1	15.2	66.7	0.6	100.8	0.9
Spot 214	502	9270	4.5	20.8657	1.3	0.0656	2.1	0.0104	1.0	0.45	66.7106	0.6	64.6	1.3	NA	NA	66.7	0.6	1.0	
Spot 17	617	14272	3.1	20.7460	0.9	0.0669	1.2	0.0104	0.8	0.67	66.7106	0.6	65.8	0.8	32.6	22.1	66.7	0.6	204.3	0.8
Spot 86	265	8897	5.2	21.4778	1.3	0.0638	1.9	0.0104	1.0	0.52	66.7165	0.7	62.8	1.2	NA	NA	66.7	0.7	1.0	
Spot 224	867	13959	2.6	20.5897	0.8	0.0674	1.1	0.0104	0.8	0.67	66.7573	0.5	66.2	0.7	45.8	20.2	66.8	0.5	145.7	0.8
Spot 123	526	94421	0.3	20.7460	0.5	0.0684	1.1	0.0104	0.9	0.89	66.7962	0.6	67.1	0.7	79.6	11.6	66.8	0.6	83.9	0.9
Spot 211	355	25483	6.5	20.1357	1.2	0.0697	1.6	0.0104	0.9	0.57	66.8065	0.6	68.4	1.0	124.7	30.4	66.8	0.6	53.6	0.9
Spot 160	308	17506	3.9	21.1181	1.2	0.0662	1.5	0.0104	0.8	0.55	66.8509	0.5	65.1	0.9	0.4	NA	66.9	0.5	17812.7	0.8
Spot 47	270	4322	3.8	20.7339	1.4	0.0636	1.7	0.0104	1.0	0.57	66.8539	0.7	62.6	1.0	NA	NA	66.9	0.7	1.0	
Spot 306	1364	198421	3.9	20.6925	0.6	0.0686	1.1	0.0104	0.9	0.80	66.8669	0.6	67.4	0.7	86.1	15.2	66.9	0.6	77.7	0.9
Spot 264	803	59167	2.3	20.5969	0.8	0.0688	1.1	0.0104	0.7	0.65	66.9341	0.5	67.6	0.7	90.3	19.9	66.9	0.5	74.1	0.7
Spot 136	497	5023	2.9	21.7669	1.5	0.0612	3.8	0.0104	3.5	0.92	66.9342	2.3	60.3	2.3	NA	NA	66.9	2.3	3.5	
Spot 64	333	22089	3.2	20.4548	1.1	0.0687	1.4	0.0104	0.7	0.50	66.9992	0.5	67.5	0.9	83.7	28.7	67.0	0.5	80.0	0.7
Spot 35	521	55401	3.3	20.9116	1.0	0.0678	1.2	0.0105	0.8	0.63	67.0208	0.5	66.6	0.8	51.5	23.0	67.0	0.5	130.2	0.8
Spot 102	519	28110	3.7	20.6648	1.0	0.0685	1.3	0.0105	0.7	0.52	67.0438	0.4	67.3	0.8	77.0	26.2	67.0	0.4	87.1	0.7
Spot 104	511	16816	4.5	20.9043	0.9	0.0673	1.3	0.0105	0.7	0.53	67.0637	0.5	66.1	0.8	31.3	26.0	67.1	0.5	214.4	0.7
Spot 226	302	551929	1.9	20.8634	1.5	0.0683	1.7	0.0105	0.9	0.53	67.1128	0.6	67.1	1.1	65.5	35.2	67.1	0.6	102.5	0.9
Spot 225	393	33364	3.7	21.2810	1.2	0.0664	1.5	0.0105	0.7	0.51	67.1153	0.5	65.2	0.9	NA	NA	67.1	0.5	0.7	
Spot 10	348	13940	2.9	20.6517	1.1	0.0677	1.7	0.0105	1.1	0.63	67.1348	0.7	66.5	1.1	43.8	32.2	67.1	0.7	153.4	1.1
Spot 279	540	23054	3.0	21.4356	1.0	0.0660	1.4	0.0105	0.9	0.66	67.1476	0.6	64.9	0.9	NA	NA	67.1	0.6	0.9	
Spot 53	508	8609	8.7	21.0218	1.5	0.0654	1.9	0.0105	1.1	0.60	67.1732	0.8	64.3	1.2	NA	NA	67.2	0.8	1.1	
Spot 263	367	11641	2.3	20.6499	1.1	0.0675	1.4	0.0105	0.9	0.64	67.2415	0.6	66.3	0.9	33.2	25.6	67.2	0.6	202.7	0.9
Spot 237	571	6153	2.6	20.9373	1.0	0.0649	1.3	0.0105	0.7	0.56	67.2452	0.5	63.8	0.8	NA	NA	67.2	0.5	0.7	
Spot 113	237	45139	0.1	20.4637	0.4	0.0697	0.8	0.0105	0.6	0.85	67.2675	0.4	68.4	0.5	107.3	9.3	67.3	0.4	62.7	0.6
Spot 122	288	30339	3.6	20.3585	1.4	0.0697	1.6	0.0105	0.9	0.54	67.2998	0.6	68.4	1.1	108.4	32.8	67.3	0.6	62.1	0.9
Spot 309	832	26680	5.1	21.3175	0.6	0.0664	1.1	0.0105	0.9	0.82	67.3045	0.6	65.2	0.7	NA	NA	67.3	0.6	0.9	
Spot 22	371	58068	15.2	20.8486	1.3	0.0683	1.5	0.0105	0.8	0.53	67.3295	0.5	67.1	1.0	60.0	30.0	67.3	0.5	112.2	0.8
Spot 192	226	5989	3.0	20.9217	1.9	0.0650	2.1	0.0105	0.8	0.39	67.3794	0.6	63.9	1.3	NA	NA	67.4	0.6	0.8	
Spot 100	236	7714	13.6	20.6299	1.4	0.0670	2.4	0.0105	0.8	0.33	67.4058	0.5	65.8	1.6	9.3	NA	67.4	0.5	722.2	0.8
Spot 242	305	5295	3.2	20.8325	1.6	0.0649	1.9	0.0105	0.9	0.50	67.4621	0.6	63.9	1.2	NA	NA	67.5	0.6	0.9	
Spot 68	501	80232	4.8	21.2233	0.8	0.0674	1.2	0.0105	0.8	0.72	67.4745	0.6	66.2	0.7	21.4	19.4	67.5	0.6	315.6	0.8
Spot 220	275	3948	3.9	21.1587	1.1	0.0624	1.5	0.0105	1.0	0.64	67.5025	0.7	61.5	0.9	NA	NA	67.5	0.7	1.0	
Spot 48	454	24743	2.9	21.0098	1.1	0.0674	1.4	0.0105	0.7	0.54	67.5308	0.5	66.3	0.9	20.6	NA	67.5	0.5	327.3	0.7
Spot 119	420	4069	3.0	20.9868	1.1	0.0633	1.4	0.0105	0.9	0.64	67.5585	0.6	62.4	0.9	NA	NA	67.6	0.6	0.9	
Spot 293	346	8494	3.2	21.0244	1.4	0.0659	1.6	0.0105	0.7	0.46	67.5639	0.5	64.8	1.0	NA	NA	67.6	0.5	0.7	
Spot 130	1268	24500	2.5	21.0491	0.7	0.0676	1.0	0.0105	0.6	0.59	67.6161	0.4	66.4	0.6	23.1	18.9	67.6	0.4	292.7	0.6
Spot 72	355	16417	6.5	21.0146	1.4	0.0673	1.7	0.0106	0.8	0.49	67.6575	0.6	66.1	1.1	10.5	NA	67.7	0.6	646.7	0.8
Spot 90	2626	74228	4.9	21.0047	0.5	0.0684	0.9	0.0106	0.7	0.82	67.6959	0.5	67.2	0.6	49.8	12.3	67.7	0.5	135.8	0.7
Spot 70	253	11904	3.4	21.2677	1.8	0.0660	2.1	0.0106	1.0	0.49	67.7272	0.7	64.9	1.3	NA	NA	67.7	0.7	1.0	
Spot 25	182	2534	3.4	20.9708	1.7	0.0603	2.2	0.0106	1.2	0.55	67.7323	0.8	59.5	1.3	NA	NA	67.7	0.8	1.2	
Spot 250	491	12516	3.9	21.3381	1.0	0.0660	1.3	0.0106	0.7	0.58	67.8882	0.5	64.9	0.8	NA	NA	67.9	0.5	0.7	
Spot 21	888	103077	3.5	20.8712	1.0	0.0690	1.3	0.0106	0.8	0.61	67.9171	0.5	67.8	0.8	63.0	23.5	67.9	0.5	107.9	0.8
Spot 73	405	24735	2.3	20.9374	1.2	0.0684	1.4	0.0106	0.7	0.48	68.1321	0.4	67.2	0.9	34.9	28.7	68.1	0.4	195.1	0.6
Spot 103	184	12538	3.1	21.5734	1.5	0.0658	1.8	0.0106	0.8	0.45	68.1946	0.6	64.7	1.1	NA	NA	68.2	0.6	0.8	
Spot 60	934	47779	0.8	20.2239	0.8	0.0713	1.1	0.0107	0.7	0.68	68.3034	0.5	69.9	0.7	126.4	18.3	68.3	0.5	54.0	0.7
Spot 81	231	55585	3.4	19.5569	1.7	0.0743	1.9	0.0107	0.7	0.40	68.4812	0.5	72.7	1.3	215.0	39.8	68.5	0.5	31.8	0.7
Spot 27	528	24459	3.5	21.4152	1.2	0.0674	1.5	0.0107	0.8	0.55	68.6736	0.6	66.2	1.0	NA	NA	68.7	0.6	0.8	
Spot 92	2530	82576	2.7	20.9060</																

Spot 277	1330	44642	7.3	20.8619	1.0	0.0725	2.6	0.0111	2.5	0.93	71.2350	1.7	71.0	1.8	64.1	22.7	71.2	1.7	111.2	2.4
Spot 175	740	34600	3.9	21.0841	1.0	0.0715	1.6	0.0111	1.2	0.75	71.4413	0.9	70.1	1.1	26.3	25.3	71.4	0.9	271.6	1.2
Spot 245	406	266801	2.4	21.1764	1.3	0.0726	2.0	0.0113	1.4	0.74	72.2791	1.0	71.2	1.3	34.6	31.6	72.3	1.0	208.8	1.4
Spot 161	475	6388	2.2	20.5389	1.0	0.0714	1.3	0.0113	0.8	0.60	72.2888	0.6	70.0	0.9	NA	NA	72.3	0.6	8.8	0.8
Spot 15	1133	50074	3.9	20.9947	0.8	0.0760	1.8	0.0118	1.6	0.91	75.4076	1.2	74.4	1.3	41.2	18.2	75.4	1.2	182.8	1.6
Spot 302	665	31303	4.3	21.2365	0.8	0.0750	1.6	0.0118	1.4	0.85	75.6058	1.0	73.4	1.1	3.7	NA	75.6	1.0	2040.7	1.4
Spot 147	966	119638	7.1	20.2002	0.8	0.0813	1.1	0.0121	0.8	0.72	77.3135	0.6	79.3	0.8	141.0	17.8	77.3	0.6	54.8	0.8
Spot 268	500	57228	1.9	19.7975	0.8	0.1981	1.0	0.0288	0.7	0.67	183.3180	1.2	183.5	1.7	186.4	17.6	183.3	1.2	98.3	0.7
Spot 54	396	58256	1.2	18.4929	0.6	0.2648	1.6	0.0361	1.5	0.92	228.7157	3.4	238.5	3.5	336.1	14.1	228.7	3.4	68.0	1.5
Spot 173	442	48112	1.1	18.6735	0.6	0.2681	1.2	0.0369	1.1	0.86	233.3871	2.4	241.1	2.6	317.3	14.0	233.4	2.4	73.5	1.0
Spot 213	250	61377	1.4	18.7282	1.0	0.2956	2.2	0.0408	2.0	0.90	257.8165	4.9	263.0	5.0	309.2	21.8	257.8	4.9	83.4	1.9
Spot 62	181	76848	2.0	18.6984	0.9	0.2976	1.6	0.0409	1.3	0.83	258.5902	3.3	264.5	3.6	317.1	20.0	258.6	3.3	81.5	1.3
Spot 12	404	26367	1.7	18.5569	0.7	0.3029	1.7	0.0416	1.5	0.91	262.7427	3.9	268.6	3.9	320.4	15.5	262.7	3.9	82.0	1.5
Spot 61	110	43555	3.0	18.6767	1.2	0.3101	1.7	0.0427	1.1	0.67	269.6656	3.0	274.3	4.0	313.6	28.0	269.7	3.0	86.0	1.1
Spot 253	227	58934	1.6	18.8136	0.9	0.3274	1.3	0.0453	0.9	0.74	285.8392	2.6	287.6	3.2	301.6	19.6	285.8	2.6	94.8	0.9
Spot 167	75	52123	2.4	18.6625	1.4	0.3304	1.8	0.0454	1.1	0.60	286.1985	3.0	289.8	4.5	319.4	32.2	286.2	3.0	89.6	1.0
Spot 19	357	92269	1.9	18.4051	0.8	0.3497	1.8	0.0473	1.6	0.90	297.9576	4.7	304.5	4.8	354.7	18.0	298.0	4.7	84.0	1.6
Spot 217	226	203375	3.0	18.8541	0.8	0.3431	1.1	0.0475	0.7	0.64	299.4445	2.0	299.5	2.8	299.8	19.0	299.4	2.0	99.9	0.7
Spot 6	501	70419	1.2	18.3562	0.6	0.3548	1.2	0.0479	1.1	0.88	301.6141	3.2	308.3	3.2	359.1	12.8	301.6	3.2	84.0	1.1
Spot 303	205	186726	0.9	18.6566	0.7	0.3498	1.3	0.0479	1.0	0.81	301.6940	3.0	304.6	3.3	326.6	17.0	301.7	3.0	92.4	1.0
Spot 98	162	59915	2.3	18.7099	0.9	0.3529	1.9	0.0485	1.7	0.89	305.0394	4.9	306.9	5.0	321.3	19.8	305.0	4.9	95.0	1.6
Spot 222	64	3970	3.3	18.6468	1.1	0.3417	3.9	0.0502	0.7	0.17	315.9167	2.1	298.5	10.2	164.3	90.8	315.9	2.1	192.2	0.7
Spot 133	114	10206	2.7	18.2904	1.1	0.3660	1.3	0.0504	0.7	0.55	316.7338	2.2	316.7	3.6	316.4	25.0	316.7	2.2	100.1	0.7
Spot 13	255	24602	0.7	18.8827	0.8	0.3603	1.4	0.0504	1.2	0.82	317.0176	3.6	312.5	3.9	278.6	19.0	317.0	3.6	113.8	1.2
Spot 124	130	13070	2.4	18.8398	0.9	0.3579	1.5	0.0504	0.9	0.59	317.1546	2.8	310.7	4.1	262.4	28.2	317.2	2.8	120.9	0.9
Spot 50	212	185854	1.3	18.3189	0.7	0.3754	0.9	0.0506	0.6	0.67	318.1206	1.9	323.7	2.5	363.7	15.3	318.1	1.9	87.5	0.6
Spot 69	158	58146	2.0	18.6001	1.0	0.3723	1.6	0.0510	1.3	0.79	320.5145	4.0	321.3	4.4	327.4	22.6	320.5	4.0	97.9	1.2
Spot 145	145	13716	2.5	18.6974	0.9	0.3658	1.4	0.0512	0.9	0.62	321.6267	2.8	316.5	3.9	279.3	26.1	321.6	2.8	115.2	0.9
Spot 232	67	17815	2.3	18.9164	1.2	0.3648	1.5	0.0515	0.8	0.50	323.5319	2.4	315.8	4.1	259.2	29.9	323.5	2.4	124.8	0.7
Spot 80	101	12724	1.4	18.4245	1.0	0.3746	1.5	0.0516	0.7	0.47	324.0639	2.2	323.0	4.1	315.6	29.8	324.1	2.2	102.7	0.7
Spot 290	179	42516	1.9	18.7239	0.7	0.3768	1.1	0.0520	0.8	0.76	326.6713	2.6	324.7	3.0	310.4	15.8	326.7	2.6	105.3	0.8
Spot 37	316	42372	2.5	18.5696	0.7	0.3806	1.0	0.0522	0.7	0.72	327.7194	2.2	327.5	2.7	325.9	15.2	327.7	2.2	100.6	0.7
Spot 93	85	31101	1.0	18.6515	1.3	0.3795	1.5	0.0522	0.6	0.42	328.3189	2.0	326.7	4.1	315.1	30.6	328.3	2.0	104.2	0.6
Spot 177	162	45066	1.3	18.7839	0.9	0.3788	1.2	0.0524	0.7	0.62	329.3988	2.4	326.2	3.3	303.1	21.0	329.4	2.4	108.7	0.7
Spot 219	156	37961	4.9	17.1376	0.7	0.4150	2.3	0.0525	2.2	0.95	330.0468	7.1	352.4	6.9	502.8	16.1	330.0	7.1	65.6	2.2
Spot 201	41	141178	1.2	18.3490	1.7	0.3904	1.9	0.0526	0.8	0.42	330.3645	2.6	334.6	5.4	364.4	38.3	330.4	2.6	90.7	0.8
Spot 110	216	44799	2.1	17.6742	0.8	0.4078	1.9	0.0530	1.8	0.91	333.0143	5.7	347.3	5.7	444.1	17.7	333.0	5.7	75.0	1.7
Spot 187	70	7806	2.1	17.3732	2.6	0.4031	3.2	0.0530	0.8	0.24	333.0983	2.4	343.9	9.2	417.4	68.7	333.1	2.4	79.8	0.7
Spot 292	119	31558	0.8	18.7620	0.9	0.3830	1.1	0.0531	0.6	0.51	333.3016	1.9	329.2	3.2	300.6	21.9	333.3	1.9	110.9	0.6
Spot 106	156	37750	1.7	18.8998	1.0	0.3891	1.5	0.0541	1.1	0.75	339.6186	3.7	333.7	4.2	292.5	22.1	339.6	3.7	116.1	1.1
Spot 202	144	51721	1.7	18.4359	0.9	0.4031	1.2	0.0547	0.8	0.65	343.5102	2.7	343.9	3.6	346.2	20.9	343.5	2.7	99.2	0.8
Spot 3	302	6895	1.7	14.0503	1.0	0.5186	1.4	0.0550	1.0	0.70	345.1795	3.4	424.2	4.9	880.1	20.9	345.2	3.4	39.2	1.0
Spot 271	477	17465	1.8	18.0518	0.5	0.4231	1.0	0.0567	0.9	0.88	355.4351	3.0	358.2	3.0	376.5	10.5	355.4	3.0	94.4	0.8
Spot 276	84	78456	2.1	18.0940	1.1	0.4431	1.2	0.0587	0.6	0.49	367.9044	2.1	372.5	3.8	400.9	23.6	367.9	2.1	91.8	0.6
Spot 155	34	7968	2.7	18.5168	1.6	0.4256	2.0	0.0598	1.1	0.54	374.1605	3.8	360.1	5.9	270.1	37.6	374.2	3.8	138.5	1.0
Spot 108	116	21639	0.6	18.1222	1.0	0.4484	1.3	0.0601	0.7	0.58	376.3646	2.7	376.2	4.0	374.8	23.3	376.4	2.7	100.4	0.7
Spot 29	395	45522	1.4	18.4702	0.5	0.4444	1.0	0.0605	0.8	0.83	378.8006	3.1	373.4	3.2	339.8	12.7	378.8	3.1	111.5	0.8
Spot 258	801	52685	2.0	17.0866	0.6	0.4821	1.9	0.0607	1.8	0.94	379.8641	6.6	399.5	6.3	514.9	14.0	379.9	6.6	73.8	1.7
Spot 286	34	8355	1.6	18.2362	1.5	0.4410	1.7	0.0608	0.7	0.43	380.2926	2.7	371.0	5.3	313.0	34.8	380.3	2.7	121.5	0.7
Spot 20	142	66320	1.5	18.3474	0.8	0.4526	1.1	0.0611	0.7	0.62	382.3233	2.4	379.1	3.4	359.2	18.9	382.3	2.4	106.4	0.6
Spot 296	226	58769	1.9	17.2901	0.7	0.6419	0.9	0.0816	0.5	0.63	505.8154	2.6	503.5	3.4	493.0	14.7	505.8	2.6	102.6	0.5
Spot 101	105	15062	1.2	16.5728	0.6	0.6851	1.8	0.0843	1.7	0.93	521.8202	8.5	529.9	7.5	564.7	14.7	521.8	8.5	92.4	1.6
Spot 300	69	15272	42.0	15.5182	1.1	0.8110	1.3	0.0936	0.6	0.46	567.9905	3.2	603.0	5.8	702.0	24.3	577.0	3.2	82.2	0.6
Spot 260	136	52468	4.2	16.6751	0.7	0.8006	1.1	0.0984	0.9	0.78	604.4863	4.9	597.2	5.0	568.1	15.0	604.8	4.9	106.5	0.8
Spot 7	92	82345	3.3	14.5439	2.0	1.0139	2.6	0.1083	1.8	0.67	663.0585	11.0	710.9	13.4	865.0	40.5	663.1	11		

Spot 212	404	190029	2.2	8.6953	1.0	4.9802	1.6	0.3179	1.3	0.80	1779.5708	19.6	1816.0	13.4	1858.0	17.3	1858.0	17.3	95.8	0.9
Spot 2	261	153436	1.6	8.7017	0.4	4.8753	0.9	0.3111	0.8	0.88	1746.2864	11.6	1798.0	7.3	1858.5	7.5	1858.5	7.5	94.0	0.4
Spot 51	137	34391	2.0	8.5986	0.7	5.2010	0.9	0.3294	0.7	0.71	1835.2668	10.6	1852.8	8.0	1872.5	11.9	1872.5	11.9	98.0	0.6
Spot 66	151	103393	1.2	8.5189	0.4	4.9826	1.0	0.3116	0.9	0.91	1748.4177	13.7	1816.4	8.3	1895.2	7.4	1895.2	7.4	92.3	0.4
Spot 282	70	355017	1.9	8.5239	0.5	5.2434	0.8	0.3265	0.7	0.80	1821.6233	10.6	1859.7	7.2	1902.5	9.1	1902.5	9.1	95.7	0.5
Spot 156	298	52105	5.2	8.3007	0.5	1.6910	2.3	0.1030	2.3	0.98	632.1922	13.6	1005.2	14.8	1941.7	9.0	1941.7	9.0	32.6	0.5
Spot 121	181	90261	4.5	8.2228	0.5	4.6282	1.0	0.2789	0.8	0.86	1585.8860	11.5	1754.4	8.0	1961.4	8.7	1961.4	8.7	80.9	0.4
Spot 31	68	103753	1.9	8.0355	0.4	6.0585	0.6	0.3572	0.5	0.81	1968.8110	8.5	1984.3	5.4	2000.5	6.4	2000.5	6.4	98.4	0.3
Spot 71	170	324590	1.8	7.4802	0.4	6.9248	0.8	0.3795	0.7	0.88	2074.0269	13.1	2101.8	7.4	2129.2	7.0	2129.2	7.0	97.4	0.3
Spot 4	409	59997	4.1	6.7326	1.0	1.7595	1.3	0.0869	0.9	0.67	537.3983	4.6	1030.7	8.6	2308.8	17.0	2308.8	17.0	23.3	0.7
Spot 65	353	274823	2.1	6.2083	0.5	8.8683	1.6	0.4038	1.5	0.94	2186.5311	27.0	2324.5	14.2	2448.1	9.1	2448.1	9.1	89.3	0.4

Key	
%	Error > 3
U/Th > 10	
U > 5,000 ppm	
suspect neo-crystalline	
ages used for MDA	

Sample 10CH01b

Analysis	U (ppm)	Isotope ratios										Apparent ages (Ma)									
		206Pb 204Pb	U/Th	206Pb* 207Pb*	± (%)	207Pb* 235U	± (%)	206Pb* 238U	± (%)	error corr.	206Pb* 238U	± (Ma)	207Pb* 235U	± (Ma)	206Pb* 207Pb*	± (Ma)	Best age (Ma)	± (Ma)	Conc (%)	% Error	
Spot 12	702	7148	6.8	20.9093	1.5	0.0634	2.5	0.0101	1.9	0.77	64.7061	1.2	62.4	1.5	NA	NA	64.7	1.2	1.9		
Sample 1 Spot 32	536	24638	8.0	20.5367	1.1	0.0786	1.6	0.0119	1.1	0.70	76.2929	0.9	76.8	1.2	92.8	27.5	76.3	0.9	82.2	1.1	
Spot 89	638	24919	17.4	20.4160	1.2	0.0917	2.3	0.0138	1.9	0.84	88.3617	1.7	89.1	2.0	108.8	29.4	88.4	1.7	81.2	1.9	
Sample 1 Spot 46	552	22022	6.5	14.2753	3.2	0.1346	3.4	0.0141	1.1	0.34	90.5075	1.0	128.2	4.1	900.2	65.3	90.5	1.0	10.1	1.1	
Sample 1 Spot 47	775	6765	5.8	18.9948	0.7	0.1053	1.3	0.0152	1.0	0.78	97.2523	1.0	101.6	1.2	205.1	18.4	97.3	1.0	47.4	1.0	
Sample 1 Spot 48	1122	14119	2.7	18.3271	0.6	0.1251	2.2	0.0170	2.1	0.96	108.8952	2.3	119.7	2.5	339.8	14.6	108.9	2.3	32.0	2.1	
Spot 120	649	288440	6.2	17.9647	1.6	0.1380	2.2	0.0181	1.5	0.68	115.3823	1.7	131.2	2.7	428.8	36.0	115.4	1.7	26.9	1.5	
Spot 9	1406	3366	4.0	11.3336	0.9	0.2453	1.4	0.0212	1.0	0.76	135.4492	1.4	222.8	2.7	1287.6	17.3	135.4	1.4	10.5	1.0	
Sample 1 Spot 3	954	25687	6.4	18.3681	1.2	0.1692	2.2	0.0229	1.9	0.83	145.7258	2.7	158.7	3.3	357.4	28.1	145.7	2.7	40.8	1.8	
Spot 113	438	10512	2.7	17.1664	1.3	0.2385	2.2	0.0305	1.7	0.75	193.9403	3.2	217.2	4.3	477.3	32.3	193.9	3.2	40.6	1.6	
Spot 29	1492	9110	5.7	12.5342	1.1	0.3381	2.0	0.0314	1.6	0.84	199.4513	3.2	295.7	5.0	1147.8	21.1	199.5	3.2	17.4	1.6	
Spot 116	386	10905	2.6	18.6074	1.1	0.2334	1.5	0.0324	0.9	0.62	205.7774	1.9	213.0	2.9	293.9	26.7	205.8	1.9	70.0	0.9	
Sample 1 Spot 45	410	15421	2.1	18.5802	0.6	0.2373	0.9	0.0327	0.6	0.67	207.5423	1.2	216.2	1.7	311.8	14.9	207.5	1.2	66.6	0.6	
Spot 31	833	28308	2.2	18.6443	0.7	0.2587	3.2	0.0354	3.1	0.96	244.1674	6.8	233.6	6.6	329.9	19.1	224.2	6.8	67.9	3.0	
Spot 34	1134	1529713	14.8	18.1994	0.8	0.2769	1.3	0.0367	1.1	0.82	232.0735	2.4	248.2	2.9	403.9	16.9	232.1	2.4	57.5	1.0	
Sample 1 Spot 27	270	10435	3.8	18.5502	0.8	0.2763	2.6	0.0383	2.3	0.87	242.4107	5.5	247.7	5.8	298.2	29.2	242.4	5.5	81.3	2.3	
Spot 48	1345	49978	2.6	18.4134	0.7	0.2919	1.3	0.0392	1.2	0.86	248.1516	2.8	260.0	3.1	368.5	15.1	248.2	2.8	67.3	1.1	
Sample 1 Spot 17	897	28501	1.3	17.2685	0.6	0.3132	4.3	0.0397	4.3	0.99	251.1008	10.5	276.6	10.4	498.6	13.3	251.1	10.5	50.4	4.2	
Sample 1 Spot 34	123	13432	2.0	17.3589	1.1	0.3203	1.4	0.0413	0.8	0.61	260.8120	2.1	282.2	3.4	463.2	24.0	260.8	2.1	56.3	0.8	
Spot 95	776	26177	1.8	18.0461	0.7	0.3126	1.2	0.0415	0.9	0.81	261.9280	2.4	276.2	2.8	398.9	15.3	261.9	2.4	65.7	0.9	
Spot 119	1016	47005	2.1	17.9600	0.7	0.3291	1.3	0.0433	1.1	0.83	273.1300	2.9	288.9	3.2	418.4	15.8	273.1	2.9	65.3	1.1	
Spot 94	1011	637328	6.0	18.4298	0.7	0.3228	2.2	0.0433	2.1	0.95	273.3271	5.6	284.1	5.5	373.4	16.3	273.3	5.6	73.2	2.1	
Sample 1 Spot 16	420	24449	2.7	18.0706	0.5	0.3302	1.1	0.0439	0.9	0.85	277.0573	2.5	289.7	2.7	393.3	12.8	277.1	2.5	70.5	0.9	
Spot 102	1284	48703	4.0	17.7783	0.8	0.3730	1.2	0.0485	0.9	0.74	305.5493	2.6	321.9	3.3	441.6	17.9	305.5	2.6	69.2	0.9	
Sample 1 Spot 44	640	29496	0.9	17.7559	0.5	0.4005	1.3	0.0523	1.2	0.92	328.4112	3.9	342.0	3.9	435.2	11.6	328.4	3.9	75.5	1.2	
Sample 1 Spot 14	338	17292	1.9	18.0452	0.7	0.3920	1.2	0.0523	0.9	0.76	328.5807	2.8	335.8	3.3	386.3	17.0	328.6	2.8	85.1	0.9	
Spot 56	403	11726	3.3	18.5322	0.9	0.3807	2.7	0.0525	2.6	0.95	329.9020	8.3	327.5	7.6	310.9	20.2	329.9	8.3	106.1	2.5	
Spot 59	309	130157	1.0	17.9466	1.1	0.4204	2.1	0.0550	1.8	0.85	344.9062	6.0	356.3	6.4	431.3	25.0	344.9	6.0	80.0	1.8	
Spot 78	916	129604	2.7	17.9768	0.6	0.4197	1.1	0.0550	0.9	0.84	345.3657	3.0	355.8	3.2	424.7	12.7	345.4	3.0	81.3	0.9	
Spot 68	871	52220	3.1	17.4676	0.8	0.4320	1.4	0.0552	1.1	0.79	346.1881	3.6	364.6	4.2	483.6	18.5	346.2	3.6	71.6	1.0	
Sample 1 Spot 42	536	88899	1.3	18.3007	0.5	0.4170	0.9	0.0558	0.8	0.85	349.7980	2.6	353.9	2.7	381.0	10.6	349.8	2.6	91.8	0.7	
Spot 88	698	217739	1.8	17.9945	0.8	0.4344	1.4	0.0570	1.2	0.84	357.3456	4.0	366.3	4.2	423.4	16.8	357.3	4.0	84.4	1.1	
Sample 1 Spot 39	283	23445	1.8	18.2704	0.7	0.4236	1.0	0.0570	0.8	0.77	357.587	2.8	358.6	3.1	365.3	14.7	357.6	2.8	97.9	0.8	
Spot 1	286	19902	1.9	18.6221	0.9	0.4193	1.4	0.0577	1.0	0.70	361.8925	3.4	355.6	4.1	314.4	22.0	361.9	3.4	115.1	0.9	
Spot 6	496	71206	1.8	18.2783	0.7	0.4363	1.3	0.0583	1.1	0.83	364.9854	3.8	367.7	4.0	384.6	16.4	365.0	3.8	94.9	1.0	
Spot 101	374	19991	1.5	18.0559	0.7	0.4419	1.1	0.0589	0.9	0.81	368.7397	3.3	371.6	3.5	389.3	14.9	368.7	3.3	94.7	0.9	
Spot 80	233	27456	1.7	17.9843	1.2	0.4532	1.7	0.0599	1.2	0.68	375.0459	4.3	379.5	5.5	406.7	28.1	375.0	4.3	92.2	1.1	
Spot 40	486	215929	0.9	18.2461	0.7	0.4559	1.0	0.0606	0.8	0.76	379.0990	2.8	381.4	3.2	395.5	14.7	379.1	2.8	95.9	0.7	
Spot 26	281	14768	0.8	18.1246	0.8	0.4582	1.9	0.0615	1.7	0.92	384.6540	6.5	383.0	6.0	373.0	17.2	384.7	6.5	103.1	1.7	
Spot 20	251	65746	1.4	18.0414	0.9	0.4665	1.2	0.0615	0.8	0.67	384.6783	2.9	388.8	3.8	413.1	19.3	384.7	2.9	93.1	0.8	
Spot 49	577	272526	3.6	17.9321	0.8	0.4719	1.2	0.0615	0.9	0.75	384.8620	3.4	392.5	4.0	437.8	18.1	384.9	3.4	87.9	0.9	
Spot 53	265	20840	1.7	17.7265	1.1	0.4723	2.1	0.0616	1.7	0.82	385.5774	6.4	392.8	6.8	435.5	26.5	385.6	6.4	88.5	1.7	
Spot 104	699	24943	1.9	16.8909	2.2	0.4969	2.4	0.0617	1.1	0.44	386.1325	4.0	409.6	8.2	544.1	47.5	386.1	4.0	71.0	1.0	
Spot 61	784	56558	1.6	17.9339	0.6	0.4728	1.0	0.0620	0.8	0.78	387.5359	3.0	393.1	3.3	426.2	14.1	387.5	3.0	90.9	0.8	
Spot 38	252	63071	1.7	18.0981	0.9	0.4691	1.4	0.0620	1.0	0.73	387.7981	3.8	390.6	4.5	407.1	21.0	387.8	3.8	95.3	1.0	
Sample 1 Spot 21	323	29405	3.2	17.9868	0.5	0.4693	0.9	0.0620	0.7	0.81	387.8785	2.7	390.7	2.9	407.6	11.8	387.9	2.7	95.2	0.7	
Spot 24	122	7084	1.6	18.5881	1.4	0.4411	2.6	0.0620	0.9	0.36	387.9501	3.5	371.0	8.1	266.7	55.9	388.0	3.5	145.5	0.9	
Spot 81	544	60263	0.7	18.2557	0.9	0.4673	1.4	0.0624	1.1	0.77	390.0918	4.0	389.3	4.4	384.7	19.4	390.1	4.0	101.4	1.0	
Spot 4	341	14632	4.5	17.7879	0.8	0.4738	1.4	0.0626	1.0	0.74	391.2774	3.8	393.8	4.4	408.8	20.5	391.3	3.8	95.7	1.0	
Spot 13	444	85001	2.0	18.2695	1.0	0.4704	1.7	0.0627	1.3	0.78	392.2502	4.9	391.5	5.4	386.8	23.4					

Sample 1 Spot 29	252	28360	2.3	18.3371	0.7	0.4789	1.0	0.0646	0.7	0.69	403.3677	2.6	397.3	3.2	362.3	15.8	403.4	2.6	111.3	0.6
Spot 99	266	147659	2.2	18.0960	1.0	0.5053	1.5	0.0667	1.1	0.72	416.1854	4.3	415.3	5.1	410.3	23.1	416.2	4.3	101.4	1.0
Spot 87	541	41125	1.0	17.8763	0.7	0.5116	0.9	0.0670	0.6	0.68	418.2202	2.5	419.5	3.2	426.5	15.2	418.2	2.5	98.1	0.6
Spot 14	93	26619	2.5	16.5008	1.4	0.5554	2.8	0.0673	2.4	0.86	419.8511	9.9	448.5	10.2	598.4	30.5	419.9	9.9	70.2	2.3
Spot 51	514	77826	1.7	17.6364	0.8	0.5242	1.2	0.0674	1.0	0.79	420.6631	4.0	427.9	4.3	467.2	16.7	420.7	4.0	90.0	1.0
Spot 52	416	26383	1.3	18.0790	0.6	0.5105	1.1	0.0678	0.8	0.73	422.7564	3.3	418.8	3.8	397.0	16.9	422.8	3.3	106.5	0.8
Spot 2	593	66244	2.5	17.9061	0.8	0.5177	1.5	0.0679	1.3	0.84	423.2065	5.3	423.6	5.3	426.0	18.5	423.2	5.3	99.3	1.2
Spot 70	332	72846	1.3	17.8828	0.9	0.5227	1.5	0.0683	1.1	0.77	425.6176	4.6	427.0	5.1	434.4	21.0	425.6	4.6	98.0	1.1
Spot 100	550	217094	3.7	17.9725	0.9	0.5232	2.7	0.0685	2.6	0.95	427.1907	10.7	427.3	9.5	427.7	19.8	427.2	10.7	99.9	2.5
Spot 127	292	32650	3.8	18.1304	1.0	0.5189	1.3	0.0690	0.7	0.56	429.9851	3.0	424.4	4.4	394.1	23.8	430.0	3.0	109.1	0.7
Spot 72	638	179375	2.8	17.7019	0.5	0.5441	1.1	0.0702	0.9	0.87	437.4120	4.0	441.1	3.9	460.7	11.8	437.4	4.0	95.0	0.9
Sample 1 Spot 11	237	20887	3.1	17.6079	0.7	0.5435	1.1	0.0705	0.9	0.81	439.4084	3.9	440.7	4.0	447.5	14.9	439.4	3.9	98.2	0.9
Spot 103	308	36321	3.5	18.1881	0.8	0.5311	1.1	0.0709	0.8	0.71	441.2766	3.5	432.5	4.0	386.2	18.0	441.3	3.5	114.3	0.8
Sample 1 Spot 43	54	28850	3.5	17.5792	0.8	0.5527	1.0	0.0714	0.6	0.59	444.6271	2.6	446.7	3.7	457.6	18.4	444.6	2.6	97.2	0.6
Spot 17	229	25394	2.3	17.6941	0.9	0.5590	1.3	0.0727	1.0	0.74	452.4691	4.2	450.9	4.7	442.7	19.5	452.5	4.2	102.2	0.9
Spot 23	479	67743	1.3	13.4137	1.8	0.7676	4.1	0.0751	3.7	0.90	466.8803	16.6	578.4	18.2	1044.7	37.0	466.9	16.6	44.7	3.6
Spot 126	246	96911	2.4	17.3448	0.9	0.5967	1.4	0.0755	1.0	0.73	468.9809	4.6	475.1	5.3	504.8	20.9	469.0	4.6	92.9	1.0
Spot 105	347	24751	1.7	16.0303	0.8	0.6538	2.0	0.0770	1.8	0.91	478.2269	8.2	510.8	7.9	659.3	17.8	478.2	8.2	72.5	1.7
Spot 39	244	80234	2.6	18.1067	1.0	0.5873	1.4	0.0776	1.0	0.68	481.7513	4.5	469.2	5.4	408.1	23.5	481.8	4.5	118.1	0.9
Sample 1 Spot 19	198	30407	2.7	17.3019	0.7	0.6243	1.0	0.0793	0.7	0.70	492.0236	3.3	492.6	3.9	495.1	15.8	492.0	3.3	99.4	0.7
Spot 55	1052	152493	3.8	15.9399	0.6	0.7052	1.7	0.0819	1.5	0.93	507.1684	7.5	541.9	7.0	690.9	13.4	507.2	7.5	73.4	1.5
Spot 71	174	16991	1.6	16.9727	1.2	0.6788	2.1	0.0851	1.6	0.78	526.4251	8.1	526.0	8.5	524.4	28.5	526.4	8.1	100.4	1.5
Sample 1 Spot 37	369	180137	3.6	16.5300	0.6	0.7326	1.7	0.0884	1.6	0.93	545.9160	8.3	558.1	7.3	608.0	13.2	545.9	8.3	89.8	1.5
Spot 60	288	45292	9.7	16.2016	0.7	0.7908	1.3	0.0936	1.1	0.84	576.9736	6.2	591.6	6.0	648.1	15.6	577.0	6.2	89.0	1.1
Sample 1 Spot 26	183	20084	1.2	16.2327	0.5	0.8364	1.0	0.1001	0.8	0.82	614.7650	4.7	617.2	4.5	626.0	11.9	614.8	4.7	98.2	0.8
Sample 1 Spot 1	288	62296	1.4	16.0875	0.6	0.9233	1.0	0.1086	0.8	0.83	664.7953	5.3	664.1	4.9	661.8	12.1	664.8	5.3	100.5	0.8
Spot 63	445	112942	6.8	13.8559	0.7	1.4583	1.1	0.1472	0.8	0.75	885.3490	6.6	913.3	6.5	981.5	14.6	981.5	14.6	90.2	1.5
Spot 106	69	33995	1.6	13.7424	1.0	1.7171	1.3	0.1728	0.9	0.69	1027.3954	8.7	1015.0	8.5	988.2	19.5	988.2	19.5	104.0	2.0
Sample 1 Spot 25	224	15177	4.3	13.5780	0.9	1.5086	1.3	0.1511	0.8	0.66	907.0714	7.0	933.9	7.7	997.6	19.3	90.9	1.9		
Spot 83	68	9443	2.4	13.4684	0.9	1.7392	1.2	0.1741	0.8	0.64	1034.8165	7.3	1023.2	7.7	998.3	18.7	998.3	18.7	103.7	1.9
Spot 67	83	252805	0.9	13.7448	1.1	1.3425	4.3	0.1343	4.1	0.97	812.6029	31.6	864.3	24.9	999.3	22.1	999.3	22.1	81.3	2.2
Spot 108	153	72419	1.2	13.4882	0.7	1.6266	1.2	0.1601	1.0	0.81	957.5576	8.5	980.5	7.5	1032.4	14.2	1032.4	14.2	92.8	1.4
Spot 50	151	13617	1.5	13.2779	0.8	1.7101	1.0	0.1672	0.6	0.58	996.8486	5.4	1012.3	6.5	1046.0	16.6	1046.0	16.6	95.3	1.6
Spot 37	300	42168	3.9	13.2402	0.7	1.7136	1.0	0.1657	0.8	0.75	988.5735	6.9	1013.6	6.4	1068.2	13.1	1068.2	13.1	92.5	1.2
Spot 86	409	67418	3.1	13.1507	0.7	1.6001	1.4	0.1537	1.2	0.84	921.9018	9.9	970.2	8.6	1081.4	14.8	1081.4	14.8	85.3	1.4
Sample 1 Spot 28	93	29911	1.0	13.0313	0.6	1.8397	1.2	0.1757	1.1	0.87	1043.2384	10.2	1059.8	8.0	1093.9	12.0	1093.9	12.0	95.4	1.1
Spot 11	268	36153	3.6	12.9216	0.8	1.8852	1.2	0.1781	0.9	0.75	1056.7606	9.2	1075.9	8.3	114.9	16.3	114.9	16.3	94.8	1.5
Spot 30	29	30452	1.3	12.5663	1.3	2.0953	1.6	0.1925	1.0	0.60	1134.8761	10.3	1147.3	11.3	1170.8	26.0	1170.8	26.0	96.9	2.2
Spot 112	249	67896	3.4	12.4829	0.6	2.2286	1.0	0.2031	0.8	0.78	1192.0730	8.4	1190.1	6.9	1186.5	12.1	1186.5	12.1	100.5	1.0
Spot 93	552	199177	1.4	11.8125	0.7	2.4831	1.1	0.2137	0.8	0.78	1248.4694	9.5	1267.1	7.8	1298.9	13.0	1298.9	13.0	96.1	1.0
Spot 130	44	5038	4.4	11.4006	1.1	2.4223	1.5	0.2075	1.0	0.69	1215.3921	11.6	1249.2	10.8	1308.0	21.0	1308.0	21.0	92.9	1.6
Sample 1 Spot 38	28	215158	2.4	11.5601	0.7	2.7445	0.9	0.2337	0.5	0.63	1353.9300	6.6	1340.6	6.3	1319.3	12.8	1319.3	12.8	102.6	1.0
Spot 128	175	60555	3.0	11.6666	0.8	2.6358	1.0	0.2243	0.7	0.66	1304.3093	7.9	1310.7	7.5	1321.1	14.9	1321.1	14.9	98.7	1.1
Spot 3	210	78834	3.4	11.4376	0.7	2.5781	1.2	0.2155	1.0	0.84	1257.9669	11.8	1294.4	9.0	1355.4	12.9	1355.4	12.9	92.8	1.0
Sample 1 Spot 40	66	399257	3.1	11.3252	0.7	2.8683	1.0	0.2367	0.7	0.69	1369.6872	8.2	1373.6	7.2	1379.7	13.4	1379.7	13.4	99.3	1.0
Sample 1 Spot 15	387	26574	3.2	11.1971	0.4	2.7170	0.7	0.2228	0.6	0.84	1296.5606	6.9	1333.1	5.2	1392.3	7.3	1392.3	7.3	93.1	0.5
Spot 110	83	36836	1.1	11.1716	0.9	2.8889	1.2	0.2360	0.8	0.66	1365.9526	9.9	1379.0	9.1	1399.3	17.3	1399.3	17.3	97.6	1.2
Spot 33	311	192017	3.2	11.1447	0.5	2.8607	0.9	0.2320	0.7	0.79	1345.0595	8.2	1371.6	6.4	1413.2	10.1	1413.2	10.1	95.2	0.7
Spot 16	27	10625	1.5	10.9593	1.4	2.4179	1.9	0.1956	1.2	0.61	1151.8580	12.3	1247.9	13.7	1417.7	28.7	1417.7	28.7	81.2	2.0
Spot 109	240	41339	2.4	10.9591	0.6	2.9329	1.1	0.2349	0.9	0.84	1360.2778	11.1	1390.4	8.1	1437.0	10.9	1437.0	10.9	94.7	0.8
Spot 96	49	37229	1.5	10.8821	0.7	3.2055	1.1	0.2550	0.8	0.78	1464.2247	10.9	1458.5	8.3	1450.1	12.8	1450.1	12.8	101.0	0.9
Spot 85	149	397700	2.3	10.8591	0.7	3.1616	1.3	0.2503	1.1	0.85	1440.0352	13.8	1447.8	9.7	1459.3	12.7	1459.3	12.7	98.7	0.9
Spot 35	347	205390	1.3	10.5066	0.5	3.3119	1.2	0.2532	1.1	0.92	1454.8974	14.6	1483.9	9.4	1525.5	8.7	1525.5	8.7	95.4	0.6
Sample 1 Spot 30	130	94381	2.1	10.2716	0.4	3.5179	0.6	0.2636	0.5	0.81	1508.0681	6.6	1531.2	4.8	1563.4	6.7	1563.4	6.7	96.5	0.4
Sample 1 Spot 41																				

Spot 44	326	131849	0.8	9.4210	0.5	3.6567	1.9	0.2505	1.9	0.96	1441.1850	24.2	1562.0	15.5	1729.3	9.9	1729.3	9.9	83.3	0.6
Sample 1 Spot 18	278	156581	4.2	9.3864	0.4	4.1499	1.6	0.2838	1.6	0.97	1610.4868	22.1	1664.2	13.1	1732.6	6.9	1732.6	6.9	93.0	0.4
Sample 1 Spot 7	88	54787	1.5	9.3688	0.5	3.7306	1.4	0.2550	1.4	0.94	1464.3275	17.8	1578.0	11.6	1733.4	9.2	1733.4	9.2	84.5	0.5
Sample 1 Spot 12	58	12364	1.3	9.2636	0.5	4.4419	0.8	0.3027	0.7	0.78	1704.5865	9.8	1720.2	6.9	1739.2	9.5	1739.2	9.5	98.0	0.5
Spot 65	121	65972	2.7	9.3111	0.6	4.4499	1.0	0.3019	0.8	0.79	1700.8651	11.6	1721.7	8.2	1747.0	11.2	1747.0	11.2	97.4	0.6
Spot 10	134	103648	2.0	9.2623	0.8	3.6849	3.3	0.2486	3.3	0.97	1431.3422	41.7	1568.1	26.7	1757.4	14.3	1757.4	14.3	81.4	0.8
Sample 1 Spot 35	242	117980	3.4	9.0735	0.3	4.0477	0.7	0.2679	0.7	0.89	1530.1365	8.9	1643.8	6.0	1792.4	6.1	1792.4	6.1	85.4	0.3
Sample 1 Spot 2	303	70640	1.5	9.0539	0.3	4.3728	0.8	0.2889	0.7	0.89	1635.8339	9.7	1707.2	6.2	1795.9	6.2	1795.9	6.2	91.1	0.3
Sample 1 Spot 8	94	19165	2.5	8.9793	0.3	4.5389	0.7	0.2989	0.7	0.91	1685.6482	9.7	1738.1	6.0	1801.9	5.6	1801.9	5.6	93.5	0.3
Spot 97	276	197627	1.8	8.8464	0.6	4.5717	1.0	0.2946	0.8	0.81	1664.6189	11.9	1744.1	8.4	1840.8	10.6	1840.8	10.6	90.4	0.6
Spot 114	134	44107	0.7	8.2829	0.5	5.7018	1.0	0.3448	0.8	0.85	1909.7075	13.6	1931.6	8.4	1955.2	9.2	1955.2	9.2	97.7	0.5
Spot 5	99	108661	1.9	8.2551	0.6	5.2177	1.0	0.3144	0.8	0.76	1762.5609	11.6	1855.5	8.4	1961.3	11.4	1961.3	11.4	89.9	0.6
Spot 92	244	266043	5.1	7.6292	0.7	6.4126	1.3	0.3562	1.1	0.84	1964.2536	18.7	2034.0	11.5	2105.5	12.5	2105.5	12.5	93.3	0.6
Sample 1 Spot 50	94	38987	2.6	6.6480	0.7	8.1430	2.7	0.3956	2.6	0.96	2148.7332	47.6	2247.0	24.5	2337.8	12.8	2337.8	12.8	91.9	0.5
Spot 84	1081	31932	9.7	6.0040	0.6	2.1365	1.2	0.0937	1.1	0.87	577.3652	5.9	1160.7	8.5	2511.4	10.2	2511.4	10.2	23.0	0.4
Spot 62	877	323660	6.6	5.6441	0.6	10.6209	1.1	0.4361	0.8	0.79	2333.1152	16.2	2490.5	9.8	2621.5	10.8	2621.5	10.8	89.0	0.4
Sample 1 Spot 4	296	85434	1.3	5.3902	0.3	12.0041	0.7	0.4714	0.7	0.89	2489.6004	13.7	2604.7	7.0	2695.5	5.6	2695.5	5.6	92.4	0.2

Key
% Error > 3
U/Th > 10
U > 5,000 ppm
suspect neo-crystalline
ages used for MDA

Sample 19CSR46

Analysis	U (ppm)	Isotope ratios						Apparent ages (Ma)												
		206Pb 204Pb	U/Th	206Pb* 207Pb*	± (%)	207Pb* 235U	± (%)	206Pb* 238U	± (%)	error corr.	206Pb* 238U	± (Ma)	207Pb* 235U	± (Ma)	206Pb* 207Pb*	± (Ma)	Best age (Ma)	± (Ma)	Conc (%)	% Error
Spot 202	2952	13579	1.7	19.5214	0.9	0.1820	1.4	0.0259	1.0	0.74	164.9876	1.6	169.8	2.1	237.7	21.0	165.0	1.6	259.4	1.0
Spot 8	910	36581	2.9	18.0944	1.0	0.3440	2.3	0.0441	2.1	0.90	278.1062	5.6	300.2	6.0	475.7	21.7	278.1	5.6	598.8	2.0
Spot 34	2326	59320	1.9	19.3495	0.8	0.3278	1.6	0.0452	1.4	0.86	284.9344	3.9	287.9	4.1	311.6	19.1	284.9	3.9	826.8	1.4
Spot 237	1007	58119	13.2	18.7687	0.8	0.3387	1.6	0.0454	1.4	0.87	286.0138	3.8	296.2	4.0	377.3	16.9	286.0	3.8	111.7	1.3
Spot 143	554	48087	2.5	19.1919	1.0	0.3333	2.0	0.0460	1.7	0.87	289.7277	4.9	292.1	5.0	310.7	22.5	289.7	4.9	638.4	1.7
Spot 19	772	13297	0.9	19.6158	0.9	0.3414	1.9	0.0482	1.5	0.80	303.4345	4.5	298.2	4.9	257.5	26.3	303.4	4.5	338.6	1.5
Spot 69	538	7023	0.4	15.6546	3.4	0.4262	3.9	0.0491	1.4	0.35	309.1091	4.1	360.5	11.8	706.1	77.6	309.1	4.1	453.1	1.3
Spot 32	809	7901471	1.7	18.7580	0.9	0.3757	1.7	0.0499	1.4	0.86	313.7415	4.4	323.9	4.7	397.3	19.5	313.7	4.4	143243.4	1.4
Spot 306	424	14486	1.0	18.8532	0.9	0.3741	1.6	0.0507	1.2	0.75	319.0437	3.7	322.7	4.3	349.3	23.1	319.0	3.7	356.4	1.1
Spot 56	156	65686	0.9	18.9560	1.3	0.3797	1.7	0.0514	1.1	0.66	323.1137	3.5	326.8	4.8	353.5	29.0	323.1	3.5	2291.8	1.1
Spot 97	544	25599	1.3	17.8810	1.0	0.4074	2.7	0.0525	2.5	0.93	329.7053	8.2	347.0	8.0	464.3	22.1	329.7	8.2	237.2	2.5
Spot 265	208	17973	1.2	18.4412	1.3	0.4063	1.8	0.0539	1.3	0.69	338.4273	4.2	346.2	5.4	398.9	29.7	338.4	4.2	382.1	1.2
Spot 18	737	66790	1.3	19.0288	0.7	0.4125	2.0	0.0554	1.8	0.92	347.4882	6.1	350.7	5.8	371.9	16.8	347.5	6.1	1332.0	1.8
Spot 220	326	10830	1.3	18.8365	0.9	0.4076	1.8	0.0560	1.2	0.70	351.3561	4.2	347.2	5.2	319.2	28.7	351.4	4.2	171.0	1.2
Spot 150	292	8180	6.1	18.3934	1.3	0.4143	1.8	0.0563	1.2	0.69	353.2405	4.2	352.0	5.2	343.8	28.9	353.2	4.2	31.2	1.2
Spot 78	264	23830	2.7	15.2370	2.3	0.5154	2.7	0.0566	1.5	0.53	354.6161	5.0	422.1	9.4	809.5	48.4	354.6	5.0	258.0	1.4
Spot 74	284	10112	5.0	18.0837	0.9	0.4320	1.7	0.0573	1.3	0.79	359.0420	4.6	364.6	5.1	399.8	23.0	359.0	4.6	45.8	1.3
Spot 292	111	2057	2.3	17.5297	1.6	0.4095	2.0	0.0578	1.2	0.58	362.1909	4.1	348.5	5.9	258.3	37.5	362.2	4.1	27.6	1.1
Spot 119	281	177829	3.6	18.3281	1.0	0.4449	1.7	0.0583	1.4	0.83	365.0653	5.1	373.7	5.4	427.3	21.6	365.1	5.1	1539.4	1.4
Spot 27	446	32149	14.7	18.4758	1.1	0.4425	2.1	0.0583	1.7	0.84	365.4164	6.2	372.0	6.4	413.3	24.9	365.4	6.2	63.3	1.7
Spot 160	814	49810	6.5	18.4532	0.8	0.4434	1.6	0.0590	1.4	0.87	369.4547	5.2	372.6	5.1	392.4	18.0	369.5	5.2	186.6	1.4
Spot 161	227	11463	1.2	18.3759	1.2	0.4401	1.9	0.0594	1.4	0.76	371.8344	5.1	370.3	5.8	360.7	27.2	371.8	5.1	210.5	1.4
Spot 166	280	38893	5.4	18.2599	1.2	0.4543	1.6	0.0598	1.1	0.70	374.3083	4.1	380.3	5.1	416.8	25.9	374.3	4.1	155.8	1.1
Spot 169	101	12665	1.9	17.8857	1.5	0.4599	2.2	0.0601	1.5	0.68	376.2054	5.3	384.2	6.9	432.5	35.4	376.2	5.3	140.4	1.4
Spot 300	249	11757	1.4	18.0147	1.2	0.4626	1.9	0.0601	1.2	0.65	376.4931	4.5	386.1	6.1	443.9	32.1	376.5	4.5	186.7	1.2
Spot 167	1946	44893	1.4	19.1645	0.9	0.4405	2.6	0.0608	2.4	0.93	380.4740	9.0	370.6	8.1	309.2	21.1	380.5	9.0	748.8	2.4
Spot 241	372	21028	1.6	17.4648	1.0	0.5006	1.5	0.0628	1.1	0.74	392.4822	4.3	412.1	5.1	523.4	22.1	392.5	4.3	247.4	1.1
Spot 54	110	2958	2.3	17.8472	1.4	0.4556	3.5	0.0632	0.8	0.23	395.2838	3.1	381.2	11.2	296.4	78.6	395.3	3.1	25.3	0.8
Spot 297	393	4355	2.4	14.9676	3.4	0.5715	4.7	0.0634	2.0	0.42	396.3685	7.7	459.0	17.5	785.8	90.2	396.4	7.7	44.6	1.9
Spot 82	332	11444	3.1	17.9832	1.0	0.4836	1.6	0.0635	1.2	0.76	396.8049	4.6	400.5	5.1	422.0	22.4	396.8	4.6	68.5	1.2
Spot 277	762	22114	2.0	18.3883	0.9	0.4830	2.0	0.0635	1.8	0.88	396.8177	6.8	400.1	6.6	419.4	21.2	396.8	6.8	181.4	1.7
Spot 31	204	20373	2.3	18.3595	1.4	0.4836	1.8	0.0637	1.1	0.59	397.8659	4.1	400.5	6.0	415.8	32.6	397.9	4.1	175.8	1.0
Spot 117	361	41117	1.7	18.0938	1.0	0.4906	1.5	0.0638	1.1	0.73	398.9436	4.4	405.3	5.1	442.0	23.2	398.9	4.4	645.3	1.1
Spot 275	277	25965	2.6	18.3445	1.4	0.4884	2.1	0.0639	1.6	0.75	399.4454	6.1	403.8	7.1	428.8	31.4	399.4	6.1	212.5	1.5
Spot 263	387	22478	2.9	18.1968	0.9	0.4903	1.3	0.0639	0.9	0.69	399.5942	3.4	405.1	4.2	436.9	20.2	399.6	3.4	148.4	0.8
Spot 137	442	41642	1.6	18.2440	1.0	0.4885	2.0	0.0641	1.8	0.86	400.5934	6.9	403.9	6.8	422.8	22.9	400.6	6.9	643.5	1.7
Spot 73	164	10006	2.2	18.3956	1.3	0.4765	2.2	0.0643	1.5	0.69	401.8963	5.9	395.7	7.1	359.6	35.4	401.9	5.9	94.3	1.5
Spot 41	708	12393	16.7	18.4386	0.8	0.4802	1.6	0.0645	1.4	0.88	402.8753	5.5	398.2	5.3	371.1	16.9	402.9	5.5	24.8	1.4
Spot 238	201	23604	2.9	17.9806	1.1	0.5044	1.9	0.0651	1.5	0.79	406.3294	5.8	414.7	6.3	461.4	25.4	406.3	5.8	165.4	1.4
Spot 307	203	12209	1.3	15.1217	2.2	0.6002	2.4	0.0652	1.1	0.45	407.1514	4.3	477.3	9.2	830.4	45.2	407.2	4.3	178.9	1.1
Spot 53	508	87254	1.5	17.6470	0.9	0.5246	1.5	0.0658	1.2	0.80	411.0069	4.9	428.2	5.4	522.0	20.5	411.0	4.9	1331.3	1.2
Spot 37	487	24046	1.5	18.1179	1.0	0.5138	1.8	0.0666	1.5	0.84	415.9323	6.1	421.0	6.2	448.9	22.0	415.9	6.1	276.5	1.5
Spot 200	387	21965	1.3	17.7725	0.9	0.5312	1.7	0.0682	1.4	0.84	425.3991	5.8	432.6	5.9	471.1	19.9	425.4	5.8	294.3	1.4
Spot 111	225	273825	1.1	18.2026	1.0	0.5277	1.4	0.0687	1.0	0.72	428.4675	4.3	430.3	5.0	439.8	22.2	428.5	4.3	5907.4	1.0
Spot 253	668	33867	2.1	17.9091	0.7	0.5405	1.6	0.0692	1.4	0.88	431.5270	5.8	438.8	5.6	476.9	16.7	431.5	5.8	349.0	1.3
Spot 118	155	8330	2.5	17.3631	1.5	0.5431	2.1	0.0695	1.3	0.65	433.1100	5.6	440.5	7.4	479.3	34.6	433.1	5.6	60.3	1.3
Spot 75	202	32336	1.5	18.0738	1.2	0.5356	1.7	0.0697	1.1	0.67	434.3079	4.8	435.5	6.0	441.9	27.8	434.3	4.8	383.5	1.1
Spot 163	2736	86444	1.5	19.0224	0.9	0.5142	1.3	0.0704	1.0	0.77	438.3856	4.3	421.2	4.6	328.5	19.4	438.4	4.3	842.9	1.0
Spot 108	32	3469	1.6	17.1944	1.9	0.5359	2.4	0.0710	1.3	0.57	442.2349	5.8	435.7	8.4	401.6	44.1	442.2	5.8	38.2	1.3
Spot 156	638	61655	3.2	18.3187	0.9	0.5435	1.7	0.0717	1.5	0.84	446.1640	6.3	440.7	6.2	412.2	20.7	446.2			

Spot 229	469	80382	0.7	16.7958	0.9	0.6302	2.3	0.0754	2.1	0.92	468.6646	9.6	496.2	9.0	625.6	19.4	468.7	9.6	2812.2	2.0
Spot 13	312	14455	3.1	17.5467	1.0	0.6093	1.6	0.0765	1.2	0.76	474.9153	5.4	483.1	6.0	522.2	22.3	474.9	5.4	77.1	1.1
Spot 226	101	6104	1.8	17.3476	1.0	0.6086	2.2	0.0782	1.1	0.49	485.1049	5.0	482.7	8.4	471.2	42.4	485.1	5.0	57.4	1.0
Spot 84	2312	53774	2.3	14.7417	1.1	0.7481	2.0	0.0788	1.6	0.82	488.9854	7.7	567.1	8.6	894.1	23.2	489.0	7.7	381.0	1.6
Spot 280	354	26679	1.1	17.3869	1.1	0.6514	1.9	0.0805	1.6	0.81	499.1061	7.6	509.3	7.8	555.5	24.5	499.1	7.6	361.5	1.5
Spot 291	1752	65306	2.0	19.0131	0.7	0.6015	1.6	0.0809	1.4	0.89	501.4690	6.8	478.2	6.0	367.8	16.5	501.5	6.8	521.9	1.3
Spot 240	274	65482	3.6	17.0234	1.0	0.6813	1.6	0.0826	1.3	0.78	511.5612	6.3	527.6	6.8	597.4	22.4	511.6	6.3	379.0	1.2
Spot 80	377	22323	3.0	16.8187	1.0	0.6865	2.2	0.0833	1.9	0.89	515.7364	9.6	530.7	9.1	595.5	22.0	515.7	9.6	106.4	1.9
Spot 45	428	31091	3.0	16.9582	0.8	0.6913	1.6	0.0843	1.4	0.85	521.5011	6.8	533.6	6.7	585.6	18.5	521.5	6.8	153.8	1.3
Spot 127	181	24159	0.6	17.5126	0.9	0.6765	1.6	0.0853	1.3	0.81	527.5930	6.7	524.6	6.7	511.8	20.8	527.6	6.7	552.0	1.3
Spot 28	1565	77676	5.3	17.5810	0.9	0.6866	2.6	0.0857	2.5	0.94	529.8627	12.5	530.7	10.8	534.5	19.8	529.9	12.5	206.2	2.4
Spot 23	356	32036	2.4	17.3269	1.0	0.7012	1.4	0.0862	1.0	0.69	533.2023	5.0	539.5	5.9	566.3	22.4	533.2	5.0	203.1	0.9
Spot 66	113	28709	1.0	16.6971	1.2	0.7359	1.7	0.0882	1.2	0.73	545.1282	6.4	560.0	7.3	620.8	25.2	545.1	6.4	400.5	1.2
Spot 295	108	17171	2.8	16.8251	1.4	0.7347	2.0	0.0884	1.4	0.70	545.8211	7.3	559.3	8.6	614.5	30.6	545.8	7.3	84.6	1.3
Spot 3	184	8589	2.0	16.5192	1.2	0.7425	2.0	0.0886	1.6	0.80	547.0863	8.5	563.9	8.8	632.2	26.5	547.1	8.5	67.8	1.6
Spot 67	377	17310	1.4	16.7052	0.7	0.7380	1.3	0.0890	1.1	0.81	549.8476	5.6	561.2	5.7	607.6	16.6	549.8	5.6	167.9	1.0
Spot 39	336	24747	2.6	17.0983	0.9	0.7275	1.5	0.0892	1.2	0.81	550.7770	6.4	555.1	6.4	572.9	19.2	550.8	6.4	138.9	1.2
Spot 147	748	41451	2.3	13.0977	0.9	0.9480	1.7	0.0892	1.5	0.85	550.9853	7.7	677.1	8.4	1122.6	17.8	551.0	7.7	220.4	1.4
Spot 290	336	51122	2.3	16.8875	0.8	0.7490	1.5	0.0895	1.2	0.83	552.7730	6.5	567.7	6.4	627.8	18.0	552.8	6.5	425.5	1.2
Spot 266	273	21558	2.4	17.1481	1.1	0.7309	1.6	0.0898	1.1	0.74	554.6042	6.1	557.1	6.7	567.2	23.0	554.6	6.1	144.2	1.1
Spot 149	172	18919	1.7	16.9872	1.1	0.7326	1.8	0.0901	1.4	0.76	556.2984	7.2	558.1	7.6	565.5	24.8	556.3	7.2	164.6	1.3
Spot 256	171	33034	0.8	17.0100	1.2	0.7404	1.8	0.0902	1.3	0.74	556.4765	7.2	562.6	7.8	587.6	26.5	556.5	7.2	612.8	1.3
Spot 89	454	32630	3.0	16.9608	0.9	0.7403	2.0	0.0902	1.8	0.89	556.6753	9.7	562.6	8.8	586.5	19.9	556.7	9.7	144.2	1.7
Spot 86	112	28988	1.3	16.7458	1.3	0.7543	2.1	0.0908	1.6	0.77	560.1600	8.8	570.7	9.3	613.0	29.1	560.2	8.8	315.8	1.6
Spot 35	206	39222	1.7	16.9376	1.2	0.7561	1.7	0.0913	1.2	0.70	562.9484	6.3	571.8	7.4	607.0	26.2	562.9	6.3	342.9	1.1
Spot 44	244	29017	0.9	16.7478	1.0	0.7578	1.4	0.0913	1.0	0.68	563.0124	5.1	572.7	6.1	611.5	22.1	563.0	5.1	446.0	0.9
Spot 185	185	21204	0.8	16.6631	1.2	0.7583	1.7	0.0914	1.2	0.72	563.6128	6.5	573.0	7.3	610.5	25.2	563.6	6.5	372.8	1.2
Spot 172	281	31570	1.3	16.9354	1.0	0.7624	1.6	0.0931	1.2	0.77	573.9046	6.8	575.4	7.1	581.2	22.4	573.9	6.8	447.3	1.2
Spot 24	78	5551	1.4	16.1831	1.3	0.7852	2.0	0.0934	1.3	0.65	575.7548	7.0	588.5	8.8	637.8	32.1	575.8	7.0	53.2	1.2
Spot 222	14	2106	0.2	15.7966	2.0	0.7429	2.7	0.0937	1.7	0.61	577.1346	9.2	564.1	11.7	512.0	47.0	577.1	9.2	129.5	1.6
Spot 305	559	97166	0.8	17.0205	0.9	0.7812	1.9	0.0941	1.7	0.88	579.4864	9.2	586.2	8.4	612.1	19.7	579.5	9.2	1910.0	1.6
Spot 7	269	12763	41.8	16.6226	1.1	0.7903	1.8	0.0942	1.3	0.72	580.0564	7.2	591.4	8.1	635.0	26.7	580.1	7.2	17.2	1.2
Spot 77	613	90162	2.2	16.8411	0.9	0.7831	1.4	0.0944	1.1	0.79	581.2453	6.1	587.3	6.2	610.6	18.5	581.2	6.1	677.0	1.0
Spot 310	640	74637	2.3	16.7527	0.7	0.7978	1.6	0.0946	1.4	0.88	582.4685	7.6	595.6	7.0	646.0	15.9	582.5	7.6	530.1	1.3
Spot 244	420	32068	0.8	17.0387	0.9	0.7794	1.6	0.0949	1.3	0.81	584.3811	7.2	585.1	7.1	588.1	20.6	584.4	7.2	477.5	1.2
Spot 102	440	197479	2.9	16.6239	0.9	0.8018	1.6	0.0952	1.3	0.81	586.0324	7.1	597.9	7.1	643.0	20.0	586.0	7.1	1163.1	1.2
Spot 187	278	20038	1.6	16.3399	1.0	0.8068	1.6	0.0954	1.3	0.79	587.1862	7.0	600.6	7.2	651.8	21.1	587.2	7.0	178.4	1.2
Spot 205	147	14719	0.5	16.4612	1.4	0.8014	2.0	0.0954	1.4	0.70	587.3232	7.7	597.6	8.9	636.9	30.4	587.3	7.7	372.2	1.3
Spot 209	249	83255	0.7	16.2310	1.0	0.8330	1.8	0.0964	1.5	0.84	593.3009	8.6	615.3	8.3	697.0	21.1	593.3	8.6	1881.2	1.4
Spot 193	107	291658	1.3	16.3523	1.3	0.8275	1.6	0.0966	0.9	0.59	594.4986	5.2	612.2	7.1	678.3	26.8	594.5	5.2	4069.9	0.9
Spot 282	174	19902	0.5	16.4376	1.2	0.8262	1.6	0.0968	1.1	0.67	595.4535	6.1	611.5	7.4	671.4	25.9	595.5	6.1	454.6	1.0
Spot 287	119	83628	2.8	16.8623	1.1	0.8144	1.5	0.0972	1.0	0.68	597.9172	6.0	604.9	7.0	631.3	24.4	597.9	6.0	512.0	1.0
Spot 299	474	198252	1.3	16.7524	0.9	0.8227	1.6	0.0972	1.3	0.84	598.1818	7.7	609.6	7.4	652.1	19.0	598.2	7.7	2516.1	1.3
Spot 109	124	16541	2.0	16.7388	1.2	0.8011	1.7	0.0973	1.1	0.65	598.4628	6.4	597.5	7.7	593.6	28.0	598.5	6.4	106.1	1.1
Spot 230	240	21937	2.1	16.5130	0.9	0.8259	1.5	0.0979	1.2	0.77	602.2755	6.8	611.3	7.0	645.1	21.1	602.3	6.8	138.5	1.1
Spot 49	255	58069	2.1	16.6917	0.9	0.8281	1.4	0.0988	1.1	0.78	607.2305	6.4	612.5	6.5	632.2	19.0	607.2	6.4	493.2	1.0
Spot 95	545	33801	1.1	16.8198	0.9	0.8179	1.6	0.0990	1.4	0.85	608.7421	8.1	606.9	7.5	600.0	19.0	608.7	8.1	319.2	1.3
Spot 271	187	119663	1.2	16.5891	0.9	0.8440	1.5	0.0992	1.2	0.82	609.4416	7.2	621.3	7.1	664.9	18.8	609.4	7.2	1682.9	1.2
Spot 72	250	33544	0.9	16.6367	0.9	0.8323	1.5	0.0996	1.1	0.76	612.0502	6.5	614.9	6.7	625.4	20.6	612.1	6.5	635.4	1.1
Spot 123	320	48752	2.1	16.5540	0.9	0.8489	1.4	0.1008	1.1	0.79	619.0792	6.7	624.0	6.7	642.1	18.7	619.1	6.7	386.9	1.1
Spot 262	1435	70918	3.1	17.4335	1.0	0.8161	1.8	0.1013	1.5	0.84	622.0593	9.2	605.9	8.4	545.8	21.9	622.1	9.2	309.5	1.5
Spot 47	154	12263	0.7	16.6189	1.0	0.8412	1.6	0.1015	1.2	0.77	623.1301	7.4	619.8	7.5	607.8	22.4	623.1	7.4	214.4	1.2
Spot 180	49	16070	0.8	16.6363	1.3	0.8415	1.7	0.1017	1.1	0.65	624.4263	6.7	620.0	8.1	603.8	28.9	624.4	6.7	246.7	1.1
Spot 272	345	33228	1.9	16.5392	0.8	0.8684	1.2	0.1023	1.0	0.77	627.5918	5.7	634.7	5.9	660.2	17.1	627.6	5.7	212.4	0.9
Spot 243	287	25779	2.1	16.5337	1.0	0.8670	1.6	0.1026	1.2											

Spot 121	166	39523	2.2	15.9716	1.0	0.9762	1.4	0.1119	0.9	0.70	683.7692	6.1	691.6	6.8	717.3	20.6	683.8	6.1	275.6	0.9
Spot 20	88	8575	1.2	16.4876	1.1	0.9406	2.2	0.1123	1.4	0.66	686.2637	9.2	673.2	10.6	629.8	34.8	686.3	9.2	81.2	1.3
Spot 268	521	49199	8.2	15.6751	1.0	1.1298	1.9	0.1258	1.6	0.86	763.9672	11.6	767.6	10.1	778.3	20.2	764.0	11.6	77.6	1.5
Spot 103	174	31582	2.3	14.6985	1.2	1.1936	1.6	0.1259	1.0	0.66	764.6709	7.4	797.6	8.6	890.8	24.2	764.7	7.4	204.1	1.0
Spot 115	76	19218	1.2	15.2511	1.0	1.1466	1.5	0.1262	1.1	0.75	766.2238	8.0	775.6	8.0	802.8	20.5	766.2	8.0	159.0	1.0
Spot 101	603	125429	1.5	15.0419	0.9	1.2233	1.8	0.1312	1.5	0.87	794.9706	11.5	811.3	9.9	856.3	17.9	795.0	11.5	947.8	1.5
Spot 207	237	97525	4.2	14.5377	0.8	1.4813	1.3	0.1535	1.0	0.79	920.6435	8.9	922.8	8.0	927.8	16.6	927.8	16.6	253.0	1.8
Spot 26	1342	787319	28.7	14.4342	1.1	1.5828	1.9	0.1616	1.6	0.83	965.9308	14.0	963.5	11.7	957.8	21.6	957.8	21.6	256.3	2.3
Spot 231	98	11786	0.8	14.0148	0.9	1.5560	1.4	0.1576	1.0	0.73	943.1689	9.1	952.9	8.7	975.4	19.6	975.4	19.6	113.7	2.0
Spot 308	575	33184	49.3	14.2356	0.8	1.6477	2.0	0.1665	1.8	0.91	992.9310	16.4	988.7	12.3	979.3	16.2	979.3	16.2	101	1.7
Spot 192	187	37967	2.3	14.0866	0.7	1.4888	1.6	0.1504	1.4	0.88	903.2373	11.8	925.8	9.6	980.0	15.3	980.0	15.3	198.9	1.6
Spot 260	195	49219	1.8	14.1185	0.9	1.5315	1.4	0.1540	1.1	0.75	923.5964	9.2	943.1	8.8	989.0	19.3	989.0	19.3	306.1	2.0
Spot 182	458	157764	4.9	14.0284	0.9	1.6522	1.8	0.1661	1.6	0.88	990.4668	14.6	990.4	11.5	990.3	17.7	990.3	17.7	300.5	1.8
Spot 162	223	10238	5.8	13.7205	1.1	1.6288	1.5	0.1634	1.1	0.72	975.4862	10.0	981.4	9.6	994.7	21.6	994.7	21.6	14.9	2.2
Spot 250	129	21102	2.1	13.9968	0.8	1.6641	1.7	0.1669	1.5	0.88	994.8504	13.6	994.9	10.7	995.1	16.5	995.1	16.5	79.2	1.7
Spot 254	410	38231	3.0	13.9117	0.9	1.6768	1.9	0.1666	1.6	0.87	993.5411	14.9	999.8	11.8	1013.5	18.5	1013.5	18.5	93.5	1.8
Spot 145	138	24455	1.8	13.7601	1.0	1.6628	1.6	0.1650	1.3	0.79	984.5443	11.9	994.4	10.4	1016.3	20.2	1016.3	20.2	107.0	2.0
Spot 259	128	12191	2.8	13.7001	1.0	1.7351	1.5	0.1716	1.1	0.72	1021.1946	10.2	1021.6	9.7	1022.5	21.3	1022.5	21.3	32.3	2.1
Spot 261	484	57078	2.5	13.8359	0.7	1.6878	1.8	0.1663	1.6	0.91	991.4852	15.1	1003.9	11.5	1031.2	15.0	1031.2	15.0	225.9	1.5
Spot 135	98	17096	3.0	13.5911	1.2	1.6947	1.9	0.1665	1.6	0.80	992.8879	14.3	1006.5	12.4	1036.3	23.3	1036.3	23.3	44.0	2.2
Spot 203	86	33881	1.1	13.6771	1.1	1.7450	2.0	0.1714	1.6	0.82	1019.8403	15.4	1025.3	12.8	1037.0	23.0	1037.0	23.0	321.7	2.2
Spot 6	247	39677	2.1	13.8978	0.8	1.6375	1.3	0.1608	1.0	0.80	961.3582	9.3	984.8	8.2	1037.3	15.8	1037.3	15.8	188.9	1.5
Spot 234	243	19917	0.6	13.6810	1.1	1.5322	1.8	0.1503	1.3	0.75	902.9221	11.2	943.4	10.9	1039.0	23.4	1039.0	23.4	296.1	2.3
Spot 184	588	52794	2.2	13.6740	1.0	1.5157	2.1	0.1487	1.9	0.88	893.5853	15.6	936.7	13.0	1039.6	20.8	1039.6	20.8	267.7	2.0
Spot 178	295	47141	2.1	13.6633	0.9	1.8261	1.6	0.1790	1.3	0.83	1061.4745	12.8	1054.9	10.3	1041.3	17.5	1041.3	17.5	216.1	1.7
Spot 218	192	49857	3.0	13.7272	0.8	1.6778	1.4	0.1643	1.2	0.84	980.6074	10.7	1000.2	8.9	1043.3	15.2	1043.3	15.2	175.7	1.5
Spot 22	454	71678	2.5	13.8672	0.9	1.7329	1.7	0.1697	1.5	0.86	1010.3098	13.6	1020.8	10.9	1043.5	17.3	1043.5	17.3	261.7	1.7
Spot 201	86	15164	1.2	13.5377	0.8	1.7679	1.4	0.1731	1.2	0.83	1029.1503	11.2	1033.7	9.2	1043.5	15.9	1043.5	15.9	93.2	1.5
Spot 106	59	34259	0.9	13.6185	1.2	1.7000	1.8	0.1663	1.4	0.76	991.9263	12.7	1008.5	11.6	1044.8	23.9	1044.8	23.9	283.9	2.3
Spot 284	106	13771	2.6	13.6909	0.9	1.6818	1.6	0.1645	1.3	0.83	981.6814	12.1	1001.6	10.2	1045.6	17.7	1045.6	17.7	41.2	1.7
Spot 12	350	219738	1.6	13.8916	0.9	1.6875	1.9	0.1648	1.7	0.88	983.5257	15.4	1003.8	12.3	1048.5	18.7	1048.5	18.7	1388.9	1.8
Spot 181	68	4784	1.4	13.1089	1.2	1.8935	2.1	0.1848	1.7	0.81	1093.3210	17.0	1078.8	13.8	1049.6	24.3	1049.6	24.3	2.3	2.3
Spot 208	979	234764	2.0	13.7023	0.8	1.9137	1.8	0.1867	1.6	0.89	1103.3661	16.0	1085.9	11.9	1051.0	16.8	1051.0	16.8	792.3	1.6
Spot 281	208	38346	3.2	13.7788	1.2	1.6974	1.5	0.1655	0.8	0.56	987.3541	7.5	1007.6	9.4	1051.8	24.6	1051.8	24.6	91.1	2.3
Spot 194	288	198704	2.3	13.6516	0.8	1.5180	1.2	0.1479	0.9	0.74	889.3950	7.4	937.7	7.4	1052.9	16.4	1052.9	16.4	1083.5	1.6
Spot 11	272	379895	2.7	13.8553	1.0	1.7090	1.4	0.1664	1.0	0.72	992.3777	9.5	1011.9	9.2	1054.5	20.0	1054.5	20.0	1455.5	1.9
Spot 43	166	19142	2.1	13.5104	1.0	1.7538	1.7	0.1705	1.4	0.79	1015.1336	12.9	1028.6	11.2	1057.2	21.6	1057.2	21.6	70.4	2.0
Spot 191	313	51795	0.8	13.5597	0.9	1.7593	1.5	0.1708	1.2	0.79	1016.6362	11.1	1030.6	9.7	1060.4	18.5	1060.4	18.5	587.4	1.7
Spot 188	227	48304	2.6	13.5089	0.9	1.7546	1.6	0.1701	1.3	0.82	1012.7682	11.9	1028.9	10.0	1063.2	17.9	1063.2	17.9	196.5	1.7
Spot 177	116	11768	1.2	13.3505	1.2	1.7974	1.8	0.1742	1.3	0.72	1035.4771	12.4	1044.5	11.8	1063.5	25.1	1063.5	25.1	71.9	2.4
Spot 165	509	71948	28.0	13.4702	0.8	1.9035	1.6	0.1840	1.4	0.87	1088.8108	14.0	1082.3	10.8	1069.2	16.3	1069.2	16.3	23.2	1.5
Spot 125	60	8809	2.1	13.2442	1.0	1.9436	1.6	0.1877	1.1	0.67	1109.1355	10.9	1096.2	10.7	1070.7	23.8	1070.7	23.8	25.5	2.2
Spot 164	176	12375	3.0	13.2563	0.9	1.8175	1.5	0.1751	1.2	0.78	1040.1905	11.3	1051.8	9.9	1075.9	19.0	1075.9	19.0	31.2	1.8
Spot 139	146	12118	2.4	13.2202	1.0	1.8018	1.5	0.1729	1.1	0.74	1027.9736	10.4	1046.1	9.6	1084.2	19.7	1084.2	19.7	36.7	1.8
Spot 228	66	39703	0.6	13.4112	1.1	1.8270	1.8	0.1749	1.4	0.80	1039.3230	13.9	1055.2	11.8	1088.2	21.4	1088.2	21.4	464.3	2.0
Spot 62	446	277921	1.6	13.4586	0.9	1.7904	2.1	0.1714	1.9	0.89	1019.9484	17.8	1042.0	13.8	1088.4	18.9	1088.4	18.9	1597.2	1.7
Spot 210	381	221435	2.9	13.4466	1.1	1.9954	1.6	0.1909	1.2	0.73	1126.5004	12.1	1114.0	10.8	1089.6	21.6	1089.6	21.6	682.1	2.0
Spot 17	278	693067	1.3	13.6144	0.8	1.8085	1.4	0.1730	1.1	0.80	1028.8310	10.7	1048.5	9.1	1089.8	16.6	1089.8	16.6	5371.9	1.5
Spot 91	112	47406	2.0	13.2945	1.0	1.9044	1.5	0.1814	1.2	0.77	1074.4072	11.5	1082.6	10.1	1099.2	19.2	1099.2	19.2	214.7	1.8
Spot 302	390	35436	1.9	13.4230	1.0	1.8248	1.7	0.1738	1.4	0.83	1032.7509	13.7	1054.4	11.3	1099.6	19.1	1099.6	19.1	124.5	1.7
Spot 144	303	46699	3.8	13.2456	0.8	1.9321	1.5	0.1838	1.3	0.86	1087.7990	13.1	1092.3	10.2	1101.2	15.8	1101.2	15.8	115.5	1.4
Spot 223	212	33474	2.3	13.2664	0.7	1.8838	1.4	0.1786	1.3	0.88	1059.0853	12.5	1075.4	9.6	1108.6	13.6	1108.6	13.6	138.1	1.2
Spot 309	94	38729	2.0	13.3411	1.0	1.8831	1.6	0.1781	1.2	0.79	1056.7520	12.2	1075.2	10.5	1112.6	19.2	1112.6	19.2	145.0	1.7
Spot 248	611	197761	2.5	13.2985	0.9	2.1067	2.0	0.198												

Spot 276	358	681232	3.4	12.8755	1.2	1.8677	1.9	0.1699	1.5	0.78	1011.3311	13.6	1069.7	12.3	1190.8	22.7	1190.8	22.7	2261.9	1.9
Spot 278	167	142925	2.8	12.8822	1.0	2.0275	2.0	0.1843	1.7	0.87	1090.3537	17.5	1124.8	13.7	1191.9	19.9	1191.9	19.9	474.8	1.7
Spot 304	205	39781	5.8	12.7464	1.0	2.2646	1.5	0.2046	1.1	0.74	1199.8706	12.5	1201.3	10.8	1204.0	20.2	1204.0	20.2	42.7	1.7
Spot 198	17	49226	1.4	12.5904	1.5	2.1072	2.1	0.1897	1.4	0.69	1119.7344	14.8	1151.1	14.5	1210.8	30.1	1210.8	30.1	320.0	2.5
Spot 4	132	52087	1.8	12.7276	1.0	2.2356	1.6	0.2004	1.2	0.77	1177.6367	13.4	1192.3	11.3	1218.9	20.3	1218.9	20.3	247.5	1.7
Spot 313	293	32086	1.2	12.6083	0.9	2.1472	1.5	0.1920	1.2	0.82	1132.1023	12.9	1164.1	10.6	1224.2	17.3	1224.2	17.3	172.1	1.4
Spot 85	362	47116	2.0	12.4839	0.8	2.0387	1.4	0.1818	1.2	0.84	1077.0197	12.1	1128.5	9.9	1229.0	15.3	1229.0	15.3	255.1	1.2
Spot 225	327	465442	3.4	12.4500	0.9	2.3472	1.5	0.2074	1.2	0.82	1215.1935	13.7	1226.7	10.7	1247.0	16.8	1247.0	16.8	1130.9	1.4
Spot 105	137	24247	2.3	12.2448	0.8	2.0250	1.7	0.1784	1.5	0.87	1058.3269	14.5	1123.9	11.6	1253.0	16.4	1253.0	16.4	82.0	1.3
Spot 132	318	33233	1.8	12.1859	0.8	2.2537	1.4	0.1970	1.1	0.81	1159.0801	12.0	1197.9	9.9	1268.8	16.0	1268.8	16.0	158.6	1.3
Spot 52	34	30462	1.2	12.2127	1.2	2.4530	1.7	0.2144	1.2	0.70	1252.0423	13.7	1258.3	12.4	1269.0	23.9	1269.0	23.9	205.5	1.9
Spot 186	383	39295	2.5	12.1098	0.9	2.5308	1.6	0.2200	1.4	0.83	1282.1211	15.8	1280.9	11.9	1278.9	17.6	1278.9	17.6	116.7	1.4
Spot 60	34	22441	0.8	12.0209	1.2	2.4868	1.9	0.2144	1.4	0.75	1252.1798	15.9	1268.2	13.5	1295.5	23.9	1295.5	23.9	158.4	1.8
Spot 269	203	34266	2.2	12.1098	0.9	2.4617	1.6	0.2119	1.2	0.79	1238.8135	13.9	1260.9	11.2	1298.7	18.5	1298.7	18.5	100.4	1.4
Spot 289	269	310114	3.1	11.6938	1.1	2.6669	1.6	0.2202	1.1	0.72	1282.8484	13.1	1319.3	11.5	1379.1	20.7	1379.1	20.7	801.6	1.5
Spot 236	364	44740	2.7	11.5820	1.0	2.7659	2.0	0.2283	1.7	0.86	1325.8272	20.1	1346.4	14.6	1379.2	19.4	1379.2	19.4	119.3	1.4
Spot 168	423	42143	2.6	11.3788	0.9	3.0465	2.0	0.2490	1.8	0.90	1433.2536	23.6	1419.4	15.6	1398.6	17.5	1398.6	17.5	107.3	1.2
Spot 303	503	399126	2.5	11.4330	1.0	3.0370	2.0	0.2451	1.7	0.86	1412.9892	21.5	1417.0	15.1	1422.9	19.2	1422.9	19.2	1025.6	1.3
Spot 301	230	32872	2.5	11.3766	0.8	2.8545	1.1	0.2302	0.8	0.72	1335.7175	9.8	1370.0	8.5	1423.9	14.9	1423.9	14.9	73.8	1.0
Spot 251	58	8734	1.6	11.1345	1.2	2.8052	1.8	0.2257	1.3	0.71	1311.8310	15.2	1356.9	13.6	1428.7	24.6	1428.7	24.6	32.5	1.7
Spot 158	387	1147565	4.1	11.2315	0.9	3.0877	1.9	0.2482	1.7	0.88	1429.3791	21.4	1429.6	14.6	1430.0	17.5	1430.0	17.5	1732.4	1.2
Spot 65	586	34025	2.4	11.1840	0.8	3.2153	1.6	0.2573	1.4	0.86	1475.8069	18.3	1460.9	12.5	1439.2	15.9	1439.2	15.9	68.2	1.1
Spot 146	313	30670	2.4	11.0610	0.9	3.0322	1.7	0.2411	1.5	0.86	1392.6343	18.6	1415.8	13.2	1450.7	17.0	1450.7	17.0	89.9	1.2
Spot 252	80	11320	2.0	11.0481	1.2	3.1216	1.8	0.2481	1.3	0.71	1428.8074	16.2	1438.0	13.7	1451.7	23.9	1451.7	23.9	29.9	1.6
Spot 61	77	19089	1.0	11.0795	0.8	2.7771	1.7	0.2205	1.5	0.87	1284.6751	17.6	1349.4	12.9	1453.5	16.0	1453.5	16.0	110.3	1.1
Spot 204	472	74400	1.8	11.0934	0.9	3.2747	1.8	0.2596	1.5	0.85	1487.9123	20.2	1475.1	13.9	1456.6	17.8	1456.6	17.8	240.9	1.2
Spot 315	227	21485	2.4	11.1608	0.9	3.0553	1.6	0.2422	1.3	0.81	1398.2356	15.9	1421.6	11.9	1456.6	17.1	1456.6	17.1	48.1	1.2
Spot 312	333	35600	1.5	11.1811	0.8	3.1920	1.3	0.2528	1.0	0.79	1452.8833	13.4	1455.2	10.0	1458.6	15.0	1458.6	15.0	119.7	1.0
Spot 206	173	14376	1.0	10.9749	0.8	3.2879	1.3	0.2594	1.0	0.78	1487.0020	13.7	1478.2	10.4	1465.6	15.9	1465.6	15.9	68.2	1.1
Spot 214	190	33722	0.8	11.0379	0.9	3.2522	1.6	0.2562	1.3	0.83	1470.5839	17.3	1469.7	12.3	1468.4	16.7	1468.4	16.7	191.2	1.1
Spot 88	375	62596	1.0	10.9408	1.0	3.0428	1.6	0.2379	1.3	0.79	1375.8224	15.6	1418.4	12.3	1483.0	18.8	1483.0	18.8	421.2	1.3
Spot 14	63	42396	2.1	11.0535	0.9	3.2318	1.6	0.2519	1.3	0.82	1448.2941	17.2	1464.8	12.6	1488.9	17.8	1488.9	17.8	138.6	1.2
Spot 96	405	85408	1.6	10.8669	1.0	3.3897	1.8	0.2636	1.6	0.85	1508.3946	21.2	1502.0	14.5	1493.0	18.4	1493.0	18.4	324.6	1.2
Spot 288	450	229482	2.0	10.9860	0.9	3.2722	1.6	0.2538	1.4	0.85	1458.2627	17.7	1474.5	12.4	1497.9	16.1	1497.9	16.1	694.8	1.1
Spot 46	162	35656	1.6	10.8438	0.8	3.3522	1.7	0.2598	1.4	0.86	1488.7786	19.1	1493.3	13.0	1499.7	15.8	1499.7	15.8	110.7	1.1
Spot 5	169	18562	3.0	10.8687	0.8	3.3268	1.2	0.2563	0.9	0.74	1471.0034	11.8	1487.4	9.4	1510.7	15.2	1510.7	15.2	32.5	1.0
Spot 2	317	40162	2.5	10.9332	1.1	3.2595	1.7	0.2511	1.3	0.75	1444.1707	16.3	1471.4	13.1	1511.0	21.0	1511.0	21.0	114.8	1.4
Spot 217	409	68218	2.6	10.8028	0.9	3.4746	1.5	0.2673	1.2	0.79	1527.0706	16.4	1521.5	12.0	1513.7	17.4	1513.7	17.4	160.1	1.2
Spot 257	65	76806	1.1	10.6330	1.0	3.4548	1.6	0.2615	1.3	0.80	1497.6079	17.0	1517.0	12.6	1544.1	18.1	1544.1	18.1	447.8	1.2
Spot 128	405	123730	1.4	10.5613	0.7	3.3844	1.9	0.2552	1.8	0.92	1465.2980	23.4	1500.8	15.2	1551.2	14.0	1551.2	14.0	538.1	0.9
Spot 227	166	83675	0.7	10.3846	0.7	3.7184	1.3	0.2745	1.0	0.81	1563.4960	14.5	1575.3	10.3	1591.2	13.9	1591.2	13.9	757.7	0.9
Spot 285	580	251369	0.7	10.3870	1.0	3.9797	2.0	0.2915	1.8	0.88	1649.2061	26.1	1630.1	16.5	1605.4	17.8	1605.4	17.8	2010.0	1.1
Spot 193	499	212323	0.5	10.2252	0.9	3.9087	1.6	0.2858	1.4	0.84	1620.6181	19.6	1615.9	13.2	1608.8	16.5	1608.8	16.5	2360.1	1.0
Spot 179	92	42934	0.8	10.0857	0.9	3.9654	1.5	0.2871	1.1	0.79	1627.1544	16.5	1627.1	11.8	1627.1	16.5	1627.1	16.5	288.7	1.0
Spot 110	21	11606	0.8	9.9914	1.0	4.1440	1.8	0.2995	1.5	0.82	1688.8809	22.1	1663.0	14.9	1630.5	19.5	1630.5	19.5	58.4	1.2
Spot 116	769	62932	18.3	10.0989	1.0	3.4692	2.6	0.2505	2.4	0.92	1441.1968	30.4	1520.2	20.2	1632.1	18.7	1632.1	18.7	13.7	1.1
Spot 174	363	421621	1.9	10.0953	0.8	3.8348	1.5	0.2767	1.3	0.86	1574.5671	18.2	1600.1	12.2	1633.8	14.2	1633.8	14.2	1337.5	0.9
Spot 55	345	68859	1.4	10.1291	0.8	3.9171	1.4	0.2819	1.2	0.83	1600.8138	17.0	1617.2	11.7	1638.6	14.9	1638.6	14.9	289.0	0.9
Spot 130	63	13072	0.8	9.9062	0.8	4.0799	1.7	0.2914	1.4	0.85	1648.6166	20.4	1650.3	13.5	1652.4	16.2	1652.4	16.2	69.1	1.0
Spot 199	160	39439	2.5	9.9604	4.9	0.9141	5.3	0.0652	1.8	0.34	407.0563	7.0	659.2	25.5	1655.5	91.7	1655.5	91.7	552.8	5.5
Spot 90	134	99522	1.4	9.9810	0.9	4.0277	1.4	0.2870	1.1	0.77	1626.4595	15.3	1639.8	11.2	1656.9	16.4	1656.9	16.4	422.6	1.0
Spot 264	116	24265	0.7	9.9936	0.9	4.0299	1.5	0.2868	1.2	0.80	1625.7565	17.5	1640.2	12.4	1658.9	16.9	1658.9	16.9	168.4	1.0
Spot 1	188	48903	1.5	10.0534	0.9	4.0919	1.6	0.2896	1.3	0.81	1639.4717	18.5	1652.7	12.9						

Spot 92	144	34573	3.1	9.3595	0.7	4.6971	1.6	0.3148	1.4	0.90	1764.4126	21.6	1766.7	13.1	1769.4	12.7	1769.4	12.7	61.3	0.7
Spot 151	203	66213	1.7	9.3214	0.8	4.5659	1.3	0.3048	0.9	0.74	1715.0143	14.1	1743.1	10.5	1776.9	15.4	1776.9	15.4	216.6	0.9
Spot 94	110	34324	1.0	8.8084	0.7	5.3331	1.2	0.3369	1.0	0.82	1871.6763	16.2	1874.2	10.4	1877.0	12.5	1877.0	12.5	169.0	0.7
Spot 215	42	32489	0.9	8.7970	1.0	5.6846	1.6	0.3566	1.3	0.80	1966.1972	21.7	1929.0	13.9	1889.3	17.3	1889.3	17.3	169.4	0.9
Spot 140	96	123755	1.3	8.6846	1.0	5.4071	1.4	0.3358	1.0	0.70	1866.6509	15.9	1886.0	11.9	1907.3	17.8	1907.3	17.8	496.9	0.9
Spot 296	228	62073	0.9	8.6205	0.8	4.6544	1.3	0.2833	1.0	0.79	1607.7504	14.9	1759.1	11.1	1943.9	14.6	1943.9	14.6	485.0	0.8
Spot 122	159	26627	1.6	8.2472	0.8	6.0489	1.5	0.3576	1.2	0.85	1970.5559	20.9	1982.9	12.6	1995.8	13.7	1995.8	13.7	63.0	0.7
Spot 314	331	260088	4.3	8.2680	0.8	5.4487	1.6	0.3178	1.4	0.87	1779.1203	21.1	1892.6	13.4	2019.4	13.6	2019.4	13.6	349.8	0.7
Spot 138	289	35781	2.2	8.0945	0.8	6.2300	1.4	0.3623	1.1	0.80	1993.1071	19.4	2008.7	12.4	2024.7	15.1	2024.7	15.1	73.5	0.7
Spot 245	117	16898	1.4	7.7272	0.9	6.9422	1.3	0.3828	1.0	0.74	2089.1203	17.2	2104.1	11.6	2118.7	15.5	2118.7	15.5	37.6	0.7
Spot 25	22	37235	1.6	7.7516	0.8	7.0581	1.6	0.3881	1.4	0.87	2113.9184	24.7	2118.8	14.1	2123.5	13.8	2123.5	13.8	99.3	0.7
Spot 58	93	150269	2.0	7.6192	0.8	7.0816	1.3	0.3839	1.0	0.79	2094.4937	18.2	2121.7	11.4	2148.2	13.8	2148.2	13.8	329.5	0.6
Spot 141	42	32545	1.5	7.3866	0.7	7.4680	1.5	0.3953	1.3	0.87	2147.4563	24.6	2169.2	13.8	2189.7	13.0	2189.7	13.0	93.3	0.6
Spot 30	218	170685	3.4	7.3192	0.7	7.8589	1.4	0.4073	1.1	0.84	2202.5035	21.4	2215.0	12.2	2226.5	12.6	2226.5	12.6	209.0	0.6
Spot 48	96	31168	2.3	7.1910	0.7	8.1688	1.4	0.4193	1.2	0.85	2257.3129	22.5	2249.9	12.5	2243.1	12.4	2243.1	12.4	44.5	0.6
Spot 249	102	24433	1.0	6.6190	0.9	8.2882	1.7	0.3904	1.5	0.86	2124.5513	26.2	2263.0	15.3	2390.6	14.7	2390.6	14.7	80.0	0.6
Spot 196	38	7807	1.2	6.3010	0.8	9.5237	1.4	0.4319	1.1	0.80	2314.4729	22.0	2389.8	13.0	2454.7	14.3	2454.7	14.3	20.4	0.6
Spot 100	232	163281	4.5	6.2661	0.7	10.3961	1.5	0.4647	1.3	0.89	2460.4870	27.2	2470.7	13.8	2479.1	11.2	2479.1	11.2	141.6	0.5
Spot 81	248	299493	0.9	5.8998	0.7	10.2152	1.2	0.4300	1.0	0.84	2305.7938	20.2	2454.5	11.5	2580.0	11.4	2580.0	11.4	1202.3	0.4
Spot 112	87	32991	30.7	5.7540	1.0	12.1116	1.5	0.4982	1.2	0.78	2606.1244	25.3	2613.1	14.2	2618.5	15.9	2618.5	15.9	3.8	0.6
Spot 129	428	514742	7.7	5.7533	1.1	12.5247	2.1	0.5142	1.7	0.84	2674.6694	38.3	2644.6	19.6	2621.6	18.7	2621.6	18.7	211.0	0.7
Spot 195	191	305071	1.0	5.7027	0.6	10.8387	1.3	0.4405	1.2	0.90	2352.7406	23.6	2509.4	12.4	2638.7	9.7	2638.7	9.7	1259.3	0.4
Spot 64	189	61125	0.7	5.5483	0.9	11.2751	1.6	0.4460	1.3	0.84	2377.6622	26.7	2546.1	15.0	2683.2	14.5	2683.2	14.5	333.0	0.5
Spot 212	173	2215158	1.1	5.5108	0.9	13.1121	1.2	0.5138	0.9	0.72	2672.7811	19.4	2687.8	11.7	2699.0	14.2	2699.0	14.2	6610.7	0.5
Spot 219	223	96090	2.3	5.4880	0.9	13.0714	1.4	0.5104	1.0	0.74	2658.2449	22.0	2684.8	12.9	2704.9	15.2	2704.9	15.2	143.7	0.6
Spot 98	125	3595866	1.3	5.4588	0.8	13.3995	1.3	0.5216	1.1	0.82	2705.9313	24.3	2708.2	12.6	2709.9	12.5	2709.9	12.5	9075.1	0.5
Spot 68	70	130126	1.4	5.4265	0.8	13.2558	1.6	0.5127	1.4	0.86	2668.0941	30.7	2698.0	15.5	2720.5	13.9	2720.5	13.9	305.1	0.5
Spot 9	199	267316	2.0	5.4325	0.8	12.8890	1.4	0.4907	1.2	0.84	2573.6512	25.6	2671.6	13.5	2746.5	12.8	2746.5	12.8	476.8	0.5
Spot 211	244	462399	1.3	5.2312	0.8	13.1981	1.3	0.4910	1.1	0.80	2574.8785	22.8	2693.9	12.7	2784.5	13.3	2784.5	13.3	1323.1	0.5
Spot 183	172	73931	1.1	5.0205	0.8	15.1559	1.4	0.5449	1.2	0.84	2804.1255	26.5	2825.1	13.3	2840.1	12.4	2840.1	12.4	226.3	0.4
Spot 233	71	3552183	2.8	4.9697	0.8	16.0963	1.4	0.5675	1.2	0.84	2897.4643	26.9	2882.5	13.2	2872.1	12.3	2872.1	12.3	3981.3	0.4
Spot 36	88	232593	1.8	4.7524	0.8	17.6314	1.4	0.5935	1.1	0.81	3003.4165	27.6	2969.8	13.6	2947.2	13.2	2947.2	13.2	338.4	0.4
Spot 51	174	73270	3.9	4.6724	0.8	17.6526	1.3	0.5873	1.0	0.77	2978.4577	23.7	2971.0	12.5	2965.9	13.4	2965.9	13.4	58.5	0.5
Spot 267	465	639435	3.4	4.0862	0.8	21.9135	1.6	0.6345	1.4	0.86	3167.3511	34.6	3179.9	15.6	3187.8	13.0	3187.8	13.0	459.4	0.4
Spot 38	320	551580	5.7	3.0820	0.8	35.2305	1.4	0.7689	1.1	0.83	3676.6548	31.7	3645.1	13.5	3627.8	11.8	3627.8	11.8	219.2	0.3

Key
% Error > 3
U/Th > 10
U > 5,000 ppm
suspect neo-crystalline
ages used for MDA

Sample 15LT03

Analysis	U (ppm)	Isotope ratios						Apparent ages (Ma)												
		206Pb 204Pb	U/Th	206Pb* 207Pb*	± (%)	207Pb* 235U	± (%)	206Pb* 238U	± (%)	error corr.	206Pb* 238U	± (Ma)	207Pb* 235U	± (Ma)	206Pb* 207Pb*	± (Ma)	Best age (Ma)	± (Ma)	Conc (%)	% Error
Spot 54	3557	1827003	0.8	21.1671	1.0	0.0384	4.9	0.0058	4.8	0.98	37.4118	1.8	38.3	1.9	93.2	23.9	37.4	1.8	136441.5	4.8
Spot 20	1823	313015	2.4	21.5843	1.0	0.0387	3.1	0.0059	2.9	0.94	38.2026	1.1	38.6	1.2	60.9	25.0	38.2	1.1	3427.7	2.9
Spot 4	3330	7163	4.8	21.5534	0.9	0.0381	3.4	0.0061	2.5	0.75	39.2073	1.0	37.9	1.3	NA	NA	39.2	1.0	255.1	2.5
Spot 74	4526	2432	5.4	8.4077	11.4	0.0988	12.9	0.0062	5.9	0.46	40.1598	2.4	95.7	11.8	1874.4	207.5	40.2	2.4	249.0	5.9
Spot 65	3939	291058	6.2	21.7929	0.7	0.0408	2.1	0.0064	2.0	0.94	40.9505	0.8	40.6	0.9	17.7	17.3	41.0	0.8	2411.3	2.0
Spot 67	7683	75141	16.6	21.2000	0.6	0.0438	1.9	0.0067	1.7	0.94	42.9511	0.7	43.5	0.8	76.2	15.4	43.0	0.7	416.4	1.7
Spot 60	5614	130967	6.8	21.6439	0.9	0.0430	2.0	0.0067	1.8	0.90	43.0107	0.8	42.8	0.9	30.4	20.8	43.0	0.8	1543.6	1.8
Spot 3	5002	114915	10.4	20.9203	1.0	0.0484	2.0	0.0072	1.8	0.88	46.3801	0.8	48.0	1.0	131.6	23.1	46.4	0.8	868.5	1.8
Spot 51	5421	108367	10.9	21.1091	0.9	0.0487	2.2	0.0074	2.0	0.92	47.3277	0.9	48.2	1.0	93.6	20.3	47.3	0.9	819.5	2.0
Spot 63	5480	59001	4.9	21.5472	1.0	0.0483	2.0	0.0075	1.8	0.88	48.1396	0.8	47.9	0.9	34.0	22.9	48.1	0.8	876.0	1.8
Spot 47	5749	73224	10.9	20.5919	1.0	0.0525	2.0	0.0078	1.7	0.85	49.7784	0.8	51.9	1.0	152.4	24.1	49.8	0.8	473.1	1.7
Spot 17	4346	108349	4.5	21.2151	0.8	0.0533	2.0	0.0081	1.9	0.92	51.7749	1.0	52.7	1.1	95.6	19.2	51.8	1.0	2089.6	1.9
Spot 15	3678	529687	4.7	20.7755	0.9	0.0553	2.0	0.0082	1.7	0.88	52.4875	0.9	54.6	1.1	150.3	21.7	52.5	0.9	10086.3	1.7
Spot 61	3286	75112	10.4	20.9765	0.9	0.0548	1.8	0.0083	1.6	0.86	53.0739	0.8	54.1	1.0	100.9	22.2	53.1	0.8	448.9	1.6
Spot 13	4300	110651	19.7	21.1060	0.9	0.0559	2.2	0.0084	2.0	0.91	54.0089	1.1	55.2	1.2	108.0	22.0	54.0	1.1	356.2	2.0
Spot 50	1195	19914	3.3	20.7422	1.1	0.0564	2.0	0.0085	1.6	0.80	54.5532	0.9	55.7	1.1	107.0	27.5	54.6	0.9	359.3	1.6
Spot 33	1772	37236	6.2	19.7468	1.1	0.0612	2.0	0.0087	1.7	0.83	55.6021	0.9	60.3	1.2	250.3	26.3	55.6	0.9	369.4	1.7
Spot 35	2896	162996	1.8	20.9268	1.0	0.0583	1.7	0.0087	1.4	0.82	55.8632	0.8	57.5	0.9	126.8	22.4	55.9	0.8	6962.3	1.4
Spot 14	1674	51632	4.5	20.9513	0.9	0.0591	2.1	0.0089	1.9	0.90	56.8391	1.1	58.3	1.2	117.8	21.7	56.8	1.1	580.9	1.9
Spot 40	2753	73083	7.6	21.2935	1.1	0.0586	2.0	0.0089	1.7	0.84	57.2543	1.0	57.9	1.1	82.9	25.7	57.3	1.0	513.3	1.7
Spot 30	2715	30700	4.1	21.4409	1.3	0.0584	2.3	0.0090	1.9	0.84	57.8964	1.1	57.7	1.3	48.1	30.0	57.9	1.1	403.6	1.9
Spot 19	3509	97687	6.1	21.3015	1.0	0.0596	2.3	0.0091	2.1	0.90	58.1284	1.2	58.8	1.3	87.0	24.1	58.1	1.2	989.1	2.1
Spot 38	1034	11379	4.0	15.0888	5.7	0.0837	6.0	0.0092	1.8	0.31	58.7912	1.1	81.7	4.7	815.7	119.9	58.8	1.1	197.6	1.8
Spot 18	1103	95333	3.7	20.9846	1.1	0.0624	2.0	0.0093	1.7	0.84	59.9490	1.0	61.5	1.2	120.7	26.2	59.9	1.0	1589.1	1.7
Spot 22	1035	102638	7.0	20.8995	1.1	0.0631	2.0	0.0094	1.7	0.84	60.4182	1.0	62.2	1.2	129.5	25.1	60.4	1.0	742.5	1.7
Spot 31	1315	64784	7.0	20.9731	1.1	0.0628	2.0	0.0094	1.7	0.84	60.4417	1.0	61.8	1.2	116.3	25.5	60.4	1.0	469.9	1.7
Spot 10	701	44036	2.6	20.0194	1.5	0.0663	2.3	0.0095	1.7	0.75	60.8448	1.0	65.1	1.4	226.1	34.2	60.8	1.0	759.1	1.7
Spot 68	1355	79534	4.3	20.8511	1.3	0.0632	2.3	0.0095	2.0	0.84	60.8801	1.2	62.3	1.4	115.3	29.9	60.9	1.2	945.1	2.0
Spot 66	940	19960	8.9	16.0206	3.6	0.0818	4.0	0.0095	1.7	0.43	60.9540	1.1	79.8	3.1	688.9	77.8	61.0	1.1	213.8	1.7
Spot 73	1356	202043	2.4	21.1265	1.2	0.0630	2.2	0.0096	1.9	0.84	61.3655	1.1	62.1	1.3	89.1	28.2	61.4	1.1	5627.1	1.9
Spot 7	294	5605	3.5	19.0600	1.6	0.0673	2.4	0.0096	1.7	0.72	61.5233	1.0	66.1	1.5	235.2	38.1	61.5	1.0	162.5	1.7
Spot 75	671	62580	4.4	20.8276	1.4	0.0640	2.3	0.0096	1.8	0.78	61.6752	1.1	63.0	1.4	114.7	33.9	61.7	1.1	681.5	1.8
Spot 6	1463	62624	2.5	21.0824	0.8	0.0642	1.6	0.0097	1.3	0.84	62.0489	0.8	63.2	1.0	108.0	20.1	62.0	0.8	1180.8	1.3
Spot 64	352	8761	3.0	21.1319	1.7	0.0616	2.2	0.0097	1.3	0.61	62.1147	0.8	60.7	1.3	7.0	NA	62.1	0.8	161.0	1.3
Spot 48	1026	45150	4.1	21.0748	1.2	0.0646	2.1	0.0098	1.8	0.84	62.8413	1.1	63.5	1.3	89.6	27.6	62.8	1.1	492.7	1.8
Spot 45	271	210281	4.6	20.7155	2.0	0.0662	2.6	0.0098	1.6	0.63	62.8727	1.0	65.1	1.6	148.5	47.2	62.9	1.0	4017.6	1.6
Spot 25	1503	29697	5.0	20.9925	1.0	0.0650	1.9	0.0098	1.6	0.85	62.9585	1.0	63.9	1.2	99.6	23.3	63.0	1.0	297.0	1.6
Spot 55	698	21518	2.8	21.3279	1.6	0.0635	2.1	0.0098	1.4	0.66	63.1276	0.9	62.5	1.3	38.3	38.2	63.1	0.9	338.5	1.4
Spot 62	292	498260	2.9	20.3729	1.5	0.0674	2.7	0.0098	2.3	0.84	63.1748	1.4	66.2	1.7	177.8	34.6	63.2	1.4	11312.6	2.2
Spot 21	520	126535	2.8	21.2883	2.1	0.0656	2.8	0.0100	1.9	0.67	63.8326	1.2	64.5	1.7	90.2	49.4	63.8	1.2	2906.3	1.9
Spot 11	350	9638	3.2	20.6605	1.9	0.0659	2.6	0.0100	1.7	0.66	64.0352	1.1	64.8	1.6	92.7	46.7	64.0	1.1	156.2	1.7
Spot 36	253	12270	4.1	21.6175	2.1	0.0635	2.5	0.0100	1.2	0.48	64.2765	0.8	62.5	1.5	NA	NA	64.3	0.8	155.6	1.2
Spot 28	828	106993	3.5	20.4377	1.5	0.0687	2.4	0.0100	1.9	0.78	64.2934	1.2	67.4	1.6	180.2	35.3	64.3	1.2	1501.1	1.9
Spot 46	123	2517	3.8	18.0570	3.8	0.0700	4.4	0.0101	1.3	0.29	64.7725	0.8	68.7	2.9	208.1	97.2	64.8	0.8	154.4	1.3
Spot 27	708	40191	1.6	21.1981	1.0	0.0667	1.8	0.0101	1.5	0.82	65.0683	1.0	65.5	1.2	82.6	24.9	65.1	1.0	1026.9	1.5
Spot 23	603	33473	4.4	21.3885	1.4	0.0664	2.6	0.0102	2.2	0.83	65.4221	1.4	65.3	1.7	59.4	34.5	65.4	1.4	352.6	2.2
Spot 9	569	29416	9.7	20.3316	1.3	0.0828	2.2	0.0120	1.8	0.81	77.1530	1.4	80.7	1.7	187.8	30.2	77.2	1.4	256.0	1.8
Spot 76	696	9408	3.8	18.8284	1.7	0.1143	2.1	0.0159	1.2	0.59	101.7002	1.3	109.9	2.2	291.2	39.4	101.7	1.3	143.9	1.2
Spot 26	483	13084	5.8	19.0209	1.0	0.1615	3.0	0.0224	2.8	0.93	142.5598	3.9	152.0	4.2	302.7	24.3	142.6	3.9	77.9	2.7
Spot 34	1117	31979	4.2	14.1032	0.8	0.2658	2.5	0.0269	2.3	0.94	170.9343	4.0	239.3	5.3	978.6	17.2	170.9	4.0	248.1	2.3
Spot 24	269	141219	1.9	18.3004	1.0	0.3113	1.5	0.0406	1.1	0.73	256.8438</									

Spot 2	730	106902	2.0	19.2199	0.7	0.3505	1.4	0.0481	1.2	0.87	302.5449	3.5	305.1	3.6	324.7	15.5	302.5	3.5	470.0	1.2
Spot 29	47	15317	4.1	14.9502	3.8	0.4622	4.0	0.0499	1.1	0.26	314.1708	3.2	385.8	12.8	841.6	80.2	314.2	3.2	49.1	1.0
Spot 69	115	29755	2.6	18.9036	1.5	0.3752	2.1	0.0514	1.5	0.70	322.8788	4.7	323.5	5.8	327.7	34.2	322.9	4.7	109.5	1.4
Spot 78	174	152114	1.0	18.8258	1.1	0.3815	1.8	0.0516	1.4	0.77	324.5681	4.3	328.1	5.0	353.5	25.7	324.6	4.3	179.21	1.3
Spot 57	78	7030	2.4	18.7703	1.6	0.3769	2.0	0.0527	1.2	0.59	331.1676	3.8	324.8	5.5	279.3	36.2	331.2	3.8	30.2	1.1
Spot 32	978	481987	2.6	15.1483	1.0	0.5899	1.8	0.0636	1.4	0.82	397.7181	5.6	470.8	6.6	844.9	20.6	397.7	5.6	1268.2	1.4
Spot 59	199	43727	1.3	17.9245	1.1	0.5033	1.8	0.0650	1.4	0.78	406.1779	5.6	413.9	6.2	457.4	25.2	406.2	5.6	241.8	1.4
Spot 58	424	159723	1.5	18.2115	1.0	0.5101	1.9	0.0666	1.6	0.86	415.8863	6.6	418.5	6.5	432.9	21.2	415.9	6.6	961.9	1.6
Spot 56	662	17867	1.3	15.1059	1.6	0.6347	2.9	0.0695	2.4	0.84	433.2102	10.1	499.0	11.4	813.5	32.9	433.2	10.1	114.4	2.3
Spot 43	235	44695	2.5	17.7380	1.0	0.6078	1.6	0.0772	1.2	0.77	479.4049	5.5	482.2	6.0	495.5	22.0	479.4	5.5	109.3	1.2
Spot 8	147	46401	1.5	16.9963	1.0	0.7627	1.4	0.0925	1.1	0.73	570.1072	5.7	575.6	6.3	597.3	21.4	570.1	5.7	158.2	1.0
Spot 37	112	8433834	1.7	14.9827	1.0	1.2654	1.5	0.1348	1.1	0.76	815.3669	8.8	830.3	8.6	870.6	20.3	815.4	8.8	24111.0	1.1
Spot 42	71	164767	2.1	12.1401	0.8	2.3688	1.6	0.2049	1.3	0.85	1201.7986	14.8	1233.2	11.3	1288.6	16.2	1288.6	16.2	254.9	1.3
Spot 41	314	7062185	2.6	9.0389	0.7	4.7676	1.6	0.3068	1.4	0.90	1724.9029	21.5	1779.2	13.2	1843.5	12.4	1843.5	12.4	5781.1	0.7
Spot 44	274	176054	2.6	9.0143	0.9	5.0981	1.6	0.3277	1.3	0.84	1827.1824	20.9	1835.8	13.3	1845.5	15.4	1845.5	15.4	128.0	0.8
Spot 71	18	284312	1.9	7.7035	1.0	7.2582	1.8	0.4013	1.4	0.81	2175.1671	26.6	2143.7	15.8	2113.6	18.0	2113.6	18.0	240.8	0.8
Spot 12	109	90332	3.0	7.4865	1.0	6.0046	1.5	0.3196	1.2	0.76	1787.6179	18.2	1976.5	13.3	2180.4	17.2	2180.4	17.2	42.9	0.8
Spot 72	72	62671	1.8	5.0892	0.8	14.0580	1.6	0.5137	1.4	0.86	2672.3701	30.8	2753.6	15.5	2813.7	13.6	2813.7	13.6	34.5	0.5

Key

	% Error > 3
	U/Th > 10
	U > 5,000 ppm
	suspect neo-crystalline ages used for MDA

Sample 21BG24

Analysis	U (ppm)	Isotope ratios						error corr.	Apparent ages (Ma)								Conc (%)	% Error		
		206Pb 204Pb	U/Th	206Pb* 207Pb*	± (%)	207Pb* 235U	± (%)		206Pb* 238U	± (Ma)	207Pb* 235U	± (Ma)	206Pb* 207Pb*	± (Ma)	Best age (Ma)	± (Ma)				
Sample 1 Spot 35	959	18911	36.7	21.1557	0.9	0.0678	1.2	0.0107	0.7	0.61	68.3604	0.5	66.6	0.7	4.7	NA	68.4	0.5	1467.6	0.7
Sample 1 Spot 67	292	2746	15.1	16.2540	3.1	0.1092	4.0	0.0142	2.6	0.64	90.9835	2.3	105.2	4.0	440.7	69.3	91.0	2.3	20.6	2.5
Sample 1 Spot 16	2956	105342	1.9	14.8765	0.8	0.3327	2.3	0.0362	2.1	0.94	229.4811	4.8	291.6	5.8	824.8	15.8	229.5	4.8	27.8	2.1
Sample 1 Spot 55	666	77309	4.0	17.8538	0.5	0.3328	1.7	0.0435	1.6	0.95	274.7623	4.3	291.7	4.2	430.0	11.7	274.8	4.3	63.9	1.6
Sample 1 Spot 66	76	11646	2.6	16.7068	1.2	0.4474	1.5	0.0559	0.9	0.61	350.3809	3.2	375.4	4.8	533.1	26.2	350.4	3.2	65.7	0.9
Sample 1 Spot 7	1071	94320	2.0	17.6353	0.6	0.4399	3.1	0.0569	3.0	0.98	356.9462	10.4	370.2	9.5	453.9	12.9	356.9	10.4	78.6	2.9
Sample 1 Spot 6	1354	203860	4.0	17.2478	0.6	0.4572	1.5	0.0578	1.4	0.91	362.0423	4.8	382.3	4.8	507.2	13.3	362.0	4.8	71.4	1.3
Sample 1 Spot 21	311	12707	3.1	17.6221	0.7	0.4399	1.9	0.0578	1.7	0.93	362.3357	6.1	370.2	5.8	419.8	15.6	362.3	6.1	86.3	1.7
Sample 1 Spot 17	1399	11757	2.5	6.3793	0.5	1.2466	2.3	0.0585	2.3	0.98	366.5983	8.1	821.9	13.1	2396.5	8.3	366.6	8.1	15.3	2.2
Sample 1 Spot 33	748	21988	1.4	17.0379	0.6	0.4955	1.5	0.0624	1.4	0.91	389.9759	5.1	408.6	5.0	515.4	13.2	390.0	5.1	75.7	1.3
Sample 1 Spot 58	287	45885	1.6	16.4645	0.7	0.5417	1.5	0.0655	1.3	0.89	408.8531	5.3	439.6	5.4	603.8	15.1	408.9	5.3	67.7	1.3
Sample 1 Spot 31	53	5067	1.5	17.0446	1.2	0.5015	2.2	0.0656	0.8	0.34	409.8854	3.0	412.7	7.6	428.4	47.1	409.9	3.0	95.7	0.7
Sample 1 Spot 61	422	16256	2.1	17.0024	1.1	0.5511	1.8	0.0695	1.5	0.80	433.2644	6.1	445.7	6.6	510.5	24.2	433.3	6.1	84.9	1.4
Sample 1 Spot 12	135	24475	3.3	17.9609	0.7	0.5369	0.9	0.0713	0.6	0.64	443.9317	2.4	436.3	3.1	396.5	15.1	443.9	2.4	112.0	0.5
Sample 1 Spot 9	730	1186647	0.9	17.5305	0.5	0.5562	0.8	0.0714	0.7	0.83	444.4411	3.0	449.1	3.1	472.8	10.6	444.4	3.0	94.0	0.7
Sample 1 Spot 46	437	24830	3.0	17.7952	0.5	0.5443	1.1	0.0716	1.0	0.91	445.5129	4.3	441.3	3.9	419.2	10.2	445.5	4.3	106.3	1.0
Sample 1 Spot 70	585	47465	1.2	17.6040	0.5	0.5556	3.0	0.0720	3.0	0.99	448.2785	12.8	448.7	10.9	450.8	11.5	448.3	12.8	99.4	2.9
Sample 1 Spot 19	560	36589	2.3	17.2753	0.6	0.5671	0.9	0.0720	0.7	0.74	448.3270	3.0	456.1	3.4	495.5	13.8	448.3	3.0	90.5	0.7
Sample 1 Spot 19	244	37226	3.7	17.7231	0.9	0.5535	1.4	0.0722	1.1	0.79	449.3385	4.9	447.3	5.1	436.5	19.5	449.3	4.9	102.9	1.1
Sample 1 Spot 50	215	26575	3.8	17.6183	0.8	0.5575	1.1	0.0725	0.7	0.68	450.9849	3.1	449.9	3.9	444.4	17.4	451.0	3.1	101.5	0.7
Sample 1 Spot 40	389	47702	1.2	17.7301	0.5	0.5608	0.9	0.0730	0.7	0.83	454.2736	3.2	452.0	3.2	440.5	10.6	454.3	3.2	103.1	0.7
Sample 1 Spot 34	112	33539	4.4	17.4816	1.0	0.5728	1.2	0.0737	0.7	0.58	458.6438	3.2	459.8	4.6	465.8	22.4	458.6	3.2	98.5	0.7
Sample 1 Spot 52	208	45972	3.0	17.4663	0.6	0.5784	2.4	0.0742	2.3	0.97	461.5485	10.2	463.5	8.8	472.9	12.5	461.5	10.2	97.6	2.2
Sample 1 Spot 60	95	77425	2.3	17.5722	0.7	0.5792	1.0	0.0746	0.7	0.71	463.8811	3.2	464.0	3.7	464.3	15.7	463.9	3.2	99.9	0.7
Sample 1 Spot 47	638	78063	3.8	17.5568	0.5	0.5829	0.8	0.0751	0.6	0.78	466.5540	2.7	466.3	2.9	465.3	10.8	466.6	2.7	100.3	0.6
Sample 1 Spot 23	243	16754	1.7	17.1483	0.7	0.6148	1.0	0.0782	0.8	0.75	485.3916	3.6	486.6	4.0	492.3	15.1	485.4	3.6	98.6	0.7
Sample 1 Spot 68	4	725	3.7	10.8707	4.3	0.8138	6.1	0.0824	1.8	0.30	510.1705	8.9	604.6	27.8	976.6	118.6	510.2	8.9	52.2	1.7
Sample 1 Spot 41	205	13276	0.9	16.8352	0.6	0.6724	1.0	0.0842	0.7	0.76	521.2913	3.7	522.1	4.0	525.9	13.8	521.3	3.7	99.1	0.7
Sample 1 Spot 22	225	91772	2.5	16.6741	0.4	0.7025	0.9	0.0858	0.7	0.85	530.7357	3.7	540.3	3.6	580.7	9.8	530.7	3.7	91.4	0.7
Sample 1 Spot 26	187	33816	1.5	16.8344	0.8	0.7110	1.1	0.0880	0.7	0.62	543.9274	3.5	545.3	4.6	551.3	18.5	543.9	3.5	98.7	0.6
Sample 1 Spot 10	102	5077	1.1	16.8801	0.8	0.6913	1.1	0.0897	0.6	0.60	553.6746	3.4	533.6	4.4	448.4	18.9	553.7	3.4	123.5	0.6
Sample 1 Spot 32	420	1907502	1.4	16.7657	0.6	0.7434	1.0	0.0910	0.9	0.83	561.7175	4.7	564.4	4.5	575.0	12.8	561.7	4.7	97.7	0.8
Sample 1 Spot 14	190	32062	1.2	16.7285	0.6	0.7447	0.8	0.0918	0.5	0.62	566.0810	2.6	565.1	3.3	561.2	13.0	566.1	2.6	100.9	0.5
Sample 1 Spot 8	99	51506	2.0	16.7579	0.9	0.7479	1.5	0.0922	1.3	0.83	568.3017	7.0	567.0	6.7	561.7	18.6	568.3	7.0	101.2	1.2
Sample 1 Spot 3	576	69451	0.6	15.8088	0.4	0.9004	0.8	0.1045	0.7	0.88	640.9558	4.4	651.9	4.0	690.1	4.4	92.9	0.7	0.0	0.0
Sample 1 Spot 63	36	14648	1.4	13.3541	0.6	1.8223	0.9	0.1801	0.6	0.64	1067.7617	5.8	1053.5	6.1	1024.1	14.4	1024.1	14.4	104.3	1.4
Sample 1 Spot 15	13	2710	3.5	12.4276	1.1	1.9262	2.3	0.1871	0.8	0.35	1105.6080	8.2	1090.2	15.6	1059.6	43.9	1059.6	43.9	104.3	4.1
Sample 1 Spot 51	121	56033	2.3	13.1531	0.8	1.7918	1.1	0.1728	0.8	0.74	1027.3086	7.9	1042.5	7.3	1074.4	15.1	1074.4	15.1	95.6	1.4
Sample 1 Spot 37	306	30550	3.5	13.0771	0.5	1.8102	0.9	0.1740	0.8	0.85	1034.1683	7.4	1049.1	6.0	1080.4	9.7	1080.4	9.7	95.7	0.9
Sample 1 Spot 45	97	11308	1.3	12.5375	1.0	1.9294	1.2	0.1796	0.6	0.49	1064.5743	5.8	1091.3	8.0	1145.1	20.9	1145.1	20.9	93.0	1.8
Sample 1 Spot 56	107	105437	0.8	12.2092	0.5	2.3088	0.8	0.2062	0.6	0.75	1208.4839	6.5	1215.0	5.6	1226.6	10.3	1226.6	10.3	98.5	0.8
Sample 1 Spot 36	118	31611	1.2	11.7105	0.7	2.6074	0.9	0.2243	0.7	0.70	1304.3448	7.8	1302.7	6.9	1300.0	13.0	1300.0	13.0	100.3	1.0
Sample 1 Spot 54	115	44770	5.1	11.7131	0.5	2.5664	0.8	0.2204	0.6	0.78	1283.9059	6.9	1291.1	5.6	1303.1	9.3	1303.1	9.3	98.5	0.7
Sample 1 Spot 43	270	66528	3.2	11.6083	0.4	2.5973	1.2	0.2208	1.1	0.93	1285.8498	12.8	1299.9	8.7	1323.1	8.7	1323.1	8.7	97.2	0.7
Sample 1 Spot 42	335	109751	4.2	11.5373	0.3	2.6044	0.8	0.2198	0.7	0.91	1280.7404	8.1	1301.9	5.6	1336.8	6.0	1336.8	6.0	95.8	0.5
Sample 1 Spot 2	128	34286	1.6	11.3845	0.5	2.8683	0.8	0.2403	0.7	0.81	1388.0652	8.4	1373.6	6.2	1351.2	9.2	1351.2	9.2	102.7	0.7
Sample 1 Spot 20	967	885337	2.7	11.0151	0.5	3.0569	0.9	0.2460	0.7	0.84	1418.0149	9.4	1422.0	6.7	1427.9	9.1	1427.9	9.1	99.3	0.6
Sample 1 Spot 48	172	62398	1.9	10.9070	0.5	3.0556	0.8	0.2442	0.6	0.78	1408.5480	7.8	1421.6	6.0	1441.3	9.3	1441.3	9.3	97.7	0.6
Sample 1 Spot 24	130	456206	2.1	10.9269	0.5	2.8594	0.9	0.2282	0.7	0.82	1324.9096	8.7	1371.3	6.7	1444.3	9.8	1444.3	9.8	91.7	0.7
Sample 1 Spot 27	90	38928	2.1	10.8084	0.7															

Sample 1 Spot 59	336	112911	2.0	9.8412	0.4	3.7417	0.8	0.2692	0.7	0.88	1536.7421	9.2	1580.3	6.1	1639.0	6.6	1639.0	6.6	93.8	0.4
Sample 1 Spot 5	230	65387	1.1	9.8041	0.4	3.3869	0.8	0.2434	0.6	0.83	1404.5269	8.0	1501.4	5.9	1640.8	7.7	1640.8	7.7	85.6	0.5
Sample 1 Spot 1	103	76527	1.3	9.7654	0.5	4.0058	0.9	0.2870	0.7	0.82	1626.4689	10.1	1635.4	7.0	1646.8	9.2	1646.8	9.2	98.8	0.6
Sample 1 Spot 11	145	83651	4.9	9.4795	0.4	4.2354	0.7	0.2941	0.6	0.81	1662.1077	8.2	1680.9	5.7	1704.4	7.4	1704.4	7.4	97.5	0.4
Sample 1 Spot 64	264	120132	2.9	9.2300	0.4	4.4826	2.9	0.3026	2.9	0.99	1704.2760	43.3	1727.7	24.3	1756.3	8.1	1756.3	8.1	97.0	0.5
Sample 1 Spot 29	602	330079	6.7	9.0897	1.2	4.0807	1.9	0.2710	1.5	0.79	1545.8528	21.0	1650.4	15.8	1786.3	21.5	1786.3	21.5	86.5	1.2
Sample 1 Spot 44	93	29536	2.4	8.8717	0.4	4.4308	0.7	0.2883	0.6	0.84	1632.9104	8.8	1718.1	6.0	1823.6	7.1	1823.6	7.1	89.5	0.4
Sample 1 Spot 30	61	36777	95.3	8.7079	0.5	5.0111	2.0	0.3198	1.9	0.97	1788.5510	30.3	1821.2	16.9	1858.7	8.8	1858.7	8.8	96.2	0.5
Sample 1 Spot 62	104	91085	1.6	8.0539	0.6	5.5748	1.6	0.3284	1.5	0.92	1830.8413	24.1	1912.2	14.2	2001.6	11.5	2001.6	11.5	91.5	0.6
Sample 1 Spot 13	114	50252	1.4	7.7104	0.4	6.5118	0.7	0.3680	0.5	0.80	2019.9530	9.1	2047.5	5.8	2075.3	6.9	2075.3	6.9	97.3	0.3

Key

- % Error > 3
- U/Th > 10
- U > 5,000 ppm
- suspect neo-crystalline
- ages used for MDA

Sample 21BG08

Analysis	U (ppm)	Isotope ratios						Apparent ages (Ma)												
		206Pb 204Pb	U/Th	206Pb* 207Pb*	± (%)	207Pb* 235U	± (%)	206Pb* 238U	± (%)	error corr.	206Pb* 238U	± (Ma)	207Pb* 235U	± (Ma)	206Pb* 207Pb*	± (Ma)	Best age (Ma)	± (Ma)	Conc (%)	% Error
Spot 77	223	880	0.1	9.1412	8.3	0.0922	8.9	0.0071	3.3	0.37	45.8524	1.5	89.5	7.6	1501.4	156.9	45.9	1.5	3.1	3.3
Spot 62	1274	24287	1.0	20.5777	1.3	0.0520	2.2	0.0078	1.8	0.81	50.3378	0.9	51.5	1.1	103.8	30.6	50.3	0.9	48.5	1.8
Spot 108	1757	6866	8.6	20.5894	1.0	0.0536	1.5	0.0084	1.0	0.71	53.7415	0.6	53.0	0.8	19.7	NA	53.7	0.6	272.2	1.0
Spot 89	1732	7122	19.2	17.7313	2.9	0.0629	3.1	0.0084	1.1	0.36	53.8356	0.6	61.9	1.9	386.9	65.6	53.8	0.6	13.9	1.1
Spot 23	2101	32117	16.2	21.0295	0.8	0.0550	1.5	0.0084	1.2	0.82	54.2199	0.6	54.3	0.8	59.1	20.1	54.2	0.6	91.7	1.2
Spot 105	5311	34576	4.2	20.7890	0.6	0.0563	2.0	0.0086	1.9	0.94	54.8976	1.0	55.6	1.1	84.7	15.4	54.9	1.0	64.8	1.8
Spot 84	2553	26934	24.1	20.9677	0.9	0.0557	1.5	0.0086	1.2	0.78	54.9632	0.6	55.1	0.8	59.6	21.9	55.0	0.6	92.2	1.1
Spot 91	3511	2606	3.1	15.0671	2.6	0.0720	4.1	0.0086	3.1	0.76	55.0548	1.7	70.6	2.8	634.9	57.1	55.1	1.7	8.7	3.1
Spot 37	4111	23345	5.8	21.1175	0.6	0.0556	1.2	0.0086	1.0	0.83	55.2324	0.5	54.9	0.6	40.6	15.4	55.2	0.5	136.0	1.0
Spot 133	2501	10112	11.7	20.0688	1.2	0.0575	1.9	0.0086	1.5	0.78	55.3400	0.8	56.8	1.1	117.3	28.4	55.3	0.8	47.2	1.5
Spot 36	982	42822	7.4	21.1182	1.2	0.0560	1.5	0.0086	0.8	0.55	55.3638	0.5	55.4	0.8	55.2	29.6	55.4	0.5	100.3	0.8
Spot 28	949	81496	4.0	21.2391	1.0	0.0559	1.3	0.0086	0.8	0.64	55.4042	0.5	55.3	0.7	49.2	23.7	55.4	0.5	112.5	0.8
Spot 46	2291	10296	14.1	20.9301	0.7	0.0555	1.3	0.0087	1.1	0.82	55.6041	0.6	54.8	0.7	21.2	17.9	55.6	0.6	262.0	1.1
Spot 154	397	5037	5.9	20.8113	1.6	0.0541	2.3	0.0087	1.2	0.52	55.8513	0.6	53.5	1.2	NA	NA	55.9	0.6	1.2	
Spot 156	3568	9472	12.5	18.6974	2.4	0.0625	3.2	0.0087	1.7	0.52	56.0399	0.9	61.5	1.9	281.3	62.9	56.0	0.9	19.9	1.7
Spot 33	1537	21396	4.0	21.0077	0.9	0.0567	1.2	0.0087	0.9	0.70	56.1485	0.5	56.0	0.7	48.2	21.0	56.1	0.5	116.4	0.9
Spot 117	2118	8455	3.6	20.8778	1.5	0.0559	1.7	0.0088	0.8	0.49	56.3296	0.5	55.3	0.9	9.5	NA	56.3	0.5	595.5	0.8
Spot 67	1275	15523	5.6	20.2909	1.0	0.0586	1.6	0.0088	1.2	0.74	56.3417	0.7	57.8	0.9	119.1	25.3	56.3	0.7	47.3	1.2
Spot 3	2044	24752	3.3	20.6571	1.0	0.0580	1.6	0.0088	1.2	0.75	56.3714	0.7	57.3	0.9	94.7	25.2	56.4	0.7	59.5	1.2
Spot 122	926	10792	6.1	21.1597	1.1	0.0556	1.7	0.0088	0.8	0.47	56.3717	0.4	54.9	0.9	NA	NA	56.4	0.4	0.8	
Spot 54	1460	67284	9.8	20.9623	0.9	0.0577	1.1	0.0088	0.7	0.63	56.4551	0.4	57.0	0.6	78.5	20.6	56.5	0.4	71.9	0.7
Spot 59	5499	73498	23.7	20.8128	0.9	0.0585	3.3	0.0088	3.2	0.97	56.7944	1.8	57.7	1.9	94.6	20.3	56.8	1.8	60.0	3.2
Spot 5	1930	1129065	5.4	20.6872	0.8	0.0594	1.2	0.0089	0.9	0.76	57.0929	0.5	58.6	0.7	121.0	18.1	57.1	0.5	47.2	0.9
Spot 96	1042	8562	4.6	20.9620	0.9	0.0566	1.2	0.0089	0.8	0.64	57.1971	0.5	55.9	0.7	-0.7	NA	57.2	0.5	-7889.4	0.8
Spot 48	467	7724	5.2	21.0012	1.3	0.0564	1.8	0.0089	1.2	0.68	57.3477	0.7	55.8	1.0	NA	NA	57.3	0.7	1.2	
Spot 12	1423	40010	5.6	21.2676	1.0	0.0579	1.3	0.0090	0.9	0.68	57.6573	0.5	57.2	0.7	37.4	23.0	57.7	0.5	154.3	0.9
Spot 44	907	7702	3.4	21.0116	1.2	0.0569	2.1	0.0090	1.0	0.47	57.8053	0.6	56.2	1.2	NA	NA	57.8	0.6	1.0	
Spot 99	749	8326	4.2	20.9790	1.1	0.0571	1.5	0.0090	0.9	0.61	57.8156	0.5	56.3	0.8	NA	NA	57.8	0.5	0.9	
Spot 24	664	17355	6.1	21.3245	1.4	0.0574	1.6	0.0090	0.9	0.55	57.8606	0.5	56.6	0.9	5.0	NA	57.9	0.5	1147.8	0.9
Spot 129	1178	10397	11.9	20.9909	1.0	0.0577	1.7	0.0090	0.8	0.47	58.0710	0.5	56.9	0.9	9.1	NA	58.1	0.5	635.0	0.8
Spot 110	765	39212	5.4	21.1100	1.1	0.0587	1.4	0.0091	0.8	0.59	58.0913	0.5	57.9	0.8	49.5	26.8	58.1	0.5	117.5	0.8
Spot 104	2351	19144	9.0	21.2248	0.8	0.0580	1.1	0.0091	0.7	0.65	58.2377	0.4	57.3	0.6	17.0	NA	58.2	0.4	342.4	0.7
Spot 53	4174	83685	3.7	20.8411	0.7	0.0601	1.0	0.0091	0.7	0.71	58.3458	0.4	59.2	0.6	95.6	16.1	58.3	0.4	61.0	0.7
Spot 102	1149	5040	3.9	21.3442	1.0	0.0551	1.4	0.0091	0.9	0.64	58.4146	0.5	54.5	0.8	NA	NA	58.4	0.5	0.9	
Spot 119	1856	24375	20.2	21.2070	0.8	0.0585	1.4	0.0091	1.1	0.78	58.4298	0.6	57.8	0.8	30.1	20.7	58.4	0.6	193.8	1.1
Spot 19	3550	74245	5.3	20.9923	1.0	0.0597	1.9	0.0091	1.6	0.84	58.4840	0.9	58.9	1.1	75.8	24.6	58.5	0.9	77.1	1.6
Spot 10	2164	48159	8.2	20.7439	0.8	0.0606	1.2	0.0092	0.9	0.74	58.7305	0.5	59.7	0.7	99.9	18.6	58.7	0.5	58.8	0.8
Spot 82	3976	31454	6.4	21.1147	0.8	0.0592	1.6	0.0092	1.3	0.85	58.7356	0.8	58.4	0.9	45.6	19.7	58.7	0.8	128.7	1.3
Spot 55	967	15786	3.5	21.3008	1.2	0.0582	1.5	0.0092	0.8	0.55	58.7721	0.5	57.4	0.8	2.1	NA	58.8	0.5	2830.5	0.8
Spot 115	46599	40047	1.6	20.8786	0.8	0.0602	3.1	0.0092	3.0	0.96	58.9416	1.7	59.3	1.8	75.3	19.4	58.9	1.7	78.2	3.0
Spot 127	989	53824	3.9	20.9610	1.1	0.0603	1.4	0.0092	0.9	0.64	59.1434	0.5	59.5	0.8	72.0	25.9	59.1	0.5	82.2	0.9
Spot 8	1930	10418	7.4	19.7009	1.2	0.0629	1.4	0.0092	0.7	0.50	59.1544	0.4	61.9	0.8	169.9	27.7	59.2	0.4	34.8	0.7
Spot 81	1617	54585	3.0	21.2141	0.9	0.0597	1.3	0.0092	0.9	0.73	59.2181	0.6	58.9	0.7	44.5	21.2	59.2	0.6	133.1	0.9
Spot 128	2757	33254	13.5	20.9080	0.8	0.0614	1.1	0.0094	0.8	0.72	60.2782	0.5	60.5	0.7	68.6	18.8	60.3	0.5	87.9	0.8
Spot 124	2907	47019	7.0	20.8338	0.7	0.0618	1.0	0.0094	0.7	0.69	60.3610	0.4	60.9	0.6	83.1	17.1	60.4	0.4	72.6	0.7
Spot 13	2476	22480	11.9	21.2900	0.8	0.0606	1.1	0.0095	0.8	0.72	60.7461	0.5	59.7	0.6	20.0	18.4	60.7	0.5	304.1	0.8
Spot 132	1071	26248	5.2	20.7292	0.8	0.0646	1.3	0.0098	1.0	0.75	63.0130	0.6	63.6	0.8	84.4	20.0	63.0	0.6	74.7	1.0
Spot 17	3623	81084	12.2	21.1950	0.7	0.0640	1.3	0.0099	1.1	0.84	63.2508	0.7	63.0	0.8	53.7	17.0	63.3	0.7	117.8	1.1
Spot 130	963	15276	6.0	20.8816	0.9	0.0639	1.3	0.0099	0.9	0.71	63.3844	0.6	62.9	0.8	45.9	21.9	63.4	0.6	138.2	0.9
Spot 61	1071	40747	7.1	20.7133	1.0	0.0655	1.4	0.0099	1.0	0.69	63.4247	0.6	64.4	0.9	100.2	24.4	63.4	0.6	63.3	1.0
Spot 83	1405	19109	3.1	20.7533	0.7	0.0653	1.2	0.0100	1.0	0.82	64.0081	0.6	64.2	0.8	72.1	16.9	64.0	0.6	88.8	1.0
Spot 92	1328	17166	7.2	21.0072	0.9	0.0653	1.2	0.0101	0.8	0.66	64.8974	0.5	64.2	0.8	39.6	21.8	64.9	0.5	163.8	0.8
Spot 112	1086	14780	3.2	20.7321	1.0	0.0684	1.6	0.0105	1.2	0.72	67.3793	0.8	67.2	1.1	60.5					

Spot 49	1303	6638	5.6	20.7852	0.8	0.0684	1.7	0.0108	1.4	0.87	69.1589	1.0	67.2	1.1	NA	NA	69.2	1.0	1.4
Spot 101	448	20686	9.5	20.8706	1.2	0.0759	1.4	0.0117	0.8	0.52	74.7380	0.6	74.3	1.0	60.9	29.4	74.7	0.6	122.6
Spot 39	1491	93544	2.7	20.7281	0.7	0.0778	1.3	0.0117	1.1	0.84	75.0444	0.8	76.1	1.0	109.6	16.8	75.0	0.8	68.5
Spot 22	1297	71789	11.5	20.2619	1.0	0.0804	1.4	0.0118	1.0	0.71	75.8927	0.8	78.5	1.1	160.0	23.7	75.9	0.8	47.4
Spot 123	1036	9956	5.4	20.8009	1.1	0.0772	1.6	0.0120	1.1	0.68	76.9966	0.8	75.5	1.1	27.7	27.6	77.0	0.8	278.0
Spot 60	730	2253	4.8	13.7357	5.8	0.1119	7.0	0.0122	1.8	0.26	78.2379	1.4	107.7	7.1	821.8	140.4	78.2	1.4	9.5
Spot 51	612	32621	3.8	20.3049	3.4	0.0850	5.5	0.0126	4.3	0.78	80.7778	3.4	82.9	4.3	143.6	80.0	80.8	3.4	56.3
Spot 131	774	4751	4.3	20.4137	1.1	0.0810	1.5	0.0128	1.0	0.65	82.0387	0.8	79.1	1.2	NA	NA	82.0	0.8	1.0
Spot 52	1335	8306	3.2	19.1413	1.2	0.0903	1.6	0.0129	1.0	0.62	82.9042	0.8	87.8	1.3	222.2	28.9	82.9	0.8	37.3
Spot 125	590	4565	6.6	20.2366	1.0	0.0839	1.3	0.0132	0.7	0.58	84.3689	0.6	81.8	1.0	6.3	NA	84.4	0.6	1331.1
Spot 45	258	3545	5.3	20.2058	1.5	0.0843	2.2	0.0135	0.9	0.40	86.1407	0.8	82.1	1.8	NA	NA	86.1	0.8	0.9
Spot 98	594	4079	6.0	18.7859	1.7	0.0922	2.5	0.0135	1.2	0.48	86.1765	1.0	89.5	2.2	179.9	51.8	86.2	1.0	47.9
Spot 15	1125	19872	27.4	20.6800	1.0	0.0907	1.4	0.0138	0.9	0.64	88.2788	0.8	88.2	1.2	86.1	24.8	88.3	0.8	102.5
Spot 85	466	4961	4.8	20.6445	1.2	0.0876	2.3	0.0140	1.1	0.48	89.4005	1.0	85.3	1.9	NA	NA	89.4	1.0	1.1
Spot 152	1253	5043	2.8	18.1453	2.0	0.1006	2.2	0.0140	1.0	0.44	89.4984	0.9	97.3	2.0	293.9	45.0	89.5	0.9	30.5
Spot 1	915	18245	2.8	20.1629	1.1	0.0949	1.6	0.0141	1.1	0.71	90.1282	1.0	92.1	1.4	142.2	26.8	90.1	1.0	63.4
Spot 109	1226	15494	2.8	20.8098	1.0	0.0917	1.3	0.0141	0.8	0.56	90.3394	0.7	89.1	1.1	54.9	26.7	90.3	0.7	164.6
Spot 157	146	7959	4.8	21.1470	2.2	0.0892	2.4	0.0142	1.0	0.43	91.1832	0.9	86.7	2.0	NA	NA	91.2	0.9	1.0
Spot 114	1711	6153850	2.3	21.1258	0.7	0.0930	1.0	0.0142	0.7	0.68	91.1955	0.6	90.3	0.9	65.6	17.4	91.2	0.6	139.1
Spot 118	510	6499	4.6	20.8502	1.0	0.0900	1.3	0.0143	0.9	0.67	91.2575	0.8	87.5	1.1	NA	NA	91.3	0.8	0.9
Spot 9	1150	35174	4.5	20.7224	0.8	0.0943	1.1	0.0143	0.7	0.66	91.2888	0.6	91.5	0.9	96.7	19.0	91.3	0.6	94.4
Spot 38	660	6021	5.7	20.3669	1.3	0.0920	1.7	0.0143	1.0	0.61	91.3073	0.9	89.3	1.4	37.2	31.6	91.3	0.9	245.5
Spot 159	1539	22640	2.3	18.8338	2.6	0.1031	2.7	0.0143	0.9	0.33	91.3191	0.8	99.7	2.6	304.3	58.8	91.3	0.8	30.0
Spot 78	506	23702	4.3	20.4522	1.1	0.0951	1.6	0.0143	1.2	0.71	91.4220	1.0	92.3	1.4	113.8	26.7	91.4	1.0	80.3
Spot 29	1154	10113	3.8	20.6427	1.0	0.0930	1.8	0.0143	0.9	0.51	91.6780	0.8	90.2	1.5	52.6	36.6	91.7	0.8	174.3
Spot 153	531	10132	5.5	20.6649	0.9	0.0927	1.8	0.0143	1.1	0.62	91.6955	1.0	90.0	1.6	45.5	34.4	91.7	1.0	201.7
Spot 16	881	58510	5.4	20.7310	0.9	0.0950	1.3	0.0143	1.0	0.73	91.7304	0.9	92.2	1.2	103.0	21.2	91.7	0.9	89.0
Spot 93	680	7776	3.4	20.8682	1.0	0.0913	1.7	0.0144	0.8	0.46	91.9487	0.7	88.7	1.5	1.6	NA	91.9	0.7	5873.0
Spot 6	832	22090	2.7	20.9105	0.8	0.0939	1.2	0.0144	0.7	0.64	92.1980	0.7	91.1	1.0	62.8	21.4	92.2	0.7	146.8
Spot 107	187	32845	3.9	20.2517	1.7	0.0974	2.1	0.0144	1.3	0.62	92.3253	1.2	94.3	1.9	145.3	38.9	92.3	1.2	63.5
Spot 47	1258	14680	2.4	20.4852	1.0	0.0956	1.7	0.0145	1.3	0.77	92.5654	1.2	92.7	1.5	95.6	24.9	92.6	1.2	96.8
Spot 2	2534	135576	2.1	20.7534	0.6	0.0962	0.9	0.0145	0.7	0.74	92.6909	0.6	93.3	0.8	107.7	14.6	92.7	0.6	86.1
Spot 40	1539	13697	2.1	20.7187	0.8	0.0948	1.1	0.0145	0.7	0.61	92.9868	0.6	91.9	0.9	64.8	20.2	93.0	0.6	143.5
Spot 79	1099	19998	2.4	20.5305	1.0	0.0963	1.3	0.0146	0.7	0.52	93.1335	0.6	93.4	1.1	99.8	26.0	93.1	0.6	93.4
Spot 25	1044	19606	3.3	20.8567	0.8	0.0954	1.2	0.0146	0.9	0.75	93.6621	0.8	92.6	1.0	64.1	18.3	93.7	0.8	146.2
Spot 56	1320	14041	2.5	20.4698	0.7	0.0967	1.3	0.0146	1.0	0.77	93.7443	0.9	93.7	1.2	93.3	19.5	93.7	0.9	100.4
Spot 100	2222	60999	2.3	20.9157	0.4	0.0963	1.0	0.0147	0.9	0.91	93.8433	0.9	93.3	0.9	80.2	10.0	93.8	0.9	117.1
Spot 50	912	5977	2.9	16.7900	4.2	0.1158	5.0	0.0147	1.7	0.34	93.9281	1.6	111.3	5.3	500.2	103.5	93.9	1.6	18.8
Spot 31	844	8026	2.7	20.8022	1.0	0.0938	2.1	0.0147	0.9	0.44	94.0045	0.9	91.0	1.9	13.2	NA	94.0	0.9	713.0
Spot 87	561	5169	4.7	20.2134	1.2	0.0945	1.7	0.0147	0.9	0.54	94.0339	0.8	91.7	1.5	31.4	NA	94.0	0.8	299.5
Spot 88	208	3359	4.0	20.8460	1.6	0.0885	5.1	0.0147	0.8	0.15	94.2150	0.7	86.1	4.2	NA	NA	94.2	0.7	0.8
Spot 64	591	226497	13.9	20.3807	1.3	0.0997	1.5	0.0147	0.8	0.55	94.2246	0.8	96.5	1.4	153.8	30.4	94.2	0.8	61.3
Spot 151	592	42244	4.9	20.9382	1.1	0.0963	1.5	0.0147	1.0	0.66	94.2277	0.9	93.3	1.3	70.6	26.4	94.2	0.9	133.4
Spot 26	446	8592	4.0	20.9451	1.1	0.0940	1.4	0.0148	0.9	0.62	94.5567	0.8	91.2	1.3	3.9	NA	94.6	0.8	2432.6
Spot 20	1359	12780	2.5	20.7748	0.9	0.0960	1.4	0.0148	0.8	0.55	94.5883	0.7	93.0	1.3	53.7	28.5	94.6	0.7	176.2
Spot 95	532	29854	6.7	20.8795	0.8	0.0967	1.3	0.0148	1.0	0.78	94.6207	0.9	93.8	1.2	72.2	19.2	94.6	0.9	131.1
Spot 134	229	4113	4.7	20.9174	1.8	0.0905	2.4	0.0148	1.1	0.45	94.9709	1.0	87.9	2.0	NA	NA	95.0	1.0	1.1
Spot 21	731	14992	4.3	21.1710	0.9	0.0953	1.3	0.0149	0.9	0.69	95.4316	0.9	92.4	1.2	15.8	NA	95.4	0.9	603.5
Spot 63	783	22571	3.4	20.4830	0.9	0.1000	1.3	0.0150	0.8	0.67	96.0577	0.8	96.7	1.2	113.5	22.1	96.1	0.8	84.7
Spot 158	585	15624	3.5	20.5885	1.0	0.0986	1.4	0.0150	0.8	0.60	96.1123	0.8	95.5	1.3	79.5	26.5	96.1	0.8	120.9
Spot 155	553	4848	5.1	20.6212	1.1	0.0946	1.9	0.0151	1.0	0.52	96.6867	1.0	91.8	1.7	NA	NA	96.7	1.0	1.0
Spot 97	1205	14503	1.8	20.7293	0.9	0.0987	1.3	0.0151	0.9	0.71	96.7969	0.9	95.5	1.2	64.2	22.0	96.8	0.9	150.7
Spot 90	801	96995	5.5	20.6108	1.2	0.1012	1.7	0.0152	1.2	0.73	97.0358	1.2	97.9	1.6	119.0	27.6	97.0	1.2	81.5
Spot 27	3444	133676	8.3	20.7319	0.5	0.1014	1.0	0.0152	0.9	0.85	97.5278	0.9	98.0	1.0	110.4	12.9	97.5	0.9	88.4
Spot 34	520	11199	5.5	21.0131	1.1	0.0981	2.4	0.0154	2.2	0.89	98.2270	2.1	95.0	2.2	15.2	NA	98.2	2.1	645.2
Spot 121	211	8710	4.3	21.1275	1.7	0.0967	2.7	0.0154	1.4	0.51	98.3126	1.4	93.7	2.4	NA	NA	98.3	1.4	1.4
Spot 106	428	16133	3.5	18.7460	3.5	0.1115	3.7	0.0154	1.1	0.29	98.6116	1.1	107.3	3.8	305.3	80.5	98.6	1.1	32.3
Spot 14	963	16917	2.5	20.6035	1.1	0.1021	1.4	0.0155	0.9	0.65	99.1591	0.9	98.7	1.3	88.6	25.6	99.2	0.9	111.9
Spot 126	837	26153	3.7	20.8493	1.0	0.1014	1.5	0.0155	1.2	0.77	99.1906	1.2	98.						